Satellite Remote Sensing and GIS Applications in Agricultural Meteorology

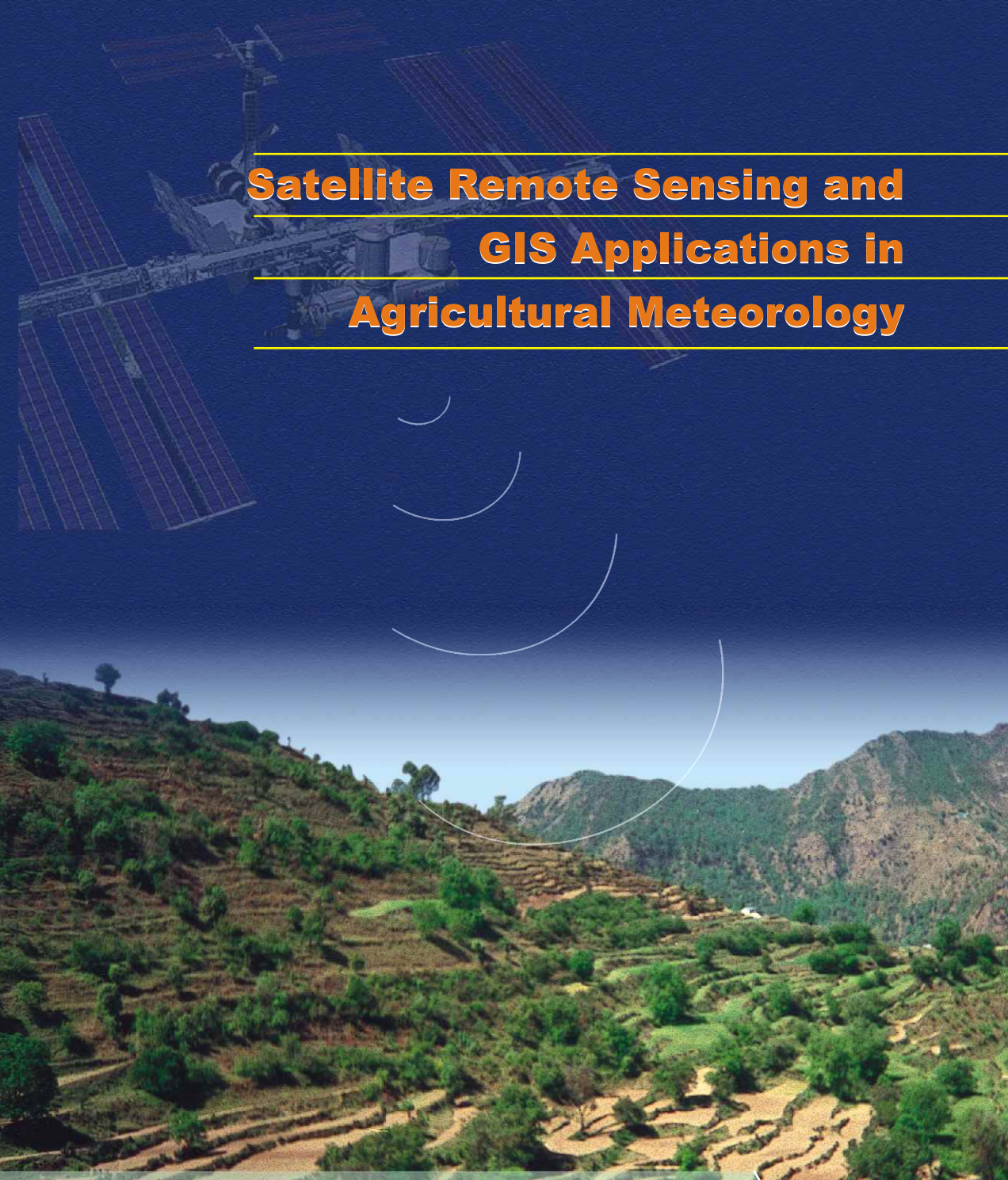

CSSTEAP iirs nrsa इसरो ISRO

Satellite Remote Sensing and GIS Applications in Agricultural Meteorology

Proceedings of the Training Workshop
7-11 July, 2003, Dehra Dun, India

Editors
M.V.K. Sivakumar
P.S. Roy
K. Harmsen
S.K. Saha

Sponsors
World Meteorological Organization (WMO)
India Meteorological Department (IMD)
Centre for Space Science and Technology Education in Asia and the Pacific (CSSTEAP)
Indian Institute of Remote Sensing (IIRS)
National Remote Sensing Agency (NRSA) and
Space Application Centre (SAC)

AGM-8
WMO/TD No. 1182

World Meteorological Organisation
7bis, Avenue de la Paix
1211 Geneva 2
Switzerland

2004

Published by
World Meteorological Organisation
7bis, Avenue de la Paix
1211 Geneva 2, Switzerland

World Meteorological Organisation

Typesetting and Printing :
M/s Bishen Singh Mahendra Pal Singh
23-A New Connaught Place, P.O. Box 137,
Dehra Dun -248001 (Uttaranchal), INDIA
Ph.: 91-135-2715748 Fax- 91-135-2715107
E.mail: bsmps@vsnl.com
Website: http://www.bishensinghbooks.com

FOREWORD

Weather and climate data systems for agricultural activities are necessary to expedite the generation of products, analyses and forecasts that affect agricultural cropping and management decisions, irrigation scheduling, commodity trading and markets, fire management and other preparedness measures against calamities, and ecosystem conservation and management. One important source of agrometeorological data that complements traditional methods of data collection is the satellite remote sensing technology. Remote sensing provides spatial coverage by measurement of reflected and emitted electromagnetic radiation, across a wide range of wavebands, from the Earth's surface and surrounding atmosphere. The improvement in technical tools of meteorological observation, during the last twenty years, has created a favourable condition for research and monitoring in many areas of science such as agriculture and forestry.

Due to the availability of new tools such as the Geographic Information Systems (GIS), management of large datasets such as traditional digital maps, databases, and models, is now possible. The quantitative data handling capability offered by GIS enables users to overlay numerous spatial data sets and statistically analyze these data and develop quantitative relationships not achievable using simple map drawing or graphics display programmes.

The Commission for Agricultural Meteorology (CAgM) of WMO recognized the potential of remote sensing applications in agricultural meteorology early in the 70s and at its sixth session in Washington in 1974 the Commission agreed that its activities should include studies on the application of remote sensing techniques to agrometeorological problems. It appointed a rapporteur to study the existing state of the knowledge of remote sensing techniques and to review its application to agrometeorological research and services. The Commission has continued to pay much attention to both remote sensing and GIS applications in agrometeorology in all its subsequent sessions including the 13th session held in Ljubljana, Slovenia in 2002.

Active promotion of the use of remote sensing and GIS in the National Meteorological and Hydrological Services (NMHSs) could enhance improved agrometeorological applications. To this end it is important to reinforce training in these new fields. The Training Workshop on Satellite Remote Sensing and GIS Applications in Agricultural Meteorology was organized in response to the recommendations of the CAgM session in Ljubljana, Slovenia in 2002 with the objective of enabling the participants from the Asian countries in learning new skills and updating their current skills in satellite remote sensing and GIS applications in agricultural meteorology. I am pleased that a number of organizations including WMO, the India Meteorological Department (IMD), the Centre for Space Science and Technology Education in Asia and the Pacific (CSSTEAP), the Indian Institute of Remote Sensing (IIRS), the National Remote Sensing Agency (NRSA) and the Space Applications Centre (SAC) have come together to organize the Training Workshop at IIRS.

The workshop dealt with a number of useful subjects including introduction to various aspects of satellite and remote sensing, digital image processing, fundamentals of GIS and Geopositioning Systems (GPS), spatial data analysis and practical demonstration of GIS software, theoretical and practical aspects of retrieval of agrometeorological parameters using satellite remote sensing data, crop growth and productivity monitoring and simulation as well as assessment and monitoring of droughts, floods, water and wind induced soil erosion, satellite applications in weather forecasting, agro-advisory services, desert locust monitoring and forest fire and degradation assessment. I hope that the proceedings of this training workshop will serve as a useful source of information to all institutions and agencies that are involved in applying agrometeorological practices in support of agricultural production and food security.

(M. Jarraud)
Secretary-General
World Meteorological Organization

CONTENTS

SATELLITE REMOTE SENSING AND GIS APPLICATIONS IN AGRICULTURAL METEOROLOGY AND WMO SATELLITE ACTIVITIES

M.V.K. Sivakumar and Donald E. Hinsman
Agricultural Meteorology Division and Satellite Activities Office
World Meteorological Organization (WMO), 7bis Avenue de la Paix,
1211 Geneva 2, Switzerland

Abstract : Agricultural planning and use of agricultural technologies need applications of agricultural meteorology. Satellite remote sensing technology is increasingly gaining recognition as an important source of agrometeorological data as it can complement well the traditional methods agrometeorological data collection. Agrometeorologists all over the world are now able to take advantage of a wealth of observational data, product and services flowing from specially equipped and highly sophisticated environmental observation satellites. In addition, Geographic Information Systems (GIS) technology is becoming an essential tool for combining various map and satellite information sources in models that simulate the interactions of complex natural systems. The Commission for Agricultural Meteorology of WMO has been active in the area of remote sensing and GIS applications in agrometeorology. The paper provides a brief overview of the satellite remote sensing and GIS Applications in agricultural meteorology along with a description of the WMO Satellite Activities Programme. The promotion of new specialised software should make the applications of the various devices easier, bearing in mind the possible combination of several types of inputs such as data coming from standard networks, radar and satellites, meteorological and climatological models, digital cartography and crop models based on the scientific acquisition of the last twenty years.

INTRODUCTION

Agricultural planning and use of agricultural technologies need application of agricultural meteorology. Agricultural weather and climate data systems are necessary to expedite generation of products, analyses and forecasts that affect

Satellite Remote Sensing and GIS Applications in Agricultural Meteorology
pp. 1-21

agricultural cropping and management decisions, irrigation scheduling, commodity trading and markets, fire weather management and other preparedness for calamities, and ecosystem conservation and management.

Agrometeorological station networks are designed to observe the data of meteorological and biological phenomena together with supplementary data as disasters and crop damages occur. The method of observation can be categorized into two major classes, manually observed and automatic weather stations (AWS). A third source for agrometeorological data that is gaining recognition for its complementary nature to the traditional methods is satellite remote sensing technology.

Remotely sensed data and AWS systems provide in many ways an enhanced and very feasible alternative to manual observation with a very short time delay between data collection and transmission. In certain countries where only few stations are in operation as in Northern Turkmenistan (Seitnazarov, 1999), remotely sensed data can improve information on crop conditions for an early warning system. Due to the availability of new tools, such as Geographic Information Systems (GIS), management of an incredible quantity of data such as traditional digital maps, database, models etc., is now possible. The advantages are manifold and highly important, especially for the fast cross-sector interactions and the production of synthetic and lucid information for decision-makers. Remote sensing provides the most important informative contribution to GIS, which furnishes basic informative layers in optimal time and space resolutions.

In this paper, a brief overview of the satellite remote sensing and GIS applications in agricultural meteorology is presented along with a description of the WMO Satellite Activities Programme. Details of the various applications alluded to briefly in this paper, can be found in the informative papers prepared by various experts who will be presenting them in the course of this workshop.

The Commission for Agricultural Meteorology (CAgM) of WMO, Remote Sensing and GIS

Agricultural meteorology had always been an important component of the National Meteorological Services since their inception. A formal Commission for Agricultural Meteorology (CAgM) which was appointed in 1913 by the International Meteorological Organization (IMO), became the foundation of the CAgM under WMO in 1951.

The WMO Agricultural Meteorology Programme is coordinated by CAgM. The Commission is responsible for matters relating to applications of meteorology to agricultural cropping systems, forestry, and agricultural land use and livestock management, taking into account meteorological and agricultural developments both in the scientific and practical fields and the development of agricultural meteorological services of Members by transfer of knowledge and methodology and by providing advice.

CAgM recognized the potential of remote sensing applications in agricultural meteorology early in the 70s and at its sixth session in Washington in 1974 the Commission agreed that its programme should include studies on the application of remote sensing techniques to agrometeorological problems and decided to appoint a rapporteur to study the existing state of the knowledge of remote sensing techniques and to review its application to agrometeorological research and services. At its seventh session in Sofia, Bulgaria in 1979, the Commission reviewed the report submitted by Dr A.D. Kleschenko (USSR) and Dr J.C. Harlan Jr (USA) and noted that there was a promising future for the use in agrometeorology of data from spacecraft and aircraft and that rapid progress in this field required exchange of information on achievements in methodology and data collection and interpretation. The Commission at that time noted that there was a demand in almost all countries for a capability to use satellite imagery in practical problems of agrometeorology. The Commission continued to pay much attention to both remote sensing and GIS applications in agrometeorology in all its subsequent sessions up to the 13th session held in Ljubljana, Slovenia in 2002. Several useful publications including Technical Notes and CAgM Reports were published covering the use of remote sensing for obtaining agrometeorological information (Kleschenko, 1983), operational remote sensing systems in agriculture (Kanemasu and Filcroft, 1992), satellite applications to agrometeorology and technological developments for the period 1985-89 (Seguin, 1992), statements of guidance regarding how well satellite capabilities meet WMO user requirements in agrometeorology (WMO, 1998, 2000) etc. At the session in Slovenia in 2002, the Commission convened an Expert Team on Techniques (including Technologies such as GIS and Remote Sensing) for Agroclimatic Characterization and Sustainable Land Management.

The Commission also recognized that training of technical personnel to acquire, process and interpret the satellite imagery was a major task. It was felt that acquisition of satellite data was usually much easier than the interpretation of data for specific applications that were critical for the

assessment and management of natural resources. In this regard, the Commission pointed out that long-term planning and training of technical personnel was a key ingredient in ensuring full success in the use of current and future remote sensing technologies that could increase and sustain agricultural production, especially in the developing countries. In this connection, WMO already organized a Training Seminar on GIS and Agroecological Zoning in Kuala Lumpur, Malaysia in May 2000 in which six participants from Malaysia and 12 from other Asian and the South-West Pacific countries participated. The programme for the seminar dealt with meteorological and geographical databases, statistical analyses, spatialization, agro-ecological classification, overlapping of agroecological zoning with boundary layers, data extraction, monitoring system organization and bulletins.

The training workshop currently being organized in Dehradun is in response to the recommendations of the Commission session in Slovenia in 2002 and it should help the participants from the Asian countries in learning new skills and updating their current skills in satellite remote sensing and GIS applications in agricultural meteorology.

GIS APPLICATIONS IN AGROMETEOROLOGY

A GIS generally refers to a description of the characteristics and tools used in the organization and management of geographical data. The term GIS is currently applied to computerised storage, processing and retrieval systems that have hardware and software specially designed to cope with geographically referenced spatial data and corresponding informative attribute. Spatial data are commonly in the form of layers that may depict topography or environmental elements. Nowadays, GIS technology is becoming an essential tool for combining various map and satellite information sources in models that simulate the interactions of complex natural systems. A GIS can be used to produce images, not just maps, but drawings, animations, and other cartographic products.

The increasing world population, coupled with the growing pressure on the land resources, necessitates the application of technologies such as GIS to help maintain a sustainable water and food supply according to the environmental potential. The “sustainable rural development” concept envisages an integrated management of landscape, where the exploitation of natural resources, including climate, plays a central role. In this context, agrometeorology can help reduce inputs, while in the framework of global

change, it helps quantify the contribution of ecosystems and agriculture to carbon budget (Maracchi, 1991). Agroclimatological analysis can improve the knowledge of existing problems allowing land planning and optimization of resource management. One of the most important agroclimatological applications is the climatic risk evaluation corresponding to the possibility that certain meteorological events could happen, damaging crops or infrastructure.

At the national and local level, possible GIS applications are endless. For example, agricultural planners might use geographical data to decide on the best zones for a cash crop, combining data on soils, topography, and rainfall to determine the size and location of biologically suitable areas. The final output could include overlays with land ownership, transport, infrastructure, labour availability, and distance to market centres.

The ultimate use of GIS lies in its modelling capability, using real world data to represent natural behaviour and to simulate the effect of specific processes. Modelling is a powerful tool for analyzing trends and identifying factors that affect them, or for displaying the possible consequences of human activities that affect the resource availability.

In agrometeorology, to describe a specific situation, we use all the information available on the territory: water availability, soil types, forest and grasslands, climatic data, geology, population, land-use, administrative boundaries and infrastructure (highways, railroads, electricity or communication systems). Within a GIS, each informative layer provides to the operator the possibility to consider its influence to the final result. However more than the overlap of the different themes, the relationship of the numerous layers is reproduced with simple formulas or with complex models. The final information is extracted using graphical representation or precise descriptive indexes.

In addition to classical applications of agrometeorology, such as crop yield forecasting, uses such as those of the environmental and human security are becoming more and more important. For instance, effective forest fire prevention needs a series of very detailed information on an enormous scale. The analysis of data, such as the vegetation coverage with different levels of inflammability, the presence of urban agglomeration, the presence of roads and many other aspects, allows the mapping of the areas where risk is greater. The use of other informative layers, such as the position of the control points and resource availability (staff, cars, helicopters, aeroplanes, fire fighting

equipment, etc.), can help the decision-makers in the management of the ecosystems. Monitoring the resources and the meteorological conditions therefore allows, the consideration of the dynamics of the system, with more adherence to reality. For instance, Figure 1 shows the informative layers used for the evaluation of fire risk in Tuscany (Italy). The final map is the result of the integration of satellite data with territorial data, through the use of implemented GIS technologies (Romanelli *et al.*, 1998).

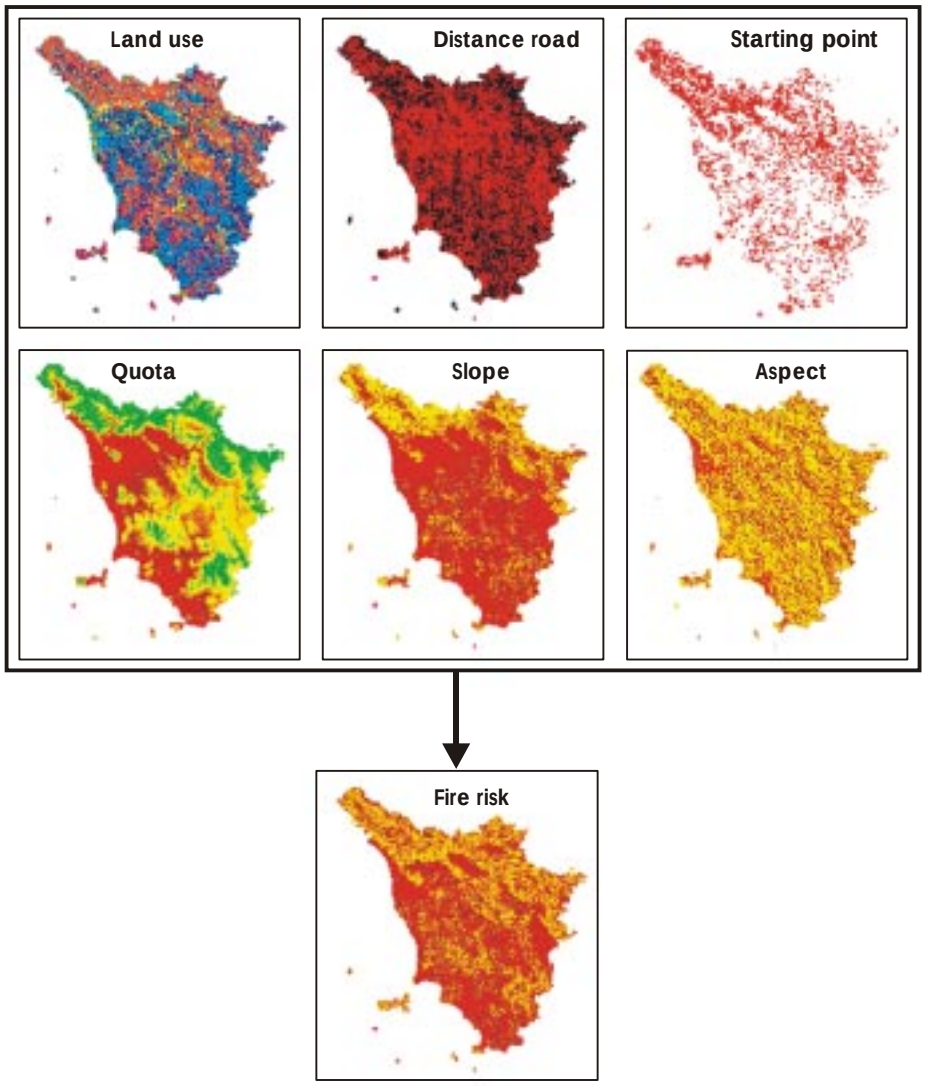

Figure 1. Informative layers for the evaluation of fire risk index (Maracchi *et al.*, 2000).

These maps of fire risk, constitute a valid tool for foresters and for organisation of the public services. At the same time, this new informative layer may be used as the base for other evaluations and simulations. Using meteorological data and satellite real-time information, it is possible to diversify the single situations, advising the competent authorities when the situation moves to hazard risks. Modelling the ground wind profile and taking into account the meteorological conditions, it is possible to advise the operators of the change in the conditions that can directly influence the fire, allowing the modification of the intervention strategies.

An example of preliminary information system to country scale is given by the SISP (Integrated information system for monitoring cropping season by meteorological and satellite data), developed to allow the monitoring of the cropping season and to provide an early warning system with useful information about evolution of crop conditions (Di Chiara and Maracchi, 1994). The SISP uses:

- Statistical analysis procedures on historical series of rainfall data to produce agroclimatic classification;
- A crop (millet) simulation model to estimate millet sowing date and to evaluate the effect of the rainfall distribution on crop growth and yield;
- NOAA-NDVI image analysis procedures in order to monitor vegetation condition;
- Analysis procedures of Meteosat images of estimated rainfall for early prediction of sowing date and risk areas.

The results of SISP application shown for Niger (Fig. 2) are charts and maps, which give indications to the expert of the millet conditions during the season in Niger, with the possibility to estimate the moment of the harvest and final production. SISP is based on the simulation of the millet growth and it gives an index of annual productivity by administrative units. These values, multiplied to a yield statistical factor, allow estimation of absolute production.

By means of such systems based on modelling and remote sensing, it is possible to extract indices relative to the main characteristics of the agricultural season and conditions of natural systems. This system is less expensive, easily transferable and requires minor informative layers, adapting it to the specific requirements of the users.

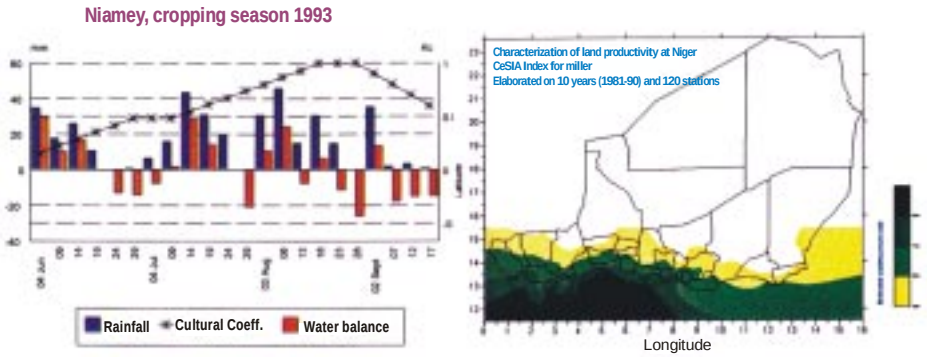

Figure 2. Examples of outputs of SISP (Maracchi *et al.*, 2000).

SATELLITE REMOTE SENSING

Remote sensing provides spatial coverage by measurement of reflected and emitted electromagnetic radiation, across a wide range of wavebands, from the earth's surface and surrounding atmosphere. The improvement in technical tools of meteorological observation, during the last twenty years, has created a favourable *substratum* for research and monitoring in many applications of sciences of great economic relevance, such as agriculture and forestry. Each waveband provides different information about the atmosphere and land surface: surface temperature, clouds, solar radiation, processes of photosynthesis and evaporation, which can affect the reflected and emitted radiation, detected by satellites. The challenge for research therefore is to develop new systems extracting this information from remotely sensed data, giving to the final users, near-real-time information.

Over the last two decades, the development of space technology has led to a substantial increase in satellite earth observation systems. Simultaneously, the Information and Communication Technology (ICT) revolution has rendered increasingly effective the processing of data for specific uses and their instantaneous distribution on the World Wide Web (WWW).

The meteorological community and associated environmental disciplines such as climatology including global change, hydrology and oceanography all over the world are now able to take advantage of a wealth of observational data, products and services flowing from specially equipped and highly sophisticated environmental observation satellites. An environmental

observation satellite is an artificial Earth satellite providing data on the Earth system and a Meteorological satellite is a type of environmental satellite providing meteorological observations. Several factors make environmental satellite data unique compared with data from other sources, and it is worthy to note a few of the most important:

- Because of its high vantage point and broad field of view, an environmental satellite can provide a regular supply of data from those areas of the globe yielding very few conventional observations;

- The atmosphere is broadly scanned from satellite altitude and enables large-scale environmental features to be seen in a single view;

- The ability of certain satellites to view a major portion of the atmosphere continually from space makes them particularly well suited for the monitoring and warning of short-lived meteorological phenomena; and

- The advanced communication systems developed as an integral part of the satellite technology permit the rapid transmission of data from the satellite, or their relay from automatic stations on earth and in the atmosphere, to operational users.

These factors are incorporated in the design of meteorological satellites to provide data, products and services through three major functions:

- Remote sensing of spectral radiation which can be converted into meteorological measurements such as cloud cover, cloud motion vectors, surface temperature, vertical profiles of atmospheric temperature, humidity and atmospheric constituents such as ozone, snow and ice cover, ozone and various radiation measurements;

- Collection of data from *in situ* sensors on remote fixed or mobile platforms located on the earth's surface or in the atmosphere; and

- Direct broadcast to provide cloud-cover images and other meteorological information to users through a user-operated direct readout station.

The first views of earth from space were not obtained from satellites but from converted military rockets in the early 1950s. It was not until 1 April 1960 that the first operational meteorological satellite, TIROS-I, was launched

by the USA and began to transmit basic, but very useful, cloud imagery. This satellite was such an effective proof of concept that by 1966 the USA had launched a long line of operational polar satellites and its first geostationary meteorological satellite. In 1969 the USSR launched the first of a series of polar satellites. In 1977 geostationary meteorological satellites were also launched and operated by Japan and by the European Space Agency (ESA). Thus, within 18 years of the first practical demonstration by TIROS-I, a fully operational meteorological satellite system (Fig. 3) was in place, giving routine data coverage of most of the planet. This rapid evolution of a very expensive new system was unprecedented and indicates the enormous value of these satellites to meteorology and society. Some four decades after the first earth images, new systems are still being designed and implemented, illustrating the continued and dynamic interest in this unique source of environmental data.

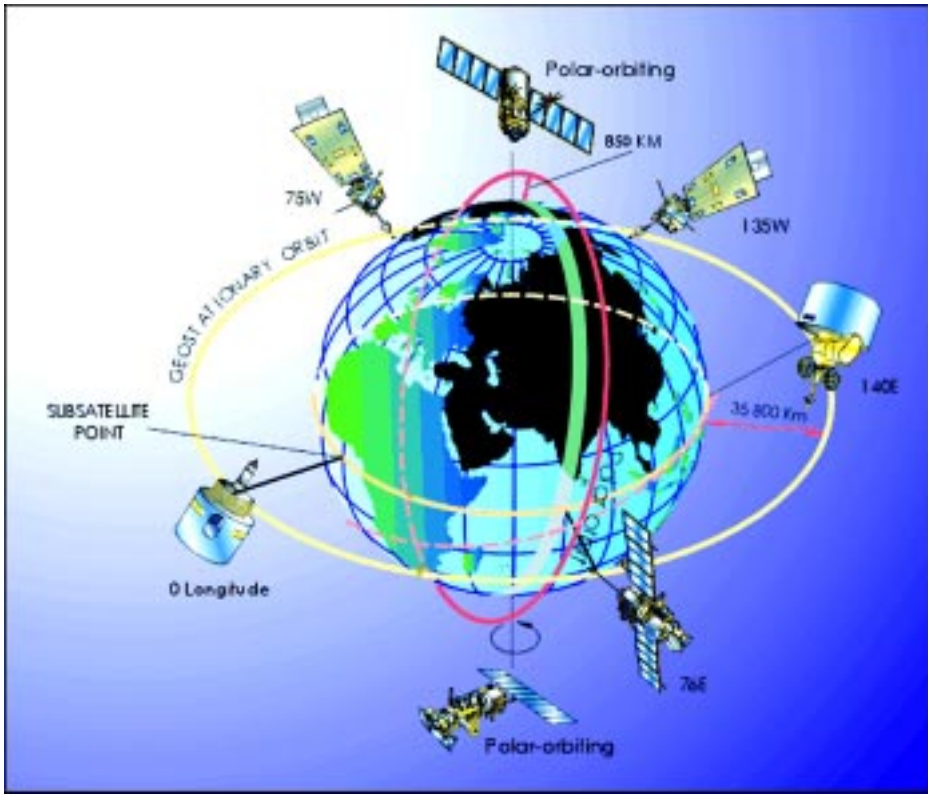

Figure 3: Nominal configuration of the space-based sub-system of the Global Observing System in 1978.

By the year 2000, WMO Members contributing to the space-based sub-system of the Global Observing System had grown. There were two major constellations in the space-based Global Observing System (GOS) (Fig. 4). One constellation was the various geostationary satellites, which operated in an equatorial belt and provided a continuous view of the weather from roughly 70°N to 70°S. The second constellation in the current space-based GOS comprised the polar-orbiting satellites operated by the Russian Federation, the USA and the People's Republic of China. The METEOR-3 series has been operated by the Russian Federation since 1991.

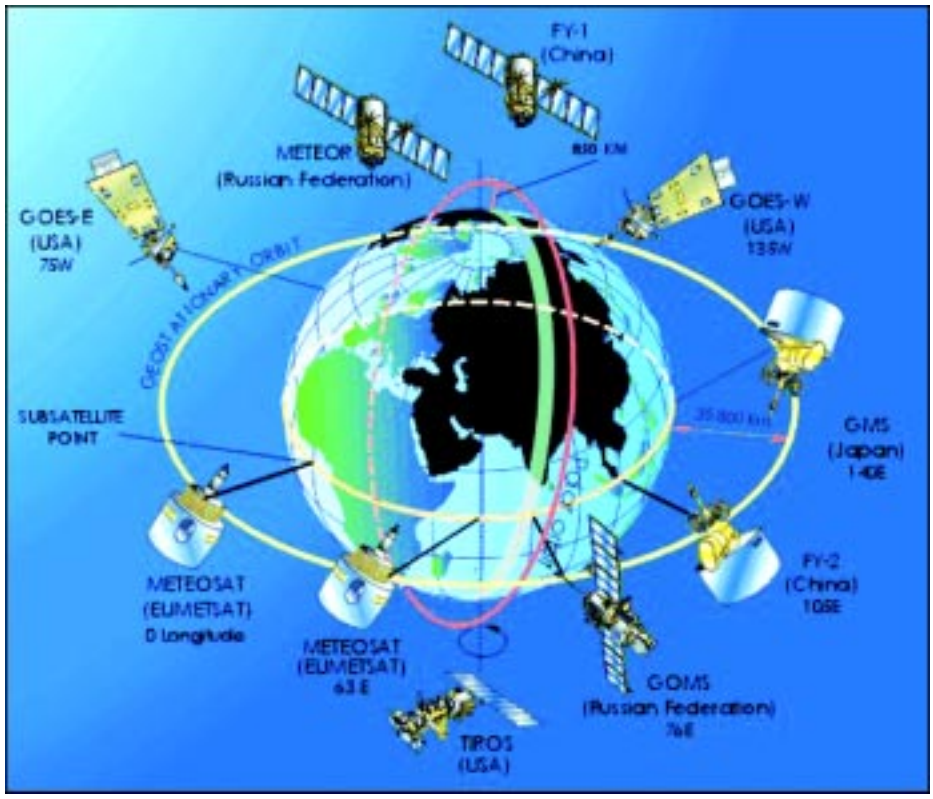

Figure 4: Nominal configuration of the space-based sub-system of the Global Observing System in 2000.

The ability of geostationary satellites to provide a continuous view of weather systems make them invaluable in following the motion, development, and decay of such phenomena. Even such short-term events such as severe thunderstorms, with a life-time of only a few hours, can be successfully recognized in their early stages and appropriate warnings of the time and area

of their maximum impact can be expeditiously provided to the general public. For this reason, its warning capability has been the primary justification for the geostationary spacecraft. Since 71 per cent of the Earth's surface is water and even the land areas have many regions which are sparsely inhabited, the polar-orbiting satellite system provides the data needed to compensate the deficiencies in conventional observing networks. Flying in a near-polar orbit, the spacecraft is able to acquire data from all parts of the globe in the course of a series of successive revolutions. For these reasons the polar-orbiting satellites are principally used to obtain: (a) daily global cloud cover; and (b) accurate quantitative measurements of surface temperature and of the vertical variation of temperature and water vapour in the atmosphere. There is a distinct advantage in receiving global data acquired by a single set of observing sensors. Together, the polar-orbiting and geostationary satellites constitute a truly global meteorological satellite network.

Satellite data provide better coverage in time and in area extent than any alternative. Most polar satellite instruments observe the entire planet once or twice in a 24-hour period. Each geostationary satellite's instruments cover about ¼ of the planet almost continuously and there are now six geostationary satellites providing a combined coverage of almost 75%. Satellites cover the world's oceans (about 70% of the planet), its deserts, forests, polar regions, and other sparsely inhabited places. Surface winds over the oceans from satellites are comparable to ship observations; ocean heights can be determined to a few centimetres; and temperatures in any part of the atmosphere anywhere in the world are suitable for computer models. It is important to make maximum use of this information to monitor our environment. Access to these satellite data and products is only the beginning. In addition, the ability to interpret, combine, and make maximum use of this information must be an integral element of national management in developed and developing countries.

The thrust of the current generation of environmental satellites is aimed primarily at characterizing the kinematics and dynamics of the atmospheric circulation. The existing network of environmental satellites, forming part of the GOS of the World Weather Watch produces real-time weather information on a regular basis. This is acquired several times a day through direct broadcast from the meteorological satellites by more than 1,300 stations located in 125 countries.

The ground segment of the space-based component of the GOS should provide for the reception of signals and DCP data from operational satellites and/or the processing, formatting and display of meaningful environmental observation information, with a view to further distributing it in a convenient form to local users, or over the GTS, as required. This capability is normally accomplished through receiving and processing stations of varying complexity, sophistication and cost.

In addition to their current satellite programmes in polar and geostationary orbits, satellite operators in the USA (NOAA) and Europe (EUMETSAT) have agreed to launch a series of joint polar-orbiting satellites (METOP) in 2005. These satellites will complement the existing global array of geostationary satellites that form part of the Global Observing System of the World Meteorological Organization. This Initial Joint Polar System (IJPS) represents a major cooperation programme between the USA and Europe in the field of space activities. Europe has invested 2 billion Euros in a low earth orbit satellite system, which will be available operationally from 2006 to 2020.

The data provided by these satellites will enable development of operational services in improved temperature and moisture sounding for numerical weather prediction (NWP), tropospheric/stratospheric interactions, imagery of clouds and land/ocean surfaces, air-sea interactions, ozone and other trace gases mapping and monitoring, and direct broadcast support to nowcasting. Advanced weather prediction models are needed to assimilate satellite information at the highest possible spatial and spectral resolutions. It imposes new requirements on the precision and spectral resolution of soundings in order to improve the quality of weather forecasts. Satellite information is already used by fishery-fleets on an operational basis. Wind and the resulting surface stress is the major force for oceanic motions. Ocean circulation forecasts require the knowledge of an accurate wind field. Wind measurements from space play an increasing role in monitoring of climate change and variability. The chemical composition of the troposphere is changing on all spatial scales. Increases in trace gases with long atmospheric residence times can affect the climate and chemical equilibrium of the Earth/ Atmosphere system. Among these trace gases are methane, nitrogen dioxide, and ozone. The chemical and dynamic state of the stratosphere influence the troposphere by exchange processes through the tropopause. Continuous monitoring of ozone and of (the main) trace gases in the troposphere and the stratosphere is an essential input to the understanding of the related atmospheric chemistry processes.

WMO SPACE PROGRAMME

The World Meteorological Organization, a specialized agency of the United Nations, has a membership of 187 states and territories (as of June 2003). Amongst the many programmes and activities of the organization, there are three areas which are particularly pertinent to the satellite activities:

- To facilitate world-wide cooperation in the establishment of networks for making meteorological, as well as hydrological and other geophysical observations and centres to provide meteorological services;

- To promote the establishment and maintenance of systems for the rapid exchange of meteorological and related information;

- To promote the standardization of meteorological observations and ensure the uniform publication of observations and statistics.

The Fourteenth WMO Congress, held in May 2003, initiated a new Major Programme, the WMO Space Programme, as a cross-cutting programme to increase the effectiveness and contributions from satellite systems to WMO Programmes. Congress recognized the critical importance for data, products and services provided by the World Weather Watch's (WWW) expanded space-based component of the Global Observing System (GOS) to WMO Programmes and supported Programmes. During the past four years, the use by WMO Members of satellite data, products and services has experienced tremendous growth to the benefit of almost all WMO Programmes and supported Programmes. The decision by the fifty-third Executive Council to expand the space-based component of the Global Observing System to include appropriate R&D environmental satellite missions was a landmark decision in the history of WWW. Congress agreed that the Commission for Basic Systems (CBS) should continue the lead role in full consultation with the other technical commissions for the new WMO Space Programme. Congress also decided to establish WMO Consultative Meetings on High-level Policy on Satellite Matters. The Consultative Meetings will provide advice and guidance on policy-related matters and maintain a high level overview of the WMO Space Programme. The expected benefits from the new WMO Space Programme include an increasing contribution to the development of the WWW's GOS, as well as to the other WMO-supported programmes and associated observing systems through the provision of continuously improved data, products and services, from both operational and R&D satellites, and

to facilitate and promote their wider availability and meaningful utilization around the globe.

The main thrust of the WMO Space Programme Long-term Strategy is:

"To make an increasing contribution to the development of the WWW's GOS, as well as to the other WMO-supported Programmes and associated observing systems (such as AREP's GAW, GCOS, WCRP, HWR's WHYCOS and JCOMM's implementation of GOS) through the provision of continuously improved data, products and services, from both operational and R&D satellites, and to facilitate and promote their wider availability and meaningful utilization around the globe".

The main elements of the WMO Space Programme Long-term Strategy are as follows:

(a) Increased involvement of space agencies contributing, or with the potential to contribute to, the space-based component of the GOS;

(b) Promotion of a wider awareness of the availability and utilization of data, products - and their importance at levels 1, 2, 3 or 4 - and services, including those from R&D satellites;

(c) Considerably more attention to be paid to the crucial problems connected with the assimilation of R&D and new operational data streams in nowcasting, numerical weather prediction systems, reanalysis projects, monitoring climate change, chemical composition of the atmosphere, as well as the dominance of satellite data in some cases;

(d) Closer and more effective cooperation with relevant international bodies;

(e) Additional and continuing emphasis on education and training;

(f) Facilitation of the transition from research to operational systems;

(g) Improved integration of the space component of the various observing systems throughout WMO Programmes and WMO-supported Programmes;

(h) Increased cooperation amongst WMO Members to develop common basic tools for utilization of research, development and operational remote sensing systems.

Coordination Group for Meteorological Satellites (CGMS)

In 1972 a group of satellite operators formed the Co-ordination of Geostationary Meteorological Satellites (CGMS) that would be expanded in the early 1990s to include polar-orbiting satellites and changed its name - but not its abbreviation - to the Co-ordination Group for Meteorological Satellites. The Co-ordination Group for Meteorological Satellites (CGMS) provides a forum for the exchange of technical information on geostationary and polar orbiting meteorological satellite systems, such as reporting on current meteorological satellite status and future plans, telecommunication matters, operations, inter-calibration of sensors, processing algorithms, products and their validation, data transmission formats and future data transmission standards.

Since 1972, the CGMS has provided a forum in which the satellite operators have studied jointly with the WMO technical operational aspects of the global network, so as to ensure maximum efficiency and usefulness through proper coordination in the design of the satellites and in the procedures for data acquisition and dissemination.

Membership of CGMS

The table of members shows the lead agency in each case. Delegates are often supported by other agencies, for example, ESA (with EUMETSAT), NASDA (with Japan) and NASA (with NOAA).

The current Membership of CGMS is:

EUMETSAT	joined 1987 currently CGMS Secretariat
India Meteorological Department	joined 1979
Japan Meteorological Agency	founder member, 1972
China Meteorological Administration	joined 1989
NOAA/NESDIS	founder member, 1972
Hydromet Service of the Russian Federation	joined 1973

WMO	joined 1973
IOC of UNESCO	joined 2000
NASA	joined 2002
ESA	joined 2002
NASDA	joined 2002
Rosaviakosmos	joined 2002

WMO, in its endeavours to promote the development of a global meteorological observing system, participated in the activities of CGMS from its first meeting. There are several areas where joint consultations between the satellite operators and WMO are needed. The provision of data to meteorological centres in different parts of the globe is achieved by means of the Global Telecommunication System (GTS) in near-real-time. This automatically involves assistance by WMO in developing appropriate code forms and provision of a certain amount of administrative communications between the satellite operators.

WMO's role within CGMS would be to state the observational and system requirements for WMO and supported programmes as they relate to the expanded space-based components of the GOS, GAW, GCOS and WHYCOS. CGMS satellite operators would make their voluntary commitments to meet the stated observational and system requirements. WMO would, through its Members, strive to provide CGMS satellite operators with operational and pre-operational evaluations of the benefit and impacts of their satellite systems. WMO would also act as a catalyst to foster direct user interactions with the CGMS satellite operators through available means such as conferences, symposia and workshops.

The active involvement of WMO has allowed the development and implementation of the operational ASDAR system as a continuing part of the Global Observing System. Furthermore, the implementation of the IDCS system was promoted by WMO and acted jointly with the satellite operators as the admitting authority in the registration procedure for IDCPs.

The expanded space-based component of the world weather watch's global observing system

Several initiatives since 2000 with regard to WMO satellite activities have culminated in an expansion of the space-based component of the Global

Observing System to include appropriate Research and Development (R&D) satellite missions. The recently established WMO Consultative Meetings on High-Level Policy on Satellite Matters have acted as a catalyst in each of these interwoven and important areas. First was the establishment of a new series of technical documents on the operational use of R&D satellite data. Second was a recognition of the importance of R&D satellite data in meeting WMO observational data requirements and the subsequent development of a set of *Guidelines for requirements for observational data from operational and R&D satellite missions.* Third have been the responses by the R&D space agencies in making commitments in support of the system design for the space-based component of the Global Observing System. And lastly has been WMO's recognition that it should have a more appropriate programme structure - a WMO Space Programme - to capitalize on the full potential of satellite data, products and services from both the operational and R&D satellites.

WMO Members' responses to the request for input for the report on the utility of R&D satellite data and products covered the full spectrum of WMO Regions as well as a good cross-section of developed and developing countries. Countries from both the Northern and Southern Hemispheres, tropical, mid- and high-latitude as well as those with coastlines and those landlocked had responded. Most disciplines and application areas including NWP, hydrology, climate, oceanography, agrometeorology, environmental monitoring and detection and monitoring of natural disasters were included.

A number of WMO Programmes and associated application areas supported by data and products from the R&D satellites. While not complete, the list included specific applications within the disciplines of agrometeorology, weather forecasting, hydrology, climate and oceanography including: monitoring of ecology, sea-ice, snow cover, urban heat island, crop yield, vegetation, flood, volcanic ash and other natural disasters; tropical cyclone forecasting; fire areas; oceanic chlorophyll content; NWP; sea height; and CO_2 exchange between the atmosphere and ocean.

WMO agreed that there was an increasing convergence between research and operational requirements for the space-based component of the Global Observing System and that WMO should seek to establish a continuum of requirements for observational data from R&D satellite missions to operational missions. WMO endorsed the *Guidelines for requirements for observational data from operational and R&D satellite missions* to provide operational users a measure of confidence in the availability of operational and R&D observational data, and data providers with an indication of its utility.

The inclusion of R&D satellite systems into the space-based component of GOS would more than double the need for external coordination mechanisms. Firstly, there will be unique coordination needs between WMO and R&D space agencies. Secondly, there will be coordination needs between operational and R&D space agencies in such areas as frequency coordination, orbit coordination including equator crossing-times, standardization of data formats, standardization of user stations. Figure 5 shows the present space-based sub-system of the Global Observing System with the new R&D constellation including NASA's Aqua, Terra, NPP, TRMM, QuikSCAT and GPM missions, ESA's ENVISAT, ERS-1 and ERS-2 missions, NASDA's ADEOS II and GCOM series, Rosaviakosmos's research instruments on board ROSHYDROMET's operational METEOR 3M Nl satellite, as well as on its future Ocean series and CNES's JASON-1 and SPOT-5.

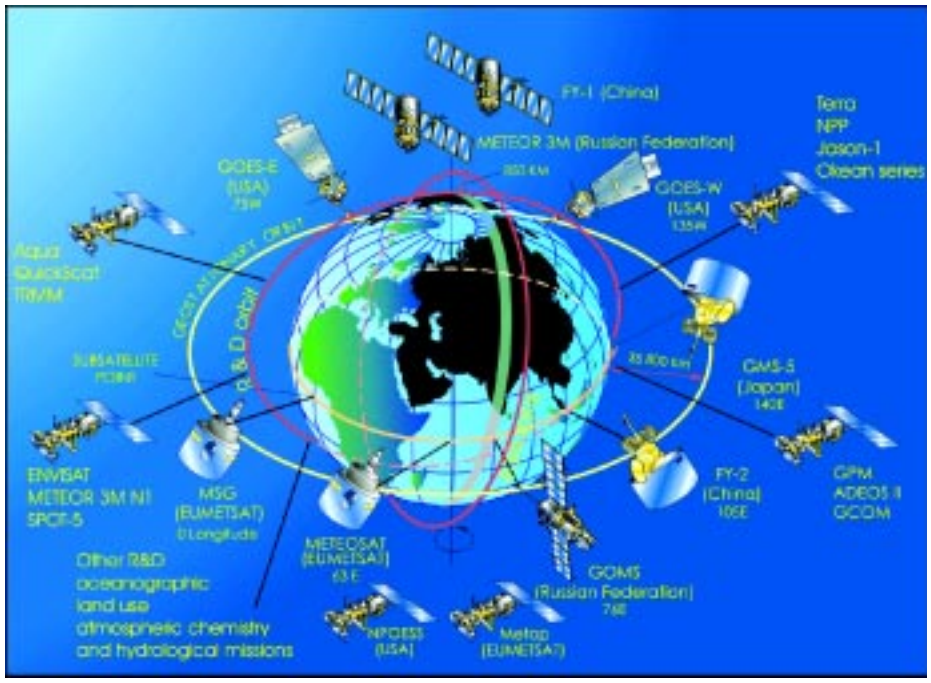

Figure 5: Space-based sub-system of the Global Observing System in 2003.

To better satisfy the needs of all WMO and supported programmes for satellite data, products and services from both operational and R&D satellites and in consideration of the increasing role of both types of satellites, WMO felt it appropriate to propose an expansion of the present mechanisms for

coordination within the WMO structure and cooperation between WMO and the operators of operational meteorological satellites and R&D satellites. In doing so, WMO felt that an effective means to improve cooperation with both operational meteorological and R&D satellite operators would be through an expanded CGMS that would include those R&D space agencies contributing to the space-based component of the GOS.

WMO agreed that the WMO satellite activities had grown and that it was now appropriate to establish a WMO Space Programme as a matter of priority. The scope, goals and objectives of the new programme should respond to the tremendous growth in the utilization of environmental satellite data, products and services within the expanded space-based component of the GOS that now include appropriate Research and Development environmental satellite missions. The Consultative Meetings on High-Level Policy on Satellite Matters should be institutionalized in order to more formally establish the dialogue and participation of environmental satellite agencies in WMO matters. In considering the important contributions made by environmental satellite systems to WMO and its supported programmes as well as the large expenditures by the space agencies, WMO felt it appropriate that the overall responsibility for the new WMO Space Programme should be assigned to CBS and a new institutionalized Consultative Meetings on High-Level Policy on Satellite Matters.

CONCLUSIONS

Recent developments in remote sensing and GIS hold much promise to enhance integrated management of all available information and the extraction of desired information to promote sustainable agriculture and development. Active promotion of the use of remote sensing and GIS in the National Meteorological and Hydrological Services (NMHSs), could enhance improved agrometeorological applications. To this end it is important to reinforce training in these new fields. The promotion of new specialised software should make the applications of the various devices easier, bearing in mind the possible combination of several types of inputs such as data coming from standard networks, radar and satellites, meteorological and climatological models, digital cartography and crop models based on the scientific acquisition of the last twenty years. International cooperation is crucial to promote the much needed applications in the developing countries and the WMO Space Programme actively promotes such cooperation throughout all WMO Programmes and provides guidance to these and other multi-sponsored programmes on the potential of remote sensing techniques in meteorology, hydrology and related

disciplines, as well as in their applications. The new WMO Space Programme will further enhance both external and internal coordination necessary to maximize the exploitation of the space-based component of the GOS to provide valuable satellite data, products and services to WMO Members towards meeting observational data requirements for WMO programmes more so than ever before in the history of the World Weather Watch.

REFERENCES

Di Chiara, C. and G. Maracchi. 1994. Guide au S.I.S.P. ver. 1.0. Technical Manual No. 14, CeSIA, Firenze, Italy.

Kleschenko, A.D. 1983. Use of remote sensing for obtaining agrometeorological information. CAgM Report No. 12, Part I. Geneva, Switzerland: World Meteorological Organization.

Kanemasu, E.T. and I.D. Filcroft. 1992. Operational remote sensing systems in agriculture. CAgM Report No. 50, Part I. Geneva, Switzerland: World Meteorological Organization.

Maracchi, G. 1991. Agrometeorologia : stato attuale e prospettive future. Proc. Congress Agrometeorologia e Telerilevamento. Agronica, Palermo, Italy, pp. 1-5.

Maracchi, G., V. Pérarnaud and A.D. Kleschenko. 2000. Applications of geographical information systems and remote sensing in agrometeorology. Agric. For. Meteorol. 103:119-136.

Romanelli, S., L. Bottai and F. Maselli. 1998. Studio preliminare per la stima del rischio d'incendio boschivo a scala regionale per mezzo dei dati satellitari e ausilari. Tuscany Region - Laboratory for Meteorology and Environmental Modelling (LaMMA), Firenze, Italy.

Seguin, B. 1992. Satellite applications to agrometeorology: technological developments for the period 1985-1989. CAgM Report No. 50, Part II. Geneva, Switzerland: World Meteorological Organization.

Seitnazarov, 1999. Technology and methods of collection, distribution and analyzing of agrometeorological data in Dashhovuz velajat, Turkmenistan. In: Contributions from members on Operational Applications in the International Workshop on Agrometeorology in the 21st Century: Needs and Perspectives, Accra, Ghana. CAgM Report No. 77, Geneva, Switzerland: World Meteorological Organization.

WMO. 1998. Preliminary statement of guidance regarding how well satellite capabilities meet WMO user requirements in several application areas, SAT-21, WMO/TD No. 913, Geneva, Switzerland: World Meteorological Organization.

WMO. 2000. Statement of guidance regarding how well satellite capabilities meet wmo user requirements in several application areas. SAT-22, WMO/TD No. 992, Geneva, Switzerland: World Meteorological Organization.

PRINCIPLES OF REMOTE SENSING

Shefali Aggarwal
Photogrammetry and Remote Sensing Division
Indian Institute of Remote Sensing, Dehra Dun

Abstract : Remote sensing is a technique to observe the earth surface or the atmosphere from out of space using satellites (space borne) or from the air using aircrafts (airborne). Remote sensing uses a part or several parts of the electromagnetic spectrum. It records the electromagnetic energy reflected or emitted by the earth's surface. The amount of radiation from an object (called radiance) is influenced by both the properties of the object and the radiation hitting the object (irradiance). The human eyes register the solar light reflected by these objects and our brains interpret the colours, the grey tones and intensity variations. In remote sensing various kinds of tools and devices are used to make electromagnetic radiation outside this range from 400 to 700 nm visible to the human eye, especially the near infrared, middle-infrared, thermal-infrared and microwaves.

Remote sensing imagery has many applications in mapping land-use and cover, agriculture, soils mapping, forestry, city planning, archaeological investigations, military observation, and geomorphological surveying, land cover changes, deforestation, vegetation dynamics, water quality dynamics, urban growth, etc. This paper starts with a brief historic overview of remote sensing and then explains the various stages and the basic principles of remotely sensed data collection mechanism.

INTRODUCTION

Remote sensing (RS), also called earth observation, refers to obtaining information about objects or areas at the Earth's surface without being in direct contact with the object or area. Humans accomplish this task with aid of eyes or by the sense of smell or hearing; so, remote sensing is day-to-day business for people. Reading the newspaper, watching cars driving in front of you are all remote sensing activities. Most sensing devices record information about an object by measuring an object's transmission of electromagnetic energy from reflecting and radiating surfaces.

Satellite Remote Sensing and GIS Applications in Agricultural Meteorology
pp. 23-38

Remote sensing techniques allow taking images of the earth surface in various wavelength region of the electromagnetic spectrum (EMS). One of the major characteristics of a remotely sensed image is the wavelength region it represents in the EMS. Some of the images represent reflected solar radiation in the visible and the near infrared regions of the electromagnetic spectrum, others are the measurements of the energy emitted by the earth surface itself i.e. in the thermal infrared wavelength region. The energy measured in the microwave region is the measure of relative return from the earth's surface, where the energy is transmitted from the vehicle itself. This is known as *active remote sensing*, since the energy source is provided by the remote sensing platform. Whereas the systems where the remote sensing measurements depend upon the external energy source, such as sun are referred to as *passive remote sensing* systems.

PRINCIPLES OF REMOTE SENSING

Detection and discrimination of objects or surface features means detecting and recording of radiant energy reflected or emitted by objects or surface material (Fig. 1). Different objects return different amount of energy in different bands of the electromagnetic spectrum, incident upon it. This depends on the property of material (structural, chemical, and physical), surface roughness, angle of incidence, intensity, and wavelength of radiant energy.

The Remote Sensing is basically a multi-disciplinary science which includes a combination of various disciplines such as optics, spectroscopy, photography, computer, electronics and telecommunication, satellite launching etc. All these technologies are integrated to act as one complete system in itself, known as Remote Sensing System. There are a number of stages in a Remote Sensing process, and each of them is important for successful operation.

Stages in Remote Sensing

- Emission of electromagnetic radiation, or EMR (sun/self- emission)
- Transmission of energy from the source to the surface of the earth, as well as absorption and scattering
- Interaction of EMR with the earth's surface: reflection and emission
- Transmission of energy from the surface to the remote sensor
- Sensor data output

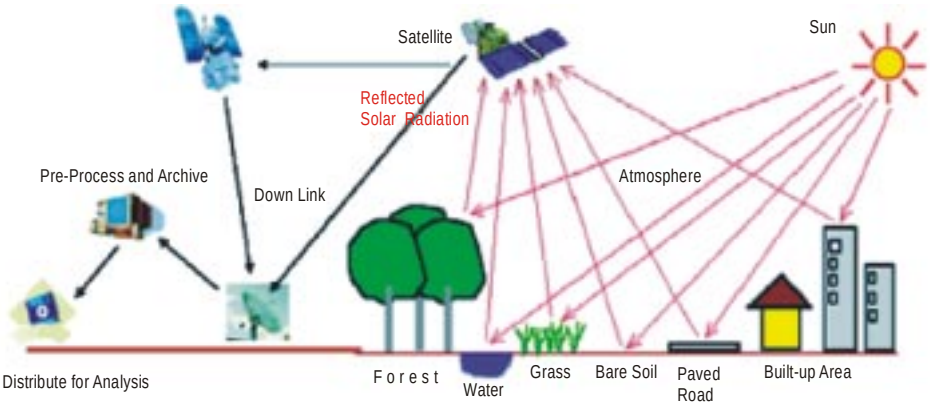

Figure 1: Remote Sensing process

- Data transmission, processing and analysis

What we see

At temperature above absolute zero, all objects radiate electromagnetic energy by virtue of their atomic and molecular oscillations. The total amount of emitted radiation increases with the body's absolute temperature and peaks at progressively shorter wavelengths. The sun, being a major source of energy, radiation and illumination, allows capturing reflected light with conventional (and some not-so-conventional) cameras and films.

The basic strategy for sensing electromagnetic radiation is clear. Everything in nature has its own unique distribution of reflected, emitted and absorbed radiation. These spectral characteristics, if ingeniously exploited, can be used to distinguish one thing from another or to obtain information about shape, size and other physical and chemical properties.

Modern Remote Sensing Technology versus Conventional Aerial Photography

The use of different and extended portions of the electromagnetic spectrum, development in sensor technology, different platforms for remote sensing (spacecraft, in addition to aircraft), emphasize on the use of spectral information as compared to spatial information, advancement in image processing and enhancement techniques, and automated image analysis in addition to manual interpretation are points for comparison of conventional aerial photography with modern remote sensing system.

During early half of twentieth century, aerial photos were used in military surveys and topographical mapping. Main advantage of aerial photos has been the high spatial resolution with fine details and therefore they are still used for mapping at large scale such as in route surveys, town planning, construction project surveying, cadastral mapping etc. Modern remote sensing system provide satellite images suitable for medium scale mapping used in natural resources surveys and monitoring such as forestry, geology, watershed management etc. However the future generation satellites are going to provide much high-resolution images for more versatile applications.

HISTORIC OVERVIEW

In 1859 Gaspard Tournachon took an oblique photograph of a small village near Paris from a balloon. With this picture the era of earth observation and remote sensing had started. His example was soon followed by other people all over the world. During the Civil War in the United States aerial photography from balloons played an important role to reveal the defence positions in Virginia (Colwell, 1983). Likewise other scientific and technical developments this Civil War time in the United States speeded up the development of photography, lenses and applied airborne use of this technology. Table 1 shows a few important dates in the development of remote sensing.

The next period of fast development took place in Europe and not in the United States. It was during World War I that aero planes were used on a large scale for photoreconnaissance. Aircraft proved to be more reliable and more stable platforms for earth observation than balloons. In the period between World War I and World War II a start was made with the civilian use of aerial photos. Application fields of airborne photos included at that time geology, forestry, agriculture and cartography. These developments lead to much improved cameras, films and interpretation equipment. The most important developments of aerial photography and photo interpretation took place during World War II. During this time span the development of other imaging systems such as near-infrared photography; thermal sensing and radar took place. Near-infrared photography and thermal-infrared proved very valuable to separate real vegetation from camouflage. The first successful airborne imaging radar was not used for civilian purposes but proved valuable for nighttime bombing. As such the system was called by the military ‘plan position indicator’ and was developed in Great Britain in 1941.

After the wars in the 1950s remote sensing systems continued to evolve from the systems developed for the war effort. Colour infrared (CIR) photography was found to be of great use for the plant sciences. In 1956 Colwell conducted experiments on the use of CIR for the classification and recognition of vegetation types and the detection of diseased and damaged or stressed vegetation. It was also in the 1950s that significant progress in radar technology was achieved.

Table1: Milestones in the History of Remote Sensing

1800	Discovery of Infrared by Sir W. Herschel
1839	Beginning of Practice of Photography
1847	Infrared Spectrum Shown by J.B.L. Foucault
1859	Photography from Balloons
1873	Theory of Electromagnetic Spectrum by J.C. Maxwell
1909	Photography from Airplanes
1916	World War I: Aerial Reconnaissance
1935	Development of Radar in Germany
1940	WW II: Applications of Non-Visible Part of EMS
1950	Military Research and Development
1959	First Space Photograph of the Earth (Explorer-6)
1960	First TIROS Meteorological Satellite Launched
1970	Skylab Remote Sensing Observations from Space
1972	Launch Landsat-1 (ERTS-1) : MSS Sensor
1972	Rapid Advances in Digital Image Processing
1982	Launch of Landsat -4 : New Generation of Landsat Sensors: TM
1986	French Commercial Earth Observation Satellite SPOT
1986	Development Hyperspectral Sensors
1990	Development High Resolution Space borne Systems
	First Commercial Developments in Remote Sensing
1998	Towards Cheap One-Goal Satellite Missions
1999	Launch EOS : NASA Earth Observing Mission
1999	Launch of IKONOS, very high spatial resolution sensor system

ELECTROMAGNETIC RADIATION AND THE ELECTROMAGNETIC SPECTRUM

EMR is a dynamic form of energy that propagates as wave motion at a velocity of c = 3 x 10^{10} cm/sec. The parameters that characterize a wave motion are wavelength (λ), frequency (ν) and velocity (c) (Fig. 2). The relationship between the above is

$$c = \nu\lambda.$$

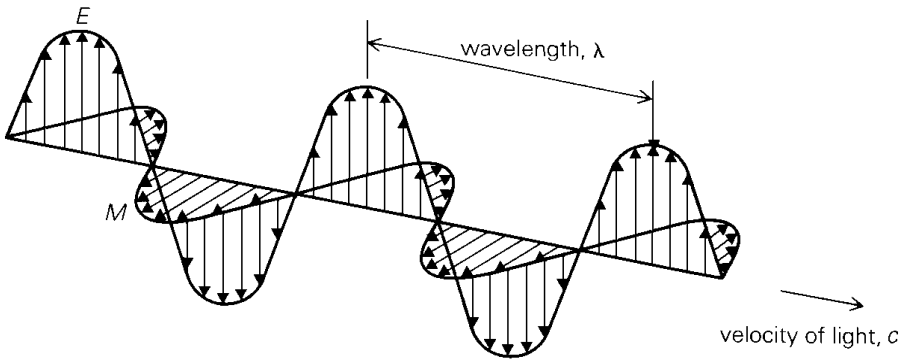

Figure 2: Electromagnetic wave. It has two components, Electric field E and Magnetic field M, both perpendicular to the direction of propagation

Electromagnetic energy radiates in accordance with the basic wave theory. This theory describes the EM energy as travelling in a harmonic sinusoidal fashion at the velocity of light. Although many characteristics of EM energy are easily described by wave theory, another theory known as particle theory offers insight into how electromagnetic energy interacts with matter. It suggests that EMR is composed of many discrete units called photons/quanta. The energy of photon is

$$Q = hc / \lambda = h \nu$$

Where

Q is the energy of quantum,

h = Planck's constant

Table 2: Principal Divisions of the Electromagnetic Spectrum

Wavelength	Description
Gamma rays	Gamma rays
X-rays	X-rays
Ultraviolet (UV) region 0.30 μm - 0.38 μm (1μm = 10^{-6}m)	This region is beyond the violet portion of the visible wavelength, and hence its name. Some earth's surface material primarily rocks and minerals emit visible UV radiation. However UV radiation is largely scattered by earth's atmosphere and hence not used in field of remote sensing.
Visible Spectrum 0.4 μm - 0.7 μm Violet 0.4 μm -0.446 μm Blue 0.446 μm -0.5 μm Green 0.5 μm - 0.578 μm Yellow 0.578 μm - 0.592 μm Orange 0.592 μm - 0.62 μm Red 0.62 μm -0.7 μm	This is the light, which our eyes can detect. This is the only portion of the spectrum that can be associated with the concept of color. Blue Green and Red are the three primary colors of the visible spectrum. They are defined as such because no single primary color can be created from the other two, but all other colors can be formed by combining the three in various proportions. The color of an object is defined by the color of the light it reflects.
Infrared (IR) Spectrum 0.7 μm – 100 μm	Wavelengths longer than the red portion of the visible spectrum are designated as the infrared spectrum. British Astronomer William Herschel discovered this in 1800. The infrared region can be divided into two categories based on their radiation properties. Reflected IR (.7 μm - 3.0 μm) is used for remote sensing. Thermal IR (3 μm - 35 μm) is the radiation emitted from earth's surface in the form of heat and used for remote sensing.
Microwave Region 1 mm - 1 m	This is the longest wavelength used in remote sensing. The shortest wavelengths in this range have properties similar to thermal infrared region. The main advantage of this spectrum is its ability to penetrate through clouds.
Radio Waves (>1 m)	This is the longest portion of the spectrum mostly used for commercial broadcast and meteorology.

Types of Remote Sensing

Remote sensing can be either passive or active. ACTIVE systems have their own source of energy (such as RADAR) whereas the PASSIVE systems depend upon external source of illumination (such as SUN) or self-emission for remote sensing.

INTERACTION OF EMR WITH THE EARTH'S SURFACE

Radiation from the sun, when incident upon the earth's surface, is either reflected by the surface, transmitted into the surface or absorbed and emitted by the surface (Fig. 3). The EMR, on interaction, experiences a number of changes in magnitude, direction, wavelength, polarization and phase. These changes are detected by the remote sensor and enable the interpreter to obtain useful information about the object of interest. The remotely sensed data contain both spatial information (size, shape and orientation) and spectral information (tone, colour and spectral signature).

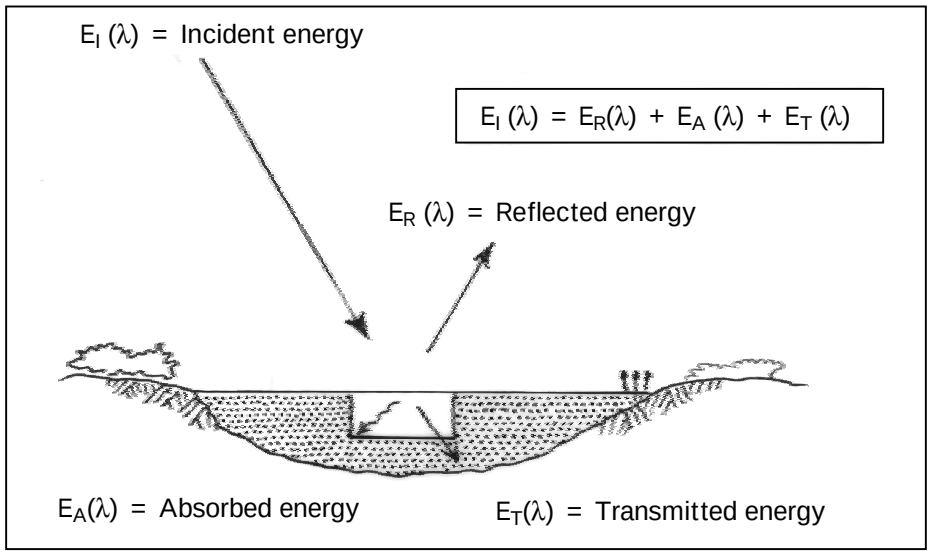

Figure 3: Interaction of Energy with the earth's surface. (source: Liliesand & Kiefer, 1993)

From the viewpoint of interaction mechanisms, with the object-visible and infrared wavelengths from 0.3 μm to 16 μm can be divided into three regions. The spectral band from 0.3 μm to 3 μm is known as the reflective region. In this band, the radiation sensed by the sensor is that due to the sun, reflected

by the earth's surface. The band corresponding to the atmospheric window between 8 μm and 14 μm is known as the thermal infrared band. The energy available in this band for remote sensing is due to thermal emission from the earth's surface. Both reflection and self-emission are important in the intermediate band from 3 μm to 5.5 μm.

In the microwave region of the spectrum, the sensor is radar, which is an active sensor, as it provides its own source of EMR. The EMR produced by the radar is transmitted to the earth's surface and the EMR reflected (back scattered) from the surface is recorded and analyzed. The microwave region can also be monitored with passive sensors, called microwave radiometers, which record the radiation emitted by the terrain in the microwave region.

Reflection

Of all the interactions in the reflective region, surface reflections are the most useful and revealing in remote sensing applications. Reflection occurs when a ray of light is redirected as it strikes a non-transparent surface. The reflection intensity depends on the surface refractive index, absorption coefficient and the angles of incidence and reflection (Fig. 4).

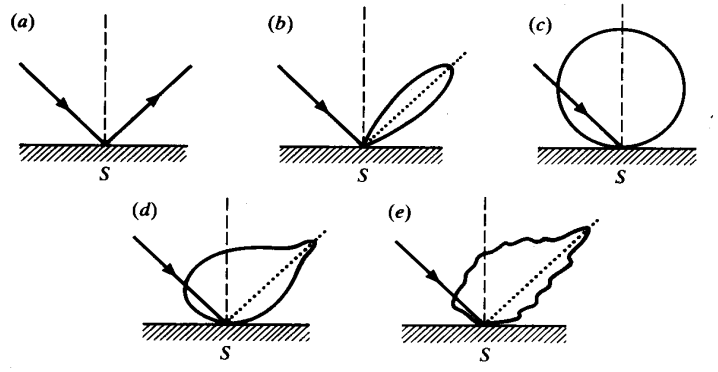

Figure 4. Different types of scattering surfaces (a) Perfect specular reflector (b) Near perfect specular reflector (c) Lambertain (d) Quasi-Lambertian (e) Complex.

Transmission

Transmission of radiation occurs when radiation passes through a substance without significant attenuation. For a given thickness, or depth of a substance, the ability of a medium to transmit energy is measured as transmittance (τ).

$$\tau = \frac{\text{Transmitted radiation}}{\text{Incident radiation}}$$

Spectral Signature

Spectral reflectance, [$\rho(\lambda)$], is the ratio of reflected energy to incident energy as a function of wavelength. Various materials of the earth's surface have different spectral reflectance characteristics. Spectral reflectance is responsible for the color or tone in a photographic image of an object. Trees appear green because they reflect more of the green wavelength. The values of the spectral reflectance of objects averaged over different, well-defined wavelength intervals comprise the spectral signature of the objects or features by which they can be distinguished. To obtain the necessary ground truth for the interpretation of multispectral imagery, the spectral characteristics of various natural objects have been extensively measured and recorded.

The spectral reflectance is dependent on wavelength, it has different values at different wavelengths for a given terrain feature. The reflectance characteristics of the earth's surface features are expressed by spectral reflectance, which is given by:

$$\rho(\lambda) = [E_R(\lambda) / E_I(\lambda)] \times 100$$

Where,

$\rho(\lambda)$ = Spectral reflectance (reflectivity) at a particular wavelength.

$E_R(\lambda)$ = Energy of wavelength reflected from object

$E_I(\lambda)$ = Energy of wavelength incident upon the object

The plot between $\rho(\lambda)$ and λ is called a spectral reflectance curve. This varies with the variation in the chemical composition and physical conditions of the feature, which results in a range of values. The spectral response patterns are averaged to get a generalized form, which is called generalized spectral response pattern for the object concerned. Spectral signature is a term used for unique spectral response pattern, which is characteristic of a terrain feature. Figure 5 shows a typical reflectance curves for three basic types of earth surface features, healthy vegetation, dry bare soil (grey-brown and loamy) and clear lake water.

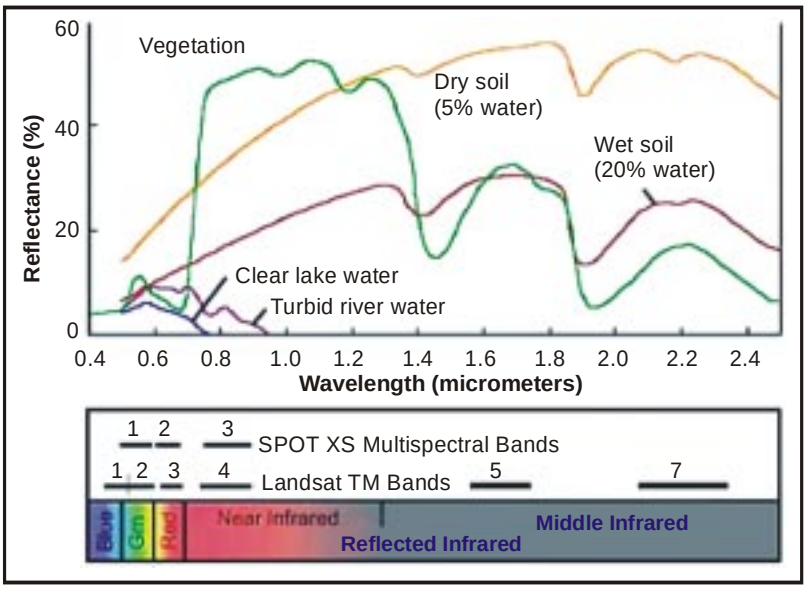

Figure 5. Typical Spectral Reflectance curves for vegetation, soil and water

Reflectance Characteristics of Earth's Cover types

The spectral characteristics of the three main earth surface features are discussed below :

Vegetation: The spectral characteristics of vegetation vary with wavelength. Plant pigment in leaves called chlorophyll strongly absorbs radiation in the red and blue wavelengths but reflects green wavelength. The internal structure of healthy leaves acts as diffuse reflector of near infrared wavelengths. Measuring and monitoring the near infrared reflectance is one way that scientists determine how healthy particular vegetation may be.

Water: Majority of the radiation incident upon water is not reflected but is either absorbed or transmitted. Longer visible wavelengths and near infrared radiation is absorbed more by water than by the visible wavelengths. Thus water looks blue or blue green due to stronger reflectance at these shorter wavelengths and darker if viewed at red or near infrared wavelengths. The factors that affect the variability in reflectance of a water body are depth of water, materials within water and surface roughness of water.

Soil: The majority of radiation incident on a soil surface is either reflected or absorbed and little is transmitted. The characteristics of soil that determine

its reflectance properties are its moisture content, organic matter content, texture, structure and iron oxide content. The soil curve shows less peak and valley variations. The presence of moisture in soil decreases its reflectance.

By measuring the energy that is reflected by targets on earth's surface over a variety of different wavelengths, we can build up a spectral signature for that object. And by comparing the response pattern of different features we may be able to distinguish between them, which we may not be able to do if we only compare them at one wavelength. For example, Water and Vegetation reflect somewhat similarly in the visible wavelength but not in the infrared.

INTERACTIONS WITH THE ATMOSPHERE

The sun is the source of radiation, and electromagnetic radiation (EMR) from the sun that is reflected by the earth and detected by the satellite or aircraft-borne sensor must pass through the atmosphere twice, once on its journey from the sun to the earth and second after being reflected by the surface of the earth back to the sensor. Interactions of the direct solar radiation and reflected radiation from the target with the atmospheric constituents interfere with the process of remote sensing and are called as "Atmospheric Effects".

The interaction of EMR with the atmosphere is important to remote sensing for two main reasons. First, information carried by EMR reflected/ emitted by the earth's surface is modified while traversing through the atmosphere. Second, the interaction of EMR with the atmosphere can be used to obtain useful information about the atmosphere itself.

The atmospheric constituents scatter and absorb the radiation modulating the radiation reflected from the target by attenuating it, changing its spatial distribution and introducing into field of view radiation from sunlight scattered in the atmosphere and some of the energy reflected from nearby ground area. Both scattering and absorption vary in their effect from one part of the spectrum to the other.

The solar energy is subjected to modification by several physical processes as it passes the atmosphere, viz.

1) Scattering; 2) Absorption, and 3) Refraction

Atmospheric Scattering

Scattering is the redirection of EMR by particles suspended in the atmosphere or by large molecules of atmospheric gases. Scattering not only reduces the image contrast but also changes the spectral signature of ground objects as seen by the sensor. The amount of scattering depends upon the size of the particles, their abundance, the wavelength of radiation, depth of the atmosphere through which the energy is traveling and the concentration of the particles. The concentration of particulate matter varies both in time and over season. Thus the effects of scattering will be uneven spatially and will vary from time to time.

Theoretically scattering can be divided into three categories depending upon the wavelength of radiation being scattered and the size of the particles causing the scattering. The three different types of scattering from particles of different sizes are summarized below:

Scattering process	Wavelength	Approximate dependence particle size	Kinds of particles
Selective			
• Rayleigh	λ^{-4}	< 1 μm	Air molecules
• Mie	λ^{0} to λ^{-4}	0.1 to 10 μm	Smoke, haze
• Non-selective	λ^{0}	> 10 μm	Dust, fog, clouds

Rayleigh Scattering

Rayleigh scattering predominates where electromagnetic radiation interacts with particles that are smaller than the wavelength of the incoming light. The effect of the Rayleigh scattering is inversely proportional to the fourth power of the wavelength. Shorter wavelengths are scattered more than longer wavelengths. In the absence of these particles and scattering the sky would appear black. In the context of remote sensing, the Rayleigh scattering is the most important type of scattering. It causes a distortion of spectral characteristics of the reflected light when compared to measurements taken on the ground.

Mie Scattering

Mie scattering occurs when the wavelength of the incoming radiation is similar in size to the atmospheric particles. These are caused by aerosols: a mixture of gases, water vapor and dust. It is generally restricted to the lower atmosphere where the larger particles are abundant and dominates under overcast cloud conditions. It influences the entire spectral region from ultra violet to near infrared regions.

Non-selective Scattering

This type of scattering occurs when the particle size is much larger than the wavelength of the incoming radiation. Particles responsible for this effect are water droplets and larger dust particles. The scattering is independent of the wavelength, all the wavelength are scattered equally. The most common example of non-selective scattering is the appearance of clouds as white. As cloud consist of water droplet particles and the wavelengths are scattered in equal amount, the cloud appears as white.

Occurrence of this scattering mechanism gives a clue to the existence of large particulate matter in the atmosphere above the scene of interest which itself is a useful data. Using minus blue filters can eliminate the effects of the Rayleigh component of scattering. However, the effect of heavy haze i.e. when all the wavelengths are scattered uniformly, cannot be eliminated using haze filters. The effects of haze are less pronounced in the thermal infrared region. Microwave radiation is completely immune to haze and can even penetrate clouds.

Atmospheric Absorption

The gas molecules present in the atmosphere strongly absorb the EMR passing through the atmosphere in certain spectral bands. Mainly three gases are responsible for most of absorption of solar radiation, viz. ozone, carbon dioxide and water vapour. Ozone absorbs the high energy, short wavelength portions of the ultraviolet spectrum ($\lambda < 0.24$ μm) thereby preventing the transmission of this radiation to the lower atmosphere. Carbon dioxide is important in remote sensing as it effectively absorbs the radiation in mid and far infrared regions of the spectrum. It strongly absorbs in the region from about 13-17.5 μm, whereas two most important regions of water vapour absorption are in bands 5.5 - 7.0 μm and above 27 μm. Absorption relatively

reduces the amount of light that reaches our eye making the scene look relatively duller.

Atmospheric Windows

The general atmospheric transmittance across the whole spectrum of wavelengths is shown in Figure 6. The atmosphere selectively transmits energy of certain wavelengths. The spectral bands for which the atmosphere is relatively transparent are known as atmospheric windows. Atmospheric windows are present in the visible part (.4 μm - .76 μm) and the infrared regions of the EM spectrum. In the visible part transmission is mainly effected by ozone absorption and by molecular scattering. The atmosphere is transparent again beyond about λ= 1mm, the region used for microwave remote sensing.

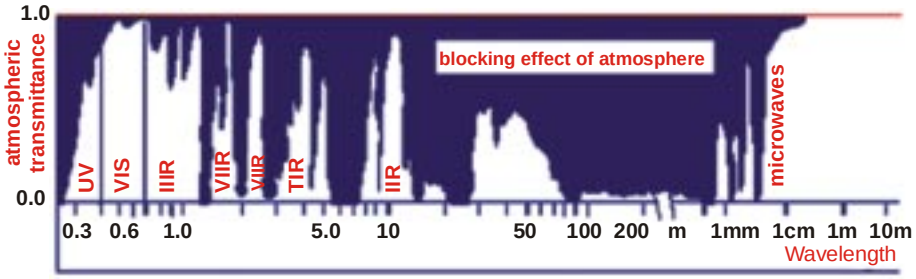

Figure 6 : Atmospheric windows

Refraction

The phenomenon of refraction, that is bending of light at the contact between two media, also occurs in the atmosphere as the light passes through the atmospheric layers of varied clarity, humidity and temperature. These variations influence the density of atmospheric layers, which in turn, causes the bending of light rays as they pass from one layer to another. The most common phenomena are the mirage like apparitions sometimes visible in the distance on hot summer days.

CONCLUSIONS

Remote sensing technology has developed from balloon photography to aerial photography to multi-spectral satellite imaging. Radiation interaction characteristics of earth and atmosphere in different regions of electromagnetic

spectrum are very useful for identifying and characterizing earth and atmospheric features.

REFERENCES

Campbell, J.B. 1996. Introduction to Remote Sensing. Taylor & Francis, London.

Colwell, R.N. (Ed.) 1983. Manual of Remote Sensing. Second Edition. Vol I: Theory, Instruments and Techniques. American Society of Photogrammetry and Remote Sensing ASPRS, Falls Church.

Curran, P.J. 1985. Principles of Remote Sensing. Longman Group Limited, London.

Elachi, C. 1987. Introduction to the Physics and Techniques of Remote Sensing. Wiley Series in Remote Sensing, New York.

http://www.ccrs.nrcan.gc.ca/ccrs/learn/tutorials/fundam/chapter1/chapter1_1_e.html

Joseph, G. 1996. Imaging Sensors. Remote Sensing Reviews, 13: 257-342.

Lillesand, T.M. and Kiefer, R.1993. Remote Sensing and Image Interpretation. Third Edition John Villey, New York.

Manual of Remote Sensing. IIIrd Edition. American Society of Photogrammtery and Remote Sensing.

Sabins, F.F. 1997. Remote Sensing and Principles and Image Interpretation. WH Freeman, New York.

EARTH RESOURCE SATELLITES

Shefali Aggarwal
Photogrammetry and Remote Sensing Division
Indian Institute of Remote Sensing, Dehra Dun

Abstract : Since the first balloon flight, the possibilities to view the earth's surface from above had opened up new vistas of opportunities for mankind. The view from above has inspired a number of technological developments that offer a wide-range of techniques to observe the phenomena on the earth's surface, under oceans, and underneath the surface of the earth. While the first imagery used for remote sensing came from balloons and later from airplanes, today the satellites or spacecraft are widely used for data collection. The uniqueness of satellite remote sensing lies in its ability to provide a synoptic view of the earth's surface and to detect features at electromagnetic wavelengths, which are not visible to the human eye. Data from satellite images can show larger areas than aerial survey data and, as a satellite regularly passes over the same area capturing new data each time, changes in the land use /land cover can be periodically monitored.

In order to use remotely sensed data, the user has to understand the characteristics of the system being used. The most important system characteristic the user has to understand is resolution. Resolution is measured in four ways, spatial, spectral, radiometric and temporal. The article describes the characteristics of satellite orbits and sensor systems, data capturing mechanisms and then highlights some of the commercially available satellites and future missions to be undertaken.

INTRODUCTION

Remote sensing is defined as the science which deals with obtaining information about objects on earth surface by analysis of data, received from a remote platform. Since the launch of the first remote sensing weather satellite (TIROS-1) in 1960 and the first Earth resources satellite in 1972 (Landsat-1), various platforms with a variety of remote sensing sensors have been launched to study the Earth land cover, the oceans, the atmosphere or to monitor the weather.

Satellite Remote Sensing and GIS Applications in Agricultural Meteorology
pp. 39-65

In the present context, information flows from an object to a receiver (sensor) in the form of radiation transmitted through the atmosphere. The interaction between the radiation and the object of interest conveys information required on the nature of the object. In order for a sensor to collect and record energy reflected or emitted from a target or surface, it must reside on a stable platform away from the target or surface being observed. Important properties of sensor system are the number of spectral bands, the spectral position of these bands, the spatial resolution or pixel size and the orbit of the satellite.

Two satellite orbits are important for remote sensing observation of the Earth: the geo-stationary orbit and the polar orbit. The geo-stationary orbit is such a position for a satellite that it keeps pace with the rotation of the Earth. These platforms are covering the same place and give continuous near hemispheric coverage over the same area day and night. These satellites are put in equatorial plane orbiting from west to east. Its coverage is limited to 70^{o}N to 70^{o}S latitudes and one satellite can view one-third globe (Figure 1). As a result it is continuously located above the same geographical position.

These are mainly used for communication and meteorological applications. Weather satellites such as Meteosat, MSG and GOES are normally positioned in this orbit. It enables the sensor aboard the satellite to take every 30 minutes a picture of the weather conditions over the same locations. This geo-stationary orbit is located at an altitude of 36,000 km above the equator.

The following are the major geo-stationary satellites:

Satellite program Launch Agency	Current Satellite	Country	Operational	Agency
METEOSAT	METEOSAT-7	International	EUMETSAT	ESA
INDOEX	METEOSAT-5	International	EUMETSAT	ESA
GOMS	GOMS-1 (ELEKTRO)	Russia		
INSAT	INSAT Series	India		
Feng-Yun*	Feng-Yun-2B	China		
GMS	GMS-5	Japan		
GOES (WEST)	GOES-10	U.S.A.	NOAA	NASA
GOES (EAST)	GOES-8	U.S.A.	NOAA	NASA

* Failed mission

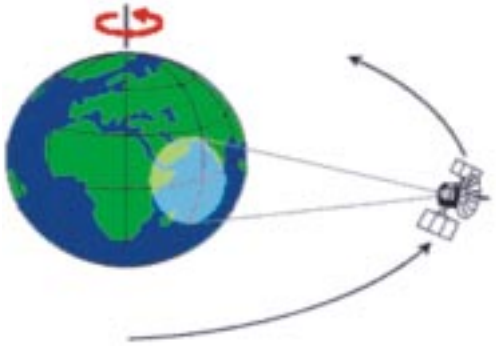

Figure 1. Geo-stationary Orbit (source CCRS website)

The second important remote sensing orbit is the polar orbit. Satellites in a polar orbit, cycle the Earth from North Pole to South Pole. The polar orbits have an inclination of approximately 99 degrees with the equator to maintain a sun synchronous overpass i.e. the satellite passes over all places on earth having the same latitude twice in each orbit at the same local sun-time. This ensures similar illumination conditions when acquiring images over a particular area over a series of days (Figure 2). Image acquisition mostly takes place in the morning when the sun position is optimal between 9.30 and 11.00 hr local time. The altitude of the polar orbits varies from approximately 650 to 900 km although spy-satellites are in a much lower orbit.

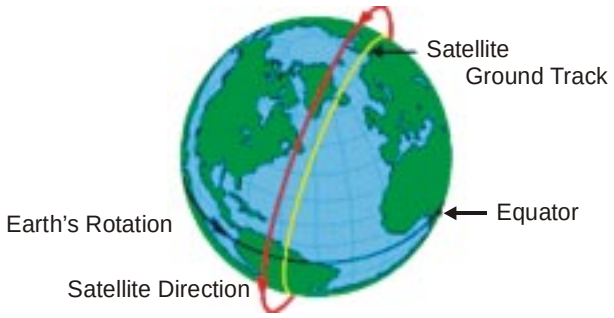

Figure 2. Near Polar Orbits (source CCRS website)

As the satellite orbits the Earth from pole to pole, its east-west position would not change if the Earth did not rotate. However, as seen from the Earth, it seems that the satellite is shifting westward because the Earth is rotating (from west to east) beneath it. This apparent movement allows the

satellite swath to cover a new area with each pass (Figure 3). The satellite's orbit and the rotation of the Earth work together to allow complete coverage of the Earth's surface, after it has completed one complete cycle of orbits (Figure 4). Through these satellites the entire globe is covered on regular basis and gives repetitive coverage on periodic basis. All the remote sensing earth resource satellites may be grouped in this category. Few of these satellites are LANDSAT series, SPOT series, IRS series, NOAA, SEASAT, TIROS, HCMM, SKYLAB, SPACE SHUTTLE etc.

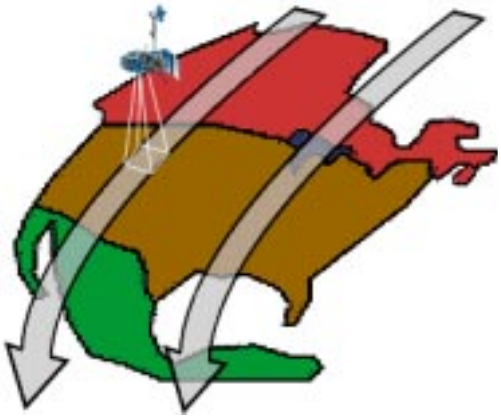

Figure 3. Area Coverage on each Consecutive pass (source: CCRS website)

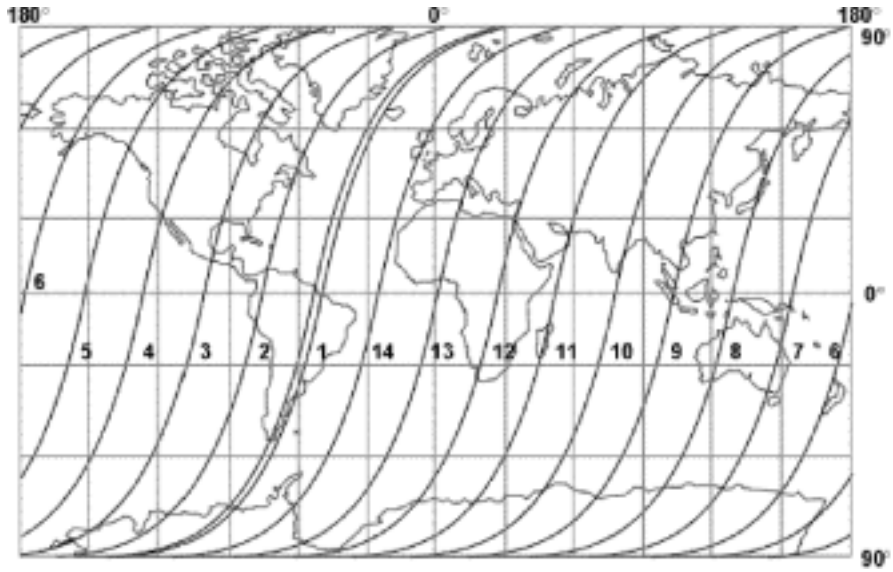

Figure 4. Complete Coverage of Earth Surface by Sun Synchronous Satellites

REMOTE SENSING SENSORS

Sensor is a device that gathers energy (EMR or other), converts it into a signal and presents it in a form suitable for obtaining information about the target under investigation. These may be active or passive depending on the source of energy.

Sensors used for remote sensing can be broadly classified as those operating in Optical-Infrared (OIR) region and those operating in the microwave region. OIR and microwave sensors can further be subdivided into passive and active.

Active sensors use their own source of energy. Earth surface is illuminated through energy emitted by its own source, a part of it is reflected by the surface in the direction of the sensor, which is received to gather the information. Passive sensors receive solar electromagnetic energy reflected from the surface or energy emitted by the surface itself. These sensors do not have their own source of energy and can not be used at nighttime, except thermal sensors. Again, sensors (active or passive) could either be imaging, like camera or sensor, which acquire images of the area and non-imaging types like non-scanning radiometer or atmospheric sounders.

Resolution

Resolution is defined as the ability of the system to render the information at the smallest discretely separable quantity in terms of distance (spatial), wavelength band of EMR (spectral), time (temporal) and/or radiation quantity (radiometric).

Spatial Resolution

Spatial resolution is the projection of a detector element or a slit onto the ground. In other words, scanner's spatial resolution is the ground segment sensed at any instant. It is also called ground resolution element (GRE).

The spatial resolution at which data are acquired has two effects – the ability to identify various features and quantify their extent. The former one relates to the classification accuracy and the later to the ability to accurately make mensuration. Images where only large features are visible are said to have coarse or low resolution. In fine resolution images, small objects can be detected.

Spectral Resolution

Spectral emissivity curves characterize the reflectance and/or emittance of a feature or target over a variety of wavelengths. Different classes of features and details in an image can be distinguished by comparing their responses over distinct wavelength ranges. Broad classes such as water and vegetation can be separated using broad wavelength ranges (VIS, NIR), whereas specific classes like rock types would require a comparison of fine wavelength ranges to separate them. Hence spectral resolution describes the ability of the sensor to define fine wavelength intervals i.e. sampling the spatially segmented image in different spectral intervals, thereby allowing the spectral irradiance of the image to be determined.

Radiometric Resolution

This is a measure of the sensor to differentiate the smallest change in the spectral reflectance/emittance between various targets. The radiometric resolution depends on the saturation radiance and the number of quantisation levels. Thus, a sensor whose saturation is set at 100% reflectance with an 8 bit resolution will have a poor radiometric sensitivity compared to a sensor whose saturation radiance is set at 20% reflectance and 7 bit digitization.

Temporal Resolution

Obtaining spatial and spectral data at certain time intervals. Temporal resolution is also called as the repetivity of the satellite; it is the capability of the satellite to image the exact same area at the same viewing angle at different periods of time. The temporal resolution of a sensor depends on a variety of factors, including the satellite/sensor capabilities, the swath overlap and latitude.

Multispectral Scanning Principle

Cameras and their use for aerial photography are the simplest and oldest of sensors used for remote sensing of the Earth's surface. Cameras are framing systems (Figure 5a), which acquire a near-instantaneous "snapshot" of an area of the Earth's surface. Camera systems are passive optical sensors that use a lens (or system of lenses collectively referred to as the optics) to form an image at the focal plane, the "aerial image plane" at which an image is sharply defined.

Many electronic (as opposed to photographic) remote sensors acquire data using scanning systems, which employ a sensor with a narrow field of view that sweeps over the terrain to build up and produce a two-dimensional image of the surface. Scanning systems can be used on both aircraft and satellite platforms and have essentially the same operating principles. A scanning system used to collect data over a variety of different wavelength ranges is called a multispectral scanner (MSS), and is the most commonly used scanning system. There are two main modes or methods of scanning employed to acquire multispectral image data - across-track scanning, and along-track scanning.

Across-track scanners scan the Earth in a series of lines (Figure 5b). The lines are oriented perpendicular to the direction of motion of the sensor platform (i.e. across the swath). Each line is scanned from one side of the sensor to the other, using a rotating mirror. As the platform moves forward over the Earth, successive scans build up a two-dimensional image of the Earth's surface. So, the Earth is scanned point by point and line after line. These systems are referred to as whiskbroom scanners. The incoming reflected or emitted radiation is separated into several spectral components that are detected independently. A bank of internal detectors, each sensitive to a specific range of wavelengths, detects and measures the energy for each spectral band and then, as an electrical signal, they are converted to digital data and recorded for subsequent computer processing.

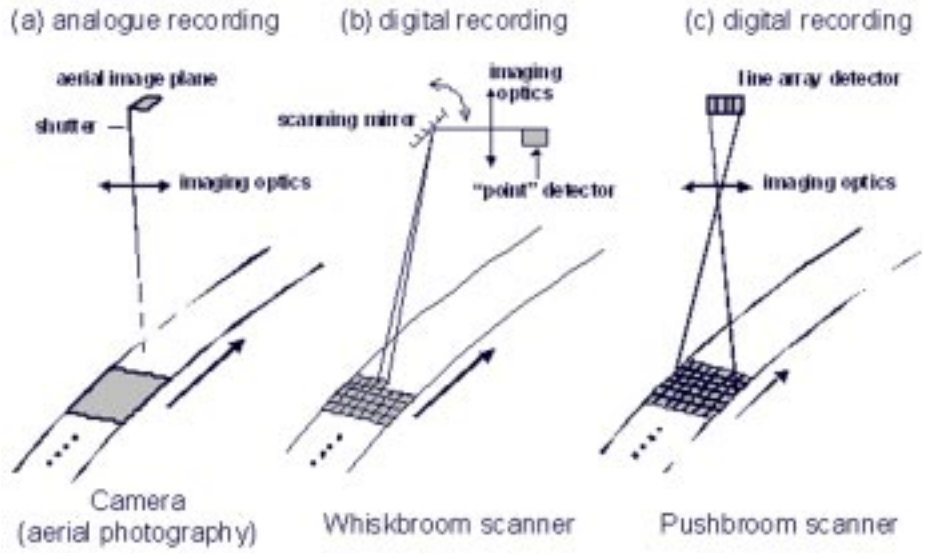

Figure 5. Principle of imaging sensor systems; (a) framing system, (b) whiskbroom scanner, (c) pushbroom scanner. (source :http://cgi.girs.wageningen-ur.nl/igi-new)

Along-track scanners also use the forward motion of the platform to record successive scan lines and build up a two-dimensional image, perpendicular to the flight direction (Figure 5c). However, instead of a scanning mirror, they use a linear array of detectors (so-called charge-coupled devices, CCDs) located at the focal plane of the image formed by lens systems, which are "pushed" along in the flight track direction (i.e. along track). These systems are also referred to as push broom scanners, as the motion of the detector array is analogous to a broom being pushed along a floor. A separate linear array is required to measure each spectral band or channel. For each scan line, the energy detected by each detector of each linear array is sampled electronically and digitally recorded.

Regardless of whether the scanning system used is either of these two types, it has several advantages over photographic systems. The spectral range of photographic systems is restricted to the visible and near-infrared regions while MSS systems can extend this range into the thermal infrared. They are also capable of much higher spectral resolution than photographic systems. Multi-band or multispectral photographic systems use separate lens systems to acquire each spectral band. This may cause problems in ensuring that the different bands are comparable both spatially and radiometrically and with registration of the multiple images. MSS systems acquire all spectral bands simultaneously through the same optical system to alleviate these problems. Photographic systems record the energy detected by means of a photochemical process which is difficult to measure and to make consistent. Because MSS data are recorded electronically, it is easier to determine the specific amount of energy measured, and they can record over a greater range of values in a digital format. Photographic systems require a continuous supply of film and processing on the ground after the photos have been taken. The digital recording in MSS systems facilitates transmission of data to receiving stations on the ground and immediate processing of data in a computer environment.

Thermal Scanner

Many multispectral (MSS) systems sense radiation in the thermal infrared as well as the visible and reflected infrared portions of the spectrum. However, remote sensing of energy emitted from the Earth's surface in the thermal infrared (3 μm to 15 μm) is different from the sensing of reflected energy. Thermal sensors use photo detectors sensitive to the direct contact of photons on their surface, to detect emitted thermal radiation. The detectors are cooled to temperatures close to absolute zero in order to limit their own thermal

emissions. Thermal sensors essentially measure the surface temperature and thermal properties of targets.

Thermal Imagers are typically across-track scanners that detect emitted radiation in only the thermal portion of the spectrum. Thermal sensors employ one or more internal temperature references for comparison with the detected radiation, so they can be related to absolute radiant temperature. The data are generally recorded on film and/or magnetic tape and the temperature resolution of current sensors can reach 0.1 °C. For analysis, an image of relative radiant temperatures is depicted in grey levels, with warmer temperatures shown in light tones, and cooler temperatures in dark tones.

Table 1. Thermal Sensors

	HCMM	TM
Operational period	1978-1980	1982 to present
Orbital altitude	620 mm	705 km
Image coverage	700 by 700 km	185 by 170 km
Acquisition time, day	1:30 p.m.	10:30 a.m.
Acquisition time, night	2:30 a.m.	9:30 p.m.
Visible and reflected IR detectors		
Number of bands	1	6
Spectral range	0.5 0 - 1.1 µm	0.4 - 2.35 µm
Ground resolution cell	500 by 500 m	30 by 30 m
Thermal IR detector		
Spectral range	10.5 - 12.5 µm	10.5 - 12.5 µm
Ground resolution cell	600 by 600 m	120 by 120m 60 m by 60 m in Landsat 7

Microwave Sensing (RADAR)

Microwave data can be obtained by both active and passive systems. Passive system monitor natural radiation at a particular frequency or range of frequency. Data may be presented numerically as line trace data or as imagery. Active systems (like SLAR and SAR) transmit their own energy and monitor the returned signal.

Characteristics of such radar imagery both in SAR and SLAR and their resolution depends on various parameters like frequency of the signal, look direction, slant range, dielectric constant of the objects, phase, antenna length etc. Spatial resolution in range and azimuth direction varies in different manners.

RADAR (SAR) imageries have been obtained from satellite SEASAT, ERS and space shuttle missions SIR-A, SIR-B and SIR-C using synthatic aperture radar, which have all weather capability. Such data products are useful for studies in cloud-covered region of the earth and in oceanography.

Table 2. Microwave Sensors

	Seasat SAR	SIR-C/X-SAR	ESA SAR	RADARSAT SAR	ENVISAT ASAR	JERS-1
Frequency	1.275 GHz	5.3 GHz 1.275 GHz	5.3 GHz	5.33 GHz	5.33 GHz	1.275 GHz
Wave length	L band 23 cm	X band 3 cm C band 6 cm L band 23 cm	C band	C band	C band	L Band (23 cm)
Swath Width	100 km, centered 20° off nadir	15 to 90 km Depend on orientation is antenna	100 km	45-510 km Varies	5 km – 100 km Varies	75 km
Ground Resolution	25 x 25 m	10 to 200 m	30 m	100x100 m to 9x9 m Varies	Varies	30 m

LAND OBSERVATION SATELLITES

Today more than ten earth observation satellites provide imagery that can be used in various applications (Table-3). The list also includes some failed as well as future missions. Agencies responsible for the distribution and trading of data internationally are also listed.

Landsat Series of Satellites

NASA, with the co-operation of the U.S. Department of Interior, began a conceptual study of the feasibility of a series of Earth Resources Technology Satellites (ERTS). ERTS-1 was launched in July 23, 1972, and it operated

until January 6, 1978. It represented the first unmanned satellite specifically designed to acquire data about earth resources on a systematic, repetitive, medium resolution, multispectral basis. It was primarily designed as an experimental system to test the feasibility of collecting earth resources data from unmanned satellites. About 300 individual ERTS-1 experiments were conducted in 43 US states and 36 nations. Just prior to the launch of ERTS-B on January 22nd 1975, NASA officially renamed the ERTS programme as the "LANDSAT" programme. All subsequent satellites in the series carried the Landsat designation. So far six Landsat satellites have been launched successfully, while Landsat-6 suffered launch failure. Table-4 highlights the characteristics of the Landsat series satellites. There have been four different types of sensors included in various combinations on these missions. These are Return Beam Vidicon camera (RBV) systems, Multispectral Scanner (MSS) systems, Thematic Mapper (TM) and Enhanced Thematic Mapper (ETM).

After more than two decades of success, the Landsat program realised its first unsuccessful mission with the launch failure of Landsat-6 on October 5, 1993. The sensor included on-board was the Enhanced Thematic Mapper (ETM). To provide continuity with Landsat -4 and -5 the ETM incorporated the same seven spectral bands and the same spatial resolutions as the TM. The ETM's major improvement over the TM was addition of an eighth panchromatic band operating in 0.50 to 0.90-µm range and spatial resolution of 15m. Landsat-7 includes two sensors: the Enhanced Thematic Mapper plus (ETM+) and the High Resolution Multispectral Stereo Imager (HRMSI).

Spot Series of Satellite

French Government in joint programme with Sweden and Belgium undertook the development of Systeme Pour l'Observation de la Terre (SPOT) program. Conceived and designed by the French Center National d'Etudes Spatiales (CNES), SPOT has developed into a large-scale international programme with ground receiving stations and data distribution outlets located in more than 30 countries. It is also the first system to have pointable optics. This enables side-to-side off-nadir viewing capabilities, and it affords full scene stereoscopic imaging from two different satellite tracks permitting coverage of the same area. SPOT-1 was retired from full-time services on December 31, 1990. The SPOT-2 satellite was launched on January 21, 1990, and SPOT-3 was launched on September 25, 1993. SPOT-4 was launched on 26 March, 1998. Characteristics of SPOT Satellites are presented in Table 5.

Table 3. Operational Earth Observation Satellites

	EUROPE		MIDDLE EAST	NORTH AMERICA			ASIA	
	France	ESA	Israel	USA		Canada	India	Japan
	SPOT1-1986 10m			LANDSAT5 -85, 30m				
	SPOT2-90 10m	ERS1-92/00 Radar		LANDSAT6-93				
	SPOT3-93/96	ERS2-95 Radar		EARLYBIRD -98	IKONOS1-99, 1m	RADARSAT-95	IRS1C-95 6m	
	SPOT4-98 10m	ENVISAT-2001Radar		LANDSAT7-99, 15m	IKONOS2 -99, 1m		IRS1D-97 6m	
			EROS A/ 1-00 2m	QUICKBIRD-01, 0.6m	ORBVIEW-01, 1m			
	SPOT5-02 3m+ HRS10		EROS B/ 1-02, 1m		ORBVIEW -02, 1m	RADARSAT -03	IRS-P6-03, 6MMSS	ALOS-03, 2.5m
	Distribution							
	SPOT IMAGING	Miscellaneous	Imagesat	SI-EOSAT, Earthwatch, Orbimage, USGS		RADARSAT	NRSA-EOSAT	JSI

Table 4. Characteristics of Landsat-1 to -7 Missions

Sensor-system	Spectral resolution (μm)	Spatial resolution (m)	Scan-width (km)	Time interval Equator	Orbital altitude	Operation period
MSS	Band 4: 0.5 - 0.6	79×79	185	18 days	918 km	Landsat 1
	Band 5: 0.6 - 0.7	79×79				23/07/1972-06/01/1978
	Band 6: 0.7 - 0.8	79×79				Landsat 2
	Band 7: 0.8 - 1.1	79×79				22/01/1975 -25/02/1982 Landsat 3 05/03/1978 - 30/11/1982
MSS	As Landsat 3					
TM	Band 1:0.45- 0.52	30×30	185	16 days	710 km	Landsat 4
	Band 2: 0.52 - 0.60	30×30				16/07/1982 - 02/1983
	Band 3:0.63 - 0.69	30×30				Landsat 5
	Band 4:0.76 - 0.90	30×30				01/03/1984 -
	Band 5:1.55 -1.75	30×30				
	Band 6:10.40-12.50	120×120				
	Band 7:2.08 - 2.35	30×30				
TM	As Landsat 4-5	30x30	185	16 days	705 km	Landsat 7
	Band 6:10.40 - 12.50	60×60				15/04/1999 -
	Panchromatic: 0.50 - 0.90	15×15				

SPOT-4 includes the additional 20m-resolution band in the mid-infrared portion of the spectrum (between 1.58 and 1.75 μm). This band is intended to improve vegetation monitoring and mineral discriminating capabilities of the data. Furthermore, mixed 20m and 10m data sets will be co-registered on-board instead of during ground processing. This will be accomplished by replacing the panchromatic band of SPOT-1, -2 and -3 (0.49 to 0.73 μm) with red band from these systems (0.61 to 0.68 μm). This band will be used to produce both 10m black and white images and 20m multispectral data. Another change in SPOT-4 is the addition of a separate wide-field-of-view, sensor called the Vegetation Monitoring Instrument (VMI).

IRS Satellite Series

The Indian Space programme has the goal of harnessing space technology for application in the areas of communications, broadcasting, meteorology and remote sensing. The important milestones crossed so far are Bhaskara-1 and 2 (1979) the experimental satellites, which carried TV Cameras and Microwave Radiometers. The Indian Remote Sensing (IRS) Satellite was the next logical step towards the National operational satellites, which directly generates resources information in a variety of application areas such as forestry, geology, agriculture and hydrology. IRS -1A/1B, carried Linear Imaging Self Scanning sensors LISS-I & LISS-II (Table 6). IRS-P2 was launched in October 1994 on PSLV-D2, an indigenous launch vehicle. IRS-1C, was launched on December 28, 1995, which carried improved sensors like LISS-III, WiFS, PAN Camera, etc. Details of IRS series platforms are given in the following section. IRS-P3 was launched into the sun synchronous orbit by another indigenous launch vehicle PSLV - D3 on 21.3.1996 from Indian launching station Sriharikota (SHAR). IRS-1D was launched on 29 September 1997 and IRS-P4 was launched on 26 – 5-1999 on-board PSLV from Sriharikota.

IRS-P4 carrying an Ocean Colour Monitor (OCM) and a Multi-frequency Scanning Microwave Radiometer (MSMR) was launched on May 26, 1999. OCM has 8 narrow spectral bands operating in visible and near-infrared bands (402-885 nm) with a spatial resolution of 360 m and swath of 1420 km. IRS-P4 OCM thus provides highest spatial resolution compared to any other contemporary satellites in the international arena during this time frame. The MSMR with its all weather capability is configured to have measurements at 4 frequencies (6.6, 10.6, 18 & 26 GHZ) with an overall swath of 1360 km. The spatial resolution is 120, 80, 40 and 40 km for the frequency bands of

Table 5. Characteristics of SPOT Satellites

Satellite Name	Launch	Sensors	Types	No. of Channels	Spectral Range (microns)	Resolution (metres)	Swath Width (km)	Revisit Time
SPOT -5	May 2002	VMI	Multi-spectral	4	0.43-0.47 (blue) 0.61-0.68(red) 0.78-0.89(NIR) 1.58-1.75(SWIR)	1000	600 x 120	1 day
		HRS	Multi-spectral	4	0.5-0.59 (green) 0.61-0.68 (red) 0.79-0.89 (NIR) 1.58-1.75 (SWIR)	10 10 10 20	60	26 days
		HRG	Pan	1	0.61-0.68	5 m, combined to generate a 2.5 metre product.	60	
			Pan	1	0.61-0.68	10 m (re-sampled at every 5 m along track)	60	
SPOT-4	March 24, 1998	VMI	Multi-spectral	4	4	Same as SPOT 4	I000	26 days
		HRV	Multi-spectral	4	0.5-0.59 (green) 0.61-0.68 (red) 0.79-0.89 (NIR) 1.58-1.75 (SWIR)	20	60	
			Pan	1	0.61-0.68	10	60	

contd...

Satellite Name	Launch	Sensors	Types	No. of Channels	Spectral Range (microns)	Resolution (metres)	Swath Width (km)	Revisit Time
SPOT-2 & 3	1990 & March 1998	HRV	Multi-spectral	3	0.5-0.59 0.61-0.68 0.79-0.89	20	60	26 days
			Pan	1	0.51-0.73	10	60	
SPOT-1	1986	HRV	Multi-spectral	3	Same as SPOT 2	20	-do-	26 days
			Pan	1	-do-	10	-do-	

Table 6. Characteristics of IRS series Satellites

Satellite Name	Launch	Sensors	Types	No. of Bands	Spectral Range (microns)	Resolution (metres)	Swath Width (km)	Revisit Time
IRS-P4 (Oceansat)	May 26, 1999	OCM	Multi-spectral	8	0.4 - 0.885	360 m	1420 km	2 days
		MSMR	RADAR	4	6.6,10.65, 18, 21 GHz	120, 80, 40 and 40 kms	1360 km	
IRS-1D	September, 1997	WiFS	Multispectral	2	0.62-0.68 (red)	189	774	5 day
					0.77-0.86 (NIR)			
		LISS-III	Multispectral	3	0.52-0.59 (green)	23	142	24-25 days
					0.62-0.68 (red)			
					0.77-0.86 (NIR)			
				1	1.55-1.70 (SWIR)	70	148	
		PAN	PAN	1		6	70	
IRS-1C	1995	WiFS	Multispectral	2	0.62-0.68 (red)	189	810	5 day
					0.77-0.86 (NIR)			
		LISS-III	Multispectral	3	0.52-0.59 (green)	23.6	142	24-25 days
					0.62-0.68 (red)			
					0.77-0.86 (NIR)			
				1	1.55-1.70 (SWIR)	70.8	148	
		PAN	PAN	1		5.8	70	

contd...

Satellite Name	Launch	Sensors	Types	No. of Bands	Spectral Range (microns)	Resolution (metres)	Swath Width (km)	Revisit Time
IRS-1B	1991	LISS-I	Multispectral	4	450-520 0.52-0.59 0.62-0.68 0.77-0.86 (NIR)	72.5	148	22 days
IRS-1A	1988	LISS-II	Multispectral	4	(same as LISS I)	36.25	74	22 days
		LISS-I	Multispectral	4	Same as above	72.5	148	
		LISS-II	Multispectral	4	Same as above	36.25	74	

6.6., 10.6, 18 and 21 GHz. MSMR will also be in a way a unique sensor as no other passive microwave radiometer is operational in the civilian domain today and will be useful for study of both physical oceanographic and meteorological parameters.

FUTURE INDIAN SATELLITE MISSIONS

Encouraged by the successful operation of the present IRS missions, many more missions have been planned for realization in the next few years. These missions will have suitable sensors for applications in cartography, crop and vegetation monitoring, oceanography and atmospheric studies.

CARTOSAT-1:

It will have a cutting-edge technology in terms of sensor systems and will provide state-of-art capabilities for cartographic applications. The satellite will have only a PAN camera with 2.5 m resolution and 30 km swath and Fore-Aft stereo capability. The 2.5 m resolution data will cater to the specific needs of cartography and terrain modeling applications.

RESOURCESAT-1:

Launched on 17th October, 2003, it is designed mainly for resources applications and having 3-band multi-spectral LISS-4 camera with a spatial resolution 5.8m and a swath of around 24 km with across – track steerability for selected area monitoring. An improved version of LISS-III, with 4 bands (green, red, near—IR and SWIR), all at 23.5 meters resolution and 140 km swath will also provide the much essential continuity to LISS-III. These payloads will provide enhanced data for vegetation applications and will allow multiple crop discrimination; species level discrimination and so on. Together with an advanced wide-field sensor, WiFS with ~ 60 m resolution and ~ 740 km swath, the payloads will aid greatly for crop and vegetation applications and integrated land and water applications. The data will also be useful for high accuracy resources management applications, where the emphasis is on multi crop mapping studies, vegetation species identification and utilities mapping.

CLIMATSAT/OCEANSAT-2:

In order to meet the information requirements to study the Planet Earth as an integrated system, satellite missions are planned which would enable

global observations of climate, ocean and the atmosphere, particularly covering the tropical regions, where sufficient data sets are not available. The instruments like radiometers, sounders, spectrometers etc. for studying the land, ocean and atmospheric interactions are being planned for these missions.

OTHER COMMERCIALLY AVAILABLE SATELLITES

IKONOS:

The IKONOS-2 satellite was launched in September 1999 and has been delivering commercial data since early 2000. IKONOS is the first of the next generation of high spatial resolution satellites. IKONOS data records 4 channels of multispectral data at 4 m resolution and one panchromatic channel with 1 m resolution (Table 7). This means that IKONOS is first commercial satellite to deliver near photographic quality imagery of anywhere in the world from space. Radiometric Resolution: Data is collected as 11 bits per pixel (2048 gray tones).

The applications for this data are boundless: in particular, it will be used for large scale mapping, creating precise height models for e.g. micro-cellular radio, and for every application requiring the utmost detail from areas which are inaccessible for aerial photography.

ENVISAT:

Envisat launched on 1st March 2002 is the most powerful European Earth-observation satellite. Envisat is a key element of the European Space Agency's plans for the next decade to monitor Earth's environment. It carries instruments to collect information that will help scientists to understand each part of the Earth system and to predict how changes in one part will affect others (Table 8). It is in a Sun synchronous orbit at an altitude of 800 km and carrying 10 instruments onboard.

Variety of earth resources satellites are currently commercially available for inventorying and monitoring earth resources. These satellites are characterised by varying spatial, spectral, radiometric and temporal resolutions (Table 9).

Table 7. Characteristic of IKONOS Satellite

Satellite Name	Launch	Sensors	Types	No. of Bands	Spectral Range (microns)	Resolution (metres)	Swath Width (km)	Revisit Time
IKONOS-2	September 24, 1999	IKONOS	Multi-spectral	4	0.45-0.52 (blue)	4		11 days
					0.52-0.60 (green)			
					0.63-0.69 (red)			
					0.76-0.90 (NIR)			
			PAN	1		1		

Table 8. Envisat's Instrument
(source: www.esa.int/export/esasa/ESADTOMBAMC_earth_O.html)

Instrument	Main purpose
Global ozone monitoring by occultation of stars (GOMOS)	To observe the concentration of ozone in the stratosphere.
Scanning Imaging Absorption Spectrometer for Atmospheric Cartography (SCIAMACHY)	To measure trace gases and aerosol concentrations in the atmosphere.
Michelson interferometer for passive atmospheric sounding (MIPAS)	To collect information about chemical and physical processes in the stratosphere, such as those that will affect ozone concentration in future.
Medium resolution imaging Spectrometer (MERIS)	Measures radiation in 15 frequency bands that give information about ocean biology, marine water quality, and vegetation on land, cloud and water vapor.
Advanced synthetic aperture Radar (ASAR)	All weather, day or night radar imaging.
Advanced along track scanning radiometer (AATSR)	To measure sea-surface temperature, a key parameter in determining the existence and/or extent of global warming.
Radar Altimeter (RA-2)	Measures distance from satellite to Earth. So can measure sea-surface height, an important measurement for monitoring El Nino, for example.
Microwave radiometer (MWR)	Allows corrections to be made to radar altimeter data.
Doppler Orbitography and Radio positioning integrated by satellite (DORIS)	Gives the position of Envisat in its orbit to within a few centimeters. This is crucial to understanding the measurements all the instruments make.
Laser retro-reflector (LRR)	Reflects pulsed laser to ground stations to help determine the satellite's exact position in its orbit.

Table 9. Characteristics of some more commercially available satellites

Satellite Name	Launch	Sensors	Types	No. of Bands	Spectral Range (microns)	Resolution (metres)	Swath Width (km)	Revisit Time
QuickBird-2	Oct. 18, 2001		Multi-spectral	4	blue (0.45-0.52)	2.5	17	
					green (0.52-0.6)			
					red (0.63-0.69)			
					NIR.(76-0.89)			
			Pan	1	0.45-0.9	0.61		
EROS 1	Dec. 5, 2000		Pan	1	0.5-0.9	1.8	12.5	1-4 days
EO 1	Nov. 21, 2000	ALI	Multi	9	0.433-0.453			
					0.45-0.515			
					0.525-0.605			
					0.63-0.69			
					0.775-0.805			
					0.845-0.89			
					1.2-1.3			
					1.55-1.75			
					2.08-2.35	30	37	16 days
			Pan	1	0.48-0.69	10		
		Hyperion	Hyper	220	0.4 to 2.5 (10nm sampling interval)	30	7.5 km x 100 km	

contd...

Satellite Name	Launch	Sensors	Types	No. of Bands	Spectral Range (microns)	Resolution (metres)	Swath Width (km)	Revisit Time
		LAC	Hyper	256	0.9-1.6 (2-6nm sampling interval)	250	185 km	
Terra (EOS AM-1)	Dec. 18, 1999	ASTER	Multi	3	VNIR - stereo (0.5-0.9)	15	60	16 days
				6	SWIR (1.6-2.5)	30		
				5	TIR (8-12)	90		
		CERES	Multi	3	SWIR, TIR, Total	20 km		
		MISR	Multi	4		250-275	360	
		MODIS	Multi	2	0.4-14.4	250	2330	
				5		500		
				29		1000		
		MOPITT	Multi	3	2.3 (CH4)	22 km	640	
					2.4 (CO)			
					4.7 (CO)			
CBERS	October 14, 1999	WFI	Multi	2	0.66 (green)	260	890	5 days
					0.83 (NIR)			
		CCD (stereo)	Multi	5	0.51-0.73 (pan)	20	113	26 days
					0.45-0.52 (blue)			
					0.52-0.59 (green)			
					0.63-0.69 (red)			
					0.7-0.89 (NIR)			

contd...

Satellite Name	Launch	Sensors	Types	No. of Bands	Spectral Range (microns)	Resolution (metres)	Swath Width (km)	Revisit Time
		IR-MSS	Multi	4	0.5-1.1 (pan) 1.55-1.75 (IR) 2.08-2.35 (IR) 10.4-12.5 (TIR)	80 160	120	
KITSAT-3	May 26, 1999	CCD	Multi	3	red, green, NIR	15		
			Pan	1		15		
NOAA-K	May - 1998	AVHRR	Multi	5		1100		
OrbView-2	August, 1997	SeaWiFS	Multi	8	0.402-0.422 0.433-0.453 0.48-0.5 0.50-0.52 0.545-0.565 0.66-0.68 0.745-0.785 0.845-0.885	1130	2,800	1 day
RADARSAT	November, 1995	SAR	Radar	1	C-band (HH polarization)	8-120		24 days
ERS-2	1995	AMI	Radar	1	5.3 GHz(C-band)	26	99	35 days
		ATSR	Multi	4		1000		

contd...

Satellite Name	Launch	Sensors	Types	No. of Bands	Spectral Range (microns)	Resolution (metres)	Swath Width (km)	Revisit Time
NOAA-14	1994	AVHRR	Multi	5		1100		
RESURS-O1-3	1994	MSU-SK	Multi	4	0.5-0.6 (green)	170	600	21 days
					0.6-0.7 (red)			
					0.7-0.8 (NIR)			
					0.8-1.1 (NIR)			
				1	10.4-12.6 (Thermal IR)	600		
JERS-1	February, 1992	SAR	Radar	1	1275 MHz (L-band, HH polarization)	18	75	44 days
		OPS	Multi	3	Visible NIR	18 x 24	75	
				4	SWIR			
ERS-1	1991	AMI	Radar	1	C band (VV polarization)	26		35 days
		ATSR	Multi	4		1000		
NOAA-12	1991	AVHRR	Multi	5		1100		

CONCLUSIONS

Since the launch of first earth resource satellite in 1972, various satellite platforms with a variety of remote sensing sensors have been launched to study the earth, the ocean, the atmosphere and the environment. These earth resources satellites data are very useful for mapping and monitoring natural resources and environment at various levels, such as global, regional, local and micro level.

REFERENCES

Campbell, J.B. 1996. Introduction to Remote Sensing. Taylor & Francis, London.

Curran, P.J. 1985. Principles of Remote Sensing. Longman Group Limited, London.

Elachi C. 1987. Introduction to the Physics and Techniques of Remote Sensing. Wiley Series in Remote Sensing, New York.

http://www.ccrs.nrcan.gc.ca/ccrs/learn/tutorials/fundam/chapter1/chapter1_2.

http://www.ersc.edu/resources/EOSC.html

Joseph, G. 1996. Imaging Sensors for Remote Sensing. *Remote Sensing Reviews*, 13: 257-342.

Lillesand, T.M. and Kiefer, R. 1993. Remote Sensing and Image Interpretation, Third Edition. John Villey, New York.

www.planetary.brown.edu/arc/sensor.html

www.spaceimage.com

www.eospso.gfc.nasa.gov

www.landsat.org

www.spotimage.fr/home

www.space.gc.ca

www.esa.int/export/esasa/ESADTOMBAMC_earth_O.html

METEOROLOGICAL SATELLITES

C.M. Kishtawal
Atmospheric Sciences Division
Meteorology and Oceanographic Group
Space Application Centre (ISRO), Ahmedabad

Abstract : The paper presents a general overview of satellite systems and characteristics of different satellite orbits viz. polar, and geostationary orbits. Various classifications of satellite sensors e.g. imaging/non-imaging, optical/microwave, and passive/active were discussed with appropriate examples. The basic concept of satellite remote sensing based on the laws of radiation, and terrestrial absorption spectrum are presented in the first part of the article. Observations from two operational satellite sensors viz. NOAA-AVHRR, and INSAT-VHRR are discussed in more detail and with ample examples.

INTRODUCTION

Meteorology is a discipline concerned with observational earth sciences and theoretical physics. From a theoretical point of view, it has to deal with a turbulent fluid whose behaviour is governed by a complex set of nonlinear, partial differential equations, which model the atmosphere as thermo-hydrodynamical system obeying the laws of an ideal gas. As a branch of observational earth sciences, it has the task of providing an accurate knowledge of the state of the atmosphere, which can only be obtained through regular, simultaneous observations covering the whole globe from the earth surface to the upper atmosphere.

Progress on the observational side other than the surface was recently limited to a network of balloon sounding stations covering practically the whole globe, albeit sparsely. The data obtained through this network permitted the discovery of previously unknown characteristics of the atmospheric motions and provided for the first time a solid basis for work for the theoreticians. Since the introduction of mathematical models and high-speed computers,

Satellite Remote Sensing and GIS Applications in Agricultural Meteorology
pp. 67-79

there has been a growing demand for adequately sampled (in space and time) and reliable observational data, since the forecast models are strongly dependent on assumed initial state of the atmosphere, as there are large areas without any conventional soundings of the atmosphere.

Before the advent of weather satellites the weathermen had been severely handicapped by having only a very limited knowledge of the state of the atmosphere at any given time. Even with the expansion of observational networks since the last world war, by various national meteorological services, the vast sparsely populated land areas of the globe and the large oceanic areas are virtually blank as far as conventional meteorological observations are concerned. Meteorological satellites have to a large extent has enabled to overcome this deficiency.

Satellite imagery is an invaluable source of information for operational forecasters. It is being used as (a) an analysis tool, especially to data sparse regions like the tropics; (b) direct aid to short period forecasts (6-12 hours ahead of cloud, rainfall, floods etc.; (c) input to numerical weather prediction models (NWP) for defining initial condition; (d) monitoring the model forecast. It also serves as a valuable indicator of dynamical and physical process at work providing the trained eye, some useful clues on atmosphere structure and its evolution. The sea-surface temperature, the sea surface/upper air winds from scatterometer/cloud motion vectors provide valuable input to numerical models. The rainfall from geostationary satellites, rain rate from microwave sensors, the OLR (Outgoing Longwave Radiation) from polar orbiting satellites are a few parameters which are frequently utilized in the initialization of the data for numerical weather prediction of monsoon.

METEOROLOGICAL SATELLITES REQUIREMENTS

a) To serve as an observing platform with appropriate sensors on board and transmitting the information (imaging & sounding) to the stations located on the earth's surface

b) To serve as a collector of meteorological data from unmanned land/ocean based instruments - Data collection platforms

c) To serve as a communication satellite for rapid exchange of meteorological data among centres and for rapid dissemination of weather forecasts, warnings etc. to user agencies.

TYPES OF METEOROLOGICAL SATELLITES

Meteorological satellites are of two types viz. Polar orbiting and Geostationary (Fig. 1). Polar orbiting satellites pass approximately over the poles at a height of about 850 kms. The whole surface of the earth is observable by these satellites which follow orbits nearly fixed in space while the earth is rotating beneath them. The areas scanned on each pass (swath) are nearly adjacent at the equator with overlapping areas further poleward. The swaths are usually about 2600 km wide. These satellites complete 14 orbits per day and thus can provide global coverage twice in 24 hours. Some of the polar orbiting satellites are NOAA, IRS, ERS-1 &ERS-2, TRMM(low inclination), DMSP, Oceansat-1 etc.

Geostationary satellites orbit around the earth over the equator at a height of about 36000 kms. They complete one orbit in 24 hours synchronised with earth's rotation about its own axis. Thus they remain over the same location on the equator. The main advantage of geostationary satellites lies in the high time-scale resolution of their data. A fresh image of the full earth's disc is available every 30 minutes. However they have limited spatial resolution as compared to the polar orbiting satellites in view of their distance from the earth. Useful information is restricted to the belt between 70 deg. N and south latitudes. Some of the examples of geostationary satellites are GMS(140^0 E), GOES-W, GOES-E, INSAT-1 and INSAT-2 Series., GEOS, METEOSAT -5 (Positioned at 64^0 E), METEOSAT-6 etc.

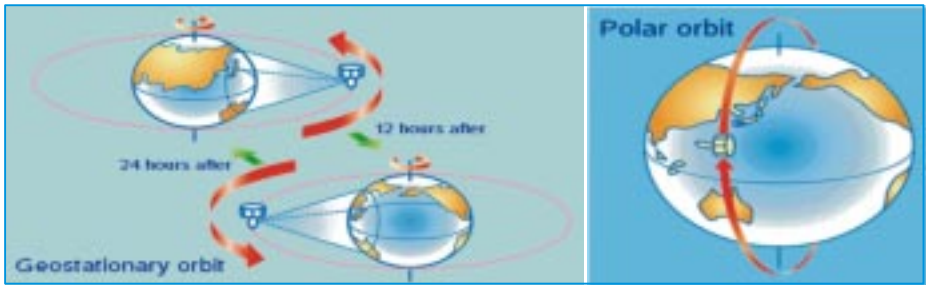

Figure 1 : Geostationary and Polar orbits

Satellite Sensor System

Most remote sensing instruments (sensors) are designed to measure photons. The fundamental principle underlying sensor operation centers on what happens in a critical component - the detector. This is the concept of

the *photoelectric effect* (for which Albert Einstein, who first explained it in detail, won his Nobel Prize). This, simply stated, says that there will be an emission of negative particles (electrons) when a negatively charged plate of some appropriate light-sensitive material is subjected to a beam of photons. The electrons can then be made to flow from the plate, collected, and counted as a signal. A key point: The magnitude of the electric current produced (number of photoelectrons per unit time) is directly proportional to the light intensity. Thus, changes in the electric current can be used to measure changes in the photons (numbers; intensity) that strike the plate (detector) during a given time interval. The kinetic energy of the released photoelectrons varies with frequency (or wavelength) of the impinging radiation. But, different materials undergo photoelectric effect release of electrons over different wavelength intervals; each has a threshold wavelength at which the phenomenon begins and a longer wavelength at which it ceases. Meteorological satellite sensors can be broadly classified as two types : passive and active (Fig. 2). Passive sensors do not use their own source of electromagnetic illumination, and depend upon the radiation emitted or reflected from the object of interest. On the other hand, active instruments use their own source of electromagnetic radiation which they use to illuminate the target, and in most cases use the properties of reflected radiation (e.g. intensity, polarization, and time delay etc.) to deduce the information about the target. These sensors can be further sub-divided into the following categories and subcategories :

Equally important is the functional classification of these sensors. Meteorological satellite sensors may be deployed to obtain one and/or more of the following characteristics of different objects of the land-ocean-atmosphere system :

(a) Spatial Information : The examples are the extent and temperature of sea surface, clouds, vegetation, soil moisture, etc. The main objective here is to obtain the required information over a 2-dimensional plane. The best suited sensors for this class are imaging radiometers operating in visible, infrared or microwave frequencies. Active sensors like Synthetic Aperture Radar (SAR) are also put to effective use for the imaging applications.

(b) Spectral Information : For certain applications, the spectral details of an electromagnetic signal are of crucial importance. A particular object of interest, for example an atmospheric layer, or, the ocean surface, interacts differently with different wavelengths of electromagnetic(EM) spectra. In most cases, this may be due to the chemical composition of the object.

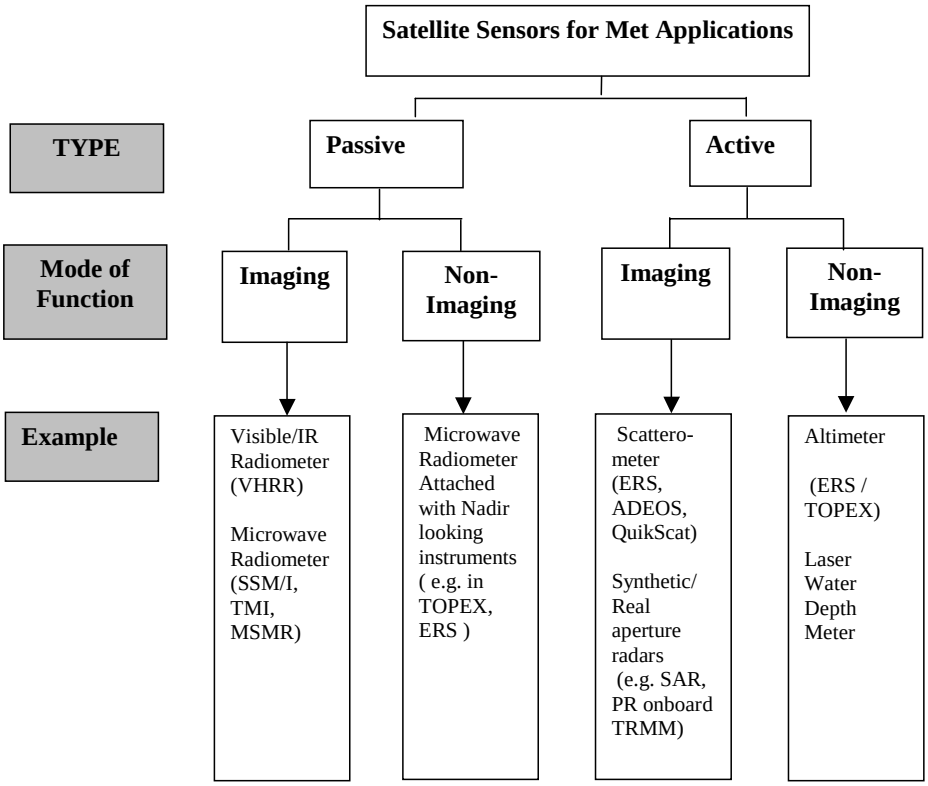

Figure 2 : Satellite sensors for Meteorological applications

Absorption, emission, or reflection of an EM radiation from an object is a function of the wavelength of EM radiation, and the temperature of the object. Thus, the spectral information can provide details of chemical composition, and/or the temperature of the object. Meteorological satellite sensors use this information for sounding applications, where the vertical structure of temperature, humidity, and in some cases, the atmospheric gases is retrieved. An example of this sensor is High Resolution IR Sounder (HIRS), and Advance Microwave Sounding Unit (AMSU) onboard NOAA series of satellites. Future satellites will carry more advanced sensors like imaging spectrometers. Geostationary Imaging Fourier Transform Spectrometer (GIFTS) is a fine example of this new-generation sensor. GIFTS, when operational, is expected to provide the vertical profiles of temperature, humidity, and winds at several atmospheric layers in vertical.

(c) Intensity Information : The intensity of EM radiation can provide several clues about the object of interest. In most cases, the satellite sensors

measure the intensity of the radiation reflected from the object to know the dielectric properties and the roughness of the object. By the use of suitable algorithms these parameters can be translated to the properties of geophysical parameters like soil moisture, ocean surface roughness, ocean surface wind speed, and wind direction, etc. The sensors that use this information are radar, scatterometer, and polarimeters.

PRINCIPLES OF SATELLITE REMOTE SENSING

All objects emit electromagnetic radiation. The hotter the source, the greater is the intensity of emission. Substances which absorb all the radiation falling on them at every wavelength are called "black bodies". The coefficient of absorption is then unity. As per Kirchhoff's law, good absorbers are good emitters as well. Hence a black body also has an emissivity unity. At any wavelength it emits the maximum amount of radiation that is appropriate to its temperature.

Most substances, however, are not perfect black bodies. Their emissivity is less than unity. Figure 3 shows wavelengths of different types of radiation and the channels used for satellite imagery. It includes the spectra of solar radiation (at temperatures of about 6000 deg. K and also of terrestrial radiation of the earth and atmosphere at temperatures between 200 and 300 deg. K). Solar radiation is in shorter wavelengths and the terrestrial radiation is in longer wavelengths. Solar radiation of significant intensity occurs at wavelengths between 0.2 and 4.0 μm, the peak intensity at about 0.5 μm in the visible part of the spectrum. Terrestrial radiation is emitted at wavelengths between 3 and 100 μm which falls entirely within the infrared region. The maximum intensity is around 11 μm.

Unlike solids and liquids, gases are not black bodies. They only absorb or emit strongly at certain wavelengths. Water vapour (H_2O), carbon dioxide (CO_2) and ozone (O_3) are such gases within the visible and infrared wave bands that are important in meteorology. Each of these gases is active in certain narrow absorption bands. There are other regions where the absorption by all the gases is so weak that the atmosphere is almost transparent. These regions are known as "windows" and are used for production of cloud imagery. Satellite imagery is obtained from radiometers that measure scattered electromagnetic radiation emitted from the sun, earth and the atmosphere.

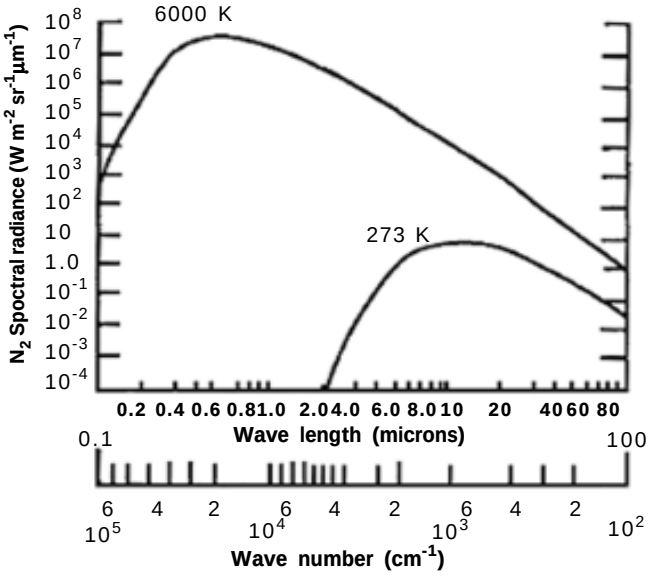

Figure 3 : Blackbody radiation emitted at temperatures corresponding to the Sun and the Earth

The satellite imageries in common operational use are :

a) Visible (VIS) - imagery derived from reflected sunlight at visible and near-infrared wavelength (0.4 - 1.1 μm).

b) Infrared (IR) imagery (Fig. 3) derived from emissions by the earth and its atmosphere at thermal infrared wavelengths (10-12 μm)

c) Water Vapour (WV) imagery derived from water vapour emissions (6-7μm) and

d) 3.7μm (often referred to as channel 3) imagery in the overlap region of solar and terrestrial radiation and hence sometimes called near IR.

e) Images from microwave radiometer such as Special Sensor Microwave/ Imager (SSM/I), and TRMM Microwave Imagers (TMI) can provide a lot of useful information. Microwave radiation is not affected by the presence of clouds and that is an important factor in the science of weather. Microwave observations are widely used for inferring sea surface temperature, sea surface wind speed and atmospheric water vapor content (over ocean surfaces), cloud liquid water content, rainfall, and the fraction of ice/snow particles within the raining systems.

DATA FROM WEATHER SATELLITES

The initial phases of the satellite era (almost for two decades) saw the use of visual imageries provided by the polar orbiting satellites. Towards the end of the seventies the sounders in polar orbiting satellites, the shifting of the US GOES satellite to the Indian latitudes during MONEX experiment and the launch of Japanese GMS satellites provided new avenues. The beginning of eighties saw the INSAT series of the meteorological satellites. The new generation of INSAT satellites to be launched in couple of years from now would have much more atmospheric information over this part of the Asian continent. Besides some experimental satellites such as the Defense meteorological satellite, ERS-1 and satellite like TRMM, are providing valuable information in describing the monsoon features, water vapour , SST, wind and rainfall (Kidder and Vonder Haar, 1995).

Tropical rainfall affects the lives and economies of a majority of the earth's population. Tropical rain systems like hurricane, typhoons and monsoons are crucial to sustaining the live hoods of those living in the tropics. Excess floods can cause drought and crop failure. The TRMM satellite's low inclination (35 degrees), non-sun synchronous, and highly processing orbits allow it to fly over each position on earths surface at different local time. The TRMM has Precipitation radar , TRMM microwave imager(TMI) and visible /infrared scanner.

Now we have launched our own Oceansat-1 onboard IRS-P4 on 26th May, 2003 which contained 8 channel onboard sensor called Ocean colour monitor (Chlorophyll content) over ocean and another microwave sensor called Muti-channel microwave radiometer (MSMR) with channel frequencies (6.6 GHz, 10.8Ghz, 18 GHz and 21 GHz) in both horizontal and vertical polarization, and is used to measure geophysical parameter related to ocean such as sea surface temperature (SST), wind speed, total integrated water vapour, and cloud liquid water vapour content (Krishna Rao, 2000).

NOAA satellites have the following meteorological payloads

i) Advanced Very High Resolution Radiometer (AVHRR)

ii) TIROS Operational Vertical Sounder (TOVS)

iii) Earth Radiation Budget (ERB)

AVHRR is a five channel scanning radiometer in visible, near infra-red and infra-red wavelengths for analysis of hydrological, oceanographic and meteorological parameters such as vegetation index (i.e. greenness), clouds, snow and ice cover and sea surface temperatures. Data are obtained by all the five channels with a resolution of 1 km. The digital AVHRR data is transmitted from the satellite in real-time (High Resolution Picture Transmission or HRPT) as well as selectively recorded on board the satellite for subsequent playback when the satellite is in communication range of the ground control station. This high resolution data is called Local Area Coverage (LAC). AVHRR data is also sampled on real-time to produce lower resolution Global Area Coverage (GAC) data. The effective resolution of the GAC data is about 4 kms. The spectral characteristics and imaging applications of AVHRR are given in Table 1.

Table 1: Spectral characteristics and applications of AVHRR.

Channel	Spectral Interval (μm)	Resolution (km)	Application
1	0.58-0.88	1.1	Cloud Mapping
2	0.73-1.0	1.1	Surface water boundaries
3	3.55-3.93	1.1	Thermal mapping, cloud distribution, fire detection
4	10.3-11.3	1.1	Cloud Distribution, SST, WV correction
5	11.5-12.5	1.1	————————do————————

TIROS operational vertical sounder (TOVS) incorporates a high resolution infrared radiation sounder (HIRS), a microwave sounding unit (MSU) and a stratospheric sounding unit (SSU). HIRS samples the atmospheric radiation in 20 IR channels and is primarily used to obtain the vertical temperature and moisture distribution in the troposphere. The HIRS uses two carbon dioxide bands for temperature sounding. Seven channels are located in the 15 μm band and six channels are located in the 4.3 μm band. The 4.3 μm channels are added to improve sensitivity (change in radiance for a given change in atmospheric temperature) at relatively warmer temperatures. Moisture is sensed with three channels in the 6.3 μm band of water vapour. The 9.7 μm channel is designed to sense ozone. Three channels are in the atmospheric

windows. The 11.1 μm and 3.76 μm channel is used to detect clouds. SSU samples the radiation from the stratosphere in 3 IR channels. MSU samples the radiation from the atmosphere in 4 channels of microwave region and is particularly useful for obtaining the vertical distribution of temperature in the atmosphere below clouds which are opaque in the infra-red radiation.

Because atmospheric motion is driven by differential absorption of solar radiation and infrared loss to space the study of Earth's radiation budget is extremely important. The latest is the Earth radiation budget experiment (ERBE), which flies on NOAA-9 and NOAA-10 as well as ERBS satellite. The ERBE is designed to make highly accurate (~ 1%) measurements of incident solar radiation, earth reflected solar radiation, and earth emitted solar radiation at scales ranging from global to 250 km.

INSAT METEOROLOGICAL COMPONENT

The Indian National Satellite (INSAT) is a multipurpose geostationary satellite, which carries both meteorological, and communications payloads. The INSAT-1D is located at 83.5 ^{0}E and INSAT-2B is located at 93.5 ^{0}E. The VHRR (very high resolution radiometer) onboard the satellite has a visible (0.55-0.75 μm) and infra-red (10.5-12.5 μm) bands with resolution of 2.75 km and 11 km for INSAT-1 series, and 2 and 8 km respectively for the INSAT–2 series. The VHRR scans are taken every 3 hours on routine basis and half hourly to even less than that, for monitoring cyclones etc. One VHRR scan takes about 30 minutes to be completed and is made up of 4096 X 4096 picture elements (pixels) in case of visible channel and 1024 x 1024 pixels in case of IR channel. The meteorological component provides:

a) Round the clock, regular half-hourly synoptic images of weather systems including severe weather, cyclones, sea surface and cloud top temperatures, water bodies, snow etc. over the entire territory of India as well as adjoining land and sea areas.

b) Collection and transmission of meteorological, hydrological and oceanographic data from unattended data collection platforms.

c) Timely warning of impending disasters from cyclones and storms etc.

d) Dissemination of meteorological information including processed images of weather systems to the forecasting offices.

INSAT-2E

The VHRR on board INSAT-2E spacecraft provides imaging capability in water vapour channel (5.7-7.1 μm) in addition to the visible and thermal IR bands with a ground resolution at the sub-satellite point of 2 km x 2 km in the visible and 8 km x 8 km in the WV (Water Vapour) & TIR (Thermal Infrared) bands. This geostationary satellite is located over 83.5 ^{0} E.

The important specifications are given in Table-2.

Table 2. INSAT 2E - VHRR Specifications

Detectors	Spectral Band (μm)	Resolution (km)
Visible (4)	0.55-0.75	2 x 2
Infra Red (1)	10.5-12.5	8 x 8
Water Vapour (1)	5.7-7.1	8 x 8

CCD Payload

The CCD camera Payload on board INSAT-2E spacecraft provides imageries in visible band (0.62 μm - 0.68 μm) & Near IR (NIR, 0.77 μm-0.86 μm) and a short-wave infrared band (SWIR, 1.55-1.69 μm). Table -3 gives the specifications of CCD.

Table 3. CCD Payload Specifications

Spatial Res.	Frame Size	Spectral Bands	Detector Array	Digitization
1 km x 1 km	10x10 deg 0.77-0.86 μm 1.55-1.7 μm	0.63-0.68 μm	Linear Si CCD (1 & 2) InGaAs	10 bits

SOME IMPORTANT MICROWAVE PAYLOADS AND THEIR APPLICATIONS

As mentioned earlier, microwave sensors have played a very important role in providing valuable information for meteorological applications. These include both active and passive type of sensors. Wind scatterometer, altimeter,

and precipitation radar are the examples of active microwave sensors. Scatterometer with operating frequencies in C-Band (~ 5 GHz), or K-Band (~ 13 GHz) is an indispensable tool for monitoring the ocean surface wind speed and wind direction with high resolution (~ 25 km) and global coverage. Ocean surface winds have a number of applications. These winds are important factors in the computation of air-sea energy and mass exchange, and they also provide input to the global ocean and wave forecast models. The use of scatterometer winds in assessing the situations leading to the formation of tropical cyclones have been demonstrated. Precipitation radar (PR) onboard Tropical Satellite Measuring Mission (TRMM) satellite is the first precipitation radar in space. This instrument operating at 13.6 GHz is capable of taking observations of vertical profiles of rainfall over the global tropics.

Among passive microwave meteorological systems, Special Sensor Microwave/Imager (SSM/I) onboard US Defense Meteorological Satellite Program (DMSP) satellite is arguably the most successful sensor. Different versions of this sensor have been providing valuable meteorological observations across the globe for nearly 16 years. The operating frequencies of this radiometer are 19.36, 22.23, 37.0, and 85.5 GHz. All the channels except 22.23 GHz operate in dual polarization (V and H), while 22.23 GHz is a single polarization (V) channel. SSM/I provides the global observations of vertically integrated water vapour (PW), sea surface wind speed (SW), cloud liquid water (CLW), and rainfall rates (RR), though due to the limitation of microwave observations, most of these observations are available only over the ocean surfaces. SSM/I provides these observations with a wide swath (~ 1400 km) and high resolution (~ 25 km). TRMM satellite launched in October 1997 carried a payload similar to SSM/I, and it is known as TRMM Microwave Imager (TMI). TMI is similar to SSM/I in characteristics however there are some significant differences. TMI is equipped with one additional channel that operates at around 10 GHz (V & H polarization). This sensor makes TMI capable of sensing global sea surface temperature (SST). A combination of observations from TMI and other visible/IR sensor onboard TRMM is being utilized operationally for measurement of daily SST with a significantly improved accuracy of ~ 0.5 K. This channel is also useful in providing improved estimates of rainfall rates. Moreover, TRMM satellite operates from a smaller altitude (~ 350 km) compared to SSM/I (~ 800 km), which ensures that the TMI observations are available at finer resolution. 85 GHz channel of TMI is highly useful in detecting the regions of active and deep convection (both over the land and the ocean surfaces) that are generally associated with the development of thunderstorm and are accompanied by heavy precipitation.

Advance Microwave Sounding Unit (AMSU) onboard the latest series of NOAA satellites, is a sounding instrument that provides the temperature and humidity sounding in presence of clouds, using the absorption bands of oxygen (~ 50 GHz), and water vapour (~ 183 GHz) respectively.

CONCLUSIONS

Various kinds of meteorological satellites such as imaging/non-imaging, optical/microwave and passive/active are available for retrieval of meteorological parameters, weather forecasting etc. INSAT-VHRR and NOAA-AVHRR satellites data are very popular in India for studing meteorological conditions.

ACKNOWLEDGEMENTS

I am thankful to my colleague and friend B. Simon who provided a lot of help in the preparation of this lecture. I also acknowledge the valuable information I received from the online tutorials by Dr. Nicholas M. Short (email : %20nmshort@epix.net).

REFERENCES

Kidder, S.Q. and Vonder Haar, T.H. 1995. Satellite Meteorology : An Introduction. Academic Press.

Krishna Rao, P. 2000. Weather Satellites System Data and Environmental Application. American Meteorological Society, London.

DIGITAL IMAGE PROCESSING

Minakshi Kumar
Photogrammetry and Remote Sensing Division
Indian Institute of Remote Sensing, Dehra Dun

Abstract : This paper describes the basic technological aspects of Digital Image Processing with special reference to satellite image processing. Basically, all satellite image-processing operations can be grouped into three categories: Image Rectification and Restoration, Enhancement and Information Extraction. The former deals with initial processing of raw image data to correct for geometric distortion, to calibrate the data radiometrically and to eliminate noise present in the data. The enhancement procedures are applied to image data in order to effectively display the data for subsequent visual interpretation. It involves techniques for increasing the visual distinction between features in a scene. The objective of the information extraction operations is to replace visual analysis of the image data with quantitative techniques for automating the identification of features in a scene. This involves the analysis of multispectral image data and the application of statistically based decision rules for determining the land cover identity of each pixel in an image. The intent of classification process is to categorize all pixels in a digital image into one of several land cover classes or themes. This classified data may be used to produce thematic maps of the land cover present in an image.

INTRODUCTION

Pictures are the most common and convenient means of conveying or transmitting information. A picture is worth a thousand words. Pictures concisely convey information about positions, sizes and inter-relationships between objects. They portray spatial information that we can recognize as objects. Human beings are good at deriving information from such images, because of our innate visual and mental abilities. About 75% of the information received by human is in pictorial form.

In the present context, the analysis of pictures that employ an overhead perspective, including the radiation not visible to human eye are considered.

Satellite Remote Sensing and GIS Applications in Agricultural Meteorology
pp. 81-102

Thus our discussion will be focussing on analysis of remotely sensed images. These images are represented in digital form. When represented as numbers, brightness can be added, subtracted, multiplied, divided and, in general, subjected to statistical manipulations that are not possible if an image is presented only as a photograph. Although digital analysis of remotely sensed data dates from the early days of remote sensing, the launch of the first Landsat earth observation satellite in 1972 began an era of increasing interest in machine processing (Cambell, 1996 and Jensen, 1996). Previously, digital remote sensing data could be analyzed only at specialized remote sensing laboratories. Specialized equipment and trained personnel necessary to conduct routine machine analysis of data were not widely available, in part because of limited availability of digital remote sensing data and a lack of appreciation of their qualities.

DIGITAL IMAGE

A digital remotely sensed image is typically composed of picture elements (pixels) located at the intersection of each row i and column j in each K bands of imagery. Associated with each pixel is a number known as Digital Number (DN) or Brightness Value (BV), that depicts the average radiance of a relatively small area within a scene (Fig. 1). A smaller number indicates low average radiance from the area and the high number is an indicator of high radiant properties of the area.

The size of this area effects the reproduction of details within the scene. As pixel size is reduced more scene detail is presented in digital representation.

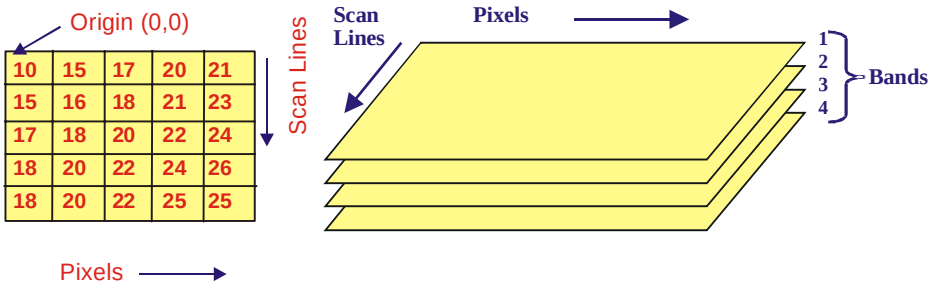

Figure 1 : Structure of a Digital Image and Multispectral Image

COLOR COMPOSITES

While displaying the different bands of a multispectral data set, images obtained in different bands are displayed in image planes (other than their own) the color composite is regarded as False Color Composite (FCC). High spectral resolution is important when producing color components. For a true color composite an image data used in red, green and blue spectral region must be assigned bits of red, green and blue image processor frame buffer memory. A color infrared composite 'standard false color composite' is displayed by placing the infrared, red, green in the red, green and blue frame buffer memory (Fig. 2). In this healthy vegetation shows up in shades of red because vegetation absorbs most of green and red energy but reflects approximately half of incident Infrared energy. Urban areas reflect equal portions of NIR, R & G, and therefore they appear as steel grey.

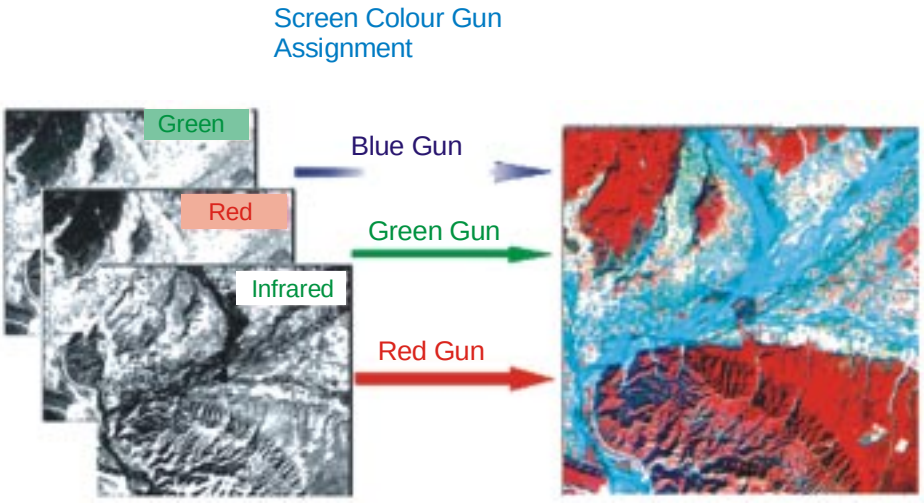

Figure 2: False Color Composite (FCC) of IRS : LISS II Poanta area

IMAGE RECTIFICATION AND REGISTRATION

Geometric distortions manifest themselves as errors in the position of a pixel relative to other pixels in the scene and with respect to their absolute position within some defined map projection. If left uncorrected, these geometric distortions render any data extracted from the image useless. This is particularly so if the information is to be compared to other data sets, be it from another image or a GIS data set. Distortions occur for many reasons.

For instance distortions occur due to changes in platform attitude (roll, pitch and yaw), altitude, earth rotation, earth curvature, panoramic distortion and detector delay. Most of these distortions can be modelled mathematically and are removed before you buy an image. Changes in attitude however can be difficult to account for mathematically and so a procedure called image rectification is performed. Satellite systems are however geometrically quite stable and geometric rectification is a simple procedure based on a mapping transformation relating real ground coordinates, say in easting and northing, to image line and pixel coordinates.

Rectification is a process of geometrically correcting an image so that it can be represented on a planar surface , conform to other images or conform to a map (Fig. 3). That is, it is the process by which geometry of an image is made planimetric. It is necessary when accurate area, distance and direction measurements are required to be made from the imagery. It is achieved by transforming the data from one grid system into another grid system using a geometric transformation.

Rectification is not necessary if there is no distortion in the image. For example, if an image file is produced by scanning or digitizing a paper map that is in the desired projection system, then that image is already planar and does not require rectification unless there is some skew or rotation of the image. Scanning and digitizing produce images that are planar, but do not contain any map coordinate information. These images need only to be geo-referenced, which is a much simpler process than rectification. In many cases, the image header can simply be updated with new map coordinate information. This involves redefining the map coordinate of the upper left corner of the image and the cell size (the area represented by each pixel).

Ground Control Points (GCP) are the specific pixels in the input image for which the output map coordinates are known. By using more points than necessary to solve the transformation equations a least squares solution may be found that minimises the sum of the squares of the errors. Care should be exercised when selecting ground control points as their number, quality and distribution affect the result of the rectification.

Once the mapping transformation has been determined a procedure called resampling is employed. Resampling matches the coordinates of image pixels to their real world coordinates and writes a new image on a pixel by pixel basis. Since the grid of pixels in the source image rarely matches the grid for

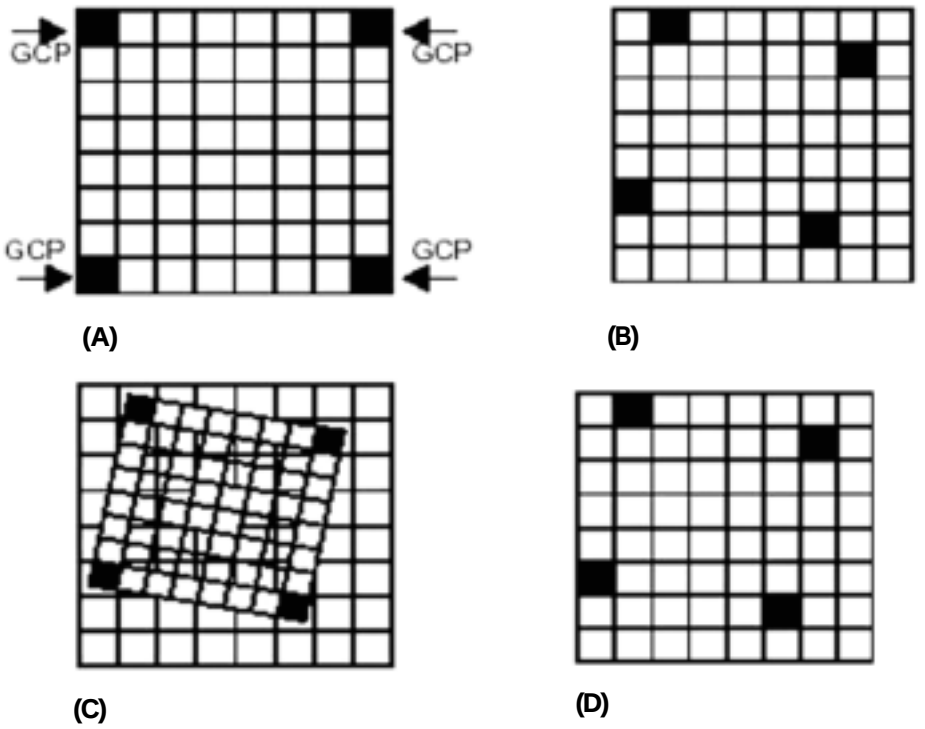

Figure 3 : Image Rectification (a & b) Input and reference image with GCP locations, (c) using polynomial equations the grids are fitted together, (d) using resampling method the output grid pixel values are assigned (source modified from ERDAS Field guide)

the reference image, the pixels are resampled so that new data file values for the output file can be calculated.

IMAGE ENHANCEMENT TECHNIQUES

Image enhancement techniques improve the quality of an image as perceived by a human. These techniques are most useful because many satellite images when examined on a colour display give inadequate information for image interpretation. There is no conscious effort to improve the fidelity of the image with regard to some ideal form of the image. There exists a wide variety of techniques for improving image quality. The contrast stretch, density slicing, edge enhancement, and spatial filtering are the more commonly used techniques. Image enhancement is attempted after the image is corrected for geometric and radiometric distortions. Image enhancement methods are applied separately to each band of a multispectral image. Digital techniques

have been found to be most satisfactory than the photographic technique for image enhancement, because of the precision and wide variety of digital processes.

Contrast

Contrast generally refers to the difference in luminance or grey level values in an image and is an important characteristic. It can be defined as the ratio of the maximum intensity to the minimum intensity over an image.

Contrast ratio has a strong bearing on the resolving power and detectability of an image. Larger this ratio, more easy it is to interpret the image. Satellite images lack adequate contrast and require contrast improvement.

Contrast Enhancement

Contrast enhancement techniques expand the range of brightness values in an image so that the image can be efficiently displayed in a manner desired by the analyst. The density values in a scene are literally pulled farther apart, that is, expanded over a greater range. The effect is to increase the visual contrast between two areas of different uniform densities. This enables the analyst to discriminate easily between areas initially having a small difference in density.

Linear Contrast Stretch

This is the simplest contrast stretch algorithm. The grey values in the original image and the modified image follow a linear relation in this algorithm. A density number in the low range of the original histogram is assigned to extremely black and a value at the high end is assigned to extremely white. The remaining pixel values are distributed linearly between these extremes. The features or details that were obscure on the original image will be clear in the contrast stretched image. Linear contrast stretch operation can be represented graphically as shown in Fig. 4. To provide optimal contrast and colour variation in colour composites the small range of grey values in each band is stretched to the full brightness range of the output or display unit.

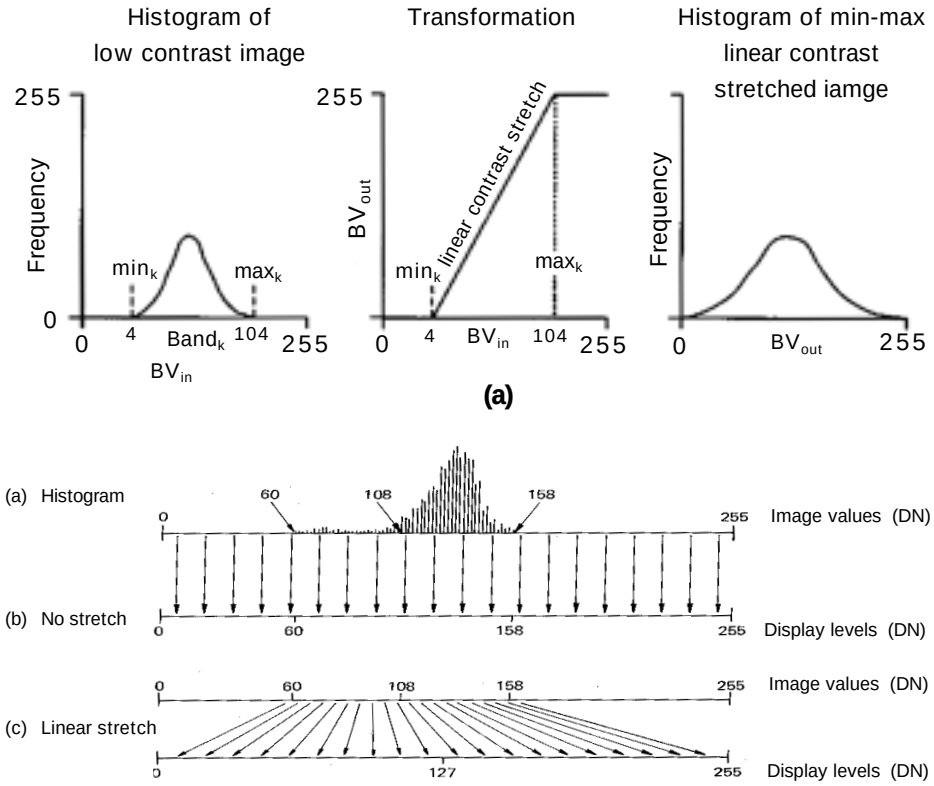

Figure 4: Linear Contrast Stretch (source Lillesand and Kiefer, 1993)

Non-Linear Contrast Enhancement

In these methods, the input and output data values follow a non-linear transformation. The general form of the non-linear contrast enhancement is defined by y = f (x), where x is the input data value and y is the output data value. The non-linear contrast enhancement techniques have been found to be useful for enhancing the colour contrast between the nearly classes and subclasses of a main class.

A type of non linear contrast stretch involves scaling the input data logarithmically. This enhancement has greatest impact on the brightness values found in the darker part of histogram. It could be reversed to enhance values in brighter part of histogram by scaling the input data using an inverse log function.

Histogram equalization is another non-linear contrast enhancement technique. In this technique, histogram of the original image is redistributed to produce a uniform population density. This is obtained by grouping certain adjacent grey values. Thus the number of grey levels in the enhanced image is less than the number of grey levels in the original image.

SPATIAL FILTERING

A characteristic of remotely sensed images is a parameter called spatial frequency defined as number of changes in Brightness Value per unit distance for any particular part of an image. If there are very few changes in Brightness Value once a given area in an image, this is referred to as low frequency area. Conversely, if the Brightness Value changes dramatically over short distances, this is an area of high frequency.

Spatial filtering is the process of dividing the image into its constituent spatial frequencies, and selectively altering certain spatial frequencies to emphasize some image features. This technique increases the analyst's ability to discriminate detail. The three types of spatial filters used in remote sensor data processing are : Low pass filters, Band pass filters and High pass filters.

Low-Frequency Filtering in the Spatial Domain

Image enhancements that de-emphasize or block the high spatial frequency detail are low-frequency or low-pass filters. The simplest low-frequency filter evaluates a particular input pixel brightness value, BV_{in}, and the pixels surrounding the input pixel, and outputs a new brightness value, BV_{out} , that is the mean of this convolution. The size of the neighbourhood convolution mask or kernel (n) is usually 3x3, 5x5, 7x7, or 9x9.

The simple smoothing operation will, however, blur the image, especially at the edges of objects. Blurring becomes more severe as the size of the kernel increases.

Using a 3x3 kernel can result in the low-pass image being two lines and two columns smaller than the original image. Techniques that can be applied to deal with this problem include (1) artificially extending the original image beyond its border by repeating the original border pixel brightness values or (2) replicating the averaged brightness values near the borders, based on the

image behaviour within a view pixels of the border. The most commonly used low pass filters are mean, median and mode filters.

High-Frequency Filtering in the Spatial Domain

High-pass filtering is applied to imagery to remove the slowly varying components and enhance the high-frequency local variations. Brightness values tend to be highly correlated in a nine-element window. Thus, the high-frequency filtered image will have a relatively narrow intensity histogram. This suggests that the output from most high-frequency filtered images must be contrast stretched prior to visual analysis.

Edge Enhancement in the Spatial Domain

For many remote sensing earth science applications, the most valuable information that may be derived from an image is contained in the edges surrounding various objects of interest. Edge enhancement delineates these edges and makes the shapes and details comprising the image more conspicuous and perhaps easier to analyze. Generally, what the eyes see as pictorial edges are simply sharp changes in brightness value between two adjacent pixels. The edges may be enhanced using either linear or nonlinear edge enhancement techniques.

Linear Edge Enhancement

A straightforward method of extracting edges in remotely sensed imagery is the application of a directional first-difference algorithm and approximates the first derivative between two adjacent pixels. The algorithm produces the first difference of the image input in the horizontal, vertical, and diagonal directions.

The Laplacian operator generally highlights point, lines, and edges in the image and suppresses uniform and smoothly varying regions. Human vision physiological research suggests that we see objects in much the same way. Hence, the use of this operation has a more natural look than many of the other edge-enhanced images.

Band ratioing

Sometimes differences in brightness values from identical surface materials are caused by topographic slope and aspect, shadows, or seasonal changes in

sunlight illumination angle and intensity. These conditions may hamper the ability of an interpreter or classification algorithm to identify correctly surface materials or land use in a remotely sensed image. Fortunately, ratio transformations of the remotely sensed data can, in certain instances, be applied to reduce the effects of such environmental conditions. In addition to minimizing the effects of environmental factors, ratios may also provide unique information not available in any single band that is useful for discriminating between soils and vegetation.

The mathematical expression of the ratio function is

$$BV_{i,j,r} = BV_{i,j,k}/BV_{i,j.l}$$

where $BV_{i,j,r}$ is the output ratio value for the pixel at rwo, i, column j; $BV_{i,j,k}$ is the brightness value at the same location in band k, and $BV_{i,j,l}$ is the brightness value in band l. Unfortunately, the computation is not always simple since $BV_{i,j} = 0$ is possible. However, there are alternatives. For example, the mathematical domain of the function is 1/255 to 255 (i.e., the range of the ratio function includes all values beginning at 1/255, passing through 0 and ending at 255). The way to overcome this problem is simply to give any $BV_{i,j}$ with a value of 0 the value of 1.

Ratio images can be meaningfully interpreted because they can be directly related to the spectral properties of materials. Ratioing can be thought of as a method of enhancing minor differences between materials by defining the slope of spectral curve between two bands. We must understand that dissimilar materials having similar spectral slopes but different albedos, which are easily separable on a standard image, may become inseparable on ratio images. Figure 5 shows a situation where Deciduous and Coniferous Vegetation crops out on both the sunlit and shadowed sides of a ridge.

In the individual bands the reflectance values are lower in the shadowed area and it would be difficult to match this outcrop with the sunlit outcrop. The ratio values, however, are nearly identical in the shadowed and sunlit areas and the sandstone outcrops would have similar signatures on ratio images. This removal of illumination differences also eliminates the dependence of topography on ratio images.

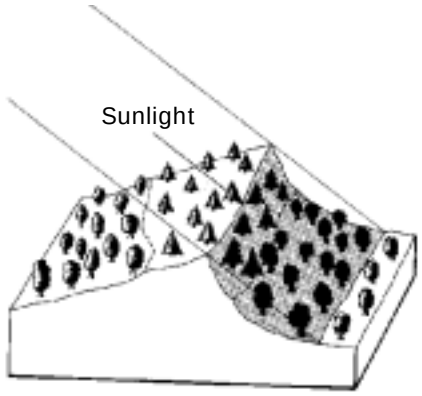

Figure 5: Reduction of Scene Illumination effect through spectral ratioing
(source Lillesand & Kiefer, 1993)

Landcover/ Illumination	Digital Number		Ratio
	Band A	Band B	
Deciduous			
Sunlit	48	50	.96
Shadow	18	19	.95
Coniferous			
Sunlit	31	45	.69
Shadow	11	16	.69

PRINCIPAL COMPONENT ANALYSIS

The multispectral image data is usually strongly correlated from one band to the other. The level of a given picture element on one band can to some extent be predicted from the level of that same pixel in another band.

Principal component analysis is a pre-processing transformation that creates new images from the uncorrelated values of different images. This is accomplished by a linear transformation of variables that corresponds to a rotation and translation of the original coordinate system.

Principal component analysis operates on all bands together. Thus, it alleviates the difficulty of selecting appropriate bands associated with the band ratioing operation. Principal components describe the data more efficiently

than the original band reflectance values. The first principal component accounts for a maximum portion of the variance in the data set, often as high as 98%. Subsequent principal components account for successively smaller portions of the remaining variance.

Principal component transformations are used for spectral pattern recognition as well as image enhancement. When used before pattern recognition, the least important principal components are dropped altogether. This permits us to omit the insignificant portion of our data set and thus avoids the additional computer time. The transformation functions are determined during the training stage. Principal component images may be analysed as separate black and white images, or any three component images may be colour coded to form a colour composite. Principal component enhancement techniques are particularly appropriate in areas where little a priori information concerning the region is available.

IMAGE FUSION TECHNIQUES

The satellites cover different portions of the electromagnetic spectrum and record the incoming radiations at different spatial, temporal, and spectral resolutions. Most of these sensors operate in two modes: *multispectral* mode and the *panchromatic* mode.

The *panchromatic* mode corresponds to the observation over a broad spectral band (similar to a typical black and white photograph) and the *multispectral* (color) mode corresponds to the observation in a number of relatively narrower bands. For example in the IRS – 1D, LISS III operates in the multispectral mode. It records energy in the green (0.52 – 0.59 μm), red (0.62-0.68 μm), near infrared (0.77- 0.86 μm) and mid-infrared (1.55 – 1.70 μm). In the same satellite PAN operates in the panchromatic mode. SPOT is another satellite, which has a combination of sensor operating in the multispectral and panchromatic mode. Above information is also expressed by saying that the multispectral mode has a better *spectral resolution* than the panchromatic mode.

Now coming to the *spatial resolution*, most of the satellites are such that the *panchromatic* mode has a better *spatial resolution* than the *multispectral* mode, for e.g. in IRS -1C, PAN has a spatial resolution of 5.8 m whereas in the case of LISS it is 23.5 m. Better is the spatial resolution, more detailed information about a landuse is present in the imagery, hence usually PAN data is used for

observing and separating various feature. Both theses type of sensors have their particular utility as per the need of user. If the need of the user is to separate two different kind of landuses, LISS III is used, whereas for a detailed map preparation of any area, PAN imagery is extremely useful.

Image Fusion is the combination of two or more different images to form a new image (by using a certain algorithm).

The commonly applied Image Fusion Techniques are

1. IHS Transformation
2. PCA
3. Brovey Transform
4. Band Substitution

IMAGE CLASSIFICATION

The overall objective of image classification is to automatically categorize all pixels in an image into land cover classes or themes. Normally, multispectral data are used to perform the classification, and the spectral pattern present within the data for each pixel is used as numerical basis for categorization. That is, different feature types manifest different combination of DNs based on their inherent spectral reflectance and emittance properties.

The term *classifier* refers loosely to a computer program that implements a specific procedure for image classification. Over the years scientists have devised many classification strategies. From these alternatives the analyst must select the classifier that will best accomplish a specific task. At present it is not possible to state that a given classifier is "best" for all situations because characteristics of each image and the circumstances for each study vary so greatly. Therefore, it is essential that the analyst understands the alternative strategies for image classification.

The traditional methods of classification mainly follow two approaches: unsupervised and supervised. The unsupervised approach attempts spectral grouping that may have an unclear meaning from the user's point of view. Having established these, the analyst then tries to associate an information class with each group. The unsupervised approach is often referred to as

clustering and results in statistics that are for spectral, statistical clusters. In the supervised approach to classification, the image analyst supervises the pixel categorization process by specifying to the computer algorithm; numerical descriptors of the various land cover types present in the scene. To do this, representative sample sites of known cover types, called training areas or training sites, are used to compile a numerical interpretation key that describes the spectral attributes for each feature type of interest. Each pixel in the data set is then compared numerically to each category in the interpretation key and labeled with the name of the category it looks most like. In the supervised approach the user defines useful information categories and then examines their spectral separability whereas in the unsupervised approach he first determines spectrally separable classes and then defines their informational utility.

It has been found that in areas of complex terrain, the unsupervised approach is preferable to the supervised one. In such conditions if the supervised approach is used, the user will have difficulty in selecting training sites because of the variability of spectral response within each class. Consequently, a prior ground data collection can be very time consuming. Also, the supervised approach is subjective in the sense that the analyst tries to classify information categories, which are often composed of several spectral classes whereas spectrally distinguishable classes will be revealed by the unsupervised approach, and hence ground data collection requirements may be reduced. Additionally, the unsupervised approach has the potential advantage of revealing discriminable classes unknown from previous work. However, when definition of representative training areas is possible and statistical information classes show a close correspondence, the results of supervised classification will be superior to unsupervised classification.

Unsupervised classification

Unsupervised classifiers do *not utilize* training data as the basis for classification. Rather, this family of classifiers involves algorithms that examine the unknown pixels in an image and aggregate them into a number of classes based on the natural groupings or clusters present in the image values. It performs very well in cases where the values within a given cover type are close together in the measurement space, data in different classes are comparatively well separated.

The classes that result from unsupervised classification are spectral classes because they are based solely on the natural groupings in the image values,

the identity of the spectral classes will not be initially known. The analyst must compare the classified data with some form of reference data (such as larger scale imagery or maps) to determine the identity and informational value of the spectral classes. In the supervised approach we define useful information categories and then examine their spectral separability; in the unsupervised approach we determine spectrally separable classes and then define their informational utility.

There are numerous clustering algorithms that can be used to determine the natural spectral groupings present in data set. One common form of clustering, called the "K-means" approach also called as ISODATA (Interaction Self-Organizing Data Analysis Technique) accepts from the analyst the number of clusters to be located in the data. The algorithm then arbitrarily "seeds", or locates, that number of cluster centers in the multidimensional measurement space. Each pixel in the image is then assigned to the cluster whose arbitrary mean vector is closest. After all pixels have been classified in this manner, revised mean vectors for each of the clusters are computed. The revised means are then used as the basis of reclassification of the image data. The procedure continues until there is no significant change in the location of class mean vectors between successive iterations of the algorithm. Once this point is reached, the analyst determines the land cover identity of each spectral class. Because the K-means approach is iterative, it is computationally intensive. Therefore, it is often applied only to image sub-areas rather than to full scenes.

Supervised classification

Supervised classification can be defined normally as the process of samples of known identity to classify pixels of unknown identity. Samples of known identity are those pixels located within training areas. Pixels located within these areas term the training samples used to guide the classification algorithm to assigning specific spectral values to appropriate informational class.

The basic steps involved in a typical supervised classification procedure are illustrated on Fig. 6.

The training stage
Feature selection
Selection of appropriate classification algorithm
Post classification smoothening
Accuracy assessment

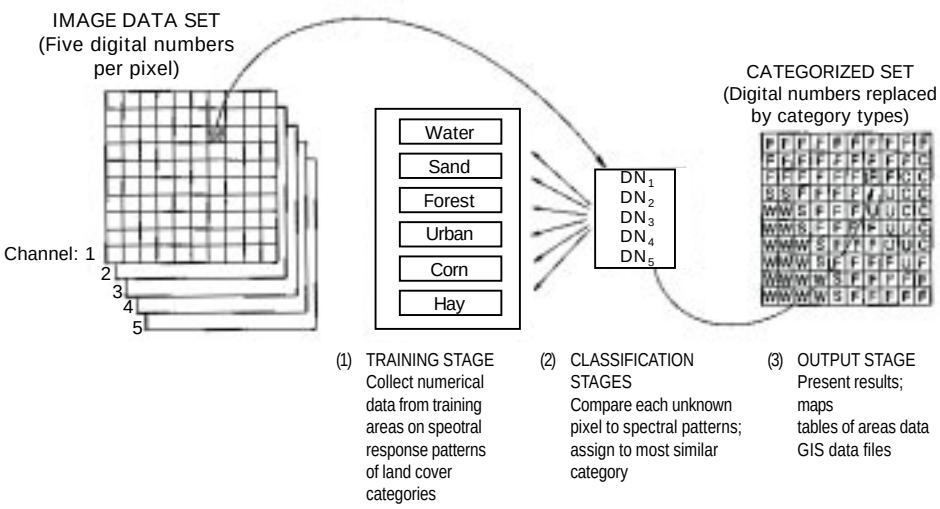

Figure 6: Basic Steps in Supervised Classification

Training data

Training fields are areas of known identity delineated on the digital image, usually by specifying the corner points of a rectangular or polygonal area using line and column numbers within the coordinate system of the digital image. The analyst must, of course, know the correct class for each area. Usually the analyst begins by assembling maps and aerial photographs of the area to be classified. Specific training areas are identified for each informational category following the guidelines outlined below. The objective is to identify a set of pixels that accurately represents spectral variation present within each information region (Fig. 7a).

Select the Appropriate Classification Algorithm

Various supervised classification algorithms may be used to assign an unknown pixel to one of a number of classes. The choice of a particular classifier or decision rule depends on the nature of the input data and the desired output. Parametric classification algorithms assume that the observed measurement vectors X_c for each class in each spectral band during the training phase of the supervised classification are Gaussian in nature; that is, they are normally distributed. Nonparametric classification algorithms make no such assumption. Among the most frequently used classification algorithms are the parallelepiped, minimum distance, and maximum likelihood decision rules.

Parallelepiped Classification Algorithm

This is a widely used decision rule based on simple Boolean "and/or" logic. Training data in n spectral bands are used in performing the classification. Brightness values from each pixel of the multispectral imagery are used to produce an n-dimensional mean vector, $M_c = (\mu_{ck1}, \mu_{c2}, \mu_{c3}, \ldots \mu_{cn})$ with μ_{ck} being the mean value of the training data obtained for class c in band k out of m possible classes, as previously defined. S_{ck} is the standard deviation of the training data class c of band k out of m possible classes.

The decision boundaries form an n-dimensional parallelepiped in feature space. If the pixel value lies above the lower threshold and below the high threshold for all n bands evaluated, it is assigned to an unclassified category (Figs. 7c and 7d). Although it is only possible to analyze visually up to three dimensions, as described in the section on computer graphic feature analysis, it is possible to create an n-dimensional parallelepiped for classification purposes.

The parallelepiped algorithm is a computationally efficient method of classifying remote sensor data. Unfortunately, because some parallelepipeds overlap, it is possible that an unknown candidate pixel might satisfy the criteria of more than one class. In such cases it is usually assigned to the first class for which it meets all criteria. A more elegant solution is to take this pixel that can be assigned to more than one class and use a minimum distance to means decision rule to assign it to just one class.

Minimum Distance to Means Classification Algorithm

This decision rule is computationally simple and commonly used. When used properly it can result in classification accuracy comparable to other more computationally intensive algorithms, such as the maximum likelihood algorithm. Like the parallelepiped algorithm, it requires that the user provide the mean vectors for each class in each hand μ_{ck} from the training data. To perform a minimum distance classification, a program must calculate the distance to each mean vector, μ_{ck} from each unknown pixel (BV_{ijk}). It is possible to calculate this distance using Euclidean distance based on the Pythagorean theorem (Fig. 7b).

The computation of the Euclidean distance from point to the mean of Class-1 measured in band relies on the equation

$$Dist = SQRT\{ (BV_{ijk} - \mu_{ck})^2 + (BV_{ijl} - \mu_{cl})^2 \}$$

Where μ_{ck} and μ_{cl} represent the mean vectors for class c measured in bands k and l.

Many minimum-distance algorithms let the analyst specify a distance or threshold from the class means beyond which a pixel will not be assigned to a category even though it is nearest to the mean of that category.

Maximum Likelihood Classification Algorithm

The maximum likelihood decision rule assigns each pixel having pattern measurements or features X to the class c whose units are most probable or likely to have given rise to feature vector x. It assumes that the training data statistics for each class in each band are normally distributed, that is, Gaussian. In other words, training data with bi-or trimodal histograms in a single band are not ideal. In such cases, the individual modes probably represent individual classes that should be trained upon individually and labeled as separate classes. This would then produce unimodal, Gaussian training class statistics that would fulfil the normal distribution requirement.

The Bayes's decision rule is identical to the maximum likelihood decision rule that it does not assume that each class has equal probabilities. A priori probabilities have been used successfully as a way of incorporating the effects of relief and other terrain characteristics in improving classification accuracy. The maximum likelihood and Bayes's classification require many more computations per pixel than either the parallelepiped or minimum-distance classification algorithms. They do not always produce superior results.

Classification Accuracy Assessment

Quantitatively assessing classification accuracy requires the collection of some in situ data or a priori knowledge about some parts of the terrain which can then be compared with the remote sensing derived classification map. Thus to assess classification accuracy it is necessary to compare two classification maps 1) the remote sensing derived map, and 2) assumed true map (in fact it may contain some error). The assumed true map may be derived from in situ investigation or quite often from the interpretation of remotely sensed data obtained at a larger scale or higher resolution.

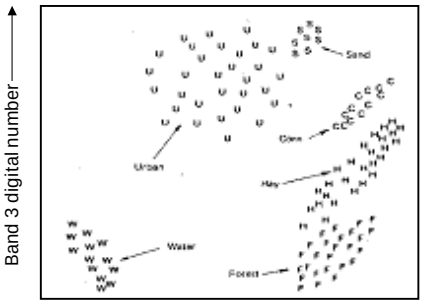

Figure 7a: Pixel observations from selected training sites plotted on scatter diagram

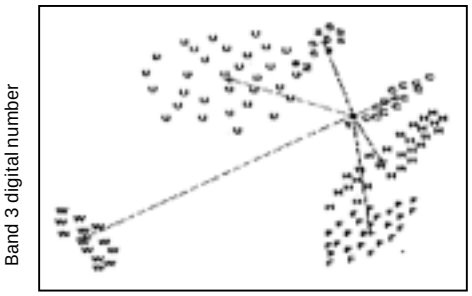

Figure 7b: Minimum Distance to Means Classification strategy

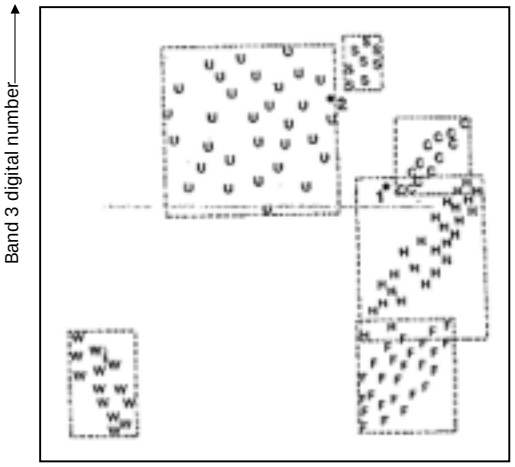

Figure 7c: Parallelepiped classification strategy

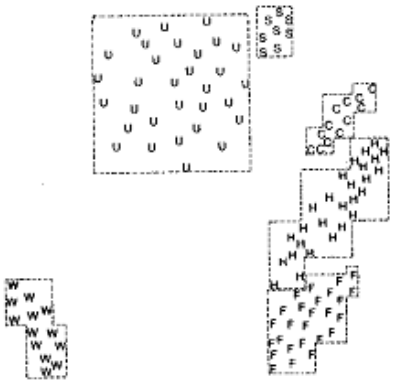

Figure 7d: Stepped parallelepipeds to avoid overlap (source Lillesand and Kiefer, 1993)

Classification Error Matrix

One of the most common means of expressing classification accuracy is the preparation of classification error matrix sometimes called confusion or a contingency table. Error matrices compare on a category by category basis, the relationship between known reference data (ground truth) and the corresponding results of an automated classification. Such matrices are square, with the number of rows and columns equal to the number of categories whose classification accuracy is being assessed. Table 1 is an error matrix that an image analyst has prepared to determine how well a Classification has categorized a representative subset of pixels used in the training process of a supervised classification. This matrix stems from classifying the sampled

training set pixels and listing the known cover types used for training (columns) versus the Pixels actually classified into each land cover category by the classifier (rows).

Table 1. Error Matrix resulting from classifying training Set pixels

	W	S	F	U	C	H	Row Total
W	480	0	5	0	0	0	485
S	0	52	0	20	0	0	72
F	0	0	313	40	0	0	353
U	0	16	0	126	0	0	142
C	0	0	0	38	342	79	459
H	0	0	38	24	60	359	481
Column Total	480	68	356	248	402	438	1992

Classification data Training set data (Known cover types) ⟶

Producer's Accuracy

W=480/480 = 100%

S = 052/068 = 16%

F = 313/356 = 88%

U =126/241l = 51%

C =342/402 = 85%

H = 359/438 = 82%

Users Accuracy

W= 480/485 = 99%

S = 052/072 = 72%

F = 313/352 = 87%

U = 126/147 = 99%

C = 342/459 = 74%

H = 359/481 = 75%

Overall accuracy = (480 + 52 + 313+ 126+ 342 +359)/1992= 84%

W, water; S, sand; F, forest; U, urban; C, corn; H, hay
(source Lillesand and Kiefer, 1993).

An error matrix expresses several characteristics about classification performance. For example, one can study the various classification errors of

omission (exclusion) and commission (inclusion). Note in Table 1 the training set pixels that are classified into the proper land cover categories are located along the major diagonal of the error matrix (running from upper left to lower right). All non-diagonal elements of the matrix represent errors of omission or commission. Omission errors correspond to non-diagonal column elements (e.g. 16 pixels that should have classified as "sand" were omitted from that category). Commission errors are represented by non-diagonal row elements (e.g. 38 urban pixels plus 79 hay pixels were improperly included in the corn category).

Several other measures for e.g. the overall accuracy of classification can be computed from the error matrix. It is determined by dividing the total number correctly classified pixels (sum of elements along the major diagonal) by the total number of reference pixels. Likewise, the accuracies of individual categories can be calculated by dividing the number of correctly classified pixels in each category by either the total number of pixels in the corresponding rows or column. Producers accuracy which indicates how well the training sets pixels of a given cover type are classified can be determined by dividing the number of correctly classified pixels in each category by number of training sets used for that category (column total). Users accuracy is computed by dividing the number of correctly classified pixels in each category by the total number of pixels that were classified in that category (row total). This figure is a measure of commission error and indicates the probability that a pixel classified into a given category actually represents that category on ground.

Note that the error matrix in the table indicates an overall accuracy of 84%. However producers accuracy ranges from just 51% (urban) to 100% (water) and users accuracy ranges from 72% (sand) to 99% (water). This error matrix is based on training data. If the results are good it indicates that the training samples are spectrally separable and the classification works well in the training areas. This aids in the training set refinement process, but indicates little about classifier performance else where in the scene.

Kappa coefficient

Kappa analysis is a discrete multivariate technique for accuracy assessment. Kappa analysis yields a Khat statistic that is the measure of agreement of accuracy. The Khat statistic is computed as

$$\text{Khat} = \frac{N\sum^{r} x_{ii}(\sum x_i + *x_{+i})}{N^2 - \sum^{r}(x_{i+} + *x_{+i})^{r}}$$

Where r is the number of rows in the matrix xii is the number of observations in row i and column i, and x_{i+} and x_{+i} are the marginal totals for the row i and column i respectively and N is the total number of observations.

CONCLUSIONS

Digital image processings of satellite data can be primarily grouped into three categories : Image Rectification and Restoration, Enhancement and Information extraction. Image rectification is the pre-processing of satellite data for geometric and radiometric connections. Enhancement is applied to image data in order to effectively display data for subsequent visual interpretation. Information extraction is based on digital classification and is used for generating digital thematic map.

REFERENCES

Campbell, J.B. 1996. Introduction to Remote Sensing. Taylor & Francis, London.

ERDAS IMAGINE 8.4 Field Guide: ERDAS Inc.

Jensen, J.R. 1996. Introduction to Digital Image Processing : A Remote Sensing Perspective. Practice Hall, New Jersey.

Lillesand, T.M. and Kiefer, R. 1993. Remote Sensing Image Interpretation. John Wiley, New York.

FUNDAMENTALS OF GEOGRAPHICAL INFORMATION SYSTEM

P.L.N. Raju
Geoinformatics Division
Indian Institute of Remote Sensing, Dehra Dun

Abstract : The handling of spatial data usually involves processes of data acquisition, storage and maintenance, analysis and output. For many years, this has been done using analogue data sources and manual processing The introduction of modern technologies has led to an increased use of computers and information technology in all aspects of spatial data handling. The software technology used in this domain is Geographic Information Systems (GIS). GIS is being used by various disciplines as tools for spatial data handling in a geographic environment. This article deals with history of GIS and fundamentals of GIS such as elements of GIS; data models; data structures & data base; and elementary spatial analysis.

INTRODUCTION

We are presently positioned at the beginning of the twenty first century with the fast growing trends in computer technology information systems and virtual world to obtain data about the physical and cultural worlds, and to use these data to do research or to solve practical problems. The current digital and analog electronic devices facilitate the inventory of resources and the rapid execution of arithmetic or logical operations. These Information Systems are undergoing much improvement and they are able to create, manipulate, store and use spatial data much faster and at a rapid rate as compared to conventional methods.

An Information System, a collection of data and tools for working with those data, contains data in analog form or digital form about the phenomena in the real world. Our perception of the world through selection, generalization and synthesis give us information and the representation of this information that is, the data constitute a model of those phenomena. So the collection of

Satellite Remote Sensing and GIS Applications in Agricultural Meteorology
pp. 103-120

data, the database is a physical repository of varied views of the real world representing our knowledge at one point in time. Information is derived from the individual data elements in a database, the information directly apparent i.e. information is produced from data by our thought processes, intuition or what ever based on our knowledge. Therefore in a database context the terms data, information and knowledge are differentiated. It can be summarized that the data are very important and add value as we progress from data to information, to knowledge. The data, which has many origins and forms, may be any of the following:

- Real, for example the terrain conditions etc.
- Captured, i.e. recorded digital data from remote sensing satellites or aerial photographs of any area.
- Interpreted, i.e. land use from remote sensing data.
- Encoded, i.e. recordings of rain-gauge data, depth of well data etc.
- Structured or organized such as tables about conditions of particular watershed.

CONCEPTS OF SPACE AND TIME IN SPATIAL INFORMATION SYSTEMS

Spatial information is always related to geographic space, i.e., large-scale space. This is the space beyond the human body, space that represents the surrounding geographic world. Within such space, we constantly move around, we navigate in it, and we conceptualize it in different ways. Geographic space is the space of topographic, land use/land cover, climatic, cadastral, and other features of the geographic world. Geographic information system technology is used to manipulate objects in geographic space, and to acquire knowledge from spatial facts.

Geographic space is distinct from small-scale space, or tabletop space. In other words, objects that are smaller than us, objects that can be moved around on a tabletop, belong to small-scale space and are not subject of our interest.

The human understanding of space, influenced by language and cultural background, plays an important role in how we design and use tools for the processing of spatial data. In the same way as spatial information is always

related to geographic space, it relates to geographic time, the time whose effects we observe in the changing geographic world around us. We are less interested in pure philosophical or physical considerations about time or space-time, but more in the observable spatio-temporal effects that can be described, measured and stored in information systems.

Spatial information systems

The handling of spatial data usually involves processes of data acquisition, storage and maintenance, analysis and output. For many years, this has been done using analogue data sources, manual processing and the production of paper maps. The introduction of modern technologies has led to an increased use of computers and information technology in all aspects of spatial data handling. The software technology used in this domain is geographic information systems (GIS).

A general motivation for the use of GIS can be illustrated with the following example. For a planning task usually different maps and other data sources are needed. Assuming a conventional analogue procedure we would have to collect all the maps and documents needed before we can start the analysis. The first problem we encounter is that the maps and data have to be collected from different sources at different locations (e.g., mapping agency, geological survey, soil survey, forest survey, census bureau, etc.), and that they are in different scales and projections. In order to combine data from maps they have to be converted into working documents of the same scale and projection. This has to be done manually, and it requires much time and money.

With the help of a GIS, the maps can be stored in digital form in a database in world co-ordinates (meters or feet). This makes scale transformations unnecessary, and the conversion between map projections can be done easily with the software. The spatial analysis functions of the GIS are then applied to perform the planning tasks. This can speed up the process and allows for easy modifications to the analysis approach.

GIS, spatial information theory, and the Geoinformatics context

Spatial data handling involves many disciplines. We can distinguish disciplines that develop spatial concepts, provide means for capturing and processing of spatial data, provide a formal and theoretical foundation, are application-oriented, and support spatial data handling in legal and

management aspects. Table 1 shows a classification of some of these disciplines. They are grouped according to how they deal with spatial information. The list is not meant to be exhaustive.

Table 1: Classification of disciplines involved in spatial analysis

Characteristics of disciplines	Sample disciplines
Development of spatial concepts	Geography Cognitive Science Linguistics Psychology
Means for capturing and processing spatial data	Remote Sensing Surveying Engineering Cartography Photogrammetry Formal and theoretical foundation Computer Science Expert Systems Mathematics Statistics
Applications	Archaeology Architecture Forestry Geo-Sciences Regional and Urban Planning Surveying
Legal Sciences	Support Economy

The discipline that deals with all aspects of spatial data handling is called Geoinformatics. It is defined as:

> Geoinformatics is the integration of different disciplines dealing with spatial information.

Geoinformatics has also been described as “the science and technology dealing with the structure and character of spatial information, its capture, its classification and qualification, its storage, processing, portrayal and dissemination, including the infrastructure necessary to secure optimal use of this information”. It is also defined as “the art, science or technology dealing with the acquisition, storage, processing, production, presentation and dissemination of geoinformation.”

A related term that is sometimes used synonymously with geoinformatics is Geomatics. It was originally introduced in Canada, and became very popular in French speaking countries. The term geomatics, however, was never fully accepted in the United States where the term geographical information science is preferred.

There is no clear-cut definition for GIS. Different people defined GIS according to capability and purpose for which it is applied. Few of the definitions are:

- "A computer - assisted system for the capture, storage, retrieval, analysis and display of spatial data, within a particular Organization" (Stillwell & Clarke, 1987).
- "A powerful set of tools for collecting, storing, retrieving at will, transforming and displaying spatial data from the real world" (Burrough, 1987).
- A GIS is also defined as follows (Aronoff, 1989):
  - A GIS is a computer-based system that provides the following four sets of capabilities to handle geo-referenced data:
  - *Input,*
  - *data management (data storage and retrieval),*
  - *manipulation and analysis, and*
  - *Output.*
- "An internally referenced, automated, spatial information system".
- "A system for capturing, storing, checking, manipulating, analyzing and displaying data which are spatially referenced to the Earth".
- "An information technology which stores, analyses and display both spatial and non–spatial data".
- "A database system in which most of the data are spatially indexed, and upon which a set of procedures operated in order to answer queries about spatial entities in the database".

- "An automated set of functions that provides professionals with advanced capabilities for the storage, retrieval, manipulation and display of geographically located data".
- "A decision support system involving the integration of spatially referenced data in a problem solving environment".
- "A system with advanced geo – modeling capabilities".

Although the above definitions cover a wide range of subjects, the activities best refer to geographical information. Some times it is also termed as Spatial Information Systems as it deals with located data, for objects positioned in any space, not just geographical, a term for world space. Similarly, the term 'a spatial data' is often used as a synonym for attribute data (i.e. rainfall/ temperature/ soil chemical parameters/ population data etc.).

Frequently used technical terms in spatial data handling are:

- Geographic (or geographical) Information System (GIS),
- Geo-information System,
- Spatial Information System (SIS),
- Land Information System (LIS), and
- Multi-purpose Cadastre.

Geographic information systems are used by various disciplines as tools for spatial data handling in a geoinformatics environment.

Depending on the interest of a particular application, a GIS can be considered to be a data store (application of a spatial database), a tool- (box), a technology, an information source or a science (spatial information science).

Like in any other discipline, the use of tools for problem solving is one thing; to produce these tools is something different. Not all are equally well suited for a particular application. Tools can be improved and perfected to better serve a particular need or application. The discipline that provides the background for the production of the tools in spatial data handling is spatial information theory (or SIT).

Geographic information technology is used to manipulate objects in geographic space, and to acquire knowledge from spatial facts. Spatial information theory provides a basis for GIS by bringing together fields that deal with spatial reasoning, the representation of space, and human understanding of space:

Spatial reasoning addresses the inference of spatial information from spatial facts. It deals with the framework and models for space and time, and the relationships that can be identified between objects in a spatio-temporal model of real world phenomena.

Scientific methods for the *representation of space* are important for the development of data models and data structures to represent objects in spatial databases. Spatial databases are distinguished from standard databases by their capability to store and manage data with an extent in space and time (spatial data types).

The *human understanding of space*, influenced by language and culture, plays an important role in how people design and use GIS.

The theory is used for the design of high-level models of spatial phenomena and processes. They are then mapped into conceptual, logical and physical models of spatial databases. The database stands central in the geoinformatics environment. It is the database that holds the data; without it, no useful function can be performed. Data are entered into the database in input processes. Later, they are extracted from the database for spatial analysis and display.

The processes of data management, analysis and display are often supported by rules that are derived from domain experts. Systems that apply stored rules to arrive at conclusions, are called rule-based or knowledge-based systems. Those that support decision making for space-related problems are known as spatial decision support systems (or SDSS). They are becoming increasingly popular in planning agencies and management of natural resources.

All these activities happen in a social, economic and legal context. It is generally referred to as spatial information infrastructure. Everything within this infrastructure and all concepts of space and time in turn are shaped and determined by the cultural background of the individuals and organizations involved.

HISTORY OF GIS

The GIS history dates back to 1960 when computer based GIS have been used and their manual procedures were in life 100 years earlier or so. The initial developments originated in North America with the organizations such as US Bureau of the Census, The US Geological Survey and The Harvard Laboratory for computer graphics and Environmental Systems Research Institute (commercial). Canadian Geographic Information Systems (CGIS) in Canada, Natural Experimental Research Center (NREC), Department of Environment (DOE) and other notable organizations in U.K. were involved in early developments. The laboratory for Computer Graphics and Spatial Analysis of the Harvard Graduate School of Design and the State University of New York at Buffalo achieved worldwide recognition. Commercial agencies started to develop and offer GIS software. Among them were today's market leaders ESRI, Intergraph, Laserscan, Autodesk etc.

A sound and stable data structure to store and analyze map data became dominant in the early 1970's. This has lead to the introduction of topology into GIS. Topology and the related graph theory proved to be effective and efficient tools to provide logically consistent two-dimensional data representations. Another significant break through occurred with the introduction and spread of personal computers in 1980's. It was possible to have a computer on the desk that was able to execute programs that previously could only be run on mainframe computers. At the same time minicomputers, and later, workstations became widely available. Relational database technology became the standard. Research on spatial data structures, indexing methods, and spatial databases made tremendous progress. The 1990's can be characterized as a period of the breakthrough of object-orientation in system and database design, recognition of geoinformatics as a professional activity, and spatial information theory as the theoretical basis for GIS. Potentiality of GIS is realized in the recent past and now it has become popular among many users for a variety of applications.

In India the major developments have happened during the last one-decade with significant contribution coming from Department of Space emphasizing the GIS applications for Natural Resources Management. Notable among them are Natural Resource Information System (NRIS), Integrated Mission for Sustainable Development (IMSD) and Bio-diversity Characterization at National Level. IIRS is also playing a major role in GIS

through education and training programs at the National and International level. Recently the commercial organizations in India have realized the importance of GIS for many applications like natural resource management, infrastructure development, facility management, business/market applications etc. and many GIS based projects according to the user organization requirements were developed.

GIS OBJECTIVES

- Maximize the efficiency of planning and decision making
- Provide efficient means for data distribution and handling
- Elimination of redundant data base - minimize duplication
- Capacity to integrate information from many sources
- Complex analysis/query involving geographical referenced data to generate new information.

For any application there are five generic questions a GIS can answer:

Location	-	What exists at a particular location?
Condition	-	Identify locations where certain conditions exist.
Trends	-	What has changed since?
Patterns	-	What spatial pattern exists?
Modeling	-	What if ……. ?

Elements of A GIS:

The GIS has been divided into four elements. They are hardware, software, data, and liveware. Table-2 gives complete details of different elements.

Table 2: Details of Elements of GIS

S. No.	Elements of GIS	Details
1.	Hardware	Type of Computer Platforms Modest Personnel Computers High performance workstations Minicomputers Mainframe computers Input Devices Scanners Digitizers Tape drivers CD Keyboard Graphic Monitor Output Devices Plotters Printers
2.	Software	Input Modules Editing MRP Manipulation/ Analysis Modules Modeling Capability
3.	Data	Attribute Data Spatial Data Remote Sensing Data Global Database
4.	Liveware	People responsible for digitizing, Implementing using GIS Trained personnel

DATA MODELS

Conversion of real world geographical variation into discrete objects is done through data models. It represents the linkage between the real world domain of geographic data and computer representation of these features. Data models discussed here are for representing the spatial information.

Data models are of two types: Raster and Vector. In raster type of representation of the geographical data, a set of cells located by coordinate is used; each cell is independently addressed with the value of an attribute. Each cell contains a single value and every location corresponds to a cell. One set of cell and associated value is a LAYER. Raster models are simple with which spatial analysis is easier and faster. Raster data models require a huge volume of data to be stored, fitness of data is limited by cell size and output is less

beautiful. Figure 1 shows vector and raster data representation of the real world phenomena.

Vector data model uses line segments or points represented by their explicit x, y coordinates to identify locations. Connecting set of line segments forms area objects. Vector data models require less storage space, outputs are appreciable, Estimation of area/perimeter is accurate and editing is faster and convenient. Spatial analysis is difficult with respect to writing the software program.

The vector model is extremely useful for describing discrete features, but less useful for describing continuously varying features such as soil type or accessibility costs for hospitals. The raster model has evolved to model such continuous features. A raster image comprises a collection of grid cells rather like a scanned map or picture. Both the vector and raster models for storing geographic data have unique advantages and disadvantages. Modern GIS packages are able to handle both models.

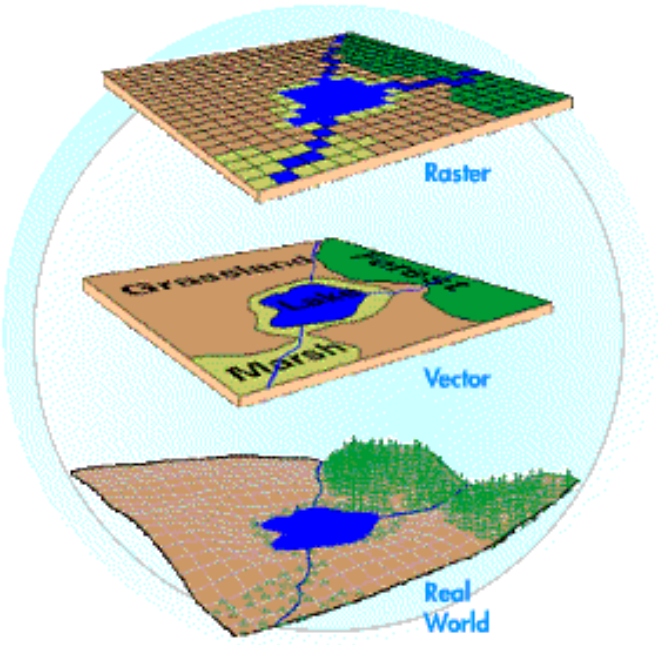

Figure 1: Vector and Raster data examples

Layers and Coverages

The common requirement to access data on the basis of one or more classes has resulted in several GIS employing organizational schemes in which all data of a particular level of classification, such as roads, rivers or vegetation types are grouped into so called layers or coverages. The concept of layers is to be found in both vector and raster models. The layers can be combined with each other in various ways to create new layers that are a function of the individual ones. The characteristic of each layer within a layer-based GIS is that all locations with each layer may be said to belong to a single Arial region or cell, whether it be a polygon bounded by lines in vector system, or a grid cell in a Raster system. But it is possible for each region to have multiple attributes. The Figure 2 shows layers and coverage concept in GIS.

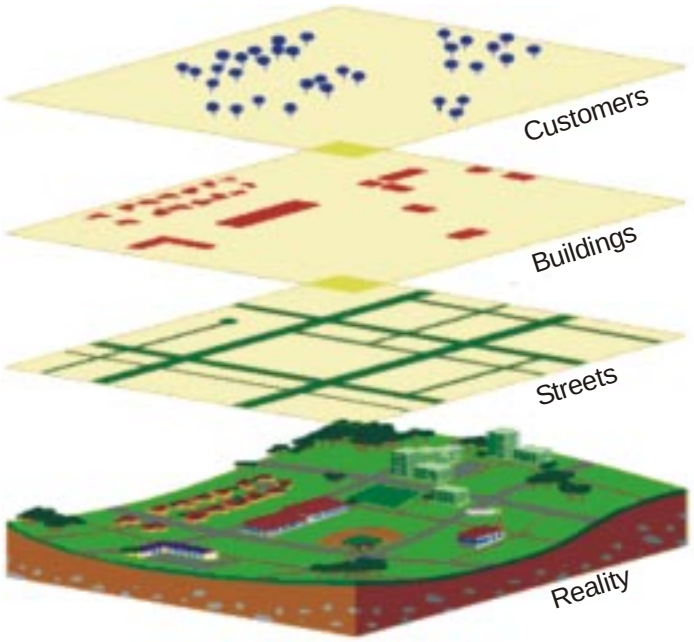

Figure 2: Layers and Coverage concept in GIS

Data Structures

There are number of different ways to organize the data inside the information system. The choice of data structure affects both Data storage volume and processing efficiency. Many GIS software's have specialized

capabilities for storing and manipulating attribute data in addition to spatial information. Three basic data structures are – Relational, Hierarchical and Network.

Relational data structure organizes the data in terms of two-dimensional tables where each table is a separate file (Table 3). Each row in the table is a record and each record has a set of attributes. Each column in the table is an attribute. Different tables are related through the use of a common identifier called KEY. Relation extracts the information, which are defined by query.

Table 3: Example of Relational Database

Settlement name	Settlement status	Settlement population	County name
Gittings	Village	243	Downshire
Bogton	Town	31520	Downshire
Puffings	Village	412	Binglia
Pondside	City	112510	Mereshire

Hierarchical data structure (Fig. 3) stores the data in a way that a hierarchy is maintained among the data items. Each node can be divided into one or more additional node. Stored data gets more and more detailed as one branches further out on the tree.

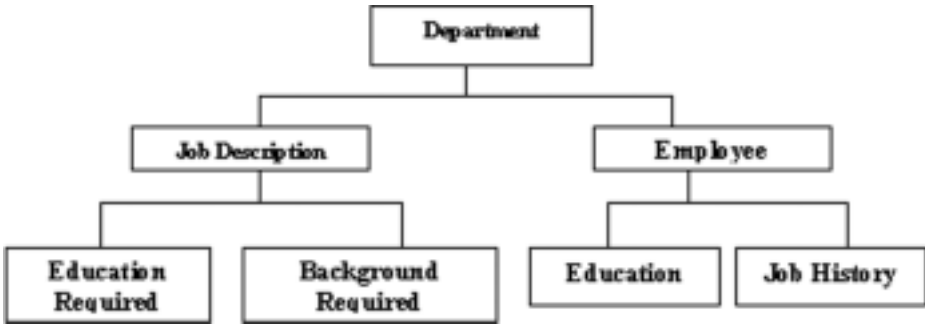

Figure 3: Hierarchical Data Structure

Network data structure (Fig. 4) is similar to hierarchy structure with the exception that in this structure a node may have more than one parent. Each node can be divided into one or more additional nodes. Nodes can have

many parents. The network data structure has the limitation that the pointers must be updated everytime a change is made to database causing considerable overhead.

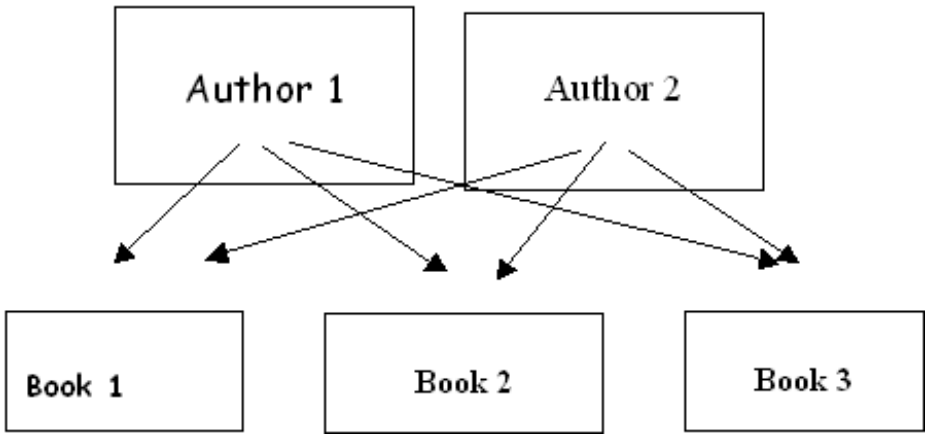

Figure 4: Network Structure

Errors in GIS

Uncertainties and errors are intrinsic to spatial data and need to be addressed properly, not sweeping away the users by high quality colour outputs. Data accuracy is often grouped according to thematic accuracy, positional accuracy and temporal accuracy occurring at various stages in spatial data handling. Given below are some of them while creating the spatial database and analysis.

(i) Errors in GIS environment can be classified into following major groups:

Age of data	-	Reliability decreases with age
Map scale	-	Non-availability of data on a proper scale or Use of data at different scales
Density of observation	-	Sparsely distributed data set is less reliable
Relevance of data	-	Use of surrogate data leads to errors
Data inaccuracy	-	Positional, elevation, minimum mapable unit etc.
Inaccuracy of contents	-	Attributes are erroneously attached

(ii) Errors associated with processing :

Map digitization errors	-	due to boundary location problems on maps and errors associated with digital representation of features
Rasteurization errors	-	due to topological mismatch arising during approximation by grid
Spatial Integration errors	-	due to map integration resulting in spurious polygons
Generalization errors	-	due to aggregation process when features are abstracted to lower scale

Attribute mismatch errors.

Misuse of Logic

The errors are also added from the source of data. Care must be taken in creating spatial databases from the accurate and reliable sources of data. Realizing the importance the users may demand in future to provide them the desired data with a tag showing how much of the data is accurate, spatial data must be presented in quantitative terms.

Spatial Analysis

Whether it is effective utilization of natural resources or sustainable development or natural disaster management, selecting the best site for waste disposal, optimum route alignment or local problems have a geographical component; geoinformatics will give you power to create maps, integrate information, visualize scenarios, solve complicated problems, present powerful ideas, and develop effective solutions like never before. In brief it can be described as a supporting tool for decision-making process. Map making and geographic analysis are not new, but a GIS performs these tasks better and faster than do the old manual methods. Today, GIS is a multibillion-dollar industry employing hundreds of thousands of people worldwide.

GIS is used to perform a variety of Spatial analysis, including overlaying combinations of features and recording resultant conditions, analyzing flows or other characteristics of networks; proximity analysis (i.e. buffet zoning) and

defining districts in terms of spatial criteria. GIS can interrogate geographic features and retrieve associated attribute information, called identification. It can generate new set of maps by query and analysis. It also evolves new information by spatial operations. Following are the analytical procedures applied with a GIS. GIS operational procedure and analytical tasks that are particularly useful for spatial analysis include:

Single layer operations

Multi layer operations/ Topological overlay

Geometric modeling

  Calculating the distance between geographic features

  Calculating area, length and perimeter

  Geometric buffers.

Network analysis

Surface analysis

Raster/Grid analysis

There are many applications of Geoinformatics, viz. facility management, planning, environmental monitoring, population census analysis, insurance assessment, and health service provision, hazard mapping and many other applications. The following list shows few applications in natural resource management:

- Agricultural development
- Land evaluation analysis
- Change detection of vegetated areas
- Analysis of deforestation and associated environmental hazards
- Monitoring vegetation health
- Mapping percentage vegetation cover for the management of land
- Crop acreage and production estimation
- Wasteland mapping

- Soil resources mapping
- Groundwater potential mapping
- Geological and mineral exploration
- Snow-melt run-off forecasting
- Monitoring forest fire
- Monitoring ocean productivity etc.
- GIS application in Forestry

With the rise of World Wide Web, new Internet protocols such as the Hypertext Transfer Protocol (HTTP), as well as easy to use interfaces (browsers), tools and languages (HTML, XML, and Java), the Internet has become a hub for GIS functionalities from the client side without even any GIS software. The GIS field is still evolving and it will be the major force in various walks of life dealing with geographic information.

CONCLUSIONS

Geographic Information System (GIS) is used by multi-disciplines as tools for spatial data handling in a geographic environment. Basic elements of GIS consist of hardware, software, data and liveware. GIS is considered one of the important tool for decision making in problem solving environment dealing with geo-information.

REFERENCES

Aronoff, S. 1989. Geographic Information Systems: A Management Perspective. Ottawa, Canada : WDC Publications.

Burrough, P.A. 1987. Principles of Geographical Information Systems for Land Resource Assessment. Oxford : Claredon Press.

Stillwell John and Clarke Graham (ed.) 1987. Applied GIS and Spatial Analysis. West Sussex : John Wiley and Sons, 2004.

http://www.ncgia.ucsb.edu/~spalladi/thesis/Chapter3.html

http://www.sli.unimelb.edu.au/gisweb/menu.html

http://www.gislinx.com/Software/Programs/MicroStation/index.shtml

http://geog.hkbu.edu.hk/geog3600/ (Hongkong Baptist University)

http://geosun.sjsu.edu/paula/137/ppt/lecture13/sld008.htm

http://www.ccrs.nrcan.gc.ca/ccrs/eduref/tutorial/tutore.html

http://www.cla.sc.edu/gis/avshtcrs/handouts.html

http://www.gisdevelopment.net

http://www.planweb.co.uk/

http://www.sbg.ac.at/geo/idrisi/wwwtutor/tuthome.htm

http://www.ed.ac.uk/

http://www.geoplace.com

FUNDAMENTALS OF GPS

P.L.N. Raju
Geoinformatics Division
Indian Institute of Remote Sensing, Dehra Dun

Abstract : Conventional methods of surveying and navigation require tedious field and astronomical observations for deriving positional and directional information. Rapid advancement in higher frequency signal transmission and precise clock signals along with advanced satellite technology have led to the development of Global Positioning System (GPS). The outcome of a typical GPS survey includes geocentric position accurate to 10 m and relative positions between receiver locations to centimeter level or better. Technological aspect as well as applications of GPS in various fields are discussed in this paper.

INTRODUCTION

Traditional methods of surveying and navigation resort to tedious field and astronomical observation for deriving positional and directional information. Diverse field conditions, seasonal variation and many unavoidable circumstances always bias the traditional field approach. However, due to rapid advancement in electronic systems, every aspect of human life is affected to a great deal. Field of surveying and navigation is tremendously benefited through electronic devices. Many of the critical situations in surveying/navigation are now easily and precisely solved in short time.

Astronomical observation of celestial bodies was one of the standard methods of obtaining coordinates of a position. This method is prone to visibility and weather condition and demands expert handling. Attempts have been made by USA since early 1960's to use space based artificial satellites. System TRANSIT was widely used for establishing a network of control points over large regions. Establishment of modern geocentric datum and its relation to local datum was successfully achieved through TRANSIT. Rapid improvements in higher frequently transmission and precise clock signals along

Satellite Remote Sensing and GIS Applications in Agricultural Meteorology
pp. 121-150

with advanced stable satellite technology have been instrumental for the development of global positioning system.

The NAVSTAR GPS (Navigation System with Time and Ranging Global Positioning System) is a satellite based radio navigation system providing precise three- dimensional position, course and time information to suitably equipped user.

GPS has been under development in the USA since 1973. The US department of Defence as a worldwide navigation and positioning resource for military as well as civilian use for 24 hours and all weather conditions primarily developed it.

In its final configuration, NAVSTAR GPS consists of 21 satellites (plus 3 active spares) at an altitude of 20200 km above the earth's surface (Fig. 1). These satellites are so arranged in orbits to have atleast four satellites visible above the horizon anywhere on the earth, at any time of the day. GPS Satellites transmit at frequencies L1=1575.42 MHz and L2=1227.6 MHz modulated with two types of code viz. P-code and C/A code and with navigation message. Mainly two types of observable are of interest to the user. In pseudo ranging the distance between the satellite and the GPS receiver plus a small corrective

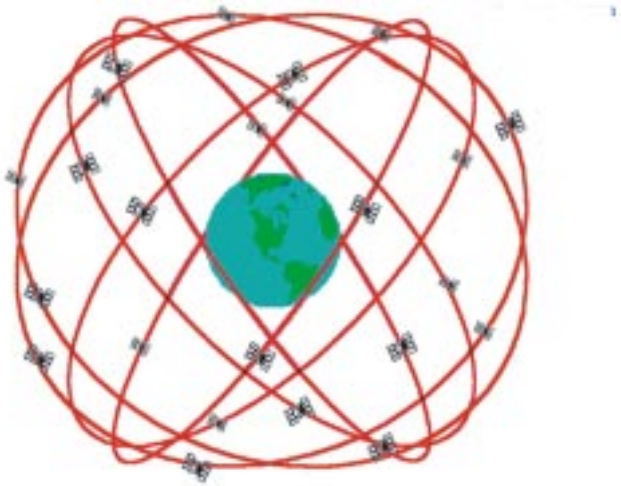

Figure 1: The Global Positioning System (GPS), 21-satellite configuration

term for receiver clock error is observed for positioning whereas in carrier phase techniques, the difference between the phase of the carrier signal transmitted by the satellite and the phase of the receiver oscillator at the epoch is observed to derive the precise information.

The GPS satellites act as reference points from which receivers on the ground detect their position. The fundamental navigation principle is based on the measurement of pseudoranges between the user and four satellites (Fig. 2). Ground stations precisely monitor the orbit of every satellite and by measuring the travel time of the signals transmitted from the satellite four distances between receiver and satellites will yield accurate position, direction and speed. Though three-range measurements are sufficient, the fourth observation is essential for solving clock synchronization error between receiver and satellite. Thus, the term "pseudoranges" is derived. The secret of GPS measurement is due to the ability of measuring carrier phases to about 1/100 of a cycle equaling to 2 to 3 mm in linear distance. Moreover the high frequency L1 and L2 carrier signal can easily penetrate the ionosphere to reduce its effect. Dual frequency observations are important for large station separation and for eliminating most of the error parameters.

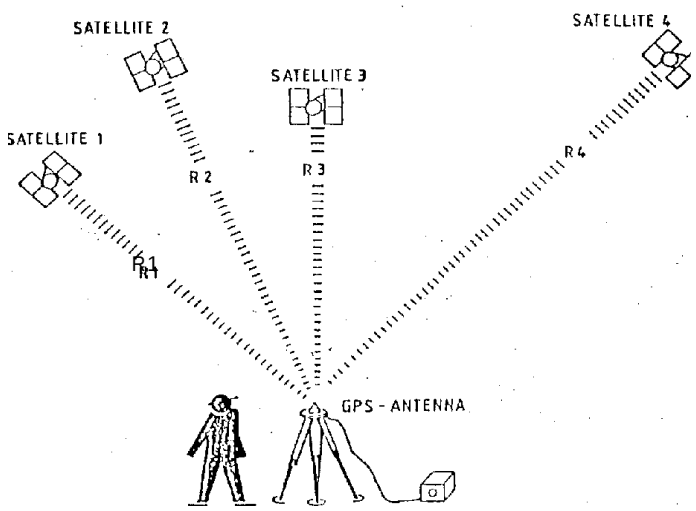

Figure 2: Basic principle of positioning with GPS

There has been significant progress in the design and miniaturization of stable clock. GPS satellite orbits are stable because of the high altitudes and no atmosphere drag. However, the impact of the sun and moon on GPS orbit though significant, can be computed completely and effect of solar radiation

pressure on the orbit and tropospheric delay of the signal have been now modeled to a great extent from past experience to obtain precise information for various applications.

Comparison of main characteristics of TRANSIT and GPS reveal technological advancement in the field of space based positioning system (Table1).

Table 1. TRANSIT vs GPS

Details	TRANSIT	GPS
Orbit Altitude	1000 Km	20,200 Km
Orbital Period	105 Min	12 Hours
Frequencies	150 MHz 400 MHz	1575 MHz 1228 MHz
Navigation data	2D : X, Y	4D : X,Y,Z, t velocity
Availability	15-20 minute per pass	Continuously
Accuracy	ñ 30-40 meters (Depending on velocity error)	ñ15m (Pcode/No. SA 0.1 Knots
Repeatability	—	ñ1.3 meters relative
Satellite Constellation	4-6	21-24
Geometry	Variable	Repeating
Satellite Clock	Quartz	Rubidium, Cesium

GPS has been designed to provide navigational accuracy of ±10 m to ±15 m. However, sub meter accuracy in differential mode has been achieved and it has been proved that broad varieties of problems in geodesy and geodynamics can be tackled through GPS.

Versatile use of GPS for a civilian need in following fields have been successfully practiced viz. navigation on land, sea, air, space, high precision kinematics survey on the ground, cadastral surveying, geodetic control network densification, high precision aircraft positioning, photogrammetry without ground control, monitoring deformations, hydrographic surveys, active control survey and many other similar jobs related to navigation and positioning,. The outcome of a typical GPS survey includes geocentric position accurate to 10 m and relative positions between receiver locations to centimeter level or better.

SEGMENTS OF GPS

For better understanding of GPS, we normally consider three major segments viz. space segment, Control segment and User segment. Space segment deals with GPS satellites systems, Control segment describes ground based time and orbit control prediction and in User segment various types of existing GPS receiver and its application is dealt (Fig. 3).

Table 2 gives a brief account of the function and of various segments along with input and output information.

Table 2. Functions of various segments of GPS

Segment	Input	Function	Output
Space	Navigation message	Generate and Transmit code and carrier phases and navigation message	P-Code C/A Code L1,L2 carrier Navigation message
Control	P-Code Observations Time	Produce GPS time predict ephemeris manage space vehicles	Navigation message
User	Code observation Carrier phase observation Navigation message	Navigation solution Surveying solution	Position velocity time

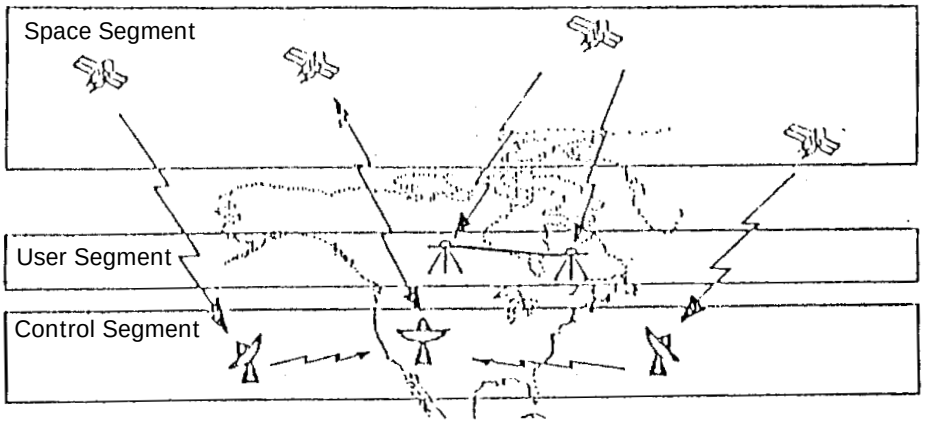

Figure 3: The Space, Control and User segments of GPS

GLONASS (Global Navigation & Surveying System) a similar system to GPS is being developed by former Soviet Union and it is considered to be a valuable complementary system to GPS for future application.

Space Segment

Space segment will consist 21 GPS satellites with an addition of 3 active spares. These satellites are placed in almost six circular orbits with an inclination of 55 degree. Orbital height of these satellites is about 20,200 km corresponding to about 26,600 km from the semi major axis. Orbital period is exactly 12 hours of sidereal time and this provides repeated satellite configuration every day advanced by four minutes with respect to universal time.

Final arrangement of 21 satellites constellation known as "Primary satellite constellation" is given in Fig. 4. There are six orbital planes A to F with a separation of 60 degrees at right ascension (crossing at equator). The position of a satellite within a particular orbit plane can be identified by argument of latitude or mean anomaly M for a given epoch.

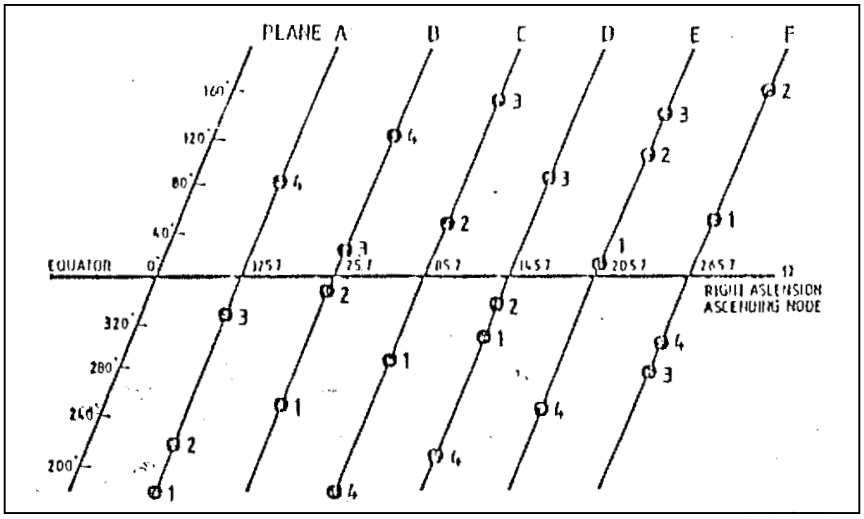

Figure 4: Arrangement of satellites in full constellation

GPS satellites are broadly divided into three blocks : Block-I satellite pertains to development stage, Block II represents production satellite and Block IIR are replenishment/spare satellite.

Under Block-I, NAVSTAR 1 to 11 satellites were launched before 1978 to 1985 in two orbital planes of 63-degree inclination. Design life of these prototype test satellites was only five years but the operational period has been exceeded in most of the cases.

The first Block-II production satellite was launched in February 1989 using channel Douglas Delta 2 booster rocket. A total of 28 Block-II satellites are planned to support 21+3 satellite configuration. Block-II satellites have a designed lifetime of 5-7 years.

To sustain the GPS facility, the development of follow-up satellites under Block-II R has started. Twenty replenishment satellites will replace the current block-II satellite as and when necessary. These GPS satellites under Block-IR have additional ability to measure distances between satellites and will also compute ephemeris on board for real time information.

Fig.5 gives a schematic view of Block-II satellite. Electrical power is generated through two solar panels covering a surface area of 7.2 square meter each. However, additional battery backup is provided to provide energy when the satellite moves into earth's shadow region. Each satellite weighs 845kg and has a propulsion system for positional stabilization and orbit maneuvers.

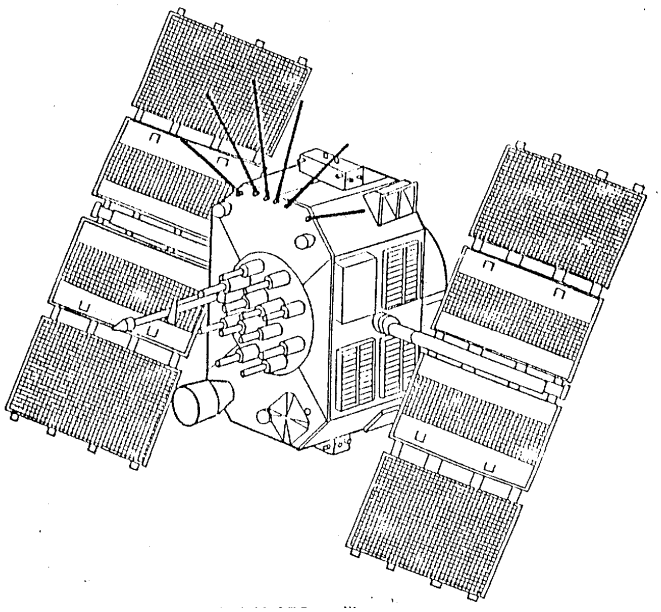

Figure 5: Schematic view of a Block II GPS satellite

GPS satellites have a very high performance frequency standard with an accuracy of between $1X10^{-12}$ to $1X10^{-13}$ and are thus capable of creating precise time base. Block-I satellites were partly equipped with only quartz oscillators but Block-II satellites have two cesium frequency standards and two rubidium frequency standards. Using fundamental frequency of 10.23 MHz, two carrier frequencies are generated to transmit signal codes.

Observation Principle and Signal Structure

NAVSTAR GPS is a one-way ranging system i.e. signals are only transmitted by the satellite. Signal travel time between the satellite and the receiver is observed and the range distance is calculated through the knowledge of signal propagation velocity. One way ranging means that a clock reading at the transmitted antenna is compared with a clock reading at the receiver antenna. But since the two clocks are not strictly synchronized, the observed signal travel time is biased with systematic synchronization error. Biased ranges are known as pseudoranges. Simultaneous observations of four pseudoranges are necessary to determine X, Y, Z coordinates of user antenna and clock bias.

Real time positioning through GPS signals is possible by modulating carrier frequency with Pseudorandom Noise (PRN) codes. These are sequence of binary values (zeros and ones or +1 and -1) having random character but identifiable distinctly. Thus pseudoranges are derived from travel time of an identified PRN signal code. Two different codes viz. P-code and C/A code are in use. P means precision or protected and C/A means clear/acquisition or coarse acquisition.

P- code has a frequency of 10.23 MHz. This refers to a sequence of 10.23 million binary digits or chips per second. This frequency is also referred to as the chipping rate of P-code. Wavelength corresponding to one chip is 29.30m. The P-code sequence is extremely long and repeats only after 266 days. Portions of seven days each are assigned to the various satellites. As a consequence, all satellite can transmit on the same frequency and can be identified by their unique one-week segment. This technique is also called as Code Division Multiple Access (CDMA). P-code is the primary code for navigation and is available on carrier frequencies L1 and L2.

The C/A code has a length of only one millisecond; its chipping rate is 1.023 MHz with corresponding wavelength of 300 meters. C/A code is only transmitted on L1 carrier.

GPS receiver normally has a copy of the code sequence for determining the signal propagation time. This code sequence is phase-shifted in time step-by-step and correlated with the received code signal until maximum correlation is achieved. The necessary phase-shift in the two sequences of codes is a measure of the signal travel time between the satellite and the receiver antennas. This technique can be explained as code phase observation.

For precise geodetic applications, the pseudoranges should be derived from phase measurements on the carrier signals because of much higher resolution. Problems of ambiguity determination are vital for such observations.

The third type of signal transmitted from a GPS satellite is the broadcast message sent at a rather slow rate of 50 bits per second (50 bps) and repeated every 30 seconds. Chip sequence of P-code and C/A code are separately combined with the stream of message bit by binary addition ie the same value for code and message chip gives 0 and different values result in 1.

The main features of all three signal types used in GPS observation viz carrier, code and data signals are given in Table 3.

Table 3. GPS Satellite Signals

Atomic Clock (G, Rb) fundamental frequency	10.23. MHz
L1 Carrier Signal	154 X 10.23 MHz
L1 Frequency	1575.42 MHz
L1 Wave length	19.05 Cm
L2 Carrier Signal	120 X 10.23 MHz
L2 Frequency	1227.60 MHz
L2 Wave Length	24.45 Cm
P-Code Frequency (Chipping Rate)	10.23 MHz (Mbps)
P-Code Wavelength	29.31 M
P-Code Period	267 days : 7 Days/Satellite
C/A-Code Frequency (Chipping Rate)	1.023 MHz (Mbps)
C/A-Code Wavelength	293.1 M
C/A-Code Cycle Length	1 Milisecond
Data Signal Frequency	50 bps
Data Signal Cycle Length	30 Seconds

The signal structure permits both the phase and the phase shift (Doppler effect) to be measured along with the direct signal propagation. The necessary bandwidth is achieved by phase modulation of the PRN code as illustrated in Fig. 6.

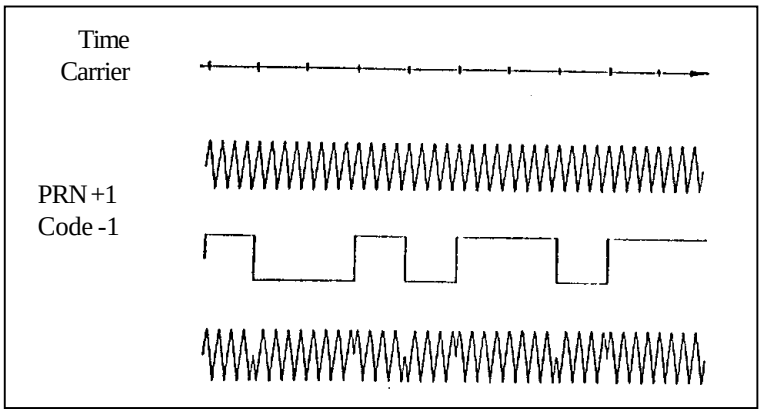

Figure 6: Generation of GPS Signals

Structure of the GPS Navigation Data

Structure of GPS navigation data (message) is shown in Fig. 7. The user has to decode the data signal to get access to the navigation data. For on line navigation purposes, the internal processor within the receiver does the decoding. Most of the manufacturers of GPS receiver provide decoding software for post processing purposes.

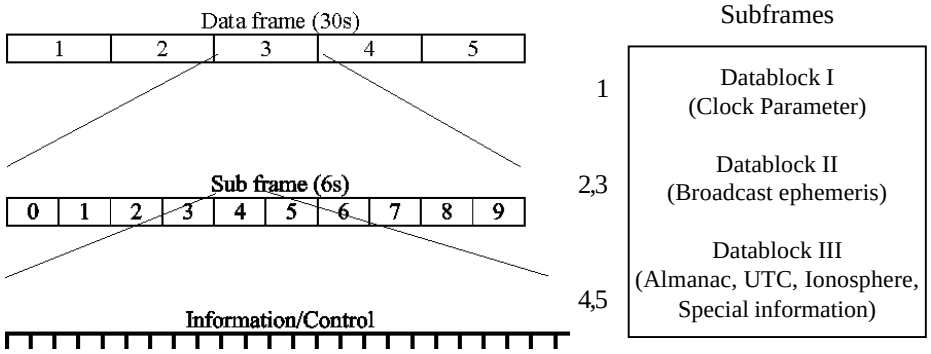

Figure 7: Structure of Navigation data

With a bit rate of 50 bps and a cycle time of 30 seconds, the total information content of a navigation data set is 1500 bits. The complete data frame is subdivided into five subframes of six-second duration comprising 300 bits of information. Each subframe contains the data words of 30 bits each. Six of these are control bits. The first two words of each subframe are the Telemetry Work (TLM) and the C/A-P-Code Hand over Work (HOW). The TLM work contains a synchronization pattern, which facilitates the access to the navigation data.

The navigation data record is divided into three data blocks:

Data Block I — appears in the first subframe and contains the clock coefficient/bias.

Data Block II — appears in the second and third subframe and contains all necessary parameters for the computation of the satellite coordinates.

Data Block III — appears in the fourth and fifth subframes and contains the almanac data with clock and ephemeris parameter for all available satellite of the GPS system. This data block includes also ionospheric correction parameters and particular alphanumeric information for authorized users.

Unlike the first two blocks, the subframe four and five are not repeated every 30 seconds.

International Limitation of the System Accuracy

Since GPS is a military navigation system of US, a limited access to the total system accuracy is made available to the civilian users. The service available to the civilians is called Standard Positioning System (SPS) while the service available to the authorized users is called the Precise Positioning Service (PPS). Under current policy the accuracy available to SPS users is 100m, 2D-RMS and for PPS users it is 10 to 20 meters in 3D. Additional limitation viz. Anti-Spoofing (AS), and Selective Availability (SA) was further imposed for civilian users. Under AS, only authorized users will have the means to get access to the P-code. By imposing SA condition, positional accuracy from Block-II satellite was randomly offset for SPS users. Since May 1, 2000 according to declaration of US President, SA is switched off for all users.

The GPS system time is defined by the cesium oscillator at a selected monitor station. However, no clock parameter are derived for this station. GPS time is indicated by a week number and the number of seconds since the beginning of the current week. GPS time thus varies between 0 at the beginning of a week to 6,04,800 at the end of the week. The initial GPS epoch is January 5, 1980 at 0 hours Universal Time. Hence, GPS week starts at Midnight (UT) between Saturday and Sunday. The GPS time is a continuous time scale and is defined by the main clock at the Master Control Station (MCS). The leap seconds is UTC time scale and the drift in the MCS clock indicate that GPS time and UTC are not identical. The difference is continuously monitored by the control segment and is broadcast to the users in the navigation message. Difference of about 7 seconds was observed in July, 1992.

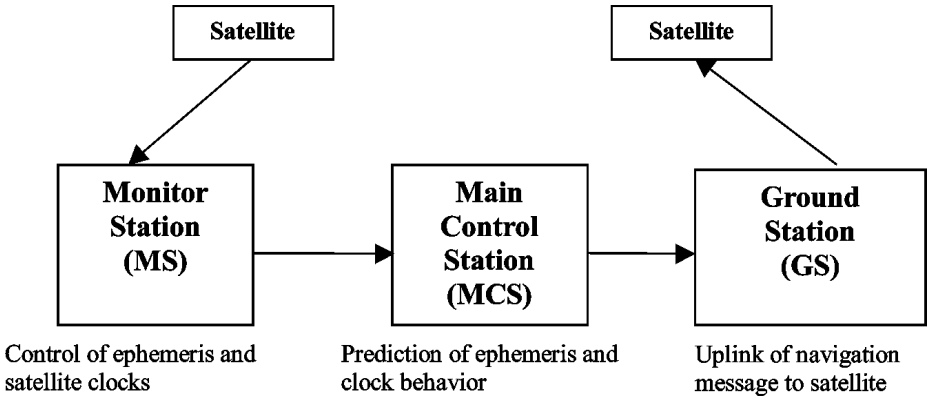

Figure 8: Data Flow in the determination of the broadcast ephemeris

GPS satellite is identified by two different numbering schemes. Based on launch sequence, SVN (Space Vehicle Number) or NAVSTAR number is allocated. PRN (Pseudo Random Noise) or SVID (Space Vehicle Identification) number is related to orbit arrangement and the particular PRN segment allocated to the individual satellite. Usually the GPS receiver displays PRN number.

Control Segment

Control segment is the vital link in GPS technology. Main functions of the control segment are:

- Monitoring and controlling the satellite system continuously
- Determine GPS system time
- Predict the satellite ephemeris and the behavior of each satellite clock.
- Update periodically the navigation message for each particular satellite.

For continuos monitoring and controlling GPS satellites a master control stations (MCS), several monitor stations (MS) and ground antennas (GA) are located around the world (Fig. 9). The operational control segment (OCS) consists of MCS near Colorado springs (USA), three MS and GA in Kwajaleian Ascension and Diego Garcia and two more MS at Colorado Spring and Hawai.

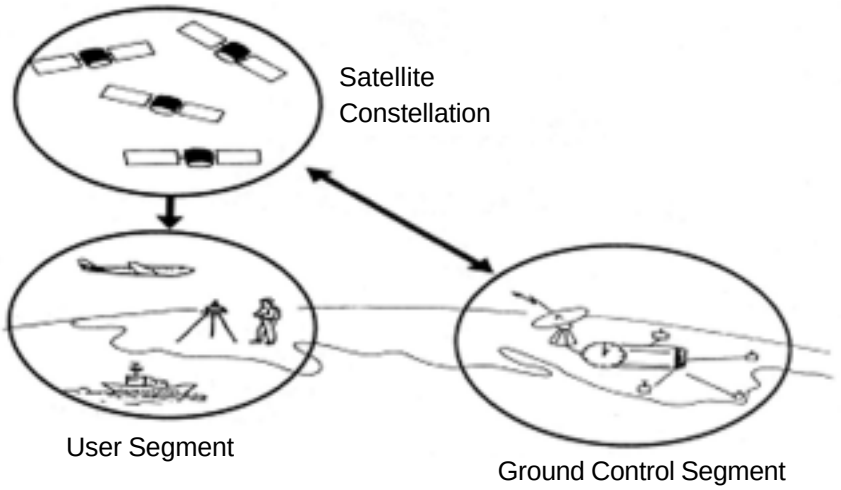

Figure 9: Control segment with observation stations

The monitor station receives all visible satellite signals and determines their pseudorages and then transmits the range data along with the local meteorological data via data link to the master control stations. MCS then precomputes satellite ephemeris and the behaviour of the satellite clocks and formulates the navigation data. The navigation message data are transmitted to the ground antennas and via S-band it links to the satellites in view. Fig. 9 shows this process schematically. Due to systematic global distribution of upload antennas, it is possible to have atleast three contacts per day between the control segment and each satellite.

User Segment

Appropriate GPS receivers are required to receive signal from GPS satellites for the purpose of navigation or positioning. Since, GPS is still in its development phase, many rapid advancements have completely eliminated bulky first generation user equipments and now miniature powerful models are frequently appearing in the market.

BASIC CONCEPT OF GPS RECEIVER AND ITS COMPONENTS

The main components of a GPS receiver are shown in Fig. 10. These are:

- Antenna with pre-amplifier
- RF section with signal identification and signal processing
- Micro-processor for receiver control, data sampling and data processing
- Precision oscillator
- Power supply
- User interface, command and display panel
- Memory, data storage

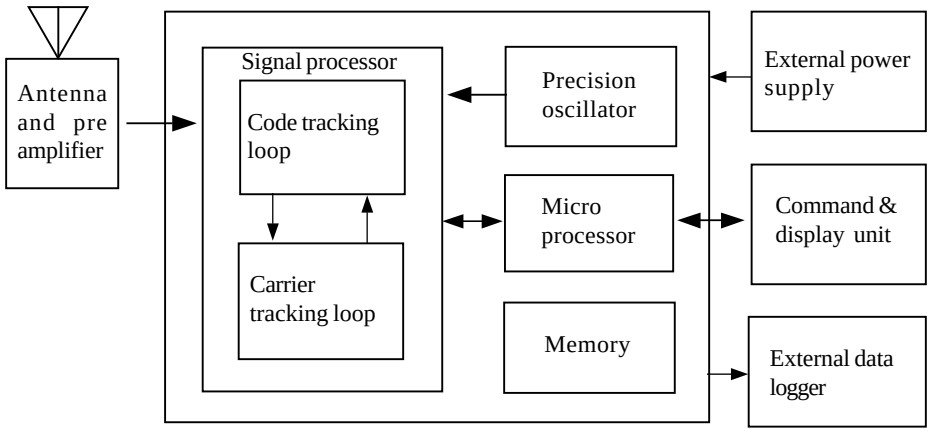

Figure 10: Major components of a GPS receiver

Antenna

Sensitive antenna of the GPS receiver detects the electromagnetic wave signal transmitted by GPS satellites and converts the wave energy to electric current] amplifies the signal strength and sends them to receiver electronics.

Several types of GPS antennas in use are mostly of following types (Fig. 11).

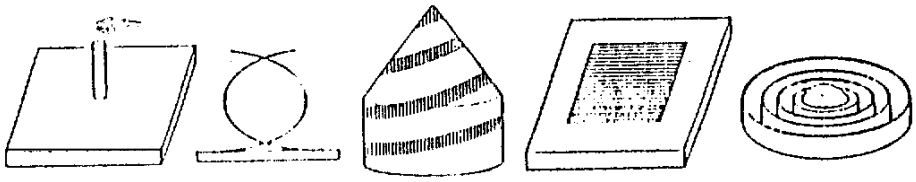

Figure 11: Types of GPS Antenna

- Mono pole or dipole
- Quadrifilar helix (Volute)
- Spiral helix
- Microstrip (patch)
- Choke ring

Microstrip antennas are most frequently used because of its added advantage for airborne application, materialization of GPS receiver and easy construction. However, for geodetic needs, antennas are designed to receive both carrier frequencies L1 and L2. Also they are protected against multipath by extra ground planes or by using choke rings. A choke ring consists of strips of conductor which are concentric with the vertical axis of the antenna and connected to the ground plate which in turns reduces the multipath effect.

RF Section with Signal Identification and Processing

The incoming GPS signals are down converted to a lower frequency in the RS section and processed within one or more channels. Receiver channel is the primary electronic unit of a GPS receiver. A receiver may have one or more channels. In the parallel channel concept each channel is continuously

franking one particular satellite. A minimum of four parallel channels is required to determine position and time. Modern receivers contain upto 12 channels for each frequency.

In the sequencing channel concept the channel switches from satellite to satellite at regular interval. A single channel receiver takes atleast four times of 30 seconds to establish first position fix, though some receiver types have a dedicated channel for reading the data signal. Now days in most of the cases fast sequencing channels with a switching rate of about one-second per satellite are used.

In multiplexing channel, sequencing at a very high speed between different satellites is achieved using one or both frequencies. The switching rate is synchronous with the navigation message of 50 bps or 20 milliseconds per bit. A complete sequence with four satellites is completed by 20 millisecond or after 40 millisecond for dual frequency receivers. The navigation message is continuous, hence first fix is achieved after about 30 seconds.

Though continuous tracking parallel channels are cheap and give good overall performance, GPS receivers based on multiplexing technology will soon be available at a cheaper price due to electronic boom.

Microprocessor

To control the operation of a GPS receiver, a microprocessor is essential for acquiring the signals, processing of the signal and the decoding of the broadcast message. Additional capabilities of computation of on-line position and velocity, conversion into a given local datum or the determination of waypoint information are also required. In future more and more user relevant software will be resident on miniaturized memory chips.

Precision Oscillator

A reference frequency in the receiver is generated by the precision oscillator. Normally, less expensive, low performance quartz oscillator is used in receivers since the precise clock information is obtained from the GPS satellites and the user clock error can be eliminated through double differencing technique when all participating receivers observe at exactly the same epoch. For navigation with two or three satellites only an external high precision oscillator is used.

Power Supply

First generation GPS receivers consumed very high power, but modern receivers are designed to consume as little energy as possible. Most receivers have an internal rechargeable Nickel-Cadmium battery in addition to an external power input. Caution of low battery signal prompts the user to ensure adequate arrangement of power supply.

Memory Capacity

For port processing purposes all data have to be stored on internal or external memory devices. Post processing is essential for multi station techniques applicable to geodatic and surveying problems. GPS observation for pseudoranges, phase data, time and navigation message data have to be recorded. Based on sampling rate, it amount to about 1.5 Mbytes of data per hour for six satellites and 1 second data for dual frequency receivers. Modern receivers have internal memories of 5 Mbytes or more. Some receivers store the data on magnetic tape or on a floppy disk or hard-disk using external microcomputer connected through RS-232 port.

Most modern receivers have a keypad and a display for communication between the user and the receivers. The keypad is used to enter commands, external data like station number or antenna height or to select a menu operation. The display indicates computed coordinates, visible satellites, data quality indices and other suitable information. Current operation software packages are menu driven and very user friendly.

Classification of GPS Receivers

GPS receivers can be divided into various groups according to different criteria. In the early stages two basic technologies were used as the classification criteria viz. Code correlation receiver technology and sequencing receiver technology, which were equivalent to code dependent receivers and code free receivers. However, this kind of division is no longer justifiable since both techniques are implemented in present receivers.

Another classification of GPS receivers is based on acquisition of data types e.g.

- C/A code receiver
- C/A code + L1 Carrier phase
- C/A code + L1 Carrier phase + L2 Carrier phase
- C/A code + p_code + L1, L2 Carrier phase
- L1 Carrier phase (not very common)
- L1, L2 Carrier phase (rarely used)

Based on technical realization of channel, the GPS receivers can be classified as:

- Multi-channel receiver
- Sequential receiver
- Multiplexing receiver

GPS receivers are even classified on the purpose as :

- Military receiver
- Civilian receiver
- Navigation receiver
- Timing receiver
- Geodetic receiver

For geodetic application it is essential to use the carrier phase data as observable. Use of L1 and L2 frequency is also essential along with P-code.

Examples of GPS Receiver

GPS receiver market is developing and expanding at a very high speed. Receivers are becoming powerful, cheap and smaller in size. It is not possible to give details of every make but description of some typical receivers given may be regarded as a basis for the evaluation of future search and study of GPS receivers.

Classical Receivers

Detailed description of code dependent T1 4100 GPS Navigator and code free Macrometer V1000 is given here:

T1 4100 GPS Navigator was manufactured by Texas Instrument in 1984. It was the first GPS receiver to provide C/A and P code and L1 and L2 carrier phase observations. It is a dual frequency multiplexing receiver and suitable for geodesist, surveyor and navigators. The observables through it are:

- P-Code pseudo ranges on L1 and L2
- C/A-Code pseudo ranges on L1
- Carrier phase on L1 and L2

The data are recorded by an external tape recorder on digital cassettes or are downloaded directly to an external microprocessor. A hand held control display unit (CDU) is used for communication between observer and the receiver. For navigational purposes the built in microprocessor provides position and velocity in real time every three seconds. T1 4100 is a bulky instrument weighing about 33 kg and can be packed in two transportation cases. It consumes 90 watts energy in operating mode of 22V - 32V. Generator use is recommended. The observation noise in P-Code is between 0.6 to 1 m, in C/A code it ranges between 6 to 10 m and for carrier phase it is between 2 to 3 m.

T1 4100 has been widely used in numerous scientific and applied GPS projects and is still in use. The main disadvantages of the T1 4100 compared to more modern GPS equipment's are

- Bulky size of the equipment
- High power consumption
- Difficult operation procedure
- Limitation of tracking four satellites simultaneously
- High noise level in phase measurements

Sensitivity of its antenna for multipath and phase centre variation if two receivers are connected to one antenna and tracking of seven satellites simultaneously is possible. For long distances and in scientific projects, T1 4100 is still regarded useful. However, due to imposition of restriction on P-code for civilian, T1 4100 during Anti Spoofing (AS) activation can only be used as a single frequency C/A code receiver.

The MACROMETER V 1000, a code free GPS receiver was introduced in 1982 and was the first receiver for geodetic applications. Precise results

obtained through it has demonstrated the potential of highly accurate GPS phase observations. It is a single frequency receiver and tracks 6 satellites on 6 parallel channels. The complete system consists of three units viz.

- Receiver and recorder with power supply
- Antenna with large ground plane
- P 1000 processor

The processor is essential for providing the almanac data because the Macrometer V 1000 cannot decode the satellite messages and process the data. At pre determined epoches the phase differences between the received carrier signal and a reference signal from receiver oscillator is measured. A typical baseline accuracy reported for upto 100 km distance is about 1 to 2 ppm (Parts per million).

Macrometer II, a dual frequency version was introduced in 1985. Though it is comparable to Macrometer V 1000, its power consumption and weight are much less. Both systems require external ephemeredes. Hence specialized operators of few companies are capable of using it and it is required to synchronize the clock of all the instruments proposed to be used for a particular observation session. To overcome above disadvantages, the dual frequency Macrometer II was further miniaturized and combined with a single frequency C/A code receiver with a brand name MINIMAC in 1986, thus becoming a code dependent receiver.

Examples of present Geodetic GPS Receivers

Few of the currently available GPS receivers that are used in geodesy surveying and precise navigation are described. Nearly all models started as single frequency C/A-Code receivers with four channels. Later L2 carrier phase was added and tracking capability was increased. Now a days all leading manufacturers have gone for code-less, non sequencing L2 technique. WILD/ LEITZ (Heerbrugg, Switzerland) and MAGNAVOX (Torrance, California) have jointly developed WM 101 geodetic receiver in 1986. It is a four channel L1 C/A code receiver. Three of the channels sequentially track upto six satellites and the fourth channel, a house keeping channels, collects the satellite message and periodically calibrates the inter channel biases. C/A-code and reconstructed L1 carrier phase data are observed once per second.

The dual frequency WM 102 was marketed in 1988 with following key features:

- L1 reception with seven C/A code channel tracking upto six satellites simultaneously.
- L2 reception of upto six satellites with one sequencing P- code channel
- Modified sequencing technique for receiving L2 when P-code signals are encrypted.

The observations can be recorded on built in data cassettes or can be transferred on line to an external data logger in RS 232 or RS 422 interface. Communication between operator and receiver is established by alpha numerical control panel and display WM 101/102 has a large variety of receiver resident menu driven options and it is accompanied by comprehensive post processing software.

In 1991, WILD GPS system 200 was introduced. Its hardware comprises the Magnavox SR 299 dual frequency GPS sensor, the hand held CR 233 GPS controller and a Nicd battery. Plug in memory cards provide the recording medium. It can track 9 satellites simultaneously on L1 and L2. Reconstruction of carrier phase on L1 is through C/A code and on L2 through P-code. The receiver automatically switches to codeless L2 when P-code is encrypted. It consumes 8.5 watt through 12-volt power supply.

TRIMBLE NAVIGATION (Sunny vale, California) has been producing TRIMBLE 4000 series since 1985. The first generation receiver was a L1 C/A code receiver with five parallel channels providing tracking of 5 satellites simultaneously. Further upgradation included increasing the number of channels upto tweleve, L2 sequencing capability and P-code capability. TRIMBLE Geodatic Surveyor 4000 SSE is the most advanced model. When P-Code is available, it can perform following types of observations, viz.,

- Full cycle L1 and L2 phase measurements
- L1 and L2, P-Code measurements when AS is on and P-code is encrypted
- Full cycle L1 and L2 phase measurement
- Low noise L1, C/A code
- Cross-correlated Y-Code data

Observation noise of the carrier phase measurement when P-code is available is about ñ 0-2mm and of the P-code pseudoranges as low as ñ 2cm. Therefore, it is very suitable for fast ambiguity solution techniques with code/ carrier combinations.

ASHTECH (Sunnyvale, California) developed a GPS receiver with 12 parallel channels and pioneered current multi-channel technology. ASHTECH XII GPS receiver was introduced in 1988. It is capable of measuring pseudoranges, carrier phase and integrated dopler of up to 12 satellites on L1. The pseudoranges measurement are smoothed with integrated Doppler. Postion velociy, time and navigation informations are displayed on a keyboard with a 40-characters display. L2 option adds 12 physical L2 squaring type channels.

ASHTECH XII GPS receiver is a most advanced system, easy to handle and does not require initialization procedures. Measurements of all satellites in view are carried out automatically. Data can be stored in the internal solid plate memory of 5 Mbytes capacity. The minimum sampling interval is 0.5 seconds. Like many other receivers it has following additional options viz.

- 1 ppm timing signal output
- Photogrammetric camera input
- Way point navigation
- Real time differential navigation and provision of port processing and vision planning software

In 1991, ASHTECH P-12 GPS receiver was marketed. It has 12 dedicated channels of L1, P-code and carrier and 12 dedicated channels of L2, P-code and carrier. It also has 12 L1, C/A code and carrier channels and 12 code less squaring L2 channels. Thus the receiver contains 48 channels and provides all possibilities of observations to all visible satellites. The signal to noise level for phase measurement on L2 is only slightly less than on L1 and significantly better than with code-less techniques. In cases of activated P-code encryption, the code less L2 option can be used.

TURBO ROGUE SNR-8000 is a portable receiver weighing around 4 kg, consumes 15-watt energy and is suitable for field use. It has 8 parallel channels on L1 and L2. It provides code and phase data on both frequencies

and has a codeless option. Full P-code tracking provides highest precision phase and pseudo rages measurements, codeless tracking is automatic "full back" mode. The code less mode uses the fact that each carrier has identical modulation of P-code/Y-code and hence the L1 signal can be cross-correlated with the L2 signal. Results are the differential phase measurement (L1-L2) and the group delay measurement (P1-P2)

Accuracy specifications are :

P-Code pseudo range	1cm (5 minutes integration)
Codeless pseudo range	10cm (5 minutes integration)
Carrier phase	0.2 - 0.3 mm
Codeless phase	0.2 - 0.7 mm

One of the important features is that less than 1 cycle slip is expected for 100 satellite hours.

Navigation Receivers

Navigation receivers are rapidly picking up the market. In most cases a single C/A code sequencing or multiplexing channel is used. However, modules with four or five parallel channels are becoming increasingly popular. Position and velocity are derived from C/A code pseudoranges measurement and are displayed or downloaded to a personal computer. Usually neither raw data nor carrier phase information is available. Differential navigation is possible with some advanced models.

MAGELLAN NAV 1000 is a handheld GPS receiver and weighs only 850 grams. It was introduced in 1989 and later in 1990, NAV 1000 PRO model was launched. It is a single channel receiver and tracks 3 to 4 satellites with a 2.5 seconds update rate and has a RS 232 data port.

The follow up model in 1991 was NAV 5000 PRO. It is a 5-channel receiver tracking all visible satellites with a 1-second update rate. Differential navigation is possible. Carrier phase data can be used with an optional carrier phase module. The quadrifilar antenna is integrated to the receiver. Post processing of data is also possible using surveying receiver like ASHTECH XII located at a reference station. Relative accuracy is about 3 to 5 metres. This is in many cases sufficient for thematic purposes.

Many hand held navigation receivers are available with added features. The latest market situation can be obtained through journals like GPS world etc.

For most navigation purpose a single frequency C/A code receiver is sufficient. For accuracy requirements better than 50 to 100 meters, a differential option is essential. For requirement below 5 meters, the inclusion of carrier phase data is necessary. In high precision navigation the use of a pair of receivers with full geodetic capability is advisable.

The main characteristics of multipurpose geodetic receiver are summarized in Table 4.

Table 4. Overview of geodetic dual-frequency GPS satellite receiver (1992)

Receiver	Channel		Code		Wavelength		Anti-spoofing
	L1	L2	L1	L2	L1	L2	
TI 4100	4	4	P	P			Single frequency
MACROMETER	6	6	-	-		/2	No influence
ASHTECH XII	12	12	C/A	-		/2	No influence
ASHTECH P 12	12	12	C/A, P	P			Squaring
TRIMBLE SST	8-12	8-12	C/A	-		/2	No influence
TRIMBLE 4000	9-12	9-12	C/A, P	P			Codeless SSE
WM 102	7 par	1 seq	C/A	P			Squaring
WILD GPS 200	9	9	C/A	p			Codeless
TURBO ROGUE	8	8	C/A, P	P			Codeless

Some of the important features for selecting a geodetic receiver are :

- Tracking of all satellites
- Both frequencies
- Full wavelength on L2
- Low phase noise-low code noise
- High sampling rate for L1 and L2
- High memory capacity

- Low power consumption
- Full operational capability under anti spoofing condition

Further, it is recommended to use dual frequency receiver to minimize ion-spherical influences and take advantages in ambiguity solution.

Accuracy

In general, an SPS receiver can provide position information with an error of less than 25 meter and velocity information with an error less than 5 meters per second. Upto 2 May 2000 U.S Government has activated Selective Availability (SA) to maintain optimum military effectiveness. Selective Availability inserts random errors into the ephemeris information broadcast by the satellites, which reduces the SPS accuracy to around 100 meters.

For many applications, 100-meter accuracy is more than acceptable. For applications that require much greater accuracy, the effects of SA and environmentally produced errors can be overcome by using a technique called Differential GPS (DGPS), which increases overall accuracy.

Differential Theory

Differential positioning is technique that allows overcoming the effects of environmental errors and SA on the GPS signals to produce a highly accurate position fix. This is done by determining the amount of the positioning error and applying it to position fixes that were computed from collected data.

Typically, the horizontal accuracy of a single position fix from a GPS receiver is 15 meter RMS (root-mean square) or better. If the distribution of fixes about the true position is circular normal with zero mean, an accuracy of 15 meters RMS implies that about 63% of the fixes obtained during a session are within 15 meters of the true position.

Types of Errors

There are two types of positioning errors: correctable and non-correctable. Correctable errors are the errors that are essentially the same for two GPS receivers in the same area. Non-correctable errors cannot be correlated between two GPS receivers in the same area.

Correctable Errors

Sources of correctable errors include satellite clock, ephemeris data and ionosphere and tropospheric delay. If implemented, SA may also cause a correctable positioning error. Clock errors and ephemeris errors originate with the GPS satellite. A clock error is a slowly changing error that appears as a bias on the pseudorange measurement made by a receiver. An ephemeris error is a residual error in the data used by a receiver to locate a satellite in space.

Ionosphere delay errors and tropospheric delay errors are caused by atmospheric conditions. Ionospheric delay is caused by the density of electrons in the ionosphere along the signal path. A tropspheric delay is related to humidity, temperature, and altitude along the signal path. Usually, a tropospheric error is smaller than an ionospheric error.

Another correctable error is caused by SA which is used by U.S Department of Defence to introduce errors into Standard Positioning Service (SPS) GPS signals to degrade fix accuracy.

The amount of error and direction of the error at any given time does not change rapidly. Therefore, two GPS receivers that are sufficiently close together will observe the same fix error, and the size of the fix error can be determined.

Non-Correctable Errors

Non-correctable errors cannot be correlated between two GPS receivers that are located in the same general area. Sources of non-correctable errors include receiver noise, which is unavoidably inherent in any receiver, and multipath errors, which are environmental. Multi-path errors are caused by the receiver “seeing” reflections of signals that have bounced off of surrounding objects. The sub-meter antenna is multipath-resistant; its use is required when logging carrier phase data. Neither error can be eliminated with differential, but they can be reduced substantially with position fix averaging. The error sources and the approximate RMS error range are given in the Table 5.

Table 5. Error Sources

Error Source	Approx. Equivalent Range Error (RMS) in meters
Correctable with Differential	
Clock (Space Segment)	3.0
Ephemeris (Control Segment)	2.7
Ionospheric Delay (Atmosphere)	8.2
Tropospheric Delay (Atmosphere)	1.8
Selective Availability (if implemented)	27.4
Total	28.9
Non-Correctable with Differential	
Receiver Noise (Unit)	9.1
Multipath (Environmental)	3.0
Total	9.6
Total user Equivalent range error (all sources)	30.5
Navigational Accuracy (HDOP = 1.5)	45.8

DIFFERENTIAL GPS

Most DGPS techniques use a GPS receiver at a geodetic control site whose position is known. The receiver collects positioning information and calculates a position fix, which is then compared to the known co-ordinates. The difference between the known position and the acquired position of the control location is the positioning error.

Because the other GPS receivers in the area are assumed to be operating under similar conditions, it is assumed that the position fixes acquired by other receivers in the area (remote units) are subject to the same error, and that the correction computed for the control position should therefore be accurate for those receivers. The correction is communicated to the remote units by an operator at the control site with radio or cellular equipment. In post-processed differential, all units collect data for off-site processing; no corrections are determined in the field. The process of correcting the position error with differential mode is shown in the Figure 12.

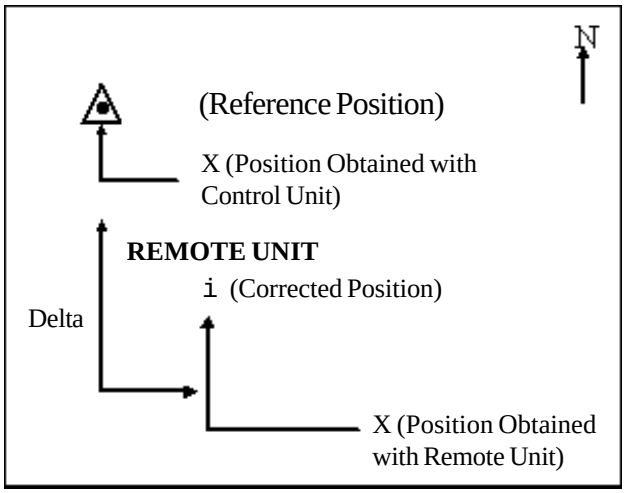

Figure 12: A Position Error Corrected with Differential

The difference between the known position and acquired position at the control point is the DELTA correction. DELTA, which is always expressed in meters, is parallel to the surface of the earth. When expressed in local co-ordinate system, DELTA uses North-South axis (y) and an East-West axis (x) in 2D operation; an additional vertical axis (z) that is perpendicular to the y and x is used in 3D operation for altitude.

APPLICATIONS OF GPS

- Providing Geodetic control.
- Survey control for Photogrammetric control surveys and mapping.
- Finding out location of offshore drilling.
- Pipeline and Power line survey.
- Navigation of civilian ships and planes.
- Crustal movement studies.
- Geophysical positioning, mineral exploration and mining.
- Determination of a precise geoid using GPS data.
- Estimating gravity anomalies using GPS.
- Offshore positioning: shiping, offshore platforms, fishing boats etc.

VARIOUS MAKES OF GPS

TRIMBLE GPS AS A ROVER

GARMIN 12 CHANNEL GPS

MAGELLAN GPS - 315 SERIES

CONCLUSIONS

Global Positioning System (GPS) is currently designed to provide navigational accuracy of ±10 m to ±15 m. However, sub meter accuracy in differential mode has been achieved and it has been proved that broad varieties of problems in geodesy and geo-dynamics can be tackled through GPS. GPS service consists of three components, viz. space, control and user.

REFERENCES

GPS Positioning Guide: A user guide to the Global Positioning System. Natural Resources, Canada. URC : uttp://www.geod.nrcan.gc.ca

GPS World Periodicals.

Proceedings of ION, GPS, 2002. Portland, Oregon, USA Sept. 2002.

Seeber, Gunter 2003. Satellite Geodesy (2nd Edition). Walter de Gruyter Inc. ISBN : 31101 75495.

SPATIAL DATA ANALYSIS

P.L.N. Raju
Geoinformatics Division
Indian Institute of Remote Sensing, Dehra Dun

Abstract : Spatial analysis is the vital part of GIS. Spatial analysis in GIS involves three types of operations- attribute query (also known as non-spatial), spatial query and generation of new data sets from the original databases. Various spatial analysis methods viz. single/multiplayer operations/overlay; spatial modeling; geometric modeling; point pattern analysis; network analysis; surface analysis; raster/grid analysis etc. are discussed in detail in this paper.

INTRODUCTION

Geographic analysis allows us to study and understand the real world processes by developing and applying manipulation, analysis criteria and models and to carryout integrated modeling. These criteria illuminate underlying trends in geographic data, making new information available. A GIS enhances this process by providing tools, which can be combined in meaningful sequence to reveal new or previously unidentified relationships within or between data sets, thus increasing better understanding of real world. The results of geographic analysis can be commercial in the form of maps, reports or both. Integration involves bringing together diverse information from a variety of sources and analysis of multi-parameter data to provide answers and solutions to defined problems.

Spatial analysis is the vital part of GIS. It can be done in two ways. One is the vector-based and the other is raster-based analysis. Since the advent of GIS in the 1980s, many government agencies have invested heavily in GIS installations, including the purchase of hardware and software and the construction of mammoth databases. Two fundamental functions of GIS have been widely realized: generation of maps and generation of tabular reports.

Satellite Remote Sensing and GIS Applications in Agricultural Meteorology
pp. 151-174

Indeed, GIS provides a very effective tool for generating maps and statistical reports from a database. However, GIS functionality far exceeds the purposes of mapping and report compilation. In addition to the basic functions related to automated cartography and data base management systems, the most important uses of GIS are spatial analysis capabilities. As spatial information is organized in a GIS, it should be able to answer complex questions regarding space.

Making maps alone does not justify the high cost of building a GIS. The same maps may be produced using a simpler cartographic package. Likewise, if the purpose is to generate tabular output, then a simpler database management system or a statistical package may be a more efficient solution. It is spatial analysis that requires the logical connections between attribute data and map features, and the operational procedures built on the spatial relationships among map features. These capabilities make GIS a much more powerful and cost-effective tool than automated cartographic packages, statistical packages, or data base management systems. Indeed, functions required for performing spatial analyses that are not available in either cartographic packages or data base management systems are commonly implemented in GIS.

USING GIS FOR SPATIAL ANALYSIS

Spatial analysis in GIS involves three types of operations: Attribute Query- also known as non-spatial (or spatial) query, Spatial Query and Generation of new data sets from the original database (Bwozough, 1987). The scope of spatial analysis ranges from a simple query about the spatial phenomenon to complicated combinations of attribute queries, spatial queries, and alterations of original data.

Attribute Query: Requires the processing of attribute data exclusive of spatial information. In other words, it's a process of selecting information by asking logical questions.

Example: From a database of a city parcel map where every parcel is listed with a land use code, a simple attribute query may require the identification of all parcels for a specific land use type. Such a query can be handled through the table without referencing the parcel map (Fig. 1). Because no spatial information is required to answer this question, the query is considered an attribute query. In this example, the entries in the attribute table that have land use codes identical to the specified type are identified.

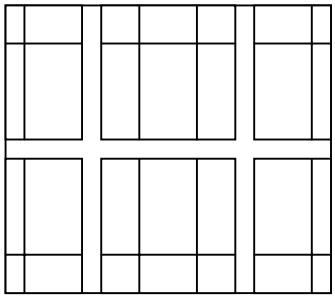

Parcel No.	*Size*	*Value*	*Land Use*
102	7,500	200,000	Commercial
103	7,500	160,000	Residential
104	9,000	250,000	Commercial
105	6,600	125,000	Residential

A sample parcel map

Attribute table of the sample parcel map

Figure 1: Listing of Parcel No. and value with land use = 'commercial' is an attribute query. Identification of all parcels within 100-m distance is a spatial query

Spatial Query: Involves selecting features based on location or spatial relationships, which requires processing of spatial information. For instance a question may be raised about parcels within one mile of the freeway and each parcel. In this case, the answer can be obtained either from a hardcopy map or by using a GIS with the required geographic information (Fig. 2).

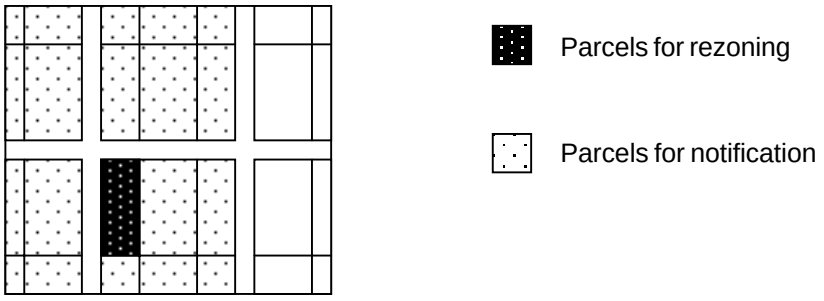

Figure 2: Land owners within a specified distance from the parcel to be rezoned identified through spatial query

Example: Let us take one spatial query example where a request is submitted for rezoning, all owners whose land is within a certain distance of all parcels that may be rezoned must be notified for public hearing. A spatial query is required to identify all parcels within the specified distance. This process cannot be accomplished without spatial information. In other words, the attribute table of the database alone does not provide sufficient information for solving problems that involve location.

While basic spatial analysis involves some attribute queries and spatial queries, complicated analysis typically require a series of GIS operations including multiple attribute and spatial queries, alteration of original data, and generation of new data sets. The methods for structuring and organizing such operations are a major concern in spatial analysis. An effective spatial analysis is one in which the best available methods are appropriately employed for different types of attribute queries, spatial queries, and data alteration. The design of the analysis depends on the purpose of study.

GIS Usage in Spatial Analysis

GIS can interrogate geographic features and retrieve associated attribute information, called identification. It can generate new set of maps by query and analysis. It also evolves new information by spatial operations. Here are described some analytical procedures applied with a GIS. GIS operational procedure and analytical tasks that are particularly useful for spatial analysis include:

- Single layer operations
- Multi layer operations/ Topological overlay
- Spatial modeling
- Geometric modeling
  - Calculating the distance between geographic features
  - Calculating area, length and perimeter
  - Geometric buffers.
- Point pattern analysis
- Network analysis
- Surface analysis
- Raster/Grid analysis
- Fuzzy Spatial Analysis
- Geostatistical Tools for Spatial Analysis

Single layer operations are procedures, which correspond to queries and alterations of data that operate on a single data layer.

Example: Creating a buffer zone around all streets of a road map is a single layer operation as shown in the Figure 3.

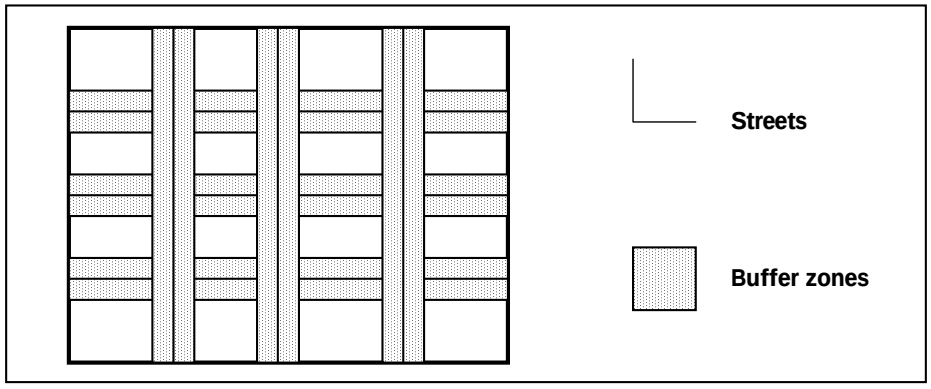

Figure 3: Buffer zones extended from streets

Multi layer operations: are useful for manipulation of spatial data on multiple data layers. Figure 4 depicts the overlay of two input data layers representing soil map and a land use map respectively. The overlay of these two layers produces the new map of different combinations of soil and land use.

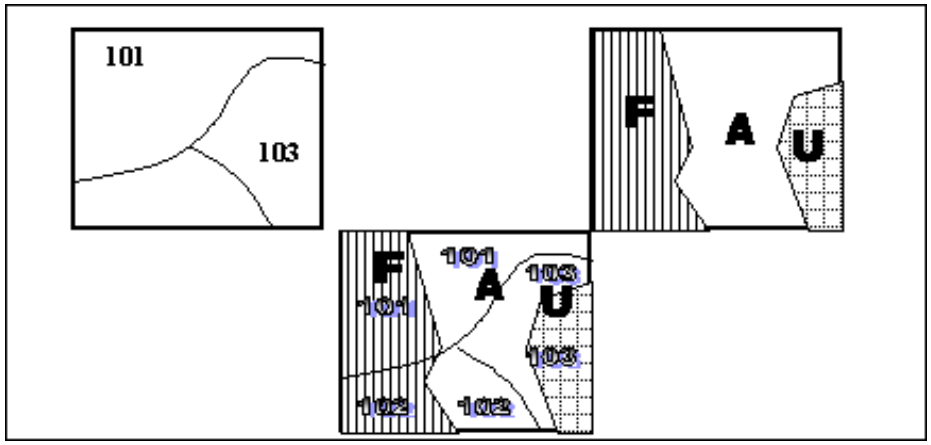

Figure 4: The overlay of two data layers creates a map of combined polygons

Topological overlays: These are multi layer operations, which allow combining features from different layers to form a new map and give new information and features that were not present in the individual maps. This topic will be discussed in detail in section of vector-based analysis.

Point pattern analysis: It deals with the examination and evaluation of spatial patterns and the processes of point features. A typical biological survey map is shown in Figure 5, in which each point feature denotes the observation of an endangered species such as big horn sheep in southern California. The objective of illustrating point features is to determine the most favourable environmental conditions for this species. Consequently, the spatial distribution of species can be examined in a point pattern analysis. If the distribution illustrates a random pattern, it may be difficult to identify significant factors that influence species distribution. However, if observed locations show a systematic pattern such as the clusters in this diagram, it is possible to analyze the animals' behaviour in terms of environmental characteristics. In general, point pattern analysis is the first step in studying the spatial distribution of point features.

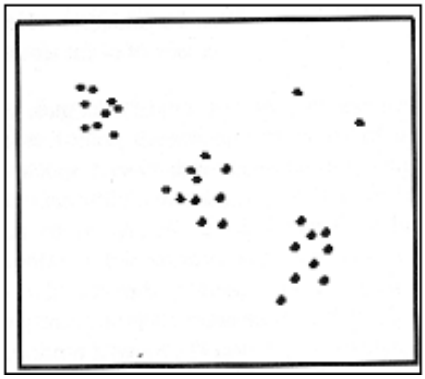

Figure 5: Distribution of an endangered species examined in a point pattern analysis

Network analysis: Designed specifically for line features organized in connected networks, typically applies to transportation problems and location analysis such as school bus routing, passenger plotting, walking distance, bus stop optimization, optimum path finding etc.

Figure 6 shows a common application of GIS-based network analysis. Routing is a major concern for the transportation industry. For instance, trucking companies must determine the most cost-effective way of connecting stops for pick-up or delivery. In this example, a route is to be delineated for a truck to pick up packages at five locations. A routing application can be developed to identify the most efficient route for any set of pick-up locations. The highlighted line represents the most cost-effective way of linking the five locations.

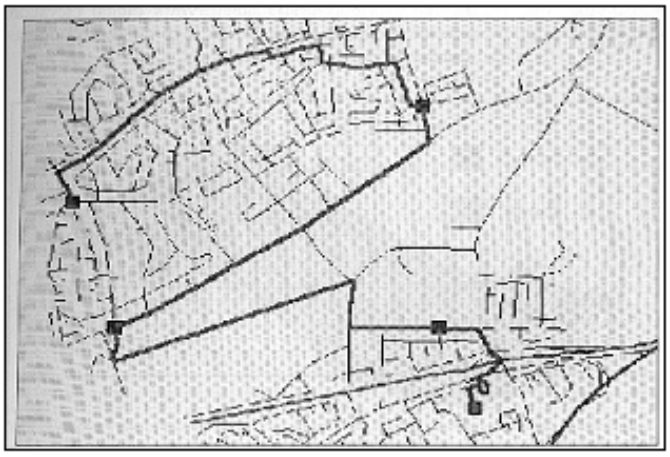

Figure 6: The most cost effective route links five point locations on the street map

Surface analysis deals with the spatial distribution of surface information in terms of a three-dimensional structure.

The distribution of any spatial phenomenon can be displayed in a three-dimensional perspective diagram for visual examination. A surface may represent the distribution of a variety of phenomena, such as population, crime, market potential, and topography, among many others. The perspective diagram in Figure 7 represents topography of the terrain, generated from digital elevation model (DEM) through a series of GIS-based operations in surface analysis.

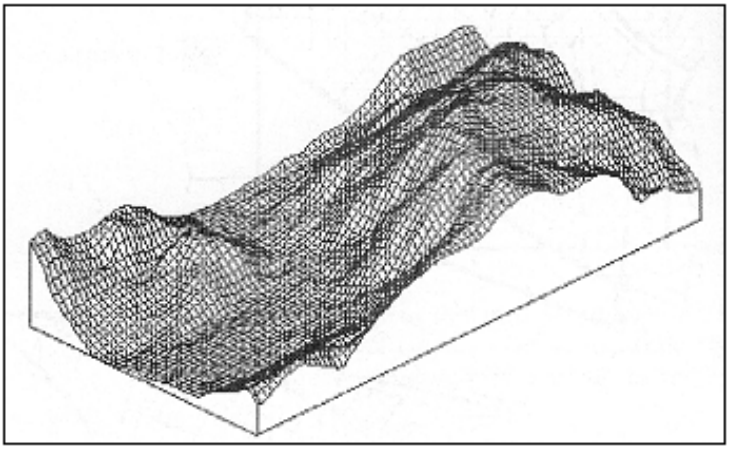

Figure 7: Perspective diagram representing topography of the terrain derived from a surface analysis

Grid analysis involves the processing of spatial data in a special, regularly spaced form. The following illustration (Figure 8) shows a grid-based model of fire progression. The darkest cells in the grid represent the area where a fire is currently underway. A fire probability model, which incorporates fire behaviour in response to environmental conditions such as wind and topography, delineates areas that are most likely to burn in the next two stages. Lighter shaded cells represent these areas. Fire probability models are especially useful to fire fighting agencies for developing quick-response, effective suppression strategies.

In most cases, GIS software provides the most effective tool for performing the above tasks.

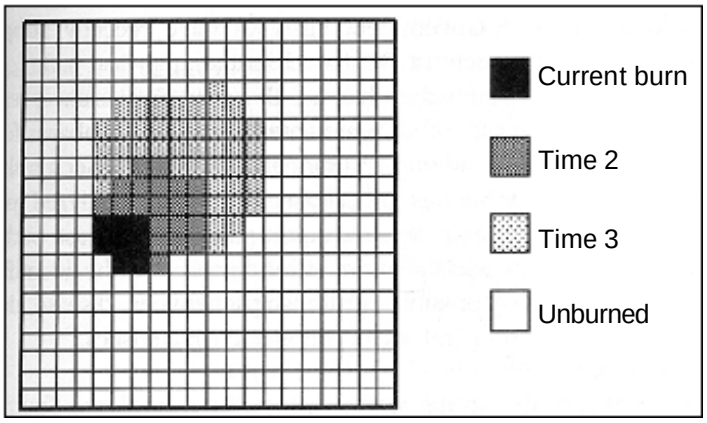

Figure 8: A fire behaviour model delineates areas of fire progression based on a grid analysis

Fuzzy Spatial Analysis

Fuzzy spatial analysis is based on Fuzzy set theory. Fuzzy set theory is a generalization of Boolean algebra to situations where zones of gradual transition are used to divide classes, instead of conventional crisp boundaries. This is more relevant in many cases where one considers 'distance to certain zone' or 'distance to road', in which case the influence of this factor is more likely to be some function of distance than a binary 'yes' or 'no'. Also in fuzzy theory maps are prepared showing gradual change in the variable from very high to very low, which is a true representation of the real world (Bonhan-Carter, 1994).

As stated above, the conventional crisp sets allow only binary membership function (i.e. true or false), whereas a fuzzy set is a class that admits the possibility of partial membership, so fuzzy sets are generalization of crisp sets to situations where the class membership or class boundaries are not, or cannot be, sharply defined.

Applications

Data integration using fuzzy operators using standard rules of fuzzy algebra one can combine various thematic data layers, represented by respective membership values (Chung and Fabbri, 1993).

Example: In a grid cell/pixel if a particular litho-unit occurs in combination with a thrust/fault, its membership value should be much higher compared with individual membership values of litho-unit or thrust/fault. This is significant as the effect is expected to be "increasive" in our present consideration and it can be calculated by fuzzy algebraic sum. Similarly, if the presence of two or a set of parameters results in "decreasive" effect, it can be calculated by fuzzy algebraic product. Besides this, fuzzy algebra offers various other methods to combine different data sets for landslide hazard zonation map preparation. To combine number of exploration data sets, five such operators exist, namely the fuzzy AND, the fuzzy OR, fuzzy algebraic product, fuzzy algebraic sum and fuzzy gamma operator.

Fuzzy logic can also be used to handle mapping errors or uncertainty, i.e. errors associated with clear demarcation of boundaries and also errors present in the area where limited ground truth exists in studies such as landslide hazard zonation. The above two kinds of errors are almost inherent to the process of data collection from different sources including remote sensing.

GEOSTATISTICAL TOOLS FOR SPATIAL ANALYSIS

Geostatistics studies spatial variability of regionalized variables: Variables that have an attribute value and a location in a two or three-dimensional space. Tools to characterize the spatial variability are:

- Spatial Autocorrelation Function and
- Variogram.

A *variogram* is calculated from the variance of pairs of points at different separation. For several distance classes or lags, all point pairs are identified which matches that separation and the variance is calculated. Repeating this process for various distance classes yields a variogram. These functions can be used to measure spatial variability of point data but also of maps or images.

Spatial Auto-correlation of Point Data

The statistical analysis referred to as spatial auto-correlation, examines the correlation of a random process with itself in space. Many variables that have discrete values measured at several specific geographic positions (i.e., individual observations can be approximated by dimensionless points) can be considered random processes and can thus be analyzed using spatial auto-correlation analysis. Examples of such phenomena are: Total amount of rainfall, toxic element concentration, grain size, elevation at triangulated points, etc.

The spatial auto-correlation function, shown in a graph is referred to as spatial *auto-correlogram*, showing the correlation between a series of points or a map and itself for different shifts in space or time. It visualizes the spatial variability of the phenomena under study. In general, large numbers of pairs of points that are close to each other on average have a lower variance (i.e., are better correlated), than pairs of points at larger separation. The auto-correlogram quantifies this relationship and allows gaining insight into the spatial behaviour of the phenomenon under study.

Point Interpolation

A point interpolation performs an interpolation on randomly distributed point values and returns regularly distributed point values. The various interpolation methods are: Voronoi Tesselation, moving average, trend surface and moving surface.

Example: Nearest Neighbor (Voronoi Tessellation)-In this method the value, identifier, or class name of the nearest point is assigned to the pixels. It offers a quick way to obtain a Thiessen map from point data (Figure 9).

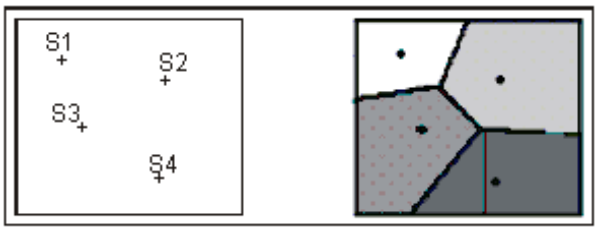

(a) (b)

Figure 9: (a) An input point map, (b) The output map obtained as the result of the interpolation operation applying the Voronoi Tessellation method

VECTOR BASED SPATIAL DATA ANALYSIS

In this section the basic concept of various vector operations are dealt in detail. There are multi layer operations, which allow combining features from different layers to form a new map and give new information and features that were not present in the individual maps.

Topological overlays: Selective overlay of polygons, lines and points enables the users to generate a map containing features and attributes of interest, extracted from different themes or layers. Overlay operations can be performed on both raster (or grid) and vector maps. In case of raster map calculation tool is used to perform overlay. In topological overlays polygon features of one layer can be combined with point, line and polygon features of a layer.

Polygon-in-polygon overlay:

Output is polygon coverage.

Coverages are overlaid two at a time.

There is no limit on the number of coverages to be combined.

New File Attribute Table is created having information about each newly created feature.

Line-in-polygon overlay:

Output is line coverage with additional attribute.

No polygon boundaries are copied.

New arc-node topology is created.

Point-in-polygon overlay:

Output is point coverage with additional attributes.

No new point features are created.

No polygon boundaries are copied.

Logical Operators: Overlay analysis manipulates spatial data organized in different layers to create combined spatial features according to logical conditions specified in Boolean algebra with the help of logical and conditional operators. The logical conditions are specified with operands (data elements) and operators (relationships among data elements).

Note: In vector overlay, arithmetic operations are performed with the help of logical operators. There is no direct way to it.

Common logical operators include AND, OR, XOR (Exclusive OR), and NOT. Each operation is characterized by specific logical checks of decision criteria to determine if a condition is true or false. Table 1 shows the true/ false conditions of the most common Boolean operations. In this table, A and B are two operands. One (1) implies a true condition and zero (0) implies false. Thus, if the A condition is true while the B condition is false, then the combined condition of A and B is false, whereas the combined condition of A OR B is true.

AND - Common Area/ Intersection / Clipping Operation

OR - Union Or Addition

NOT - (Inverter)

XOR - Minus

Table 1: Truth Table of common Boolean operations

A	B	A AND B	A OR B	A NOT B	B NOT A	A XOR B
0	0	0	0	0	0	0
0	1	0	1	0	1	1
1	0	0	1	1	0	1
1	1	1	1	0	0	0

The most common basic multi layer operations are union, intersection, and identify operations. All three operations merge spatial features on separate data layers to create new features from the original coverage. The main difference among these operations is in the way spatial features are selected for processing.

Overlay operations

The Figure 10 shows different types of vector overlay operations and gives flexibility for geographic data manipulation and analysis. In polygon overlay, features from two map coverages are geometrically intersected to produce a

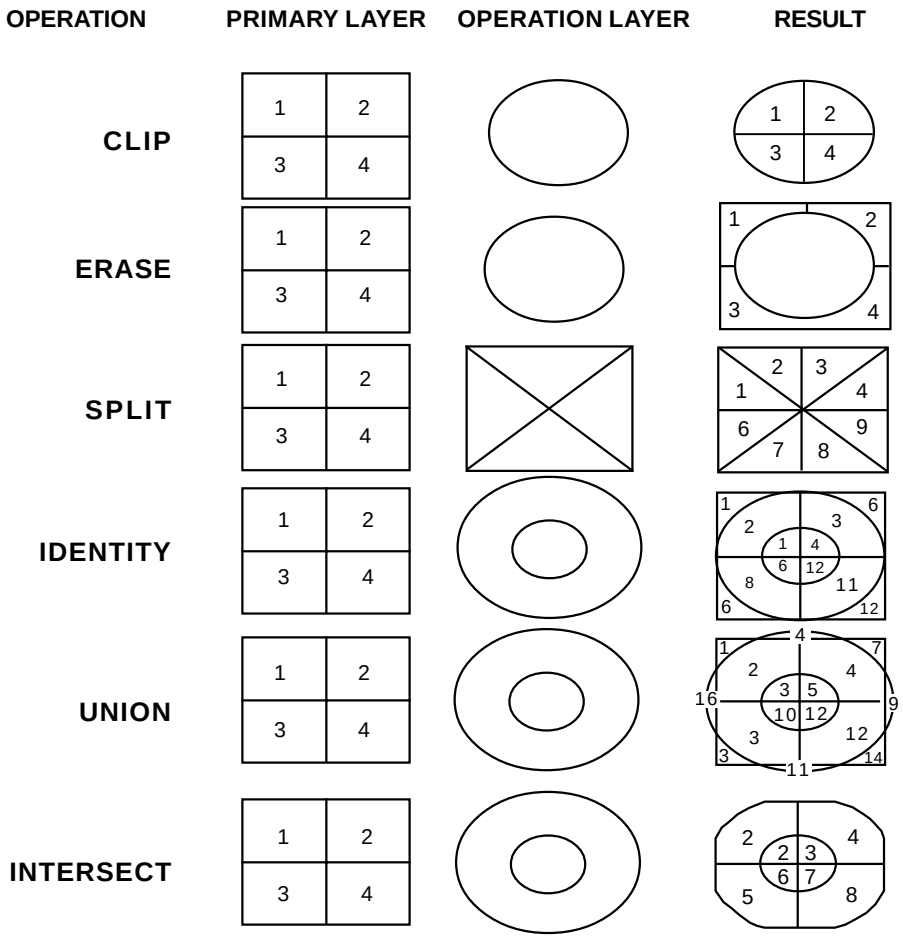

Figure 10 : Overlay operations

new set of information. Attributes for these new features are derived from the attributes of both the original coverages, thereby contain new spatial and attribute data relationships.

One of the overlay operation is AND (or INTERSECT) in vector layer operations, in which two coverages are combined. Only those features in the area common to both are preserved. Feature attributes from both coverages are joined in the output coverage.

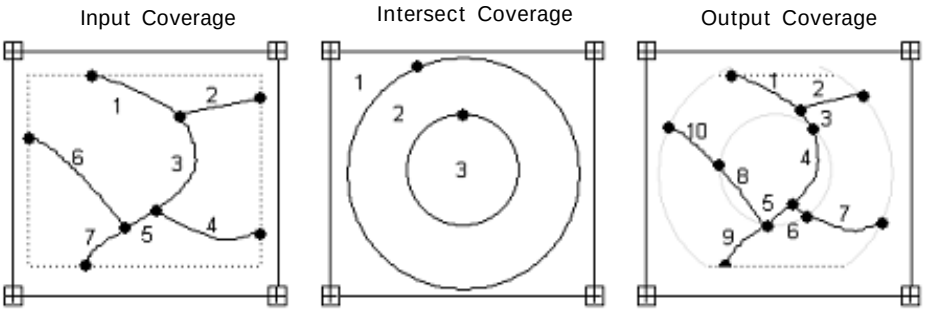

INPUT COVERAGE	
#	ATTRIBUTE
1	A
2	B
3	A
4	C
5	A
6	D
7	A

INTERSECT COVERAGE	
#	ATTRIBUTE
1	
2	102
3	103

OUTPUT COVERAGE	INPUT COVERAGE		INTERSECT COVERAGE	
#	#	ATTRIBUTE	#	ATTRIBUTE
1	1	A	2	102
2	2	B	2	102
3	3	A	2	102
4	3	A	3	103
5	5	A	3	103
6	4	C	3	103
7	4	C	2	102
8	6	D	3	103
9	7	A	2	102
10	6	D	2	102

RASTER BASED SPATIAL DATA ANALYSIS

Present section discusses operational procedures and quantitative methods for the analysis of spatial data in raster format. In raster analysis, geographic units are regularly spaced, and the location of each unit is referenced by row and column positions. Because geographic units are of equal size and identical shape, area adjustment of geographic units is unnecessary and spatial properties of geographic entities are relatively easy to trace. All cells in a grid have a positive position reference, following the left-to-right and top-to-bottom data scan. Every cell in a grid is an individual unit and must be assigned a value. Depending on the nature of the grid, the value assigned to a cell can be an integer or a floating point. When data values are not available for particular cells, they are described as NODATA cells. NODATA cells differ from cells containing zero in the sense that zero value is considered to be data.

The regularity in the arrangement of geographic units allows for the underlying spatial relationships to be efficiently formulated. For instance, the distance between orthogonal neighbors (neighbors on the same row or column) is always a constant whereas the distance between two diagonal units can also be computed as a function of that constant. Therefore, the distance between any pair of units can be computed from differences in row and column positions. Furthermore, directional information is readily available for any pair of origin and destination cells as long as their positions in the grid are known.

Advantages of using the Raster Format in Spatial Analysis

Efficient processing: Because geographic units are regularly spaced with identical spatial properties, multiple layer operations can be processed very efficiently.

Numerous existing sources: Grids are the common format for numerous sources of spatial information including satellite imagery, scanned aerial photos, and digital elevation models, among others. These data sources have been adopted in many GIS projects and have become the most common sources of major geographic databases.

Different feature types organized in the same layer: For instance, the same grid may consist of point features, line features, and area features, as long as different features are assigned different values.

Grid Format Disadvantages

- Data redundancy: When data elements are organized in a regularly spaced system, there is a data point at the location of every grid cell, regardless of whether the data element is needed or not. Although, several compression techniques are available, the advantages of gridded data are lost whenever the gridded data format is altered through compression. In most cases, the compressed data cannot be directly processed for analysis. Instead, the compressed raster data must first be decompressed in order to take advantage of spatial regularity.
- Resolution confusion: Gridded data give an unnatural look and unrealistic presentation unless the resolution is sufficiently high. Conversely, spatial resolution dictates spatial properties. For instance, some spatial statistics derived from a distribution may be different, if spatial resolution varies, which is the result of the well-known scale problem.
- Cell value assignment difficulties: Different methods of cell value assignment may result in quite different spatial patterns.

Grid Operations used in Map Algebra

Common operations in grid analysis consist of the following functions, which are used in Map Algebra to manipulate grid files. The Map Algebra language is a programming language developed to perform cartographic modeling. Map Algebra performs following four basic operations:

- Local functions: that work on every single cell,
- Focal functions: that process the data of each cell based on the information of a specified neighborhood,
- Zonal functions: that provide operations that work on each group of cells of identical values, and
- Global functions: that work on a cell based on the data of the entire grid.

The principal functionality of these operations is described here.

Local Functions

Local functions process a grid on a cell-by-cell basis, that is, each cell is processed based solely on its own values, without reference to the values of other cells. In other words, the output value is a function of the value or values of the cell being processed, regardless of the values of surrounding cells. For single layer operations, a typical *example* is changing the value of each cell by adding or multiplying a constant. In the following example, the input grid contains values ranging from 0 to 4. Blank cells represent NODATA cells. A simple local function multiplies every cell by a constant of 3 (Fig. 11). The results are shown in the output grid at the right. When there is no data for a cell, the corresponding cell of the output grid remains a blank.

Input Grid

2	0	1	1
2	3	0	4
4		2	3
1	1		2

X 3 =

Output Grid

6	0	3	3
6	9	0	12
12		6	9
3	3		6

Figure 11: A local function multiplies each cell in the input grid by 3 to produce the output grid

Local functions can also be applied to multiple layers represented by multiple grids of the same geographic area (Fig. 12).

Input Grid

2	0	1	1
2	3	0	4
4		2	3
1	1		2

X

Multiplier Grid

1	1	2	2
1	2	2	2
2	2	3	3
2	3	3	4

=

Output Grid

2	0	2	2
2	6	0	12
8		6	9
2	3		8

Figure 12: A local function multiplies the input grid by the multiplier grid to produce the output grid

Local functions are not limited to arithmetic computations. Trigonometric, exponential, and logarithmic and logical expressions are all acceptable for defining local functions.

Focal Functions

Focal functions process cell data depending on the values of neighboring cells. For instance, computing the sum of a specified neighborhood and assigning the sum to the corresponding cell of the output grid is the "focal sum" function (Fig. 13). A 3 x 3 kernel defines neighborhood. For cells closer to the edge where the regular kernel is not available, a reduced kernel is used and the sum is computed accordingly. For instance, a 2 x 2 kernel adjusts the upper left corner cell. Thus, the sum of the four values, 2,0,2 and 3 yields 7, which becomes the value of this cell in the output grid. The value of the second row, second column, is the sum of nine elements, 2, 0, 1, 2, 3, 0, 4, 2 and 2, and the sum equals 16.

Input Grid

2	0	1	1
2	3	0	4
4	2	2	3
1	1	3	2

Focal Sum =

Output Grid

7	8	9	6
13	16	16	11
13	18	20	14
8	13	13	10

Figure 13: A Focal sum function sums the values of the specified neighborhood to produce the output grid

Another focal function is the mean of the specified neighborhood, the "focal mean" function. In the following example (Fig. 14), this function yields the mean of the eight adjacent cells and the center cell itself. This is the smoothing function to obtain the moving average in such a way that the value of each cell is changed into the average of the specified neighborhood.

Input Grid

2	0	1	1
2	3	0	4
4	2	2	3
1	1	3	2

Focal Mean =

Output Grid

1.8	1.3	1.5	1.5
2.2	2.0	1.8	1.8
2.2	2.0	2.2	2.3
2.0	2.2	2.2	2.5

Figure 14: A Focal mean function computes the moving average of the specified neighborhood to produce the output grid

Other commonly employed focal functions include standard deviation (focal standard deviation), maximum (focal maximum), minimum (focal minimum), and range (focal range).

Zonal Functions

Zonal functions process the data of a grid in such a way that cell of the same zone are analyzed as a group. A zone consists of a number of cells that may or may not be contiguous. A typical zonal function requires two grids – a zone grid, which defines the size, shape and location of each zone, and a value grid, which is to be processed for analysis. In the zone grid, cells of the same zone are coded with the same value, while zones are assigned different zone values.

Figure 15 illustrates an example of the zonal function. The objective of this function is to identify the zonal maximum for each zone. In the input zone grid, there are only three zones with values ranging from 1 to 3. The zone with a value of 1 has five cells, three at the upper right corner and two at the lower left corner. The procedure involves finding the maximum value among these cells from the value grid.

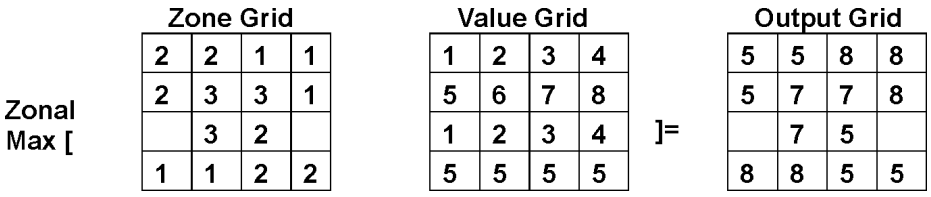

Figure 15: A Zonal maximum function identifies the maximum of each zone to produce the output grid

Typical zonal functions include zonal mean, zonal standard deviation, zonal sum, zonal minimum, zonal maximum, zonal range, and zonal variety. Other statistical and geometric properties may also be derived from additional zonal functions. For instance, the zonal perimeter function calculates the perimeter of each zone and assigns the returned value to each cell of the zone in the output grid.

Global Functions

For global functions, the output value of each cell is a function of the entire grid. As an example, the Euclidean distance function computes the distance from each cell to the nearest source cell, where source cells are defined in an input grid. In a square grid, the distance between two orthogonal neighbors is equal to the size of a cell, or the distance between the centroid locations of adjacent cells. Likewise, the distance between two diagonal

neighbors is equal to the cell size multiplied by the square root of 2. Distance between non-adjacent cells can be computed according to their row and column addresses.

In Figure 16, the grid at the left is the source grid in which two clusters of source cells exist. The source cells labeled 1 are the first clusters, and the cell labeled 2 is a single-cell source. The Euclidean distance from any source cell is always equal to 0. For any other cell, the output value is the distance from its nearest source cell.

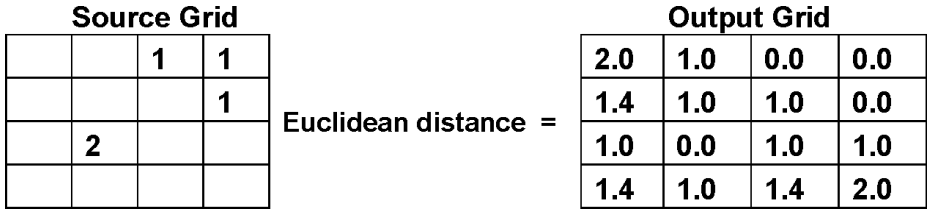

Figure 16: A Euclidean distance function computes the distance from the nearest source cell

In the above example, the measurement of the distance from any cell must include the entire source grid; therefore this analytical procedure is a global function.

Figure 17 provides an example of the cost distance function. The source grid is identical to that in the preceding illustration. However, this time a cost grid is employed to weigh travel cost. The value in each cell of the cost grid indicates the cost for traveling through that cell. Thus, the cost for traveling from the cell located in the first row, second column to its adjacent source cell to the right is half the cost of traveling through itself plus half the cost of traveling through the neighboring cell.

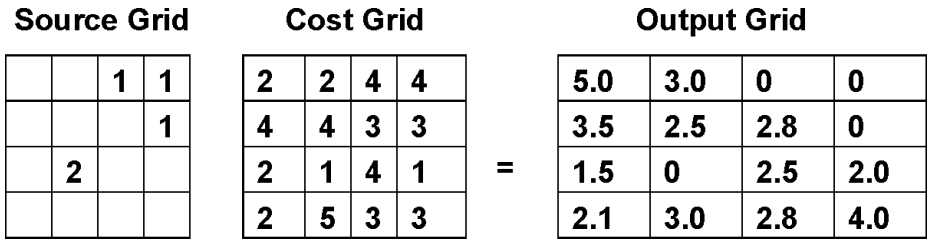

Figure 17: Travel cost for each cell is derived from the distance to the nearest source cell weighted by a cost function

Another useful global function is the cost path function, which identifies the least cost path from each selected cell to its nearest source cell in terms of cost distance. These global functions are particularly useful for evaluating the connectivity of a landscape and the proximity of a cell to any given entities.

SOME IMPORTANT RASTER ANALYSIS OPERATIONS

In this section some of the important raster based analysis are dealt:

- Renumbering Areas in a Grid File
- Performing a Cost Surface Analysis
- Performing an Optimal Path Analysis
- Performing a Proximity Search

Area Numbering: Area Numbering assigns a unique attribute value to each area in a specified grid file. An area consists of two or more adjacent cells that have the same cell value or a single cell with no adjacent cell of the same value. To consider a group of cells with the same values beside each other, a cell must have a cell of the same value on at least one side of it horizontally or vertically (4-connectivity), or on at least one side horizontally, vertically, or diagonally (8-connectivity). Figure 18 shows a simple example of area numbering.

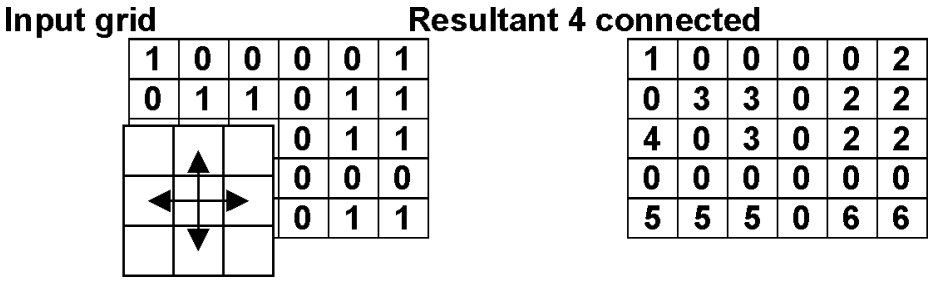

Figure 18. Illustrates simple example of Area numbering with a bit map as input. The pixels, which are connected, are assigned the same code. Different results are obtained when only the horizontal and vertical neighbors are considered (4-connected) or whether all neighbors are considered (8-connected)

One can renumber all of the areas in a grid, or you can renumber only those areas that have one or more specific values. If you renumber all of the

areas, Area Number assigns a value of 1 to the first area located. It then assigns a value of 2 to the second area, and continues this reassignment method until all of the areas are renumbered. When you renumber areas that contain a specified value (such as 13), the first such area is assigned the maximum grid value plus 1. For example, if the maximum grid value is 25, Area Number assigns a value of 26 to the first area, a value of 27 to the second area, and continues until all of the areas that contain the specified values are renumbered.

Cost Surface Analysis: Cost Surface generates a grid in which each grid cell represents the cost to travel to that grid cell from the nearest of one or more start locations. The cost of traveling to a given cell is determined from a weight grid file. Zero Weights option uses attribute values of 0 as the start locations. The By Row/Column option uses the specified row and column location as the start location.

Optimal Path: Optimal Path lets us analyze a grid file to find the best path between a specified location and the closest start location as used in generating a cost surface. The computation is based on a cost surface file that you generate with Cost Surface.

One must specify the start location by row and column. The zeros in the input cost surface represent one endpoint. The specified start location represents the other endpoint.

Testing the values of neighboring cells for the smallest value generates the path. When the smallest value is found, the path moves to that location, where it repeats the process to move the next cell. The output is the path of least resistance between two points, with the least expensive, but not necessarily the straightest, line between two endpoints. The output file consists of only the output path attribute value, which can be optionally specified, surrounded by void values.

Performing A Proximity Search: Proximity lets you search a grid file for all the occurrences of a cell value or a feature within either a specified distance or a specified number of cells from the origin.

You can set both the origin and the target to a single value or a set of values. The number of cells to find can also be limited. For example, if you

specify to find 10 cells, the search stops when 10 occurrences of the cell have been found within the specified distance of each origin value. If you do not limit the number of cells, the search continues until all target values are located.

The output grid file has the user-type code and the data-type code of the input file. The gird-cell values in the output file indicate whether the grid cell corresponds to an origin value, the value searched for and located within the specified target, or neither of these.

The origin and target values may be retained as the original values or specified to be another value.

GRID BASED SPATIAL ANALYSIS

Diffusion modeling and *Connectivity analysis* can be effectively conducted from grid data. Grid analysis is suitable for these types of problems because of the grid's regular spatial configuration of geographic units.

Diffusion Modeling: It deals with the process underlying spatial distribution. The constant distance between adjacent units makes it possible to simulate the progression over geographic units at a consistent rate. Diffusion modeling has a variety of possible applications, including wildfire management, disease vector tracking, migration studies, and innovation diffusion research, among others.

Connectivity Analysis: Connectivity analysis evaluates inter separation distance, which is difficult to calculate in polygon coverage, but can be obtained much more effectively in a grid.

The connectivity of a landscape measures the degree to which surface features of a certain type are connected. Landscape connectivity is an important concern in environmental management. In some cases, effective management of natural resources requires maximum connectivity of specific features. For instance, a sufficiently large area of dense forests must be well connected to provide a habitat for some endangered species to survive. In such cases, forest management policies must be set to maintain the highest possible level to connectivity. Connectivity analysis is especially useful for natural resource and environmental management.

CONCLUSIONS

GIS is considered as a decision making tool in problem solving environment. Spatial analysis is a vital part of GIS and can be used for many applications like site suitability, natural resource monitoring, environmental disaster management and many more. Vector, raster based analysis functions and arithmetic, logical and conditional operations are used based on the recovered derivations.

REFERENCES

Bonhan - Carter, G.F. 1994. Geographic Information Systems for Geoscientists. Love Printing Service Ltd., Ontario, Canada.

Burrough, P.A. 1987. Principles of Geographical Information System for Land Assessment. Oxford : Clardon Press.

Chung, Chang-Jo F. and Fabbri, A.G. 1993. The representation of Geoscience Information for data integration. *Nonrenewable Resources*, Vol. 2, No. 2, Oxford Univ. Press.

RETRIEVAL OF AGROMETEOROLOGICAL PARAMETERS USING SATELLITE REMOTE SENSING DATA

S. K. Saha
Agriculture and Soils Division
Indian Institute of Remote Sensing, Dehra Dun

Abstract : The recent development of satellite meteorology has allowed us to estimate spatially and frequently number of basic agro-meteorological parameters. This paper discusses approaches of retrieval of several agro-meteorological parameters viz. surface albedo, land surface temperature, evapotranspiration, absorbed photosynthetically active radiation by integrated use of optical and thermal infrared sensors satellite data.

INTRODUCTION

Countries in the Asia-Pacific region have networks of agro-meteorological ground stations in order to monitor the agricultural production and weather forecasting. But, such networks are generally less dense than they should be for a correct representation of the high spatial climatic variability which exists in Asia-Pacific region. Also the agro-meteorological data from various ground stations are not delivered in real time to a central collecting point. So, conventional agro-meteorological techniques have severe limitations to use their data for real time agricultural monitoring and yield forecasting.

The recent development of satellite meteorology has allowed us to obtain frequent and accurate measurements of a number of basic agro-meteorological parameters (e.g. surface albedo, surface temperature, evapotranspiration, solar radiation, rainfall etc.). The satellite estimated agro-meteorological parameters have several advantages compared to conventional measurements of agro-meteorological data in ground meteorological network.

Satellite Remote Sensing and GIS Applications in Agricultural Meteorology
pp. 175-194

- The spatial scale, from 50 m to 5 km depending on the satellite resolution, is more precise than ground climatic data (typically near 100 km for synoptic stations and 10-50 km for local less regular stations).
- High temporal data (e.g. every half an hour for METEOSAT).
- Remote sensing has access to surface agromet properties, as opposed to screen height agromet data in conventional method which attempts to characterize air mass properties.

The various approaches of retrieval of several agro-meteorological parameters viz. Surface albedo, Surface temperature, Evapotranspiration (ET), Absorbed photo-synthetically active radiation (APAR) using satellite data are discussed in following sections.

APPROACHES OF RETRIEVAL OF AGRO-METEOROLOGICAL PARAMETERS USING SATELLITE DATA

Surface Albedo

The amount of solar radiation (0.4 – 4.0 μm) reflected by a surface is characterized by its hemispherical albedo, which may be defined as the reflected radiative flux per unit incident flux. Surface albedo is an important parameter used in global climatic models to specify the amount of solar radiation absorbed at the surface. Moreover, variations in surface albedo can serve as diagnostic of land surface changes and their impact on the physical climatic system can be assessed when routinely monitored surface albedo is used in climatic models. Albedo information is useful for monitoring crop growth, prediction of crop yield, and monitoring desertification.

For clear sky conditions, the surface albedo may be estimated by remote sensing measurements covering optical spectral bands.

The albedo 'A', can generally be expressed by the following equations (Valientez *et al.*, 1995) :

$$A = (\pi.L\_) / (\mu s. Es)$$

where L is the integral of the spectral irradiance weighted by the filter function of the band ($W/m^2/Sr$) and Es is the integral of the spectral solar irradiance weighted by the filter function (W/m^2).

$\mu s = \text{Cos } \theta s$

$\pi . L = \int_{\lambda^a}^{\lambda^b} \pi . L(\lambda) . S(\lambda) . d\lambda$

$\mu s . Es = \int_{\lambda^a}^{\lambda^b} \mu s . Es(\lambda) . S(\lambda) . d\lambda$

where, L (λ) is the spectral radiance reflected from the surface ($W/m^2/Sr/\mu m$); S (λ) is the spectral response of the filter function; Es (λ) is the normal spectral irradiance coming from the sun ($W/m^2/\mu m$).

Goita and Royer (1992) suggested the following equation for computation of albedo, using atmospherically uncorrected reflectance :

$$A = \sum_{i=1}^{n} \rho i . Ei / \sum_{i=1}^{n} Ei$$

$\rho = \pi . L\lambda . d^2 / Ei . \text{Cos } \theta s$

$L\lambda = \alpha . DN + \beta$

where, ρi is the apparent reflectance in band i; Ei is the exo-atmosphere solar irradiance in band i, $L\lambda$ is the spectral radiance; d^2 is the sun to earth distance correction factor; θs is the solar zenith angle; DN is the digital number; α and β are the gain and off-set values obtained from the sensor calibration parameters.

The general term "narrow-band" include Landsat, IRS, AVHRR channels, while the general term "broad-band" include METEOSAT. The term "Planetary" and "Surface" refer to either albedo when they are calculated or measured from top of the atmosphere as seen by a satellite or at ground level without any intermediate atmosphere, respectively.

Several factors complicate the estimation of surface albedo from remotely sensed data-atmospheric effect, degree of isotropy of the surface and spectral interval of the narrow band interval (Brest and Goward, 1987).

Rugged terrain, the geometry between the sun, the surface orientation and the satellite sensor, which can vary from one pixel to another is a factor which makes the estimation of surface reflectance from remotely sensed data difficult.

Saunders (1990) suggested a detailed complex methodology to retrieve surface albedo from NOAA – AVHRR visible and infrared bands by considering Rayleigh scattering, aerosol scattering and gaseous absorption as the principal radiation attenuating mechanisms, wherein the accuracy of the atmospheric correction would be dependent on input profiles of atmospheric constituents.

Prasad *et al.* (1995) suggested a dark body radiance method for computation of albedo from NOAA – AVHRR data and found albedo values comparable to those retrieved by Saunders (1990) method. The methodology adopted by them is discussed below :

The albedo (A) is given by

$$A = W_1 . \rho_1 + W_2 . \rho_2$$

where, ρ_1 and ρ_2 are atmospherically corrected reflectance factors for the visible and near IR band, respectively. W_1 and W_2 are the weightages specific to spectral bands (given by Saunders, 1990). The atmospherically corrected reflectance for the pixel in a given band (ρ_1) is given by :

$$\rho_1 = (L_p - H_p) / [S.Sin (r) - B_p . H_p]$$

where, L_p is the radiance for pixel 'p'; S. Sin (r) represents the extra-terrestrial solar spectral radiation which depends on the sun elevation angle 'r' and the day of the year; H_p is the atmospheric radiance component for a given pixel 'p' at scan/view angle θ_p (from local vertical) :

$$H_p = H_n . \text{Sec } \theta_p$$

$$H_n = H_B . \text{Sec } \theta_B$$

$$B_p = [1 - (f)_p] / (b)_p$$

where, H_B is the base radiance of dark body pixels (water body for NIR and the cloud shadow region for visible band) due to atmospheric effects; H_n is the normalized atmospheric radiance for nadir, θ_B is the scan angle for the base pixels; $(f)_p$ and $(b)_p$ refer to forward and backward scattering for the pixel at wavelength.

Saha and Pande (1995a) used Landsat TM optical bands data for computation of regional surface albedo following the approach suggested by Goita and Royer (1992) (Fig. 1). An albedo image was generated by Kant (2000) for the snow and forest covered Himalayan mountain of India by using NOAA – AVHRR Ch1 and Ch2 data following an empirical relationship relating broad band albedo and narrow band albedo (Fig. 2).

(a)

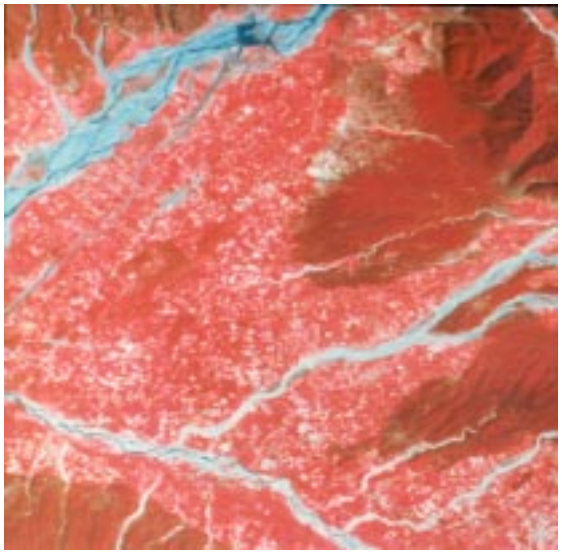

(b)

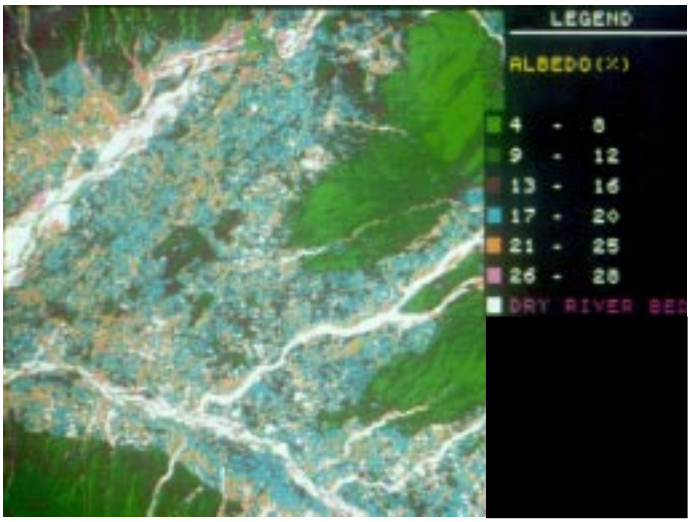

Figure 1: (a) FCC and (b) Albedo image of part of Doon Valley generated by using Landsat-TM optical data

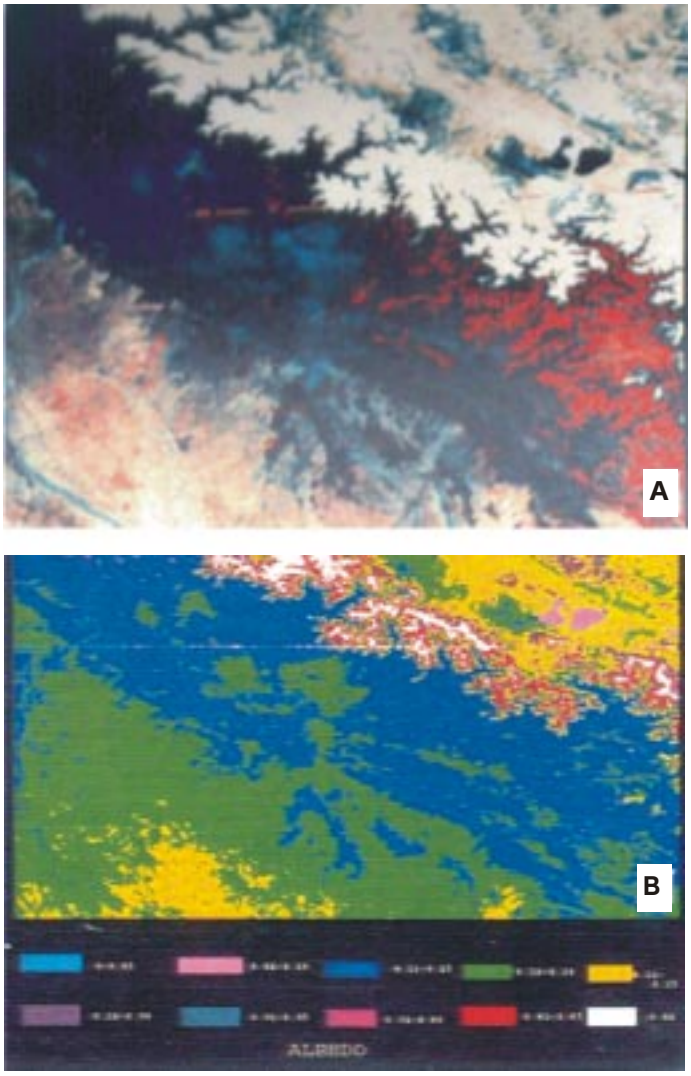

Figure 2: (A) FCC (NOAA-AVHRR-Ch2,Ch1,Ch1) and (B) Albedo image of Part of Himalayan mountain, India

Land Surface Temperature

It is the temperature of the land surface i.e. kinetic temperature of the soil plus the canopy surface (or in the absence of vegetation, the temperature of the soil surface).

Surface temperature can be used for various agro-meteorological applications –

- surface heat energy balance study
- characterization of local climate in relation with topography and land use
- mapping of low temperature for frost conditions (night-time) or winter cold episodes (day/night)
- derivation of thermal sums (using surface temperature instead of air temperature) for monitoring crop growth and development conditions.

The land surface temperature can be estimated from remote sensing measurement at thermal IR wavelength (8-14 μm) of the emitted radiant flux (Li) and some estimate of the surface emissivity (ϵ). Land surface temperature (Ts) can be expressed using inverse Plank's equation (Mansor and Cracknell, 1994) :

$$Ts = C_2 / \lambda \, 1n \, [(\epsilon . C_1 . \lambda^{-5} / \pi . L\lambda) + 1]$$

where, C_1 and C_2 are the first and second radiation constants (C_1 = 3.742 x 10^{-16} Wm^2 & C_2 = 0.01444 mK); λ is wavelength in m; ϵ is the emissivity and $L\lambda$ is the spectral radiance ($mw/cm^2/Sr/\mu m$).

The Normalised Difference Vegetation Index (NDVI) is used as a parameter for evaluating emissivity. The surface emissivity of a surface can be calculated using the following relationship (van de Griend, 1993) :

$$\epsilon = a + b.1n \, (i) + \Delta\epsilon$$

where, a = 1.0094 and b = 0.047, 'i' is the NDVI of mixed pixel, $\Delta\epsilon$ is the error in emissivity values. 'i' can be estimated by using following expressions (Valor and Caselles, 1996) :

$$i = i_v . P_v + i_g \, (1 - P_v)$$

$$P_v = (1 - i/i_g) / (1 - i/_g) - K \, (1 - i/i_v)$$

$$K = (\rho_{2v} - \rho_{1v}) / ((\rho_{2g} - \rho_{1g})$$

where, P_v is the vegetation proportion; 'i' is the NDVI value of mixed pixel; i_g and i_v are the NDVI values of pure soil and pure vegetation pixel, respectively,

ρ_{2v} and ρ_{1v} are the reflectances in NIR and red region for pure vegetation pixels; ρ_{2g} , ρ_{1g} are the reflectances in NIR and red region for pure soil pixels.

$$\Delta\epsilon = 4 < d\epsilon > P_v (1 - P_v)$$

where, $\Delta\epsilon$ is mean weighed value taking into account the different vegetation in the area, their structure and their proportion in it.

The NOAA – AVHRR channels 4 & 5 (10.3 – 10.3 and 11.5 – 12.5 μm) are widely used for deriving surface temperature for the day time passes. The temperatures derived from channels 4 and 5 are slightly different due to atmospheric water vapour absorption. Thus, in the land surface retrieval algorithm, the incorporation of the difference between channels 4 & 5 could be useful in correcting for the atmospheric water vapour effect as a first degree approximation. An approach based on the differential absorption in two adjacent infrared channels is called "split-window" technique and is used for determination of surface temperature.

In split-window algorithm, brightness temperatures in AVHRR channel 4 (T_4) and channel 5 (T_5), mean emissivity ϵ, i.e. $(\epsilon_4 + \epsilon_5)/2$; difference in emissivity $\Delta\epsilon$, i.e. $(\epsilon_4 - \epsilon_5)$, have been used for the estimation of land surface temperature using the following relation (Becker and Li, 1990) :

$$T_s = A + B [(T_4 + T_5) / 2] + C [(T_4 - T_5) / 2]$$

where, A, B and C are co-efficients worked out by statistical analysis and given by :

$$A = 1.274; \quad B = 1 + \{0.15616 (1- \epsilon) / \epsilon\} - 0.482 \ (\Delta\epsilon / \epsilon^2)$$

$$C = 6.26 + \{ 3.98 (1- \epsilon) / \epsilon\} + 38.33 (\Delta\epsilon / \epsilon^2)$$

Brightness temperature (T_B) values have been calculated by using the inverse of Planck's radiation equation :

$$T (B) = C_2 . V / 1_n (1 + C_1 . V^3 / E_i)$$

$$E_i = S_i . C + I_i \text{ (Kidwell, 1991)}$$

where, V is the wave number of (Cm^{-1}) of channel filter;

C_1 = 1.1910659 x 10^{-5} ($mw/m^2/Sr/cm^4$)

C_2 = 1.43883 cm^ok

E_i, is radiance ($mw/m^2/Sr/cm$); C is digital number; S_i scaled slope; I_i is the intercept value.

Flow diagram of the methodology for deriving land surface temperature following "split-window" approach using NOAA – AVHRR data is shown in Fig. 3. Landsat TM (Saha and Pande, 1995a) and NOAA – AVHRR derived (Kant, 2000) land surface temperature images generated following above approaches are presented in Fig. 4 and Fig. 5, respectively.

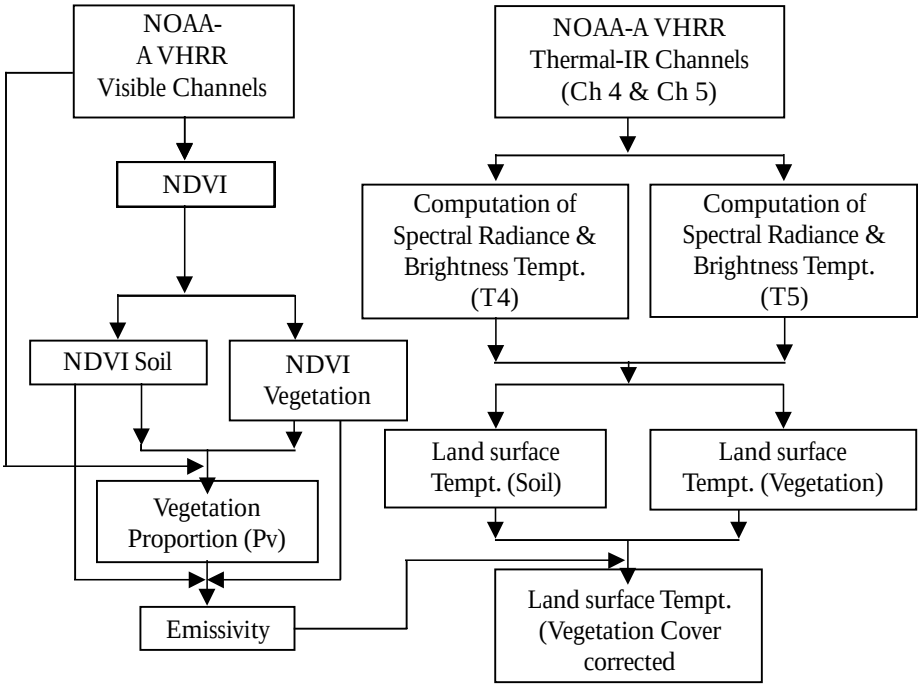

Figure 3: Flow diagram of methodology of retrieval of land surface temperature using NOAA-AVHRR data.

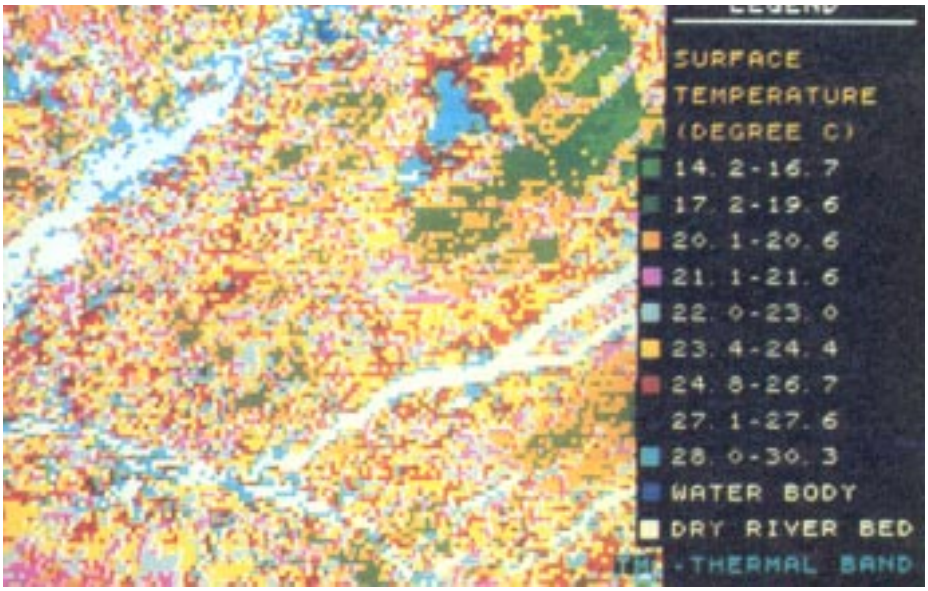

Figure 4: Surface temperature image generated by processing of Landsat – TM in part of western Doon Valley, Dehra Dun

Evapotranspiration (ET)

The concept of using remotely sensed surface temperature in evapotranspiration estimation has been demonstrated by Bartholic *et al.* (1972) and Brown (1974).

The model used to estimate evapotranspiration from remote sensing data and agro-meteorological data is based on surface energy balance equation.

$$R_n = G + H + LE$$

$$LE = R_n - H - G$$

where, R_n is the net radiation flux; LE is the latent heat flux (corresponding to evaporation for a bare soil and evapotranspiration for a vegetation canopy); H is the sensible heat flux; G is the soil heat flux. All above terms have unit W / m^2. The net radiation (R_n) can be expressed as :

$$R_n = (1\text{-}A)\, R_s + E_a.Rl - E_s \,.\, \sigma \,.\, T_s^4$$

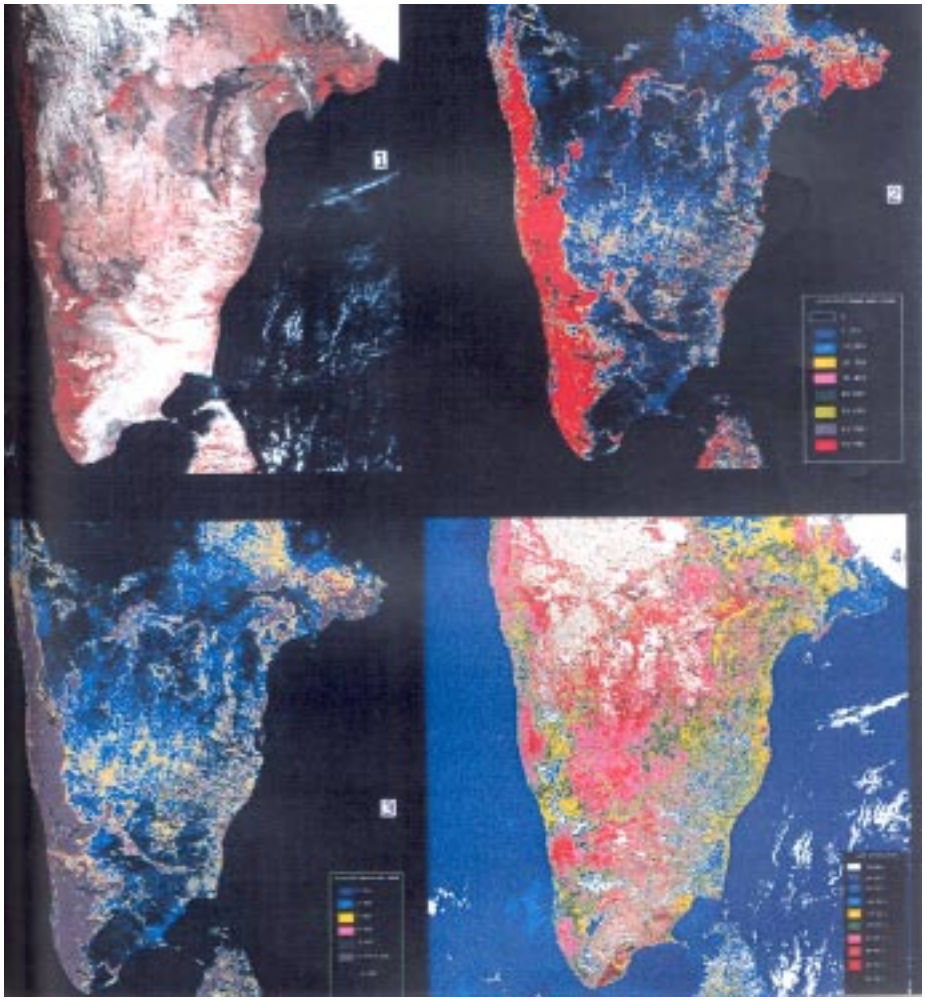

Figure 5: (1) FCC (Ch2, Ch1, Ch1, R,G,B) ; (2) Vegetation proportion image; (3) Surface emissivity image and (4) Surface Temperature image - derived from processings of NOAA - AVHHR data (southern India)

where, A is surface albedo; Rs is the incident short wave radiation (w/m^2); E_a is the atmospheric emissivity; Rl is the incoming long wave radiation (w/m^2); E_s is the surface emissivity; σ is the Stefan – Boltzman constant and T_s is the surface temperature (^oK).

Atmospheric emissivity (E_a) and incoming long wave radiation (Rl) can be computed using following expressions given by Brutsaert (1975) :

$E_a = 1.24\ (e_a / T_a)^{1/7}$

$R_{L} = \sigma . Ta^4$

where, e_a is the vapour pressure of air at ambient air temperature Ta. The sensible heat flux may be written as :

$$H = \rho . C_p (T_s - T_a) / \Upsilon_a$$

where, ρ is the air density; C_p is the specific heat of air, Υ_a is the aero-dynamic resistance for sensible heat flux (S/m). The aero-dynamic resistance (Υ_a) can be expressed as (Hatfield *et al.*, 1984) :

$$\gamma_a = \frac{1_n \{(z-d)/zo\}^2}{K^2 U}$$

where, Z is the reference height (2m); d is the zero plane of displacement (m) (= 2 h/3 h is the height of vegetation); Zo is the surface roughness height (m) (= h/8); K is the Von Karman's constant (≈ 0.38) and U is the wind speed at Z (m/s).

Soil heat flux can be written as function of net radiation (Ma *et al.*, 1999):

$$G = \frac{Ts}{A}\ (0.003.A + A^2)\ (1\text{-}0.978\ NDVI\ 4)\ .R_n \quad \text{(for vegetated surface)}$$

$G = 0.20 . R_n$ (for bare surface)

Since, H, G and R_n are instantaneous, it is necessary to apply a procedure to integrate to daily totals. The evaporative fraction (Brutsaert and Sugita, 1992) is the energy used for evaporation process divided by the total amount of energy available for the evaporation process.

$$\wedge = \frac{LH}{LH + H} = \frac{LE}{R_n - G}$$

Although, the H and LE fluctuate strongly on daily basis, the evaporative fraction behaves steady during day time. Then, the link between the instantaneous and the integrated daily case is given by

$\wedge_{24\ hrs} = \wedge_{inst.}$

The final equation that can be used to evaluate the daily ET is based on the evaporative fraction –

$ET_{24} = \wedge_{inst.} (R_n\ day - G\ day)$

Figure 6 illustrates flow chart for a daily ET model based on remote sensing data. Various researchers investigated several approaches of ET modeling using satellite data using Landsat TM and NOAA – AVHRR data (for reference see Chen *et al.*, 2003). ET and R_n estimated from Landsat TM data following surface energy balance modeling approach for western part of Doon Valley is presented in Fig. 7 (Saha and Pande, 1995b).

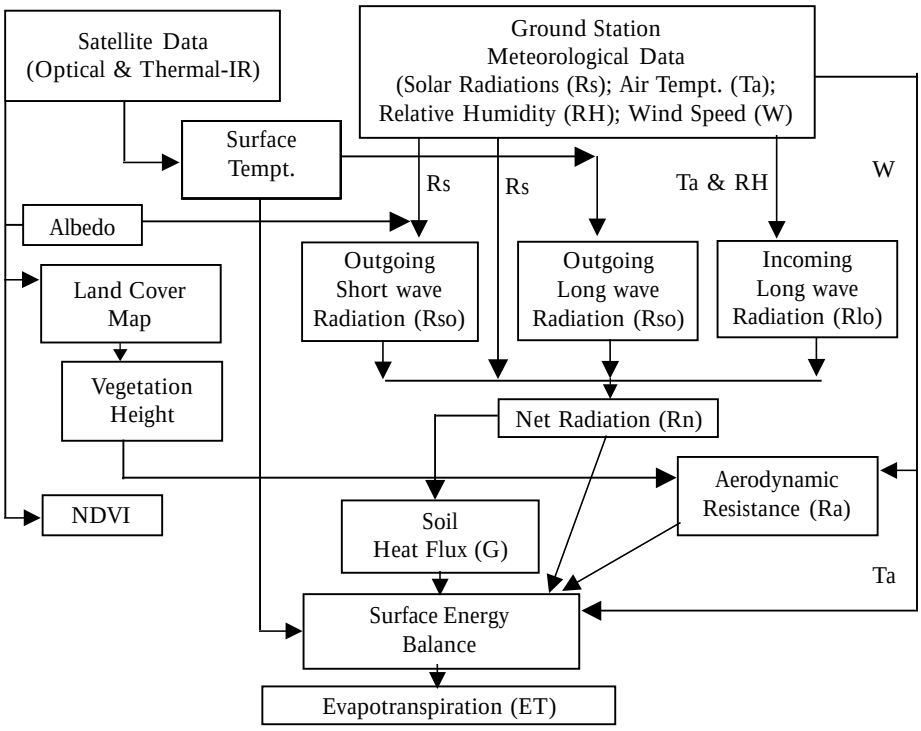

Figure 6: Flow chart for daily regional ET estimation using satellite data

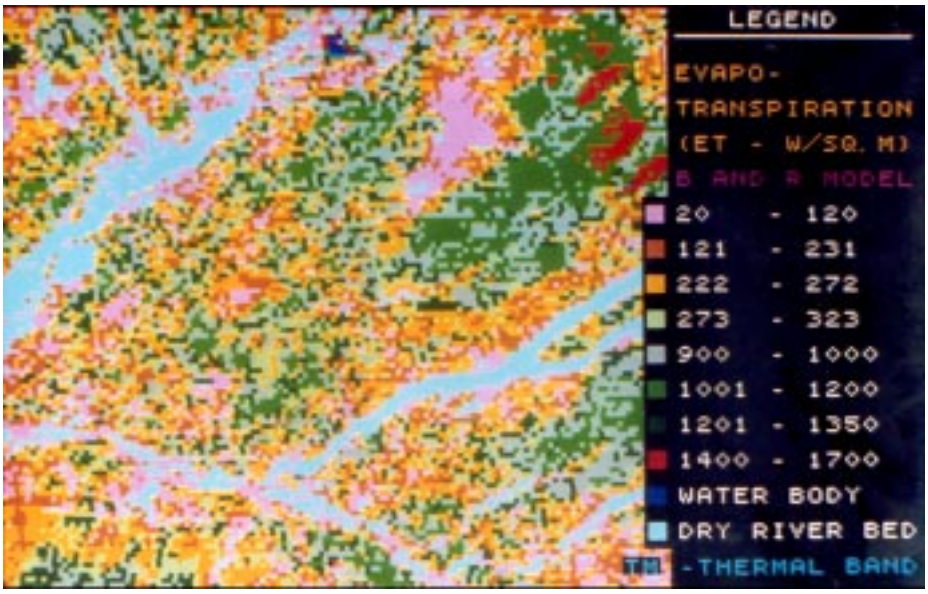

Figure 7: Evapotranspiration image of part of western Doon Valley generated by processing of Landsat – TM data

Absorbed Photosynthetically Active Radiation (APAR)

APAR is the fraction of the PAR (Photosynthetically Active Radiation) absorbed by the canopy and used for carbon dioxide assimilation. PAR refers to the visible part of the solar spectrum between 0.4 and 0.7 μm, where chlorophyll absorbs solar radiation. APAR is a key parameter in productivity analysis and ecosystem modeling. The productivity of vegetation canopies can be studied from estimation of APAR derived from optical remote sensing data.

The APAR results from a leaf radiation balance :

$$APAR = PAR - pp_{AR} . PAR - PAR_{trans} + PAR_{soil}$$

where, p_{PAR} is the canopy reflectance at the upper side of the canopy in the 0.4 to 0.7μm spectral range, PAR_{trans} is the amount of PAR that is transmitted through the canopy and directed to the soil; PAR_{soil} that is reflected from the soil underneath the canopy and is received back at the lower side of the canopy.

APAR can be deduced directly from PAR after simplifying the previous equation into :

$$APAR = fPAR \cdot PAR$$

where, f PAR is the fractional photosynthetically active radiation.

Asrar *et al.* (1992) showed that f PAR is related to NDVI and relation is expressed by :

$$f\ PAR = 1.222 - 0.1914 \cdot NDVI$$

Variation in canopy optical properties, architecture as well as background spectral reflectance could affect f PAR – NDVI relation, with background spectral properties producing a large effect.

It was observed that APAR was linearly related to NDVI and curvulinearly to LAI (Leaf Area Index) approaching asymptotically value of LAI, where virtually all incident short wave radiation observed by crop canopy. Fig. 8 illustrates APAR map of wheat crop derived by processing of IRS- WiFS data from a case study of part of U.P. and U.A., India (ASD, 2003).

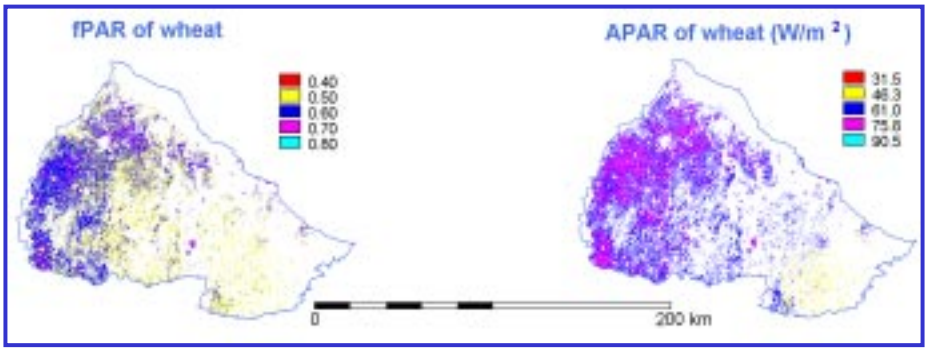

Figure 8: Estimated f PAR and APAR values of wheat (using NDVI of IRS –WiFS).

Clevers (1989) suggested an approach for reducing soil background to some extend on the relation between f PAR and remote sensing derived spectral indices. According to him f PAR can be related with WDVI (Weighted Difference Vegetation Index).

$$f\ PAR = WDVI \cdot f\ PAR\alpha / WDVI\alpha$$

where, f PARα is asymptotically limiting value of f PAR (usually 0.94); WDVIα is the asymptotically limiting value of WDVI which is given by :

$$WDVI = NIR_r - C.\ R_r$$

$$C = \frac{NIR_s}{R_s}$$

where, NIR_r is the total measured NIR reflectance, R_r is the total measured red reflectance, NIR_s and R_s are the NIR and red reflectance of soil, respectively.

The relation between LAI and f PAR was described as :

$$LAI = -1/K_{PAR}\ .\ 1n\ [\ 1 - f\ PAR/\ fPAR\alpha]$$

where, K_{PAR} is the function of extinction and scattering co-efficient.

Experimental evidence indicated that the growth rate of several agricultural crop species increases linearly with increasing amounts of APAR, when soil water nutrients are not limiting (Myneni and Choudhury, 1993).

Therefore, integration of APAR over period e.g. growth cycle (i.e. emergence to maturity) represents total photosynthetic capacity of crops :

$$APAR = \int_{t=0}^{m} e.APAR(t) = \int_{t=0}^{m} e.f\ (NDVI).0.48.R_s$$

where, e is the radiation use efficiency, defined as the ratio of canopy net photosynthesis to incident PAR; f (NDVI) is a function relating NDVI with f PAR and R_s is the incoming solar radiation. Field *et al.* (1995) developed a global ecology model for net primary production in which e is calculated as :

$$e = e'\ .\ T_1.\ T_2\ .\ W$$

where, e' is the typical maximum conversion factor for above ground biomass for C_3 and C_4 crops when the environmental conditions are all optimum (e = 2.5 for C_3 crops and e = 4 for C_4 crops).

$$W = \wedge$$

$$T_1 = 0.8 + 0.02\ .\ T_{opt} - 0.005\ .\ T^2_{opt}$$

$$T_2 = 1.185 \frac{1}{1+\exp(0.2.T_{opt} - 10 - T_{mon})} \cdot \frac{1}{1+\exp(-0.3T_{opt}^{-10} + T_{mon})}$$

where, $\wedge$ is the evaporative fraction, T_{opt} (^oC) is the mean air temperature during the month of maximum LAI or NDVI and T_{mon} (^oC) is the mean monthly air temperature.

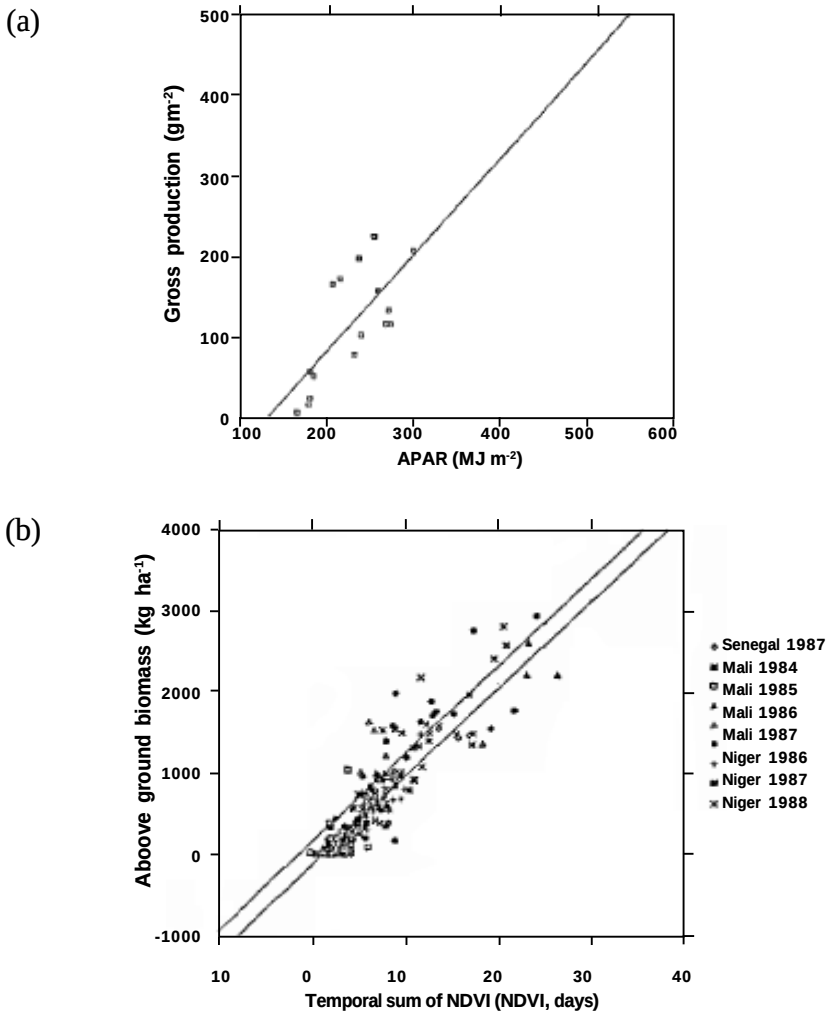

Figure 9: (a) Relation between gross production and accumulated APAR and (b) Relation between above ground biomass and accumulated NDVI

Therefore, temporal sums of NDVI which is giving cumulative values of APAR, can be used for estimation of crop/vegetation productivity. Prince (1990) observed a good linear relationship between APAR and vegetation gross production and also strong positive relationship between above ground vegetation biomass and temporal sum of NOAA – AVHRR NDVI (Fig. 9) in parts of Africa.

CONCLUSIONS

Remotely sensed satellite optical and thermal infrared can be synergistically used to estimate surface agro-meteorological properties. Optical data can be used to estimate land surface albedo by integrating narrow-band directional spectral reflectances. Thermal IR data from various satellites appear as valuable tool for vegetation growth and conditions assessment by retrieval of land surface temperature and estimation of evapotranspiration following various modeling approaches. Optical data in the form of spectral indices are found to be related to solar radiation absorbed by vegetation canopies and this is useful for assessing regional vegetation potential productivity.

REFERENCES

Asrar, G. Myneni, R.B. and Choudhury, B.J. 1992. Spatial heterogeneity in vegetation canopies and remote sensing of absorbed photosynthetically active radiation : a modeling study. Remote Sensing Environment, 41 : 85-103.

Bartholic, J. F., Namken, K.N. and Wiegand, C.L. 1972. Aerial thermal scanner to determine temperature of soil and crop canopies differing in water stress. Agronomy Journal, 6 : 603.

Becker, F. and Li, L. 1990. Towards a local split window method over land surface. Remote Sensing Environment, 32 (17) : 17-33.

Brest, C.L. and Goward, S.N. 1987. Deriving surface albedo from narrow band satellite data. International Journal of Remote Sensing, 8 : 351-367.

Brown, K.W. 1974. Calculation of evapotranspiration from crop surface temperature. Agricultural Meteorology, 14 : 199-209.

Brutsaert, W. 1975. On a derivable formula of long wave radiation from clear skies. Water Resource Research, 11 : 742 – 744.

Brutsaert, W. and Sugita 1992. Application of self-preservation in the diurnal evolution of the surface energy budget to determine daily evaporation. *Journal of Geophysical Research*, 19 (17) : 18, 377 – 18, 382.

Chen, Y.; Li, X.; Jing, G. and Shi, P. 2003. An estimation model for daily regional evapotranspiration. International Journal of Remote Sensing, 24 : 199 – 205.

Clevers, J.G.P.W. 1988. A simplified reflectance model for the estimation of Leaf Area Index. Remote Sensing Environment, 25 : 53-69.

Field, C.B.; Randerson, J.J. and Malmstrom, C.M. 1995. Global net primary productivity production : Combining ecology and remote sensing. Remote Sensing Environment, 51 (1) : 74-88.

Goita, K. and Royer, A. 1992. Land surface climatology and land cover change monitoring since 1973 over a north-Sahelian zone using Landsat data. Geocarto-International, 2: 15-28.

Hatfield, J.L.; Reginato, R.J. and Idso, S.B. 1984. Evaluation of canopy temperature evapotranspiration models over various crops. Agricultural and Forest Meteorology, 32: 41 – 53.

Kant, Yogesh 2000. Studies on Land Surface Process using Satellite Data. *Ph.D. Thesis* in Physics, Omania University, India.

Myneni, R.B. and Choudhary, B.J. 1993. Synergistic use of Optical and Microwave data in agro-meteorological applications. Advances in Space Research, 13 (5) : 239-248.

Mansor, S.B. and Cracknell, A.P. 1994. Monitoring of coal fires using thermal infrared data. International Journal of Remote Sensing, 15 (8) : 1675 – 1685.

Prasad, S.; Gupta, R.K. and Sesa Sai, M.V.R. 1995. Computation of surface albedo from NOAA – AVHRR data. Pages 51-57. In Proc. National Symposium on Remote Sensing Environment with special emphasis on Green Revolution. ISRS, India.

Prince, S.D. 1990. High temporal frequency remote sensing of primary production using NOAA – AVHRR. Pages 169-184. In book "Applications of Remote Sensing in Agriculture" (Eds. M.D. Steven and J.A. Clark). Butterworth.

Saha, S.K. and Pande, L.M.1995a. Regional surface albedo and ET modeling using combination of optical and thermal IR data. Pages 70-78. In book "Advances in Tropical Meteorology" (R.K. Dutta, Ed.). Concept Publishers, New Delhi, India.

Saha, S.K. and Pande, L.M.1995b. Modeling land surface energy balance components and assessment of crop water stress – a satellite thermal IR remote sensing approach. Proc. ISRS Silver Jubilee Year Seminar, Dehra Dun.

Saunders, R.W. 1990. In determination of broad band surface albedo from AVHRR visible and near infrared radiances. International Journal of Remote Sensing, 11 (1) : 49 – 67.

Valor, E. and Caselles, V. 1996. Mapping land surface emissivity from NDVI; application to European, Africa and South American areas. Remote Sensing Environment, 57 : 167 – 184.

van de Gried, A.A. and Owe, M.1993. On the relationship between thermal emissivity and the normalized difference vegetation index for natural surfaces. International Journal of Remote Sensing, 14 : 1119 – 1131.

Valientz, J.A.; Nunez, M.; Lopez – Baeza E. and Poreno, J.F. 1995. Narrow band to broad band conversion for Meteosat – visible channel and broad – band albedo using both AVHRR –1 and 2 channels. International Journal of Remote Sensing, 16 (6) : 1147 – 1166.

RETRIEVAL OF AGROMETEOROLOGICAL PARAMETERS FROM SATELLITES

C.M. Kishtawal
Atmospheric Sciences Division
Meteorology and Oceanographic Group
Space Application Centre (ISRO), Ahmedabad

Abstract: In this article the techniques of the retrieval of agro-meteorological parameters like cloudiness, rainfall, soil moisture, solar radiation, surface temperature, and shelter temperature/humidity using different approaches are discussed. A discussion is presented on the state-of-the-art sensors, and how they can be helpful in providing some additional parameters and also, the conventional parameters (as mentioned above) with better accuracy.

INTRODUCTION

Satellites offer a unique source of information for many agricultural applications. Among their attributes are: (1) regular, repetitive observation patterns; (2) large scale synoptic view of the earth surface from space; and (3) availability of a permanent information archive for establishing baseline data. In the following sections a brief outline of the weather parameters of agro-meteorological importance is provided, and a discussion about the usefulness of satellite observations in the retrieval of these parameters is given.

PARAMETERS OF AGRO-METEOROLOGICAL INTEREST

Although a large number of atmospheric parameters can affect the agricultural production in short and long time scale, we will confine the current discussion to a few parameters. Also, we will see how the satellite observations can play a role in determination of these parameters. The parameters discussed in the following subsections are:

Satellite Remote Sensing and GIS Applications in Agricultural Meteorology
pp. 195-211

- Clouds
- Rainfall
- Soil Moisture
- Solar Radiation
- Surface Temperature
- Temperature and Humidity Profiles.

Meteorological satellites play an important role in retrieval of the above parameters at large spatial scales. The following subsections provide the discussion on this aspect.

Clouds

Interpretation of Cloud in Visible/Infrared Imageries

The cloud configuration seen in satellite imagery represents a visible manifestation of all types of atmospheric processes. The complete interpretation of cloud structure must make use of both satellite imagery and other available observational data. One should remember that the satellite sensors view only tops of clouds while in surface observations their bases are seen. Basically following six characteristic features of satellite pictures are helpful in extracting information for weather forecasting:

i) Brightness - The brightness depends strongly upon the albedo of the underlying surface in visible pictures. Highly reflecting surfaces like cumulonimbus (Cb) tops and snow appear pure white whereas the sea looks black. Other clouds and land appear in varying degrees of gray. In IR images warm land surfaces appear very dark while cold ones are white (e.g. Cb tops, thick cirrus, snow etc.). Lower level clouds and thin cirrus appear gray.

ii) Pattern - Cloud elements are seen to be organised into identifiable patterns like lines, bands, waves etc.

iii) Structure - In a VIS image, shadows of taller clouds fall on lower surfaces. Shadows and highlights thus give an idea of the cloud structure. In IR

imagery this information is provided by the cloud top temperature (CTT) more directly.

iv) Texture - The cloud surfaces when viewed by the satellite vary in degree of apparent smoothness. Some clouds appear smooth while some may look ragged.

v) Shape - Clouds assume a variety of shapes - rounded, straight, serrated, scalloped, diffused or curved.

vi) Size - The size of a pattern or the size of individual elements in a pattern are useful indicators of the scale of weather systems.

While interpreting satellite pictures continuity in time has to be maintained. The pictures should not be viewed in isolation but must be interpreted with reference to past weather and earlier imageries. It is necessary to keep in mind the time of the day, season and local peculiarities while interpreting satellite imageries. In VIS pictures illumination depends on the position of the sun which will vary the brightness of clouds. Similarly in different seasons (e.g. summer and winter) the image disc of the northern and southern hemisphere will have different brightness. Local features like mountains and valleys introduce their own effects. In IR imagery elevated land like Tibetan Plateau will be cold at night and would appear very bright whereas tropical oceans would maintain about the same gray shade throughout the diurnal cycle.

Interpretation of Visible Imageries

Clouds have higher albedo than land (apart from snow cover) and appear white or light grey in a VIS imagery. Their brightness depends on their physical properties. Clouds with high albedo have large depth, high cloud water (ice) content, small cloud-droplet size whereas clouds with low albedo have shallow depth, low cloud water (ice) content, large average cloud-droplet size. The water content and depth of the cloud are the most important. Typical Albedo values are given in Table 1.

Table 1. Albedo values of different surfaces and clouds

Earth surface	(%)	Clouds	(%)
Oceans, Lakes	8	Shallow broken clouds Cu, Ci, Cs, Cc	30 35
Land Surfaces	14-18	St	40
Sand, Desert	27	Thick clouds (Cs)	74
Ice and Snow		Ac, As, Sc	68
Sea ice	35	Cu	75
Old snow	59	Ns	85
Fresh snow	80	Cb	90

VIS imagery is useful for distinguishing between sea, land and clouds (Figure 1). Seas and lakes have low albedo and hence appear dark. Land appears brighter than sea but darker than clouds. Albedo of land varies with the type of surface. Deserts appear very bright in contrast to the darkness of forests and vegetated areas. When the sun shines obliquely onto clouds the shadow thrown by an upper cloud layer onto a lower layer reveals the vertical structure of the cloud in VIS imagery.

The texture of the cloud in VIS imagery can help in its identification, (for example) its cellular pattern can distinguish stratocumulus clouds (Sc) from stratus (St). No VIS imagery can be obtained at night. To distinguish clouds from snow covered ground a knowledge of the surface topography is essential. Thin clouds have low albedo and do not show up very brightly in VIS imagery so that the cloud cover over dark surfaces may be underestimated. In the same manner thin cloud over a high albedo desert surface may look misleadingly bright and thick. Mesoscale cumulus (Cu) clouds which are smaller than the resolution of the satellite will be depicted in rather lighter grey shades in VIS imagery quite unlike the normal view of convective clouds.

Interpretation of IR Imagery

IR imagery indicates the temperature of the radiating surfaces. In black and white image warm areas are shown in dark tones and cold areas in light tones. Clouds will generally appear whiter than the earth surface because of their lower temperature. In this respect IR and VIS images have some similarity.

Because cloud top temperature decreases with height IR images show good contrast between clouds at different levels. This is not possible in VIS imagery.

Coast lines show up clearly in IR images whenever there is strong contrast between land and sea surface temperatures. During the day the land may appear darker (warmer) than the sea but at night may appear lighter (cooler). At times when land and sea temperatures are almost same, it becomes impossible to detect coastlines in IR imagery. The most marked contrast between land and sea is normally found in Summer and Winter and is least in Spring and Autumn. Thin Ci which is often transparent in the VIS can show up clearly in IR especially when it lies over much warmer surface.

IR imagery is inferior to VIS in providing information about cloud texture as it is based upon emitted and not scattered radiation. Low clouds and fog can rarely be observed in IR at night because they have almost the same temperature as the underlying surface. But during day, such clouds are easily detected in.

Interpretation of WV Imagery

Water vapor imagery is derived from radiation at wavelengths around 6-7 μm. Though this is not an atmospheric window, it is part of the spectrum where water vapor is the dominant absorbing gas. It has a strong absorption band centered on 6.7 μm. In regions of strong absorption, most of the radiation reaching the satellite originates high in the atmosphere. The stronger the absorption, the higher is the originating level of the emission that ultimately reaches the satellite. As the Relative Humidity (RH) decreases the main contribution of the radiance received by the satellite comes from lower in the troposphere.

WV imagery is usually displayed with the emitted radiation converted to temperature like IR imagery. Regions of high upper tropospheric humidity appear cold (bright) and regions of low humidity appear warm (dark) i.e. when the upper troposphere is dry, the radiation reaching the satellite originates from farther down in the atmosphere where it is warmer and appears darker on the image. In a normally moist atmosphere most of the WV radiation received by the satellite originates in the 300-600 hPa layer. But when the air is dry some radiation may come from layers as low as 800 hPa. Due to the general poleward decrease of water vapor content, the height of the contributing layer gets lower and lower towards the poles.

Since clouds do emit radiation in this wave band, high clouds may be seen in this type of imagery. Thick high clouds as Cb anvils stand out prominently in both WV and IR imageries. Broad-scale flow patterns are particularly striking in WV imagery. This is because WV acts as passive tracer of atmospheric motions. WV imagery is therefore useful for displaying the mid tropospheric flow (for example), upper tropospheric cyclones are defined clearly by moist spirals or comma-shaped patterns. Subsidence areas appear dark. Jet streams are delineated by sharp gradients in moisture with dry air on the poleward side. Even when a WV image indicates a very dry upper troposphere, there may well be moist air near the surface. Moist air or cloud in the lower half of the troposphere is not depicted well in WV imagery.

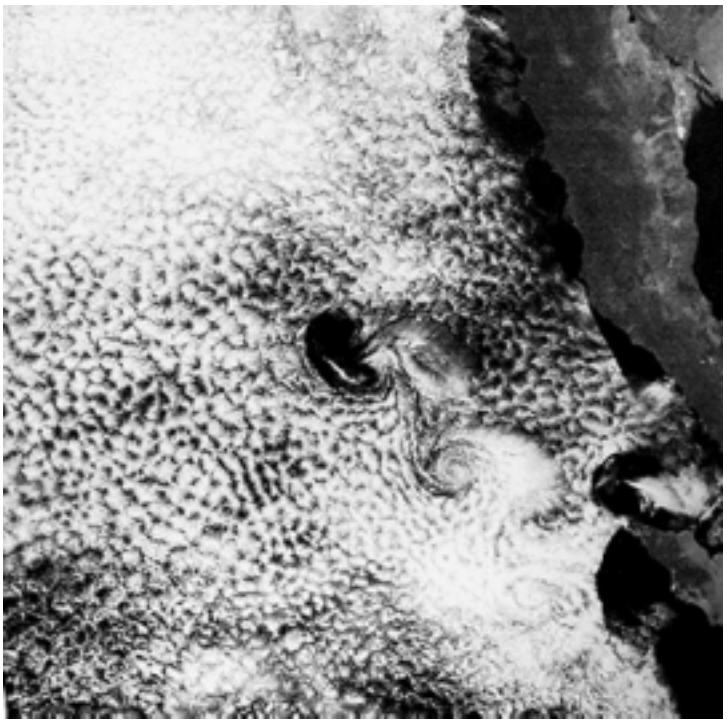

Figure 1: Karman cloud vortices in Pacific Ocean as they are seen in visible images

Rainfall

Rainfall is not only an important parameter for agro-meteorology, it is also a vital component of earth's hydrological cycle. Oceans receive heat from the sun, and the evaporation takes place. When the same evaporation travels

vertically, it gets condensed to form clouds and eventually precipitation. During this process, enormous amount of energy is released which is called the latent heat of condensation. This is one of the major sources of energy that drives the circulation in tropical atmosphere. Hence, the knowledge of rainfall and its distribution at current time is also important for its future prediction.

There are several techniques to derive rainfall from satellite observations. The earliest developed methods that are useful even today are based on the visible/infrared observations from satellites. Techniques based on visible sensors rely on the identification of cloud types. Each cloud type is assumed to have different rain intensity, and then the rain is derived based upon the extent of each cloud type. In infrared-based methods, the most common approach is to find cold clouds (say, colder than 250^{o}K) within an overcast area. The raining potential of the clouds is proportional to the fractional area covered by cold clouds, and thus the rainfall derived. More complex techniques use both visible and infrared observations to create a bi-spectral histogram of the cloud images. Bi-spectral histogram method is a simple technique in which the clouds can be classified based on the combination of cloud signatures in visible and infrared frequencies. Then the rainfall is derived by estimating the extent of each type of cloud and multiplying it by the a-priori rain potential of respective classes. However, all the rain-retrieval techniques based on visible/IR observations are basically "inferential" in nature, because these sensors can sense the clouds (that too, the top surfaces of the clouds) but not the actual rain, that occurs at several layers below the clouds. Visible/IR techniques make a "guess" about the rainfall based on the cloud features. Due to this shortcoming, the estimates of rainfall based on visible/IR technique are not very accurate on instantaneous time scale. However, long time averages (e.g. daily, weekly, and monthly) of rainfall are better and usable for practical purposes.

On the other hand, rainfall estimation techniques based on microwave frequencies (0.1 cm to 100 cm wave length) are more direct in nature. Due to their large wavelengths, these frequencies can easily penetrate clouds. However, these frequencies interact effectively with rainfall. Let us consider the case of passive microwave methods. In these techniques, the microwave instrument onboard satellite does not have any source of microwave illumination. It has just a receiver that can gather the microwave emission coming from earth, ocean or atmosphere. Due to small emissivity in microwave region, ocean surface emits small amount of microwave radiation. When the rainfall occurs over a layer in the atmosphere, two different processes take place.

The atmospheric rain layer itself emits microwave radiation and thus the radiation received at satellite is greater than the radiation received in no-rain situation. This process is predominant at lower frequencies (e.g. 19 GHz, or about 1.5 cm wavelength). On the other hand, the rain drops, ice and snow particles, scatter the microwave radiation (particularly at higher frequencies, e.g. 85 GHz, or about 0.3 cm wavelength) that is coming up from the ground. In this case the radiation received at satellite will be smaller than that in no-rain situation. In both the cases, the change in the microwave radiation (measured in terms of brightness temperature) can be related to the intensity of rainfall. Various algorithms have been developed in the past that use either low frequency or high frequency, or a combination of both. It is to be noted that for emission based algorithms (using lower frequencies of microwave e.g. 19 GHz), it is important that the emission from the background should be uniform and also as little as possible, so that the emission from rainfall can be detected clearly. So emission based algorithms are effective only over the ocean surfaces, while the scattering based algorithms using higher frequencies of microwave, can be used over the ocean as well as over the land. Special Sensor Microwave Imager (SSM/I), and TRMM Microwave Imager (TMI) are good examples of passive microwave sensors that are quite effective in the determination of global rainfall (Figure 2).

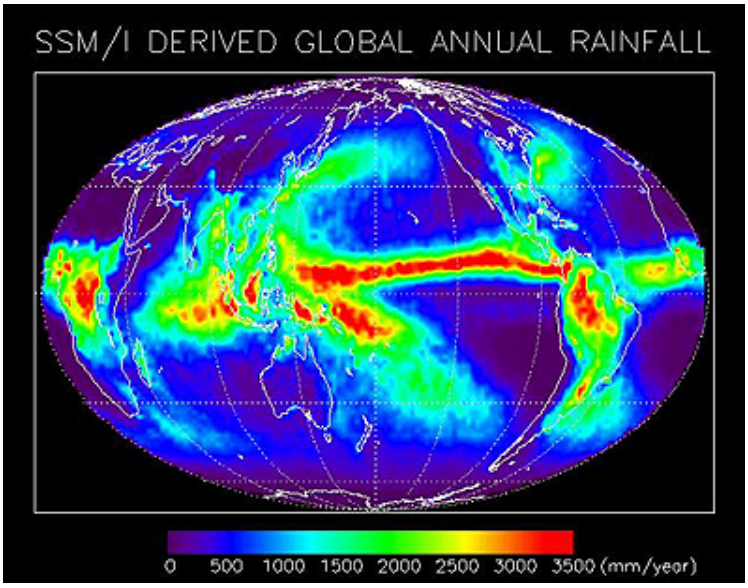

Figure 2: Global annual rainfall observed by Special Sensor Microwave/Imager (SSM/I) (Picture courtesy : rst.gsfc.nasa.gov)

Soil Moisture

Recent advances in remote sensing have shown that soil moisture can be measured by a variety of techniques. However, only microwave technology has demonstrated a quantitative ability to measure soil moisture under a variety of topographic and vegetation cover conditions so that it could be extended to routine measurements from a satellite system. Both active and passive microwave techniques have been applied by researchers for the estimation of soil moisture. Two material properties provide clues about composition and surface state by the manner in which these attributes interact with the microwave radiation. One property is the dielectric constant (its symbol is the small Greek letter, *k*), which is the ratio of the capacitance of a material to that of a vacuum. It is a dimensionless number that is set at 1.00. This electrical property describes a material's capability (capacity) to hold a charge, which also measures its ability to polarize when subjected to an electric field. Microwave radiation penetrates deeper into materials with low dielectric constants and reflect more efficiently from those with high constants. Values for *k* range from 3 to 16 for most dry rocks and soils, and up to 80 for water with impurities. Moist soils have values typically between 30 and 60. Thus, variation in emitted microwave radiances (in case of passive microwave observations e.g. by radiometers) or reflected-pulse intensities (in case of active microwave observations e.g. by radar) may indicate differences in soil moisture, other factors being constant. Dry soil has a high emittance; water surfaces have low emittance in microwave region. If one adds water to the soil, the emittance falls and becomes polarized. With the knowledge of "normal" emittance at a particular location (which depends upon soil type and vegetation), microwave observations can be used to detect changes in emittance and therefore of soil moisture. Since the soil moisture is changed by precipitation, these emittance changes between two satellite passes can serve as a proxy of precipitation, known as Antecedent Precipitation Index (API).

The second material property is roughness that can be used to define the *soil texture*. Materials differ from one another in their natural or cultivated state of surface roughness. Roughness, in this sense, refers to minute irregularities that relate either to textures of the surfaces or of objects on them (such as, closely-spaced vegetation that may have a variety of shapes). Examples include the textural character of pitted materials, granular soils, gravel, grass blades, and other covering objects whose surfaces have dimensional variability on the order of millimeters to centimeters. The height of an irregularity, together with radar wavelength and grazing angle at the point of contact,

determines the behavior of a surface as smooth (specular reflector), intermediate, or rough (diffuse reflector). A surface with an irregularity height averaging 0.5 cm will reflect Ka band (l= 0.85 cm), X band (l= 3 cm), and L band (l= 25 cm) radar waves as if it were a smooth, intermediate, and rough surface, respectively. Other average heights produce different responses, from combinations of "all smooth" to "all rough" for the several bands used. This situation means radar, broadcasting three bands simultaneously in a quasi-multi-spectral mode, can produce color composites, if we assign a color to each band. Patterns of relative intensities for images made from different bands may serve as diagnostic tonal signatures for diverse materials whose surfaces show contrasted roughness.

Solar Radiation

Incoming solar radiation is the primary source of energy for plant photosynthesis. Solar radiation also plays a key role in evapotranspiration. Visible observations from satellites provide an excellent source of information about the amount of solar radiation reaching the plant canopy. A measurement of solar energy reflected to space from earth-atmosphere system immediately specifies the maximum amount of solar energy that can be absorbed at the surface. Incoming solar radiation can be known by adjusting the amount absorbed. Hence, for the computation of downwelling solar radiation, the albedo of the surface must be known. This is especially important over the regions of high reflectivity such as snow and desert. Tarpley (1979) used a statistical regression technique to obtain surface fluxes over the land from Visible channel observations from geostationary satellites. In this model, cloud amount is estimated for a given location from satellite visible data. Three separate regression equations are then used to estimate solar radiation for three categories of clouds. This method provides an accuracy of 10% for clear sky, 30% for partly cloudy and 50% for overcast conditions. Other algorithms like those by Moser and Raschke (1984), and Pinker and Ewing (1985) used physical approaches, and treated the interaction of incoming and reflected solar radiation with the atmosphere and land surfaces in physical manner. The transmittance of solar radiation in these approaches is solved by the use of radiative transfer equations that take into account the concentration profile of different atmospheric components. These physical schemes also take into account the cloudiness and atmospheric water vapor. These methods provide relatively higher accuracy. However, statistical techniques have remained the choice for operational use. These methods require coincident satellite and

ground (pyranometer) observations to develop the coefficients in the regression equations. These methods produce daily total insolation, based on hourly estimates made from geostationary satellite data between 0800 and 1600 LST, with interpolation used toward both sunrise and sunset and for any other missing hourly values.

Surface Temperature

Air temperature is significantly related to crop development and conditions. Operational crop and soil moisture models require daily minimum and maximum shelter temperature and dew point temperature. Canopy (or skin) temperature may be more directly related to growth and evapotranspiration than the shelter temperature. The difference between the two is a measure of crop stress. The ability to observe canopy temperature directly is an advantage of satellite observations. However, it is to be noted that the satellite derived "skin temperature" and "crop canopy temperature" are equivalent only when a satellite field of view (FOV) is filled with vegetation. If FOV constitutes a mixture of bare soil, water bodies, etc. the relation between the two becomes complex. Satellite observations in the thermal IR window (10-12 μm) are used to obtain estimates of canopy or skin temperature. Price (1984) found that surface temperatures over vegetated land can be estimated with an accuracy of 2-3^{o} C using AVHRR split window technique. The errors can largely be attributed to imperfect knowledge about atmospheric water vapor content and wavelength dependent surface emissivity. Clouds pose a serious problem in the estimation of surface temperature by infrared techniques.

Satellite surface temperature estimates have been used to delineate areas of freezing for frost warning and for monitoring freezing events that can affect food production. In U.S., the infrared observations from geostationary satellite GOES are used for freeze forecasting by following the diurnal progression of the freeze line. Accurate freeze forecasts permit farmers to protect crops only when there is a significant freeze threat.

Shelter Temperature

Shelter temperature, its minimum/maximum values along with canopy temperature are important factors of consideration for assessment of crop development and crop stress. Shelter temperature is more directly related to the air temperature than the surface temperature. Observations from

atmospheric sounders like TOVS (TIROS-N Operational Vertical Sounder) are used in methods for estimating shelter temperature. A simple linear regression approach is generally used to derive shelter temperature from satellite soundings. (A brief description of sounding principles is given in next section). Collocated and coincident sets of satellite soundings and shelter temperature observations are used to develop regression coefficients (Davis and Tarpley, 1983). This method provides the shelter temperature with an accuracy of about 2^{o} C. In winter time, a temperature inversion generally persists over the cold ground. This results in a bias of 1-2^{o} C (satellite estimates being warmer) in the nighttime estimates of shelter temperature during winter.

Temperature and Humidity Profiles (Sounding)

Temperature and moisture structures of earth's atmosphere are some of the most significant factors that influence the weather and climate patterns on the local as well as on global scale. The vertical structure of temperature and humidity is retrieved by satellite "sounders" that operate in infrared and microwave frequencies. Sounders use the principle of gaseous absorption for the retrieval of temperature and humidity profiles. For the retrieval of temperature, absorption spectra of some uniformly mixed gas such as CO_2, or, O_2 is used (Fig. 3). These gases absorb earth's upwelling radiation. However, at some wavelengths (say, l_1) their efficiency of absorption is very strong, while at some neighboring wavelengths (say, l_2), it is very weak. Now, any radiation of wavelength l_1 coming from lower layers of atmosphere has very little chance of reaching up to satellite, because it is getting strongly absorbed by the given gas. So, at this wavelength, most of the radiation will be coming from the upper layers of the atmosphere. Similarly, the radiation emitted from the ground at wavelength l_2 will reach the satellite without much interruption, because the atmospheric gases absorb this radiation very weakly. It means that the radiation at wavelength l_2 contains information about the atmospheric layers near the surface. Similarly, radiation at other wavelengths lying between l_1 and l_2 is sensitive to different atmospheric layers in vertical.

Since the radiance from these layers is highly sensitive to the temperature of these layers, the temperature information can be retrieved if we know the radiances reaching the satellite at different wavelengths. A sounder is designed to measure the upwelling radiances at different wavelengths, which are used for retrieving the temperature information. However the actual mathematical procedure of retrieval is quite complex.

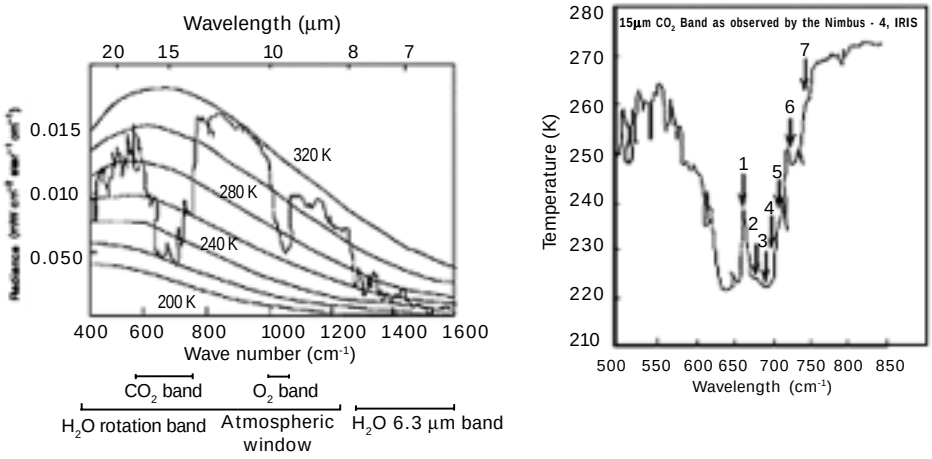

Figure 3: (a) Curve showing the absorption of infrared radiation by different gases in the atmosphere. (b) Numbers shown in this curve (1,2,3,4…7) denote the central wavelengths of CO_2 absorption band used for sounding of atmospheric temperature profiles

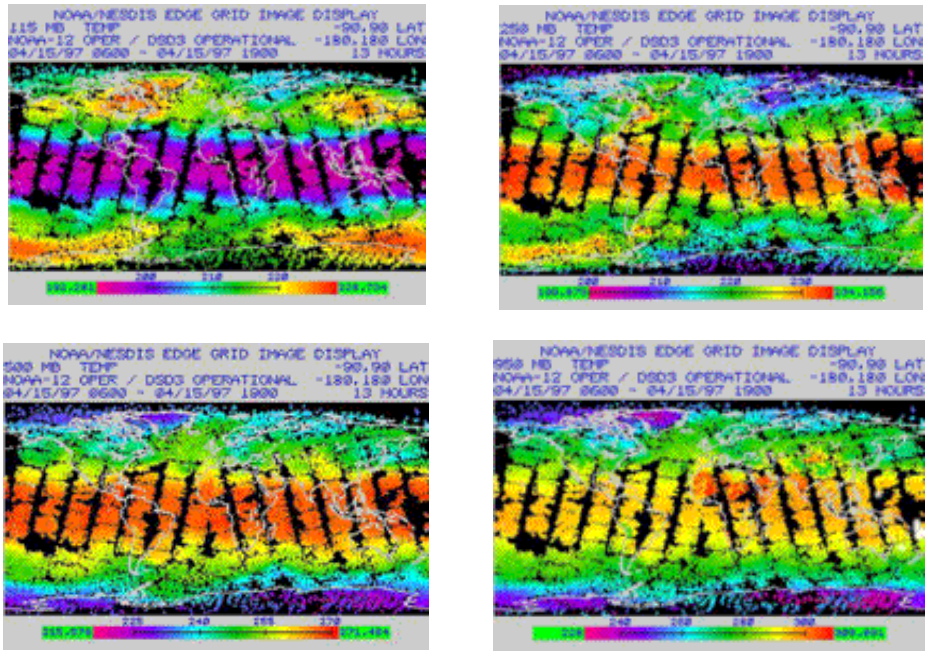

Figure 4: Distribution of global temperature at four vertical levels by TOVS (Picture courtesy : rst.gsfc.nasa.gov)

The principle of the sounding of humidity profiles is similar to that of temperature. However, water vapor is not a uniformly mixed gas, and also it changes phase (i.e. ice, water, snow, or vapor) very frequently within the atmosphere. Satellite water vapor sounders use the water vapor absorption frequencies (~ 6 lm in IR sounder, and ~ 183 GHz in microwave sounders). However, the upwelling radiation at these wavelengths/frequencies not only depends upon the water vapor amount in different atmospheric layers, but also on the temperature of those layers. In this case a-priori information about the temperature structure of the atmosphere is crucial for the retrieval of humidity profiles.

An example of infrared sounders is TIROS Operational Vertical Sounder (TOVS), onboard NOAA series of satellites. This instrument is designed to profile temperature and water vapor. The TOVS is actually a three instrument complex: the High Resolution IR Sounder (HIRS-2), with 20 channels; the Stratospheric Sounding Unit (SSU), with three channels near 15 μm, and the Microwave Sounding Unit (MSU), a passive scanning microwave spectrometer with four channels in the 5.5 μm interval. Advance Microwave Sounding Units (AMSU-A, and AMSU-B onboard recent series of NOAA) are the examples of microwave sounders that are designed to sense temperature and humidity profiles respectively.

OBSERVATIONS OF THE EARTH'S SURFACE

The brightness of the earth's surface in VIS imageries depends on the time of the day, season of the year, the geographical location etc. It is easy to distinguish dry land from a water surface and to identify shorelines, rivers, lakes, islands etc. Dry land, depending on the type of relief, assumes various grey shades in VIS imageries.

The tone of the underlying surface in IR imageries depends on temperature and so its appearance is affected on the latitudinal, diurnal and seasonal variations. During day light hours and in summer dry land surfaces appear darker than the water surface but at night it has a lighter tone than a water surface. IR imageries reveal only large irregularities of relief of vegetation pattern which are associated with marked temperature gradients whereas VIS pictures can reveal even small terrain variations.

Deserts and Vegetated Areas

Dense vegetated areas appear relatively dark in VIS imageries. Mountains with thick forests can be easily identified when sparsely vegetated plains surround it. Deserts with very sparse vegetation combined with red and yellow soils and rocks make the earth's surface highly reflective. These areas appear brightest in satellite pictures.

Surface temperature differences between deserts and vegetated regions are often modified diurnally by water vapor absorption in moist low levels of the atmosphere. Hence the radiation emitted from the surface reaches the satellite undiminished only when the atmosphere is dry. When it is moist the radiation from the high cold levels only reach and hence the IR imagery is not much influenced by the surface characteristics.

Snow

Knowledge of surface geography together with an appreciation of the climatological variation of snow cover through the seasons is a basic prerequisite for the analysis of satellite imagery in respect of snow.

The tone of snow on VIS imagery varies from bright white to light grey depending on the nature of the relief, vegetation, the age of snow and the illumination. In areas of relatively flat terrain without trees snow surfaces appear uniformly white in tone. In areas covered by extensive forests a snow-covered surface appears patchy, brighter patches correspond to areas where there are no trees and dark patches to forest areas.

In IR imagery, snow covered terrain often appears whiter than its surroundings. At night the snow surface cools more rapidly than its surroundings and during the day it warms gradually. Light snow on the tops of high mountain ranges is less detectable in IR than in VIS data as the temperature difference between cold land and snow is small while the difference in albedo between snow and land is large.

ATMOSPHERIC POLLUTANTS

Dust and Haze

Dust is characterized by a dull, hazy and filmy appearance similar to thin cirrostratus. Dust can extend to adjacent water bodies and sometimes obscure the coastline. The edges of dust areas are ill defined.

Blowing dust and sand can be observed in satellite imageries when the reflectivity of the suspended particles differs greatly from the reflectivity of the underlying surface.

Haze particles scatter quite effectively at the blue end of the visible wavelength (channel 1) and hence areas of haze show up better in images of this channel.

Particles of dust or sand carried by the wind form a cloud that causes land marks to appear blurred or to disappear in VIS images. To be detected in IR imagery a dust cloud must be very deep. There are two reasons for the same. Firstly the dust must be composed of large enough particles (over 15 m) to obscure radiation emitted from the ground at least partially. Secondly it must be deep enough to have low temperature otherwise it will not be able to distinguish it from the surface.

Forest Fires

The usefulness of weather satellites are not limited to meteorological observations alone. Their camera systems, sensors and their global coverage enable them to perform a variety of non-meteorological tasks as well. These are detection of forest fires, the tracking of locust clouds, observing volcanoes etc. The sensors of weather satellite enable detection of forest fires characterized by a dull, hazy appearance as in the case of dust. Detection becomes difficult in VIS imagery if the smoke is not prominent. Under such condition it might be possible to spot the fire in IR imagery by sensing the thermal radiation given off. But the detection depends on the intensity of forest fire, its extent, the resolution of the satellite, presence or absence of clouds etc. If a thick cloud system covers the area of forest fire or if clouds have been generated by hot air rising above the forest fire zone it may not be possible to detect forest fires efficiently.

CONCLUSIONS

Various agrometeorological parameters such as clouds, rainfall, soil moisture, solar radiation, land surface temperature, temperature and humidity profiles etc. can be effectively retrieved by using optical, thermal-IR and microwave sensors data onboard various meteorological and earth resources satellites. This information is vital for management of agro-resources and environment.

ACKNOWLEDGEMENTS

I am thankful to my colleague and friend B. Simon who provided a lot of help in the preparation of this lecture. I also acknowledge the valuable information I received from the online tutorials by Dr. Nicholas M. Short (email : %20nmshort@epix.net).

REFERENCES

Ananthkrishnan, R. and Soman, M.K. 1988. The onset of Southwest monsoon over Kerala: 99 (1901-1980). Journal of Climate, 8, 283-296.

Arkin, P.A. and Ardanuy, P.E. 1989. Estimating climatic scale precipitation from space: a review. Journal of Climate, 2, 1229-1238.

Bader, M.J., Forbes, G.S., Grant, J.R., Lilley, R.B.E. and Waters, A.J. Images in weather forecasting, a practical guide for interpreting satellite and radar imagery. Syndicate of Cambridge Uni., The Pitts bldg, Cambridge, CB21RP, New York, NY1001-4211, USA.

Das, P.K. 1968. The Monsoon. Published by the Director, Nat. Book Trust, New Delhi.

Davis, P.A. and Tarpley, J.D. 1983. Estimation of shelter temperature from operational satellite sounder data. Journal of Climate and Applied Meteorology, 22, 369-376.

Fein, J.S. and Stephens, P.L. 1986. Monsoons. John Wiley & Sons, USA.

Kelkar, R.R. and Yadav, B.S. A basic guide for the use of INSAT imagery. IMD, New Delhi.

Kidwell, K.D. 1986. NOAA polar orbiter data : user guide, pp 1-7.

Moser, W. and Raschke, E. 1984. Incident solar radiation over Europe estimated from METEOSAT data. Journal of Climate and Applied Meteorology, 23, 166-170.

Pinker, R.T. and Ewing, J.A. Modeling surface solar radiation : Model formulation and validation. Journal of Climate and Applied Meteorology, 24, 389-401.

Price, J.C. 1984. Land surface temperature measurements from the split window channels of the NOAA-7 AVHRR. J. Geophysics Res., 89, 7231-7237.

Smith, W.L., Woolf, H.M., Hayden, C.M., Mark, D.Q. and Mc Milan, L.M. 1979. The TIROS-N operational vertical sounder. Bull. Am. Soc., 60, 1177-1187.

Tarpley, J.D. 1979. Estimating incident solar radiation at the surface from geostationary satellite data. J. Applied Meteorology, 18, 1172-1181.

REMOTE SENSING AND GIS APPLICATION IN AGRO-ECOLOGICAL ZONING

N.R. Patel
Agriculture and Soils Division
Indian Institute of Remote Sensing, Dehra Dun

Abstract : Sustainable agricultural development requires a systematic effort towards the planning of land use activities in the most appropriate way, apart from several other institutional and policy programme initiatives. Agro-ecological zoning (AEZ) is one of the most important approaches for agricultural developmental planning because survival and failure of particular land use or farming system in a given region heavily relies on careful assessment of agro-climatic resources. This approach is used to categorize agro-climatically uniform geographical areas for agricultural developmental planning and other interventions. Modern tools such as satellite remote sensing and Geographical Information System (GIS) have been providing newer dimensions to effectively monitor and manage land resources in an integrated manner for agro-ecological characterization. The application of AEZ is limited by lack of geospatial data, particularly in mountainous areas. This paper tries to demonstrate incorporation of new tools to extend applicability of AEZ in mountainous areas like Kumaon Himalayas, India.

INTRODUCTION

Sustainable agricultural development requires a systematic effort towards the planning of land use activities in the most appropriate way, apart from several other institutional and policy programmme initiatives. Agro-ecological zoning (AEZ) is one of the most important bases for agricultural developmental planning because survival and failure of particular land use or farming system in a given region heavily relies on careful assessment of agro-climatic resources. A practical zoning approach thus arises because climate represented by thermal and moisture regimes forms small geographic areas, resulting in a variable mosaic of specialized areas, capable of supporting varied land use systems (Troll, 1965). The approach is used to categorize agroclimatically uniform

Satellite Remote Sensing and GIS Applications in Agricultural Meteorology
pp. 213-233

geographical areas for agricultural developmental planning and other interventions. A framework of agro-ecological zoning describing concepts, methods and procedures was conceptualized for the first time by FAO (1976). Agro-ecological zoning refers to the division of an area of land into land resource mapping units, having unique combination of landform, soil and climatic characteristics and or land cover having a specific range of potentials and constraints for land use (FAO, 1996). The particular parameters used in the definition focus attention on the climatic and edaphic requirements of crop and on the management systems under which the crops are grown. Each zone has a similar combination of constraints and potentials for land use and serves as a focus for the targeting of recommendations designed to improve the existing land use situation, either through increasing production or by limiting land degradation. The addition of further layers of information on such factors as land tenure, land availability, nutritional requirement of human and livestock populations, infrastructure and costs and prices, has enabled the development of more advanced applications in natural resource analysis and land use planning. AEZ can be regarded as a set of core applications, leading to an assessment of land suitability and potential productivity. An output of AEZ studies includes maps showing agro-ecological zones and land suitability, quantitative estimates on potential crop yields and production. Such information provides the basis for advanced applications such as land degradation assessment, livestock productivity modeling, population support capacity assessment and land use optimization modeling.

IMPORTANCE OF AEZ IN SUSTAINABLE AGRICULTURAL DEVELOPMENT PLANNING

The ability of the world's natural resources to provide for the needs of its growing population is a fundamental issue for the international community. World's population is increasing rapidly and at the same time, essential natural resources, such as land and water, are declining both in quantity and quality due to such factors as competition with industrial and urban demands. The basic problem is that limits to the productive capacity of land resources are set by climate, soil and land forms condition. In this context AEZ can be regarded as a set of applications, leading to an assessment of land suitability and potential productivity in terms of climate, soil and land forms condition.

Agro-Ecological Zoning (AEZ) is one of the most important bases of sustainable agricultural development planning of a region. It is applicable in micro or local level planning mainly for rainfed agriculture. It assesses basically the yield potentialities of various crop conditions; evolves future plan of action

involving crop diversification; determines suitability of different crops for optimizing land use, disseminates research results and agro-technology. As a result sustainable agricultural development planning is increasingly being based on agro-ecological zones. In this process agro climate zoning has become very popular (Verma and Partap, 1989). The initial focus of the FAO agro-ecological zoning system was to assess the suitability of different types of land use for selected land uses. It is an important starting point for selected land use planning with an overview of the whole region. It diagnoses the present situation with regard to farming and land use by categorizing, describing and analyzing, farming systems components.

DEFINITIONS

Agro-Ecological Zoning (AEZ) refers to the division of an area of land into smaller units, which have similar characteristics related to land suitability potential production and environmental impact.

Agro-Ecological Zone is a land resource mapping unit, having a unique combination of land form, soil and climatic characteristics and/or land cover having a specific range of potentials and constraints for land use (FAO, 1996).

Agro-Ecological Cell (AEC) is defined by a unique combination of land form, soil and climatic characteristics

TRADITIONAL APPROACH

Several attempts have been made to classify the land area into climatic regions. Many of the earlier efforts to delineate agro-climates used manual overlay of isolines representing either potential evapotranspiration or temperature or their combinations and superimposed on soil resource maps. Carter (1954) divided India into six climatic regions, ranging from arid to per humid, based on the criteria of Thornthwaite system of climate classification. Sehgal *et al*. (1987) prepared a computerized bio-climatic map of NW India, based on the criteria of dry month. Krishnan (1988) delineated 40 soil climatic zones based on major soil types and moisture index. Murthy and Pandey (1978) brought out a 8 agro-ecological region map of India on the basis of physiography, climate, soils and agricultural regions. The approach depicts a good beginning of agro-ecological zoning in the country, but it suffers from several limitations due to over generalizations such as grouping together the areas having different physiography, temperature and soil in zone.

Subramanian (1983) based on the data of 160 meteorological stations in the country and using the concept of moisture adequacy index, delineated 29 agro-ecological zones with the possible 36 combinations of IMA and dominated soil groups as per FAO/UNESCO Soil Map (1974).The planning commission, as a result of mid-term appraisal of the planning targets of VII Plan (1985-1990), divided the country into 15 broad agro-climatic zones based on physiography and climate (Sehgal *et al*., 1992).

NEW TOOLS FOR AEZ

Modern tools such as satellite remote sensing and GIS have been providing newer dimensions to effectively monitor and manage natural resources. It has been well conceived that remote sensing and GIS have great role to play in agro-ecological zoning for sustainable development due to multi-stage character of the comprehensive approach to agro-ecological zoning (Pratap *et al*., 1992). Several approaches of AEZ in past involved manual integration of agro-climatic and other natural resource data (Mavi, 1984; Venkateswaralu *et al*., 1996). As a result, large amount of agro-ecological data could not be handled easily and aggregation was required at an early stage in the analysis. This led to loss of information on spatial variability. On the other hand, GIS technology is very useful for automated logical integration of bio-climate, terrain and soil resource inventory information (Patel *et al*., 2000). The system is capable of containing all data required to solve resource management problems. Topographic maps, land resource map and contour map having physiographic, geographic and bio-climatic information forms primary input for GIS for agro-ecological zoning activities. The system also facilitates the enlargement of a particular geographic pocket to render more details on retrieval. After collecting the basic data on zonal resource information, the data can be manipulated to create relevant profiles of applied use that can be retrieved on demand. A zonal database can also be integrated with non-geographic information such as socioeconomic data, which is relevant for making decision on development priority interventions about the sustainable management of zonal resources. Remote sensing provides digital or hard copy data base information on natural resources. This information can be stored and retrieved as and when required and also data can be classified and aggregated for any number of planning exercises. This AEZ concept involves the representation of land in layers of spatial information and combination of layers of spatial information using geographic information system (GIS).

STRUCTURE OF AEZ

The structure of AEZ includes the comprehensive framework for the appraisal and planning of land resources (Figure 1). The nature of analysis, which involves the combination of layers of spatial information to define zones, lends itself to application of a GIS. The major requirements of computerized GIS for an activity like agro-ecological zoning and zonal resource information of mountain areas are topographic maps, land resource maps and contour maps. These maps, containing physiographic, geographic, and bio-climatic information form primary inputs. Various outputs are generated in both tabular and map forms. Till date, good progress has been made in developing GIS based tools for land resources planning, management and monitoring at different scales.

ELEMENTS OF AEZ

The essential elements of the core applications of AEZ include :

- Land resource inventory, comprising
  - Analysis of length of growing period or moisture availability index
  - Defining thermal zones
  - Compilation of climatic resource inventory
  - Compilation of soil and landform resource inventory
  - Compilation of present land use inventory
  - Combination of above to make land resource inventory based on agro-ecological zones or agro-ecological cells.
- Inventory of land utilization types and crop requirements
- Land suitability evaluation, including
  - Potential productivity computations
  - Matching of constraints and requirements

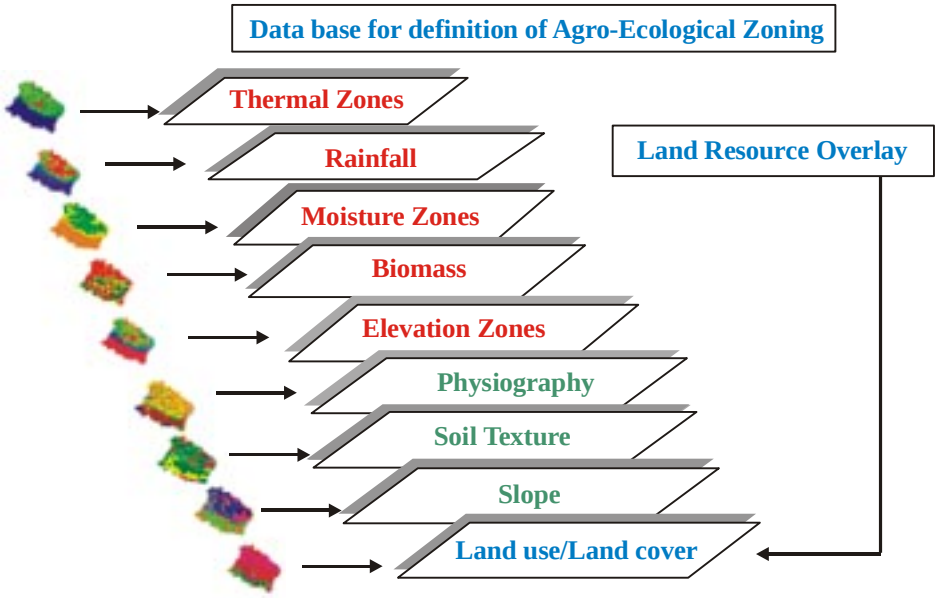

Figure 1: Structure of land resource

A CASE STUDY ON AGRO-ECOLOGICAL ZONING IN MOUNTAIN ECOSYSTEM

Sustainable development of mountain regions is a challenging task because the areas have highly diverse and fragile ecosystems. One of the most striking characteristics of mountains is their spatial variability. This makes the planning of the use of natural resources in the mountains more complex than any other area. In view of this, the present study was conducted in part of Kumaon Himalayas (latitudes 28°45' to 30°00'N, longitude 78°45' to 80°15') to demonstrate the use of remote sensing and GIS as a tools for agro-ecological zoning with mountain perspective (Patel *et al*., 2002). The methodology used in this study is outlined in the flow diagram in Figure 2. This methodology is further described as following sub heads.

Climate

Long term (approximately 10 years) monthly maximum and minimum temperatures were collected from six meteorological stations falling in the

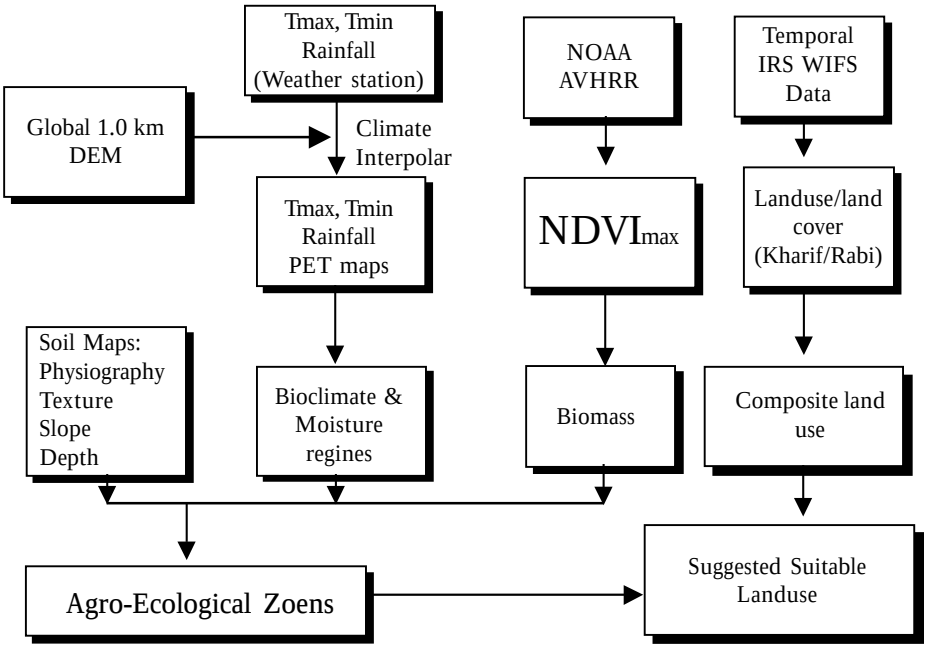

Figure 2 : Flow diagram of the method for agro-ecological zoning

western Himalayas. However, monthly rainfall data for eight years were collected from eleven rain gauge stations within the study area. The details about location of meteorological and rain gauge stations are shown in Table 1. Digital elevation data with one-kilometer grid size was taken from Global Digital Elevation Model (USGS GDEM) and geometrically registered in UTM projection. Validation and accuracy check for digital elevation data derived from Global DEM was done with spot height observation from Survey of India toposheets on 1:250000 scale. A close agreement was observed between spot height observations and Global DEM based elevation data (R^2 = 0.98). Long term monthly and annual averages of mean temperatures of six meteorological stations were regressed against corresponding elevation using MICROSTA statistical software (Table 2). A good agreement was also observed between annual mean temperature and elevation (annual mean temperature = 24.443 - 0.0045 × elevation, R^2 = 0.97). Similarly long term average annual rainfall recorded at different rain gauge stations were regressed against elevation for developing rainfall – elevation relationship (annual rainfall = 515.1 + 0.3843 × elevation, R^2 = 0.75) representing the region under study. The empirical relations thus developed were used to utilize inherent spatial quality of digital elevation model in GIS environment for depicting spatial variation in normal

monthly and annual mean temperatures as well as annual rainfall condition over Kumaon region. These monthly spatial distribution of mean temperatures were used for computation of spatial potential evapotranspiration (PET) based on Thornthwaite (1948) as:

$$PET = 1.6 \left[(10\ T_{ijk}/I_{jk})^{ajk} \right]$$

where,

$$I_{jk} = \sum_{i=Jan}^{Dec} (T_{ijk}/5)^{1.514}$$

T = Mean air temperature (°C)

i = Month of a year (i = Jan, Feb, ……Dec)

j = Pixel value of i th row

k = Pixel value of j th column

$ajk = 67.5*10^{-8}(I_{jk})^3 - 7.71*10^{-5}*(I_{jk})^2 + 0.01792(I_{jk}) + 0.4923$

These monthly potential evapotranspiration were summed over twelve months in a year to obtain spatial distribution of annual PET for use in computation of moisture index (MI). The moisture index with positive and negative values indicates moist or dry climate and seasonal variation of effective moisture. The revised moisture index of Thornwaite and Mather (1955) method based on annual rainfall and potential evapotranspiration was calculated as,

$$MI = [(P - PET)/PET] * 100$$

where,

MI = Moisture Index

P = Rainfall (mm)

PET = Potential Evapotranspiration (mm)

This information on moisture index is vital to congenial biotic environment and has been used to classify the climatic types. To arrive at homogeneous zones, the limit of moisture index of the various climatic types was scaled as shown in Table 3.

Table 1. Data for fields and location of meteorological and rain gauge stations

No.	Met/rain gauge station	Data fields Monthly	Period (years)	- Latitude - Longitude	Elevation (meter)	Source
1.	Mukteswar	Rainfall, Temperature	10	29° 27' 28.7" N 79° 39' 27.2" E	2275	Institute Temperate Horticulture Station
2.	Hawalbagh	Rainfall, Temperature	10	29° 36' 00.0" N 79° 40' 00.0" E	1250	Met. Station
3.	Almora	Rainfall, Temperature	10	29° 35' 22.4" N 79° 38' 42.2" E	1528	Vivekanand ICAR Institute
4.	Pantnagar	Rainfall, Temperature	10	29° 02' 27.2" N 79° 24' 30.5" E	232	Agriculture University, Pantnagar
5.	Nainital	Rainfall, Temperature	10	29° 21' 30.7" N 79° 27' 26.3" E	1945	Astronomy State Observatory, Nainital
6.	Dehra Dun	Rainfall,Temperature	10	30° 19' 00.0" N 78° 02' 00.0" E	682	Met. Station
7.	Mussoorie	Rainfall, Temperature	10	30° 27' 00.0" N 78° 05' 00.0" E	2024	Met. Station, CSWCRII Dehra Dun
8.	Chaukhutia	Rainfall	8	29° 52' 32.1" N 79° 22' 15.6' E	976	Forest Conservation Department, Ranikhet
9.	Kedar	Rainfall	8	29° 47' 07.8' N 79° 15' 26.8" E	958	Forest Conservation Department, Ranikhet

No.	Met/rain gauge station	Data fields Monthly	Period (years)	- Latitude - Longitude	Elevation (meter)	Source
10.	Naula	Rainfall	8	29° 44' 13.5" N 79° 15 11.8" E	886	Forest Conservation Department, Ranikhet
11.	Tamadhaun	Rainfall	8	29° 50' 49.0" N 79° 12' 05.4" E	912	Forest Conservation Department, Ranikhet
12.	Sauni	Rainfall	8	29° 37' 47.9" N 79° 22' 05.8" E	1599	Forest Conservation Department, Ranikhet
13.	Deolikhet	Rainfall	8	29° 38' 51.1" N 79° 27' 00.6" E	1715	Forest Conservation Department, Ranikhet
14.	Binta	Rainfall	8	29° 47' 10.0" N 79° 28' 14.5" E	1887	Forest Conservation Department, Ranikhet

Table 2. Mean Temperature v/s Elevation Relationship

Month	Regression Equation	R^2
January	y = - 0.0031 x + 14.106	0.89
February	y = - 0.004 x + 17.012	0.95
March	y = - 0.0047 x + 22.122	0.97
April	y = - 0.0051 x + 27.95	0.96
May	y = - 0.0057 x + 31.485	0.98
June	y = - 0.0059 x + 31.925	0.96
July	y = - 0.0058 x + 30.642	0.99
August	y = - 0.0054 x + 29.755	0.98
September	y = - 0.0053 x+ 28.855	0.99
October	y = - 0.0044 x + 25.133	0.95
November	y = - 0.003 x + 19.284	0.89
December	y = - 0.0018 x + 15.045	079

Table 3. Scaling of moisture index into different agro-climate types

Climatic type	Moisture Index	Symbol
Semi arid	-66.7 to – 33.3	D
Dry sub-humid	- 33.3 to 0	C1
Moist sub-humid	0 to 20	C2
Humid (4 classes)	20 to 100	B1, B2, B3 and B4
Per-humid	> 100	A

Vegetation Biomass variability

Using NDVI to estimate standing green biomass proved to be a reliable source of biomass data. The existing functional relationship between monthly cutting of green dry matter (DM) and maximum normalized difference vegetation index (NDVI) derived from NOAA AVHRR (Advanced Very High Resolution Radiometer) was used. Monthly NDVI images of NOAA AVHRR during year 1999 were used to derive the maximum NDVI in a year for estimating biomass or dry matter (DM) as per equation.

$DM = (1.615*NDVI_{max})^{1.318}$; $R^2 = 0.90$

DM = Dry matter

$NDVI_{max}$ = Maximum NDVI in a year.

Land use/land cover

Land use/land cover was derived from coarse resolution IRS WiFS satellite data. Ground truth was collected through integrated use of previous year IRS LISS III hard copy (1:250,000 scale) satellite data, Survey of India (SOI) toposheets and handheld Global Positioning System (GPS). Combination of satellite data acquired during *kharif* (September and October, 2001) and *rabi* (January and March, 2002) seasons were digitally classified to land use/land cover information classes for *kharif* and *rabi*, respectively using MXL classifier. Agricultural land use classes in *rabi* season were refined with respect to land use information in *kharif* season and crop calendar of major crops cultivated in the region. Finally, classified land use /land cover information of *kharif* and *rabi* seasons were logically integrated on a pixel by pixel basis in raster GIS for deriving cropping system or composite land use/land cover (Fig. 3).

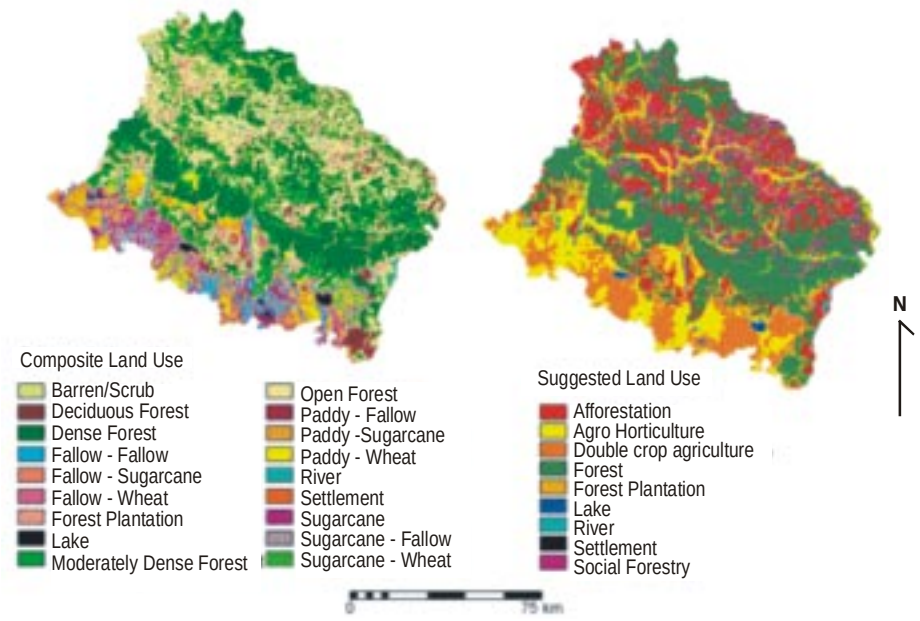

Figure 3: Suggested land use based on AEZs and present land use

Soils

Forty-six soil mapping unit along with their characteristics such as depth, texture, slope, erosion status, and drainage condition for the study area were obtained from soil map (1:250000 scale) prepared by National Bureau of Soil Survey and Land Use Planning, India. These spatial and non spatial data on soils were converted into digital soil resource databases for AEZ. In general terms, coarse loamy and skeletal soils are in side slope and top of Lesser Himalayas and piedmont plain while fine textured soils mainly found in alluvial plain and fluvial valleys. The soils are mostly moderately deep to deep, however, approximately 25 % of the area having shallow soils were mainly found in Lesser Himalayas and piedmont plain (Fig. 4).

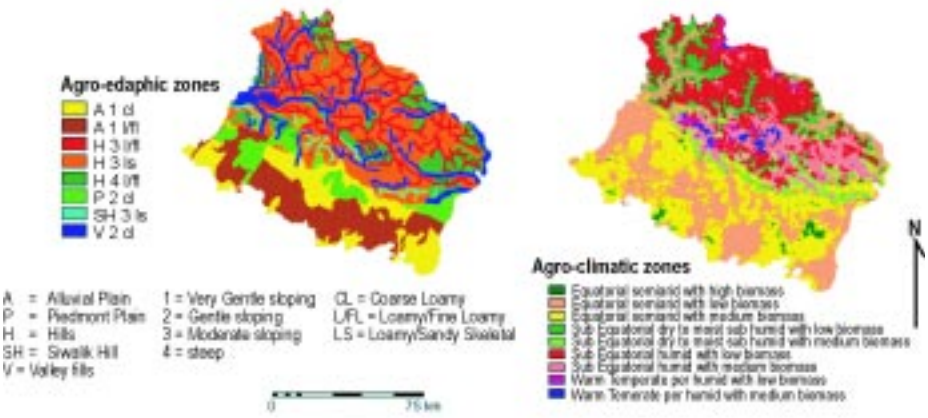

Figure 4: Characteristics of agro-edaphic and agro-climatic zones

All the land resource databases and characteristics (Fig. 1) described above as layer or combination of layers of spatial information were integrated or overlaid to derive different unique agro-ecological cells. These agro-ecological cells were further aggregated to arrive at agro-ecological zones and sub zones based on their potential to support agriculture and vegetation patterns.

Delineation of agro-climatic zones

Agro-climatic zones are of paramount importance for defining or delineation of agro-ecological zoning for sustainable use of land resources. The essential elements in demarcating or defining of an agro-climatic zone are bioclimates based on thermal regimes, moisture regime and biomass variability

(Fig. 5). Thermal regimes indicate to the amount of heat available for plant growth and development during the growing period. Moisture regimes represent water availability for crop production and hence they are the vital to classify the agro-climatic zones. Nine different agro-climatic zones were delineated by GIS aided integration of thermal regimes, moisture regimes and biomass map layers (Fig. 5).

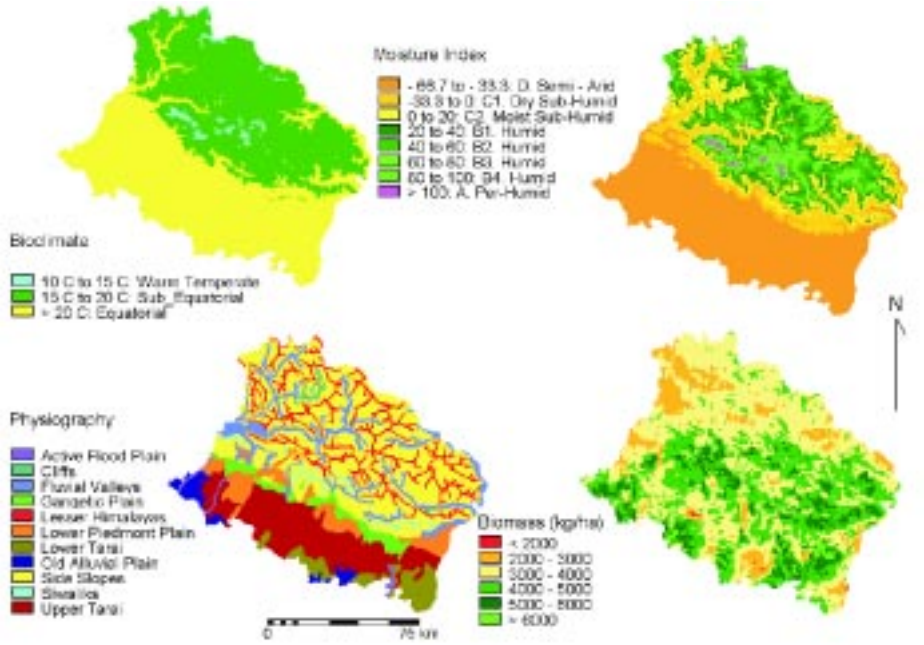

Figure 5: Input layers for agro-ecological zoning

Delineation of Agro-ecological zones and sub-zones

Thirty agro-ecological sub zones (AEZIa to AEZXIIc) were delineated in the study area (Table 4) by GIS aided integration of nine agro-climatic and eight agro-edaphic zones (Fig. 6). Results revealed that the majority of area falls in XIa whereas minimum area is occupied by Via (Patel *et al.*, 2002). The other larger sub-zones are Ib and VIIIa, respectively. AEZIc and AEZIIc are the most potential zones for intensive cropping with possibility of two and three crops such as paddy – wheat or sugarcane – wheat (Table-4). Further sub-ecological zones are reclassified by GIS aided integration in which sub-zones are clubbed into main agro-ecological zones. Therefore, twelve agro-ecological zones (AEZI to AEZXII) are identified in the study area. The spatial

Table 4. Spatial extent of Agro-Ecological Sub Zones

Sl.No.	AEZ	AE Sub Zone	Description	Area (ha)	(%)
1.	I	a	Equatorial, semiarid very gently sloping alluvial plain with loamy to fine loamy soils and low biomass	74487.48	6.50
2.	I	b	Equatorial, semiarid very gently sloping alluvial plain with loamy to fine loamy soils and medium biomass	107997.1	9.42
3.	I	c	Equatorial, semiarid very gently sloping alluvial plain with loamy to fine loamy soils and high biomass	10111.92	0.88
4.	II	a	Equatorial, semiarid very gently sloping in alluvial plain with coarse loamy soils and low biomass	80015.28	6.98
5.	II	b	Equatorial, semiarid very gently sloping in alluvial plain with coarse loamy soils and medium biomass	64135.22	5.59
6.	II	c	Equatorial, semiarid very gently sloping in alluvial plain with coarse loamy soils and high biomass	2371.58	0.21
7.	III	a	Equatorial, semiarid gently sloping valley fills with coarse loamy soils and low biomass	46335.98	4.04
8.	III	b	Equatorial, semiarid gently sloping valley fills with coarse loamy soils and medium biomass	24758.47	2.16
9.	III	c	Equatorial, semiarid gently sloping valley fills with coarse loamy soils and high biomass	77.76	0.01
10.	IV	a	Sub equatorial, Sub humid to humid gently sloping valley fills with coarse loamy soils and low biomass	34531.08	3.02

Sl.No.	AEZ	AE Sub Zone	Description	Area (ha)	(%)
11.	IV	b	Sub equatorial, Sub humid to humid gently sloping valley fills with coarse loamy soils and medium biomass	11631.71	1.01
12.	V	a	Equatorial, semiarid gently sloping piedmont plain with coarse loamy soil and low biomass	42151.25	3.68
13.	V	b	Equatorial, semiarid gently sloping piedmont plain with coarse loamy soil and medium biomass	34266.01	2.99
14.	V	c	Equatorial, semiarid gently sloping piedmont plain with coarse loamy soil and high biomass	968.43	0.08
15.	VI	a	Sub equatorial, Sub humid to humid gently sloping piedmont plain with coarse loamy soils and low biomass	7.07	0.00
16.	VI	b	Sub equatorial, Sub humid to humid gently sloping piedmont plain with coarse loamy soils	1180.48	1.10
17.	VII	a	Warm temperate, per humid moderately steep to steep sloping piedmont plain with coarse loamy soils and low biomass	5444.59	0.57
18.	VII	b	Warm temperate, per humid moderately steep to steep sloping piedmont plain with coarse loamy soils	6976.9	0.61
19.	VIII	a	Sub equatorial, Sub humid to humid moderate steep to steep sloping Hills with loam to fine loam soils and low biomass	123103.1	10.75
20.	VIII	b	Sub equatorial, Sub humid to humid moderate steep to steep sloping Hills with loam to fine loam soils	65662.08	5.72

Sl.No.	AEZ	AE Sub Zone	Description	Area (ha)	(%)
21.	IX	a	Equatorial, semiarid moderate steep to steep sloping in Hills with loam to fine loamy soils and low biomass	35354.6	3.08
22.	IX	b	Equatorial, semiarid moderate steep to steep sloping in Hills with loam to fine loamy soils and medium biomass	15561.97	2.67
23.	IX	c	Equatorial, semiarid moderate steep to steep sloping in Hills with loam to fine loamy soils and high biomass	498.35	.05
24.	X	a	Warm temperate, per humid moderately steep to steep sloping Hills with coarse loamy skeletal soils and low biomass	2286.76	0.20
25.	X	b	Warm temperate, per humid moderately steep to steep sloping Hills with coarse loamy skeletal soils and medium biomass	3990.33	0.34
26.	XI	a	Sub equatorial, Sub humid to humid moderate steep to steep sloping Hills with loamy skeletal soils and low biomass	182201.9	15.88
27.	XI	b	Sub equatorial, Sub humid to humid moderate steep to steep sloping Hills with loamy skeletal soils and medium biomass	106272	9.27
28.	XII	a	Equatorial, semiarid moderate steep to steep sloping Hills with loamy skeletal soils and low biomass	2940.62	0.26
29.	XII	b	Equatorial, semiarid moderate steep to steep sloping Hills with loamy skeletal soils and medium biomass	43830.09	3.82
30.	XII	c	Equatorial, semiarid moderate steep to steep sloping Hills with loamy skeletal soils and high biomass	353.44	0.03

Table 5. Spatial extent of Agro-Ecological Zones

Sl.No.	AEZ	Description	Area (ha)	(%)
1.	I	Equatorial, semiarid very gently sloping in alluvial plain with loamy to fine loamy soils	192596.5	16.8
2.	II	Equatorial semiarid very gently sloping in alluvial plain with coarse loamy soils	146522.1	12.78
3.	III	Equatorial, semiarid gently sloping in valley fills with coarse loamy soils	71172.21	6.21
4.	IV	Sub equatorial, Sub humid to humid gently sloping valley fills with coarse loamy soils	4842.13	4.03
5.	V	Equatorial, semiarid gently sloping piedmont plain with coarse loamy soil	77385.69	6.75
6.	VI	Sub equatorial, Sub humid to humid gently sloping piedmont plain with coarse loamy soils	1187.55	1.10
7.	VII	Warm temperate, per humid moderately steep to steep sloping piedmont plain with coarse loamy soils	12421.49	1.18
8.	VIII	Sub equatorial, Sub humid to humid moderate steep to steep sloping Hills with loamy to fine loamy soils	188765.2	16.47
9.	IX	Equatorial, semiarid moderate steep to steep sloping in Hills with loam to fine loamy soils	51414.92	6.80
10.	X	Warm temperate, per-humid moderately steep to steep sloping Hills with coarse loamy skeletal soils	6277.09	0.54
11.	XI	Sub equatorial, Sub humid to humid moderate steep to steep sloping Hills with loamy skeletal soils	288474.2	25.15
12.	XII	Equatorial, semiarid moderate steep to steep sloping Hills with loamy skeletal soils	47124.15	4.11

distribution of these zones is presented in Figure 6. The area covered ranges from 0.54 % in AEZ X to 25.15 % in AEZ XI. The whole hilly portion falls in AEZ VIII whereas lower alluvial plain in AEZ I and AEZ II (Table-5). A suitable land use (Fig. 3) plan for sustainable use of land resource for the Kumaon region was suggested based on characteristics of AEZs and existing land use pattern.

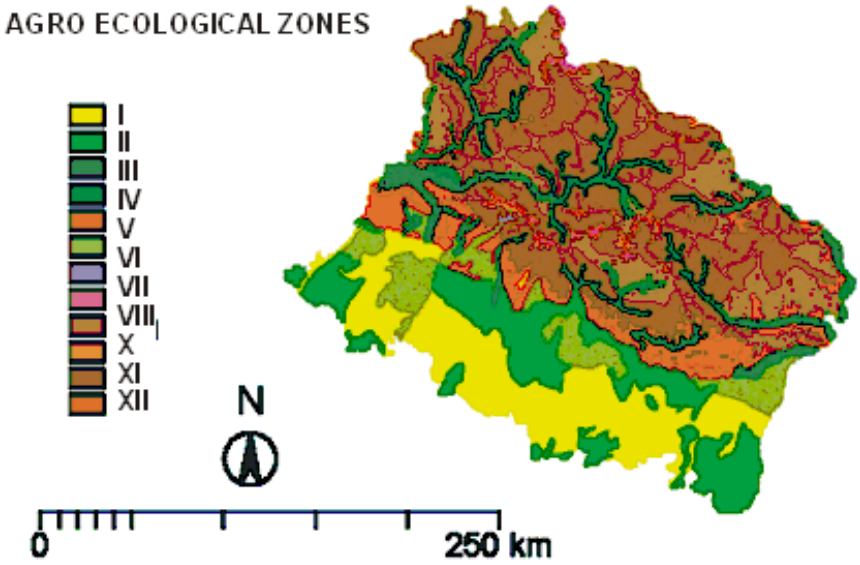

Figure 6. Agro-ecological zones

CONCLUSIONS

A Remote Sensing and Geographical Information System based approach to delineate Agro-Ecologically homogeneous geographical areas was developed using soil resources, temperature, rainfall, moisture, and biomass as input layers. Based on delineated Agro-ecological Zones, suitable land use were suggested in Kumaon region of Almora, Nainital, Champawat and Udham Singh Nagar districts.

Following conclusions were drawn from the study,

1. Strong negative relations between temperatures and elevation (i.e. lapse rate) would provide basis for estimating spatial variations in temperature, particularly in the mountain ecosystems.

2. Spatial distribution of PET and Moisture index would help in defining micro-Environment more accurately in the mountains environment.

3. Integration of bio-climate, moisture regimes and regional vegetation biomass in GIS environment could provide a more dynamic way of characterizing homogeneous agro-climatic zones for identifying biophysical and climate characteristics to agricultural productivity.

REFERENCES

Carter, D.B. 1954. Climates of Africa and according to Thornthwaite (1948) Classification. John Hopkins University Publication (in) Climatology, 7(14).

FAO, 1976. A framework for land evaluation. Food and Agricultural Organisation, Soils Bulletin 32, Rome, Italy.

FAO, 1996. Guidelines: Agro-ecological zoning. Food and Agricultural Organisation, Soils Bulletin, Rome, Italy.

Krishnan, A. 1988. Delineation of soil climatic zones of India and its practical applications in Agriculture. Fertilizer News, 33 (4).

Mavi, H.S. 1984. Introduction to Agrometeorology, IInd edition. Raju Primlani for Oxford & IBH Publishers Co. Pvt. Ltd.

Murthy, R.S. and Pandey, S. 1978. Delineation of agro-ecological regions of India. Paper presented in Commission V, 11th Congress of ISSS, Edmonton, Canada, June 19-27.

Pariyar, M.P. and Singh, G. 1994. GIS based model for agro-ecological zoning: a case study of Chitwan district, Nepal. Proc. 15th Asian Conference Rem. Sens., Bangalore, India. Vol. 1 : A4-1 to A4-6.

Pratap, T., Pradhan, P., Lotta, P.K., Mya, S., Karim and Nakarmi, G. 1992. Geographic Information Systems and Technology application in Agro-ecological zonation of mountain agriculture. Eds. N.S. Jodha, M. Banskota and Tej Pratap, Oxford & IBH Publishing Co. Pvt. Ltd., New Delhi.

Patel, N.R., Mandal, U.K. and Pande, L.M. 2000. Agro-ecological zoning system. A Remote Sensing and GIS Perspective. Journal of Agrometeorology, 2 (1) : 1-13.

Patel, N.R., Endang, P., Suresh Kumar and Pande, L.M. 2002. Agro-ecological zoning using remote sensing and GIS – A case study in part of Kumaon region. In: Sustainable agriculture development, Proce. of 2nd International Conference on Sustainable Agriculture, Water Resources Development and Earth Care Policies, 18-20 December, 2002, New Delhi (In Press).

Sehgal, J.L., Vernemmen, C. and Tavernier, R. 1987. Agro-climatic Environments and Moisture Regimes in NW India - Their Applications in Soils and Crop Growth. Research Bull. NBSS Publ. 17, Nagpur, India, NBSS & LUP.

Sehgal, J.L., Mandal, D.K., Mandal, C. and Vadivelu, S. 1992. Agro-ecological Region of India. NBSS & LUP (ICAR) Publication 24, Nagpur.

Subramanian, A.R. 1983. Agro-ecological Zones of India. Arch. Met. Geoph. Biocl. Ser. B32; 329-333.

Thornthwaite, C.E. and Mathew, J.R. 1955. The Water Balance. Publications in Climatology, Vol.8, No.1. Drexel Institute of Technology, Laboratory of Climatology, Centerton, N.J. pp. 104.

Thornthwaite, C.W. 1948. An Approach towards a rational classification of climate. Geographical Review, 38: 55-94.

Troll, C. 1965. Seasonal Climates of the earth. World maps of Climatology. Eds. E. Rodenwalt and H. Jusatz. Berlin : Springer – Verlag, pp. 28.

Venkateshwarlu, J., Ramakrishna, Y.S. and Rao, A.S. 1996. Agro-climatic zones of India. Annals of Arid Zone, 35 (1); 1-8.

Verma and Pratap, 1989. Agro climatic zones. Profiles and Issues. Agro-climatic Regional Planning UNIT (ARPU) Working paper, Ahmedabad: Sardar Patel Inst. of Econ. and Soc. Res. 1989.

CROP GROWTH MODELING AND ITS APPLICATIONS IN AGRICULTURAL METEOROLOGY

V. Radha Krishna Murthy
Department of Agronomy, College of Agriculture
ANGR Agricultural University, Rajendranagar, Hyderabad

Abstract: This paper discusses various crop growth modeling approaches viz. Statistical, Mechanistic, Deterministic, Stochastic, Dynamic, Static and Simulation etc. Role of climate change in crop modeling and applications of crop growth models in agricultural meteorology are also discussed. A few successfully used crop growth models in agrometeorology are discussed in detail.

INTRODUCTION

Crop is defined as an "Aggregation of individual plant species grown in a unit area for economic purpose".

Growth is defined as an "Irreversible increase in size and volume and is the consequence of differentiation and distribution occurring in the plant".

Simulation is defined as "Reproducing the essence of a system without reproducing the system itself". In simulation the essential characteristics of the system are reproduced in a model, which is then studied in an abbreviated time scale.

A model is a schematic representation of the conception of a system or an act of mimicry or a set of equations, which represents the behaviour of a system. Also, a model is "A representation of an object, system or idea in some form other than that of the entity itself". Its purpose is usually to aid in explaining, understanding or improving performance of a system. A model is, by definition

Satellite Remote Sensing and GIS Applications in Agricultural Meteorology
pp. 235-261

"A simplified version of a part of reality, not a one to one copy". This simplification makes models useful because it offers a comprehensive description of a problem situation. However, the simplification is, at the same time, the greatest drawback of the process. It is a difficult task to produce a comprehensible, operational representation of a part of reality, which grasps the essential elements and mechanisms of that real world system and even more demanding, when the complex systems encountered in environmental management (Murthy, 2002).

The Earth's land resources are finite, whereas the number of people that the land must support continues to grow rapidly. This creates a major problem for agriculture. The production (productivity) must be increased to meet rapidly growing demands while natural resources must be protected. New agricultural research is needed to supply information to farmers, policy makers and other decision makers on how to accomplish sustainable agriculture over the wide variations in climate around the world. In this direction explanation and prediction of growth of managed and natural ecosystems in response to climate and soil-related factors are increasingly important as objectives of science. Quantitative prediction of complex systems, however, depends on integrating information through levels of organization, and the principal approach for that is through the construction of statistical and simulation models. Simulation of system's use and balance of carbon, beginning with the input of carbon from canopy assimilation forms the essential core of most simulations that deal with the growth of vegetation.

Systems are webs or cycles of interacting components. Change in one component of a system produces changes in other components because of the interactions. For example, a change in weather to warm and humid may lead to the more rapid development of a plant disease, a loss in yield of a crop, and consequent financial adversity for individual farmers and so for the people of a region. Most natural systems are complex. Many do not have boundaries. The bio-system is comprised of a complex interaction among the soil, the atmosphere, and the plants that live in it. A chance alteration of one element may yield both desirable and undesirable consequences. Minimizing the undesirable, while reaching the desired end result is the principle aim of the agrometerologist. In any engineering work related to agricultural meteorology the use of mathematical modeling is essential. Of the different modeling techniques, mathematical modeling enables one to predict the behaviour of design while keeping the expense at a minimum. Agricultural systems are basically modified ecosystems. Managing these systems is very difficult. These

systems are influenced by the weather both in length and breadth. So, these have to be managed through systems models which are possible only through classical engineering expertise.

TYPES OF MODELS

Depending upon the purpose for which it is designed the models are classified into different groups or types. Of them a few are :

a. Statistical models: These models express the relationship between yield or yield components and weather parameters. In these models relationships are measured in a system using statistical techniques (Table 1).

   Example: Step down regressions, correlation, etc.

b. Mechanistic models: These models explain not only the relationship between weather parameters and yield, but also the mechanism of these models (explains the relationship of influencing dependent variables). These models are based on physical selection.

c. Deterministic models: These models estimate the exact value of the yield or dependent variable. These models also have defined coefficients.

d. Stochastic models: A probability element is attached to each output. For each set of inputs different outputs are given alongwith probabilities. These models define yield or state of dependent variable at a given rate.

e. Dynamic models: Time is included as a variable. Both dependent and independent variables are having values which remain constant over a given period of time.

f. Static: Time is not included as a variables. Dependent and independent variables having values remain constant over a given period of time.

g. Simulation models: Computer models, in general, are a mathematical representation of a real world system. One of the main goals of crop simulation models is to estimate agricultural production as a function of weather and soil conditions as well as crop management. These models use one or more sets of differential equations, and calculate both rate and state variables over time, normally from planting until harvest maturity or final harvest.

Table 1. Prediction models for crop growth, yield components and seed yield of soybean genotypes with meteorological observations

	GENOTYPE	
	MACS-201	MACS-58
Plant height	-89.98+0.77 MAT_1 +0.39 SS_2 -1.10 MIT_3 +12.91 MT_3 -12.50 GDD_3 -0.09 HTU_3 R^2 = 0.97	57.60-0.24 MIT_1 -0.06 RH_{12} -0.07 HTU_3 R^2 = 0.92
Branches per plant	2.97+0.08 SS_1 +0.08 MAT_2 -0.01 HTU_2-0.07 MAT_3 R^2 = 0.91	6.44-0.01 RH_{21} +0.03 MAT_2 -0.12 MAT_3 R^2 = 0.83
Green leaves	-1.20-0.20 MT_1 -0.03 RH_{11} +0.19 GDD_2 -0.18 RH_{13} +0.13 RH_{23} +2.92 MT_3 -3.55 GDD_3 R^2 = 0.98	19.95-0.29 MIT_2 -0.05 RH_{12} -0.60 SS_3 R^2 = 0.78
Leaf area (dm^2 m^{-2})	754.01-25.97 SS_1 -20.65 MAT_2 -29.85 SS_2 +0.15 HTU_2 -23.23 MIT_3 -5.66 RH_{13} -0.73 RH_{23} R^2 = 0.99	451.89-2.28 RH_{11} -7.06 SS_1 - 1.90 MIT_2 +1.02 RH_{22} +1.34 HTU_2-2.04 GDD_3 R^2 = 0.99
Leaf area index	-13.46+0.40 SS_1 -0.09 MAT_2 +0.17 MAT_3 +0.15 RH_{23} +1.02 SS_3 -0.02 HTU_3 R^2 = 0.98	18.30-0.03 RH_{11} -0.03 RH_{21} -0.02 HTU_1 +0.02 HTU_2 - 0.35 MAT_3 R^2 = 0.96
Canopy dry weight	-1610.10+3.16 RH_{11} +16.65 MT_1 +2.73 HTU_2 +76.04 MAT_3 -6.77 RH_{13} +126.81 SS_3 -14.12 HTU_3 R^2 = 0.99	2018.40-7.14 RH_{11} -2.21 HTU_1 -1.74 RH_{12} -16.14 MAT_3 R^2 = 0.94
No. of pods per plant	-697.79+4.14 MIT_1 +0.94 RH_{11} +13.01 SS_1 +11.14 MAT_3 +2.20 RH_{23} +29.93 SS_3 -1.65 HTU_3 R^2 = 0.99	56.89+3.86 SS_1-0.33 HTU_3 R^2 = 0.88
Seeds per pod	-5.08 + 0.03 MAT_1 + 0.94 RH_{11} +0.05 MIT_2 -0.03 RH_{13} +0.04	4.13-0.07 MIT_1 -0.02 GDD_1 -0.86 GDD_3 R^2 = 0.95 RH_{23} +0.11 SS_3 -0.07 GDD_3 R^2 = 0.99
100 seed weight	3.18-0.05 RH_{11} -0.09 GDD_2 +1.95 MT_3 -2.34 GDD_3 R^2 = 0.93	15.32-0.11 RH_{11} -0.06 RH_{21} -0.10 HTU_1 -0.04 RH_{22} +0.02 HTU_2 +0.74 MT_3 -1.24 GDD_3 R^2 = 0.97
Harvest index	56.16 +0.11 RH_{11} -0.13 RH_{21} +0.38 MAT2 -0.07 HTU_2 -0.69 MAT_3 R^2 = 0.94	151.36-0.20 RH_{11} -0.06 RH_{21} -0.10 HTU_1 -0.63 MAT_2 +0.17 HTU_2 -2.30 MAT_3 -0.06 RH_{13} R^2 = 0.98
Yield	6370.20-7.73 RH_{21} -5.57 HTU_2 -93.85 MAT_3 R^2 = 0.93	6899.70-21.84 RH_{11} -62.83 MT_1-10.89 HTU_3 R^2 = 0.95
Plant height	42.38+0.70 SS_1 -0.07 HTU_3 R^2 = 0.92	110.89-0.36 MIT_1-0.05 RH_{21} +0.042 HTU_1 -0.11 RH_{12} -0.03 RH_{22} -0.01 HTU_2 -0.91 MAT_3 -0.12 RH_{13}-1.1 SS_3 R^2 = 0.99

	GENOTYPE	
	MACS-201	MACS-58
Branches per plant	6.31-0.01 RH_{12} +0.02 MT_2 -0.09 MAT_3 R^2 = 0.91	5.79-0.01 RH_{12} -0.01 RH_{22} -0.06 MAT_3 R^2 = 0.81
Green leaves	2.81+0.68 MAT_1 -0.05 RH_{21} -0.04 HTU_1 -0.25 MIT_2 -0.23 MAT_3 R^2 = 0.77	28.68-0.72 RH_{21} +0.05 SS_1 -0.73 MIT_2 +0.01 RH_{12} -0.48 SS_2 +0.67 GDD_2 -0.05 RH_{13} -0.72 SS_3 -0.27 GDD_3 R^2 = 0.99
Leaf area (dm^2 m^{-2})	190.28-2.01 RH_{11} +1.02 RH_{21} -6.68 SS_1 -4.98 MAT_2 +1.19 HTU_2 +26.48 MT_3 -40.32 GDD_3 R^2 = 0.99	346.96-0.20 RH_{21} +0.02 HTU_1 -0.53 RH_{12} -0.32 RH_{22} +0.013 HTU_2 +1.16 MIT_3 -0.64 RH_{13} -3.80 SS_3 -10.10 GDD_3 R^2 = 0.99
Leaf area index	17.47-0.01 RH_{21} -0.25 SS_1 -0.02 HTU_1 -0.36 MAT_2 +0.06 HTU_2 -0.35 MAT_3 +0.06 RH_{23} +0.39 SS_3 R^2 = 0.99	6.21-0.02 RH_{22} -0.02 HTU_3 R^2 = 0.87
Canopy dry weight	751.46+19.21 MIT_1 -4.19 RH_{11} -2.16 HTU_1 -18.80 MAT_2 +1.47 RH_{12} +4.36 HTU_2 +70.36 SS_3 -4.71 HTU_3 R^2 = 0.99	1568.40-5.00 MAT_1 -6.30 RH_{11} -0.91 HTU_1 +2.20 MAT_2 +0.80 MT_2 +5.40 GDD_2 +0.49 HTU_2 +2.68 RH_{13} -14.91 SS_3 -22.65 MJ_1 R^2 = 0.99
No. of pods per plant	152.48-0.25 RH_{21} -0.28 RH_{12} +0.01 HTU_2 -0.05 MAT_3 -1.24 MIT_2 R^2 = 0.89	56.54+3.39 MAT_1 +6.44 SS_1 +2.80 MT_2 -0.70 HTU_1 -0.53 RH_{12} -0.72 RH_{13} -0.32 HTU_3 R^2 =0.98
Seeds per pod	4.93-0.00 HTU_1 -0.01 RH_{12} +0.01 HTU_2 -0.05 MAT_3 R^2 = 0.86	4.99-0.01 MIT +0.01 RH_{11} +0.06 GDD_1 +0.01 MAT_2 -0.01 RH_{12} -0.04 HTU_2 -0.02 MAT_3 -0.03 RH_{13} +0.02 RH_{23} R^2 = 0.99
100 seed weight	15.45+0.06 MAT_2 -0.28 GDD_3 R^2 = 0.90	28.08-0.12 MAT_1 -0.02 RH_{11} -0.03 RH_{21} +0.01 MAT_2 -0.02 RH_{12} +0.02 RH_{23} -0.45 SS_3 - 0.44 GDD_3 +0.02 HTU_3 R^2 = 0.99
Harvest index	44.25+1.10 SS_1 -0.10 HTU_3 R^2 = 0.92	58.90 +1.02 MAT_1 -0.07 RH_{21} -0.10 HTU_1 -0.11 RH_{22} -0.31 SS_{22} -0.62 GDD_2 -0.65 MAT_3 -0.32 GDD_3 R^2 = 1.000
Yield	6373.5-128.52 MAT_3 R^2 = 0.90	7115.90-27.53 MIT_1 -22.21 RH_{11} -4.51 HTU_1 -3.22 RH_{12} - 3.00 HTU_2 -66.31 MAT_3 -7.45 HTU_3 R^2 = 0.99

GENOTYPE -MACS-330	
Plant height	85.15-0.67 MAT_1 +0.77 SS_1 -1.10 MAT_2 -0.42 RH_{12} +0.09 RH_{22} +1.07 SS_2 -0.14 RH_{13} +1.64 MT_3 -0.14 HTU_3 R^2 = 0.99
Branches per plant	-5.05-0.32 MT_1 +0.39 GDD_1 +1.03 MT_2 -1.04 GDD_2 -0.06 MIT_3 R^2 = 0.85
Green leaves	12.40-0.64 RH_{21} +0.032 SS_2 -0.037 HTU_2 R^2 = 0.81
Leaf area ($dm^2 m^2$)	-203.25-0.47 RH_{11} -1.06 RH_{12} +40.96 MT_2 -41.82 GDD_2 -0.17 HTU_2 +6.01 MAT_3 -1.12 RH_{13} -1.04 HTU_3 R^2 = 0.83
Leaf area index	-2.17+0.0067 RH_{21} +0.39 SS_1 -0.09 GDD_1 +0.016 RH_{22} +0.18 SS_2 +0.22 MAT_3 +0.0069 RH_{13} -0.60 SS_3 -0.17 GDD_3 R^2 = 0.87
Canopy dry weight	144.72-6.41 MAT_1 -3.51 RH_{11} +1.33 RH_{21} -9.53 RH_{12} +3.58 RH_{22} +48.55 SS_2 -3.84 HTU_2 -29.11 SS_3 +1.61 HTU_3 R^2 = 0.99
No. of pods per plant	24.67-2.29 MIT_1 +0.63 RH_{11} +6.79 SS_1 -3.37 MAT_2 +0.32 HTU_2 +4.17 MAT_3 -10.42 SS_3 -0.35 HTU_3 R^2 = 0.95
Seeds per pod	7.47-0.09 SS_1 -0.08 MAT_2 -0.04 RH_{12} +0.10 MAT_3 -0.01 RH_{13} -0.01 HTU_3 R^2 = 0.96
100 seed weight	-2.02-0.07 RH_{11} +0.03 RH_{21} +0.26 SS_1 +0.68 MAT_2 +0.08 RH_{22} -0.67 GDD_2 +0.02 RH_{13} -0.022 MT_3 -0.013 HTU_3 R^2 = 0.99
Harvest index	24.39-0.22 RH_{11} +0.06 RH_{21} -0.12 MT_1 +1.75 MAT_2 -0.20 RH_{12} +0.24 RH_{22} -1.64 GDD_2 +0.55 MAT_3 -0.10 HTU_3 R^2 = 0.99
Yield	1899+1.27 RH_{23} -5.63 HTU_3 R^2 = 0.77

ABBREVIATIONS

MAT_1 – Maximum temperature in phase 1
MAT_2 – Maximum temperature in phase 2
MAT_3 – Maximum temperature in phase 3
MIT_1 – Minimum temperature in phase 1
MIT_2 – Minimum temperature in phase 2
MIT_3 – Minimum temperature in phase 3
MT_1 – Mean temperature in phase 1
MT_2 – Mean temperature in phase 2
MT_3 – Mean temperature in phase 3
RH_{11} – Relative humidity in the morning in phase 1
RH_{12} – Relative humidity in the morning in phase 2
RH_{13} – Relative humidity in the morning in phase 3
RH_{21} – Relative humidity in the evening in phase 1
RH_{22} – Relative humidity in the evening in phase 2
RH_{23} – Relative humidity in the evening in phase 3
SS_1 – Sunshine hours in phase 1
SS_2 – Sunshine hours in phase 2
SS_3 – Sunshine hours in phase 3
GDD_1 – Growing degree days in phase 1
GDD_2 – Growing degree days in phase 2
GDD_3 – Growing degree days in phase 3
HTU_1 – Heliothermal units in phase 1
HTU_2 – Heliothermal units in phase 2
HTU_3 – Heliothermal units in phase 3

h. Descriptive model: A descriptive model defines the behaviour of a system in a simple manner. The model reflects little or none of the mechanisms that are the causes of phenomena. But, consists of one or more mathematical equations. An example of such an equation is the one derived from successively measured weights of a crop. The equation is helpful to determine quickly the weight of the crop where no observation was made.

i. Explanatory model: This consists of quantitative description of the mechanisms and processes that cause the behaviour of the system. To create this model, a system is analyzed and its processes and mechanisms are quantified separately. The model is built by integrating these descriptions for the entire system. It contains descriptions of distinct processes such as leaf area expansion, tiller production, etc. Crop growth is a consequence of these processes.

WEATHER DATA FOR MODELING

The national meteorological organizations provide weather data for crop modeling purposes through observatories across the globe (Sivakumar *et al.*, 2000). In many European countries weather records are available for over 50 years. In crop modeling the use of meteorological data has assumed a paramount importance. There is a need for high precision and accuracy of the data. The data obtained from surface observatories has proved to be excellent. It gained the confidence of the people across the globe for decades. These data are being used daily by people from all walks of life. But, the automated stations are yet to gain popularity in the under developed and developing countries. There is a huge gap between the old time surface observatories and present generation of automated stations with reference to measurement of rainfall. The principles involved in the construction and working of different sensors for measuring rainfall are not commonly followed in automated stations across the globe. As of now, solar radiation, temperature and precipitation are used as inputs in DSSAT.

Weather as an Input in Models

In crop modeling weather is used as an input. The available data ranges from one second to one month at different sites where crop-modeling work in the world is going on. Different curve fitting techniques, interpolation, extrapolation functions etc., are being followed to use weather data in the model operation. Agrometeorological variables are especially subject to variations in space. It is reported that, as of now, anything beyond daily data proved

unworthy as they are either over-estimating or under-estimating the yield in simulation. Stochastic weather models can be used as random number generators whose input resembles the weather data to which they have been fit. These models are convenient and computationally fast, and are useful in a number of applications where the observed climate record is inadequate with respect to length, completeness, or spatial coverage. These applications include simulation of crop growth, development and impacts of climate change. In 1995 JW Jones and Thornton described a procedure to link a third-order Markov Rainfall model to interpolated monthly mean climate surfaces. The constructed surfaces were used to generate daily weather data (rainfall and solar radiation). These are being used for purposes of system characterization and to drive a wide variety of crop and live stock production and ecosystem models. The present generation of crop simulation models particularly DSSAT suit of models have proved their superiority over analytical, statistical, empirical, combination of two or all etc., models so far available. In the earliest crop simulation models only photosynthesis and carbon balance were simulated. Other processes such as vegetative and reproductive development, plant water balance, micronutrients, pest and disease, etc., are not accounted for as the statistical models use correlative approach and make large area yield prediction and only final yield data are correlated with the regional mean weather variables. This approach has slowly been replaced by the present simulation models by these DSSAT models. When many inputs are added in future the models become more complex. The modelers who attempt to obtain input parameters required to add these inputs look at weather as their primary concern. They may have to adjust to the situation where they develop capsules with the scale level at which the input data on weather are available.

Role of Weather in Decision Making

Decisions based solely upon mean climatic data are likely to be of limited use for at least two reasons. The first is concerned with definition of success and the second with averaging and time scale. In planning and analyzing agricultural systems it is essential not only to consider variability, but also to think of it in terms directly relevant to components of the system. Such analyses may be relatively straightforward probabilistic analyses of particular events, such as the start of cropping seasons in West Africa and India. The principal effects of weather on crop growth and development are well understood and are predictable. Crop simulation models can predict responses to large variations in weather. At every point of application weather data are the most important input. The main goal of most applications of crop models

is to predict commercial out-put (Grain yield, fruits, root, biomass for fodder etc.). In general the management applications of crop simulation models can be defined as: 1) strategic applications (crop models are run prior to planting), 2) practical applications (crop models are run prior to and during crop growth) and 3) forecasting applications (models are run to predict yield both prior to and during crop growth).

Crop simulation models are used in USA and in Europe by farmers, private agencies, and policy makers to a greater extent for decision making. Under Indian and African climatic conditions these applications have an excellent role to play. The reasons being the dependence on monsoon rains for all agricultural operations in India and the frequent dry spells and scanty rainfall in crop growing areas in Africa. Once the arrival of monsoon is delayed the policy makers and agricultural scientists in India are under tremendous pressure. They need to go for contingency plans. These models enable to evaluate alternative management strategies, quickly, effectively and at no/low cost. To account for the interaction of the management scenarios with weather conditions and the risk associated with unpredictable weather, the simulations are conducted for at least 20-30 different weather seasons or weather years. If available, the historical weather data, and if not weather generators are used presently. The assumption is that these historical data will represent the variability of the weather conditions in future. Weather also plays a key role as input for long-term crop rotation and crop sequencing simulations.

CLIMATE CHANGE AND CROP MODELING

Climate change

Climate change is defined as “Any long term substantial deviation from present climate because of variations in weather and climatic elements”.

The causes of climate change

1. The natural causes like changes in earth revolution, changes in area of continents, variations in solar system, etc.

2. Due to human activities the concentrations of carbon dioxide and certain other harmful atmospheric gases have been increasing. The present level of carbon dioxide is 325 ppm and it is expected to reach 700 ppm by the end of this century, because of the present trend of burning forests,

grasslands and fossil fuels. Few models predicted an increase in average temperature of 2.3 to 4.6°C and precipitation per day from 10 to 32 per cent in India.

Green house effect

The effect because of which the earth is warmed more than expected due to the presence of atmospheric gases like carbon dioxide, methane and other tropospheric gases. The shortwave radiation can pass through the atmosphere easily, but, the resultant outgoing terrestrial radiation can not escape because atmosphere is opaque to this radiation and this acts to conserve heat which rises temperature.

Effects of climate Change

1. The increased concentration of carbon dioxide and other green house gases are expected to increase the temperature of earth.

2. Crop production is highly dependent on variation in weather and therefore any change in global climate will have major effects on crop yields and productivity.

3. Elevated temperature and carbon dioxide affects the biological processes like respiration, photosynthesis, plant growth, reproduction, water use etc. In case of rice increased carbon dioxide levels results in larger number of tillers, greater biomass and grain yield. Similarly, in groundnut increased carbon dioxide levels results in greater biomass and pod yields.

4. However, in tropics and sub-tropics the possible increase in temperatures may offset the beneficial effects of carbon dioxide and results in significant yield losses and water requirements.

Proper understanding of the effects of climate change helps scientists to guide farmers to make crop management decisions such as selection of crops, cultivars, sowing dates and irrigation scheduling to minimize the risks.

Role of Climate Change in Crop Modeling

In recent years there has been a growing concern that changes in climate will lead to significant damage to both market and non-market sectors. The climate change will have a negative effect in many countries. But farmers

adaptation to climate change-through changes in farming practices, cropping patterns, and use of new technologies will help to ease the impact. The variability of our climate and especially the associated weather extremes is currently one of the concerns of the scientific as well as general community. The application of crop models to study the potential impact of climate change and climate variability provides a direct link between models, agrometeorology and the concerns of the society. Tables 2 and 3 present the results of sensitivity analysis for different climate change scenarios for peanut in Hyderabad, India. As climate change deals with future issues, the use of General Circulation Models (GCMs) and crop simulation models proves a more scientific approach to study the impact of climate change on agricultural production and world food security compared to surveys.

Cropgro (DSSAT) is one of the first packages that modified weather simulation generators/or introduced a package to evaluate the performance of models for climate change situations. Irrespective of the limitations of GCMs it would be in the larger interest of farming community of the world that these DSSAT modelers look at GCMs for more accurate and acceptable weather generators for use in models. This will help in finding solutions to crop production under climate changes conditions, especially in underdeveloped and developing countries.

FUTURE ISSUES RELATED TO WEATHER ON CROP MODELING

For any application of a crop model weather data is an essential input and it continues to play a key role. So:

1. There is an urgent need to develop standards for weather station equipment and sensors installation and maintenance.

2. It is also important that a uniform file format is defined for storage and distribution of weather data, so that they can easily be exchanged among agrometeorologists, crop modelers and others working in climate and weather aspects across the globe.

3. Easy access to weather data, preferably through the internet and the world wide web, will be critical for the application of crop models for yield forecasting and tactical decision making.

4. Previously one of the limitations of the current crop simulation models was that they can only simulate crop yield for a particular site. At this

Table 2. Results of sensitivity analysis for different climate change scenarios showing the simulated mean peanut seed yield (kg ha^{-1}) at maturity and standard deviation (SD) for 25 years (1975-1999) of weather under irrigated and rainfed conditions at Hyderabad, India

Temperature increase (°C)	Irrigated				Rainfed			
	330 ppm CO_2		555 ppm CO_2		330 ppm CO_2		555 ppm CO_2	
	Yield	SD	Yield	SD	Yield	SD	Yield	SD
0.0	1570	112	2223	144	1431	219	2041	297
1.0	1526	120	2168	157	1369	234	1977	319
1.5	1484	119	2127	153	1322	224	1926	318
2.0	1451	130	2100	173	1294	236	1891	330
2.5	1436	132	2095	178	1274	240	1876	334
3.0	1437	134	2104	192	1260	251	1857	359
3.5	1450	139	2115	195	1187	354	1749	510
4.0	1210	551	1754	797	1060	480	1560	699
4.5	741	735	1077	1064	770	589	1148	869
5.0	377	621	555	916	530	560	662	818

Table 3. Results of sensitivity analysis for different climate change scenarios showing the simulated mean peanut seed yield (kg ha^{-1}) at maturity and standard deviation (SD) for 25 years (1975-1999) of weather under rainfed conditions at Hyderabad, India with 20% increase or decrease in rainfall

Temperature increase (°C)	Rainfed (+20 % rainfall)				Rainfed (-20 % rainfall)			
	330 ppm CO_2		555 ppm CO_2		330 ppm CO_2		555 ppm CO_2	
	Yield	SD	Yield	SD	Yield	SD	Yield	SD
0.0	1494	106	2140	129	1430	219	1948	354
1.0	1437	95	2060	117	1298	294	1873	380
1.5	1400	88	2018	114	1254	283	1821	378
2.0	1368	82	1990	110	1222	295	1780	394
2.5	1356	82	1980	122	1195	295	1762	416
3.0	1367	93	2005	135	1177	315	1742	440
3.5	1385	106	2035	157	1095	394	1628	556
4.0	1346	301	1971	444	1015	452	1518	646
4.5	1238	475	1795	693	700	563	1048	830
5.0	1000	640	1213	1016	416	493	647	764

site weather (soil and management) data also must be available. It is a known fact that the weather data (and all these other details) are not available at all locations where crops are grown. To solve these problems the Geographical Information System (GIS) approach has opened up a whole field of crop modeling applications at spatial scale. From the field level for site-specific management to the regional level for productivity analysis and food security the role of GIS is going to be tremendous (Hoogenboom, 2000).

APPLICATIONS AND USES OF CROP GROWTH MODELS IN AGRICULTURAL METEOROLOGY

The crop growth models are being developed to meet the demands under the following situations in agricultural meteorology.

1. When the farmers have the difficult task of managing their crops on poor soils in harsh and risky climates.

2. When scientists and research managers need tools that can assist them in taking an integrated approach to finding solutions in the complex problem of weather, soil and crop management.

3. When policy makers and administrators need simple tools that can assist them in policy management in agricultural meteorology.

The potential uses of crop growth models for practical applications are as follows (Sivakumar and Glinni, 2000).

On farm decision-making and agronomic management

The models allow evaluation of one or more options that are available with respect to one or more agronomic management decisions like:

- Determine optimum planting date.
- Determine best choice of cultivars.
- Evaluate weather risk.
- Investment decisions.

The crop growth models can be used to predict crop performance in regions where the crop has not been grown before or not grown under optimal

conditions. Such applications are of value for regional development and agricultural planning in developing countries (Van Keulen and Wolf, 1986). A model can calculate probabilities of grain yield levels for a given soil type based on rainfall (Kiniry and Bockhot, 1998). Investment decisions like purchase of irrigation systems (Boggess and Amerling, 1983) can be taken with an eye on long term usage of the equipment thus acquired. Kiniry *et al.* (1991) showed that for maize, both simulated and measured mean yields with weeds are 86% of the weed-free yields.

Understanding of research

In agro-meteorological research the crop models basically helps in:

- Testing scientific hypothesis.
- Highlight where information is missing.
- Organizing data.
- Integrating across disciplines.
- Assist in genetic improvement;
  - Evaluate optimum genetic traits for specific environments.
  - Evaluate cultivar stability under long term weather.

Penning de Vries (1977) emphasized that simulation models contribute to our understanding of the real system which in-turn helps to bridge areas and levels of knowledge. It is believed that in conversion of conceptual models into mathematical simulation models the agrometeorologists can understand the gaps in their knowledge. So, the interdisciplinary nature of simulation modeling efforts leads to increased research efficacy and improved research direction through direct feedback. In this direction de Wit and Goudriaan (1978) developed BAsic CROp growth Simulator (BACROS) which was used as a reference model for developing other models and as a basis for developing summary models. Also O Toole and Stockle (1987) described the potential of simulation models in assessing trait benefits of winter cereals and their capacity to survive and reproduce in stress-prone environment. Crop growth models have been used in plant breeding to simulate the effects of changes in the morphological and physiological characteristics of crops which aid in identification of ideotypes for different environments (Hunt, 1993; Kropff *et al.*, 1995).

Policy management

The policy management is one very useful application of crop simulation models. The issues range from global (impacts of climate change on crops) to field level (effect of crop rotation on soil quality) issues. Thornton *et al.* (1997) showed that in Burkina Faso, crop simulation modeling using satellite and ground-based data could be used to estimate millet production for famine early warning which can allow policy makers the time they need to take appropriate steps to ameliorate the effects of global food shortages on vulnerable urban and rural populations. In Australia Meinke and Hammer (1997) found that when November-December SOI (Southern Oscillation Index) phase is positive, there is an 80% chance of exceeding average district yields. Conversely, in years when the November-December SOI phase is either negative or rapidly falling, there is only a 5% chance of exceeding average district yields, but a 95% chance of below average yields. This information allows the industry to adjust strategically for the expected volume of production.

Crop models can be used to understand the effects of climate change such as :

a) Consequences of elevated carbon-dioxide, and

b) Changes in temperature and rainfall on crop development, growth and yield. Ultimately, the breeders can anticipate future requirements based on the climate change.

A FEW SUCCESSFULLY USED MODELS IN AGROMETEOROLOGY

Large scale evolution of computers since 1960 allowed to synthesize detailed knowledge on plant physiological processes in order to explain the functioning of crops as a whole. Insights into various processes were expressed using mathematical equations and integrated in simulation models. In the beginning, models were meant to increase the understanding of crop behaviour by explaining crop growth and development in terms of the understanding physiological mechanisms. Over the years new insights and different research questions motivated the further development of simulation models. In addition to their explanatory function, the applicability of well-tested models for extrapolation and prediction was quickly recognized and more application-oriented models were developed. For instance demands for advisory systems for farmers and scenario studies for policy makers resulted in the evolution of models, geared towards tactical and strategic decision support respectively.

Now, crop growth modeling and simulation have become accepted tools for agricultural research.A few models used in agrometeorological studies are:

1. The de Wit school of models

In the sixties, the first attempt to model photosynthetic rates of crop canopies was made (de Wit, 1965). The results obtained from this model were used among others, to estimate potential food production for some areas of the world and to provide indications for crop management and breeding (de Wit, 1967; Linneman *et al.*, 1979). This was followed by the construction of an Elementary CROp growth Simulator (ELCROS) by de Wit *et al.* (1970). This model included the static photosynthesis model and crop respiration was taken as a fixed fraction per day of the biomass, plus an amount proportional to the growth rate. In addition, a functional equilibrium between root and shoot growth was added (Penning de Vries *et al.*, 1974). The introduction of micrometeorology in the models (Goudriaan, 1977) and quantification of canopy resistance to gas exchanges allowed the models to improve the simulation of transpiration and evolve into the BAsic CROp growth Simulator (BACROS) (de Wit and Goudriaan, 1978).

2. IBSNAT and DSSAT Models

In many countries of the world, agriculture is the primary economic activity. Great numbers of the people depend on agriculture for their livelihood or to meet their daily needs, such as food. There is a continuous pressure to improve agricultural production due to staggering increase in human population. Agriculture is very much influenced by the prevailing weather and climate. The population increase is 2.1 per cent in India. This demands a systematic appraisal of climatic and soil resources to recast an effective land use plan. More than ever farmers across the globe want access to options such as the management options or new commercial crops. Often, the goal is to obtain higher yields from the crops that they have been growing for a long time. Also, while sustaining the yield levels they want to :

1. Substantially improve the income.
2. Reduce soil degradation.
3. Reduce dependence on off-farm inputs.
4. Exploit local market opportunities.

5. Farmers also need a facilitating environment in which;

   a. Affordable credit is available.

   b. Policies are conducive to judicious management of natural resources.

   c. Costs and prices of production are stable.

6 Another key ingredient of a facilitating environment is information, such as :

   a. An understanding of which options are available.

   b. How these operate at farm level.

   c. The impact on issues of their priority.

To meet the above requirements of resource poor farmers in the tropics and sub tropics IBSNAT (International Benchmark Sites Network for Agro-technology Transfer) began in 1982. This was under a contract from the U.S. Agency for International Development to the University of Hawaii at Manoa, USA. IBSNAT was an attempt to demonstrate the effectiveness of understanding options through systems analysis and simulation for ultimate benefit of farm households across the globe. The purposes defined for the IBSNAT project by its technical advisory committee were to :

1. Understand ecosystem processes and mechanisms.
2. Synthesize from an understanding of processes and mechanisms, a capacity to predict outcomes.
3. Enable IBSNAT clientele to apply the predictive capability to control outcomes.

The models developed by IBSNAT were simply the means by which the knowledge scientists have and could be placed in the hands of users. In this regard, IBSNAT was a project on systems analysis and simulation as a way to provide users with options for change. In this project many research institutions, universities, and researchers across the globe spent enormous amount of time and resources and focused on:

1 Production of a “decision support system” capable of simulating the risks and consequences of alternative choices, through multi-institute and multi-disciplinary approaches.

2. Definition of minimum amount of data required for running simulations and assessing outcomes.

3. Testing and application of the product on global agricultural problems requiring site-specific yield simulations.

The major product of IBSNAT was a Decision Support System for Agro-Technology Transfer (DSSAT). The network members lead by J.W. Jones, Gainesville, USA developed this. The DSSAT is being used as a research and teaching tool. As a research tool its role to derive recommendations concerning crop management and to investigate environmental and sustainability issues is unparalleled. The DSSAT products enable users to match the biological requirements of crops to the physical characteristics of land to provide them with management options for improved land use planning. The DSSAT is being used as a business tool to enhance profitability and to improve input marketing.

The traditional experimentation is time consuming and costly. So, systems analysis and simulation have an important role to play in fostering this understanding of options. The information science is rapidly changing. The computer technology is blossoming. So, DSSAT has the potential to reduce substantially the time and cost of field experimentation necessary for adequate evaluation of new cultivars and new management systems. Several crop growth and yield models built on a framework similar in structure were developed as part of DSSAT package. The package consists of : 1) data base management system for soil, weather, genetic coefficients, and management inputs, 2) Crop-simulation models, 3) series of utility programs, 4) series of weather generation programs, 5) strategy evaluation program to evaluate options including choice of variety, planting date, plant population density, row spacing, soil type, irrigation, fertilizer application, initial conditions on yields, water stress in the vegetative or reproductive stages of development, and net returns.

Other Important Models

Crop models can be developed at various levels of complexity. The level of complexity required depends on the objective of the modeling exercise. The top-down approach to model design (Hammer *et al*., 1989; Shorter *et al*., 1991) is appropriate for models aimed at yield prediction. In this approach, complexity is kept to a minimum by commencing with a simple framework and only incorporating additional phenomena or processes if they improve

the predictive ability of the model. Sinclair (1986), Muchow *et al*. (1990) and Hammer and Muchow (1991) have adopted this method in developing models of soybean, maize and sorghum respectively.

The EPIC, ALAMANC, CROPSYST, WOFOST, ADEL models are being successfully used to simulate maize crop growth and yield. The SORKAM, SorModel, SORGF as also ALMANAC models are being used to address specific tasks of sorghum crop management. CERES – pearl millet model, CROPSYST, PmModels are being used to study the suitability and yield simulation of pearl millet genotypes across the globe. Similarly, the two most common growth models used in application for cotton are the GOSSYM and COTONS models. On the same analogy the PNUTGRO for groundnut, CHIKPGRO for chick pea, WTGROWS for wheat, SOYGRO for soybean, QSUN for sunflower are in use to meet the requirements of farmers, scientists, decision makers, etc., at present. The APSIM, GROWIT added with several modules are being used in crop rotation, crop sequence and simulation studies involving perennial crops.

Under Indian sub-continent conditions, crop yield forecasting based on meteorological data is very important from several points of view. Using crop yield as dependent variable and weather factors as independent variables, empirical statistical models for predicting crop yield have been reported by Mall *et al*. (1996). Also, Mall and Gupta (2000) reported a successful empirical statistical – yield weather model for wheat in the Varanasi district of Uttar Pradesh, India. Rajesh Kumar *et al*. (1999) developed a stepwise regression model which states that the pigeonpea yield variation by weather variables is upto 94 per cent in Varanasi District, U.P., India. Using a thermal time and phasic development model. Patel *et al.* (1999) found that pigeonpea phenophases depended upon the available heat units and accounted for 98 per cent of total variation in Anand, Gujarat State, India.

Elsewhere in the world there were studies (Robertson and Foong, 1977; Foong, 1981), which predicted yields based on climatic factors using mathematical modeling. Factors such as water deficit, solar radiation, maximum and minimum temperatures which play a vital role at floral initiation were taken into consideration to construct these models. In Southern Malaysia Ong (1982) found a high correlation between yield of oil palm and rainfall and dry spells as also temperature and sunshine using a step-wise regression approach. Chow (1991) constructed a statistical model for predicting crude palm oil production with trend, season, rainfall, etc. Amissah-Arthur and Jagtap

(1995) successfully assessed nitrogen requirements by maize across agro ecological zones in Nigeria using CERES-maize model. Hammer *et al*. (1995) using local weather and soil information correlated peanut yields with estimates from PEANUTGRO, a model in the CERES family and gave a regression with high coefficient (r^2 = 0.93) of variation. The construction of contemporary crop models entails the combination of many algorithms for physiological processes and impact of environmental factors on process rates (Monteith, 2000). This clearly indicates that in the development of models and their application for solving problems at field level on agrometeorological aspects are given due weightage.

APPLICATION OF MODELS IN AGRICULTURAL METEOROLOGY – PRECAUTIONS

Hunger demands food. Food grains come from agriculture, but it is risk-prone. So research efforts are necessary. Unfortunately, funding for research worldwide is declining at an alarming rate. The agricultural scientists and planners are facing formidable challenges to ensure continued increases in agricultural productivity to meet the food grain requirements of burgeoning population across the globe. Nowadays, the traditional field experimentation is becoming very expensive. So, the works on development and use of crop growth models to answer strategic and tactical questions concerning agricultural planning as well as on-farm soil and crop management are essential.

Although these models are useful in more than one way as detailed earlier in this lecture, much of the modeling uses and applications to date have been mainly in the area of research. The products of research need to be disseminated to the farmers. Otherwise the present works on crop modeling cannot sustain in the long run. So far, much of crop modeling applications in the literature are based on sole cropping and only in the recent past this work has been extended to intercrops, crop rotations, crop sequences, etc. The works on crop rotations shall be taken up on priority. If one considers the attention given to individual crops so far maize and cotton rank more than 50% of the work but there are many other crops that meet food requirements of the population in tropical and sub-tropical areas of the world. So, it is essential to understand fully the physical and physiological processes of these crops that govern their growth and yield under valuable soil and climatic conditions through crop models.

The development of agrometerological and agroclimatological models include climate crop and soil. The availability of water (which is an observed

parameter through rainfall) and water requirement (expressed by PET which is an estimated parameter) are basic inputs in majority of these studies. The suitability of individual models for the estimation of PET depends not only on accurate predictive ability of the model but also on the availability of necessary input data. In addition, the following points shall be taken into considerations in model development and their application as precautions in agricultural meteorological studies.

1. Adequate human resource capacity has to be improved to develop and validate simulation models across the globe.

2. Multi-disciplinary research activities are essential for qualitative works in crop growth modeling.

3. Linkages shall be made and strengthened among research – education – extension to quickly disseminate the outcomes of models to farmers.

4. Majority of models use rainfall data at monthly interval, which is too long a period when compared to short duration of dry land crops (Sorghum, pearlmillet mature in 100 days). So, there is an urgent need to correct this anomaly by selecting proper methodologies.

5. It is important to differentiate between models of interest for research and for practical application. So, models useful to farmers with minimum input parameters shall find right place in the society.

6. It is always preferable to use one or more methods / models in conjunction to get more realistic conclusions useful to the farmers, who are the ultimate beneficiary alongwith industries.

7. The requirements in terms of details for local agricultural planning and operations are quite different from regional agricultural planning. Therefore, while selecting / using any model, it must be kept in mind the clear objective of study on one hand and verifying with ground truth (irrespective of the claims of the modal author) on the other hand.

8. The results / output of the models must be interpreted in an appropriate way by integrating soil, weather and crop. This interpretation is the key for success of agrometerological models. So, application of crop growth models shall form a part of studies of agrometeorologists on a regular and more continuous basis.

9. One should trust contemporary models particularly those concerned with yields. Wide variations may be found in the yield predicted by different models for specific crop in a defined environment. There is a need to develop test and improve the models with similar basis till they achieve comparable success for use by farmers, extension workers industry, etc. The reason is that the farmer needs them for decision-making, because It was found that the model can be used to identity new sites suitable for development of crop which finally results in generation of income to them.

10. It will be important to link the crop simulation models to local short and long-term weather forecasts. This will improve the yield predictions and provide policy makers with advanced yield information to help manage expected famines and other associated problems.

CONCLUSIONS

Various kinds of models such as Statistical, Mechanistic, Deterministic, Stochastic, Dynamic, Static, Simulations are in use for assessing and predicting crop growth and yield. Crop growth model is a very effective tool for predicting possible impacts of climatic change on crop growth and yield. Crop growth models are useful for solving various practical problems in agriculture. Adequate human resource capacity has to be improved to be develop and validate simulation models across the globe.

ACKNOWLEDGEMENTS

The author wishes to acknowledge the excellent encouragement, technical review and recommendations provided by Dr. M.V.K. Sivakumar, Professor C.J. Stigter, Professor Gerrit Hoogenboom and Dr. P.V.V. Prasad in preparation of the manuscript.

REFERENCES

Allen, L.H., Valle, P.R., Jones, J.W. and Jones, P.H. 1998. Soybean leaf water potential responses to carbon dioxide and drought. Agronomy Journal 90: 375-383.

Amissah-Arthur, A. and Jagtap, S.S. 1995. Application of models and geographic information system based decision support system in analysis the effect of rainfall on maize yield stability. Sustain Africa 3: 2-15.

Boggess, W.G. and Amerling, C.B. 1983. A bioeconomic simulation analysis of irrigation environments. S.J. Agric. Econ. 15: 85-91.

Boote, K.J., Jones, J.W., Hoogenboom, G., Wilkerson, G.G. and Jagtap, S.S. 1989. PNUTGRO VI.0, Peanut crop growth simulation model, user's guide. Florida Agricultural Experiment Station, Journal No. 8420. University of Florida, Gainesville, Florida, USA.

Chow, C.S. 1991. Seasonal and rainfall effects on oil palm yield in Malaysia. Second National Seminar on Agrometeorology, Petaling Jaya, Malaysia, pp. 109-128.

Clifford, S.C., Stronach, I.M., Black, C.R., Singleton-Jones, P.R., Azam-Ali, S.N. and Crout, N.M. 2000. Effects of elevated CO_2, drought and temperature on the water relations and gas exchange of groundnut (*Arachis hypogaea* L.) stands grown in controlled environment glasshouses. Physiological Plantarum 110: 78-88.

de Wit, C.T. and J. Goudriaan. 1978. Simulation of assimilation, respiration and transpiration of crops. Simulation monograph. PUDOC, Wageningen, The Netherlands.

de Wit, C.T., R. Brouwer and F.W.T. Penning de Vries. 1970. The simulation of photosynthetic systems, in prediction and measurement of photosynthetic productivity. Proceedings of International Biological Program/Plant Production Technical Meeting. Setlik, I., Ed., Trebon, PUDOC, Wageningen, The Netherlands.

de Wit, C.T. 1965. Photosynthesis of leaf canopies. Agricultural Research Report No. 663. PUDOC, Wageningen, The Netherlands.

de Wit, C.T. 1967. Photosynthesis: its relationship to overpopulation. p. 315-320. *In* Harvesting the sun. Academic Press, New York.

Foong, S.F. 1981. An improved weather model for estimating oil palm fruit yield. The Oil Palm in Agriculture in the Eighties. ISP, Malaysia.

Goudriaan, J. 1977. Crop micrometeorology: a simulation study. Simulation monograph. PUDOC. Wageningen, The Netherlands.

Hammer, G.L., Hoizworth, D.P., Mulo, S. and Wade, L.J. 1989. Modeling adaptation and risk of production of grain sorghum in Australia. p. 257-267. *In* M.A., Foale, B.W. Hare and R.G. Henzell (eds.) Proc. of the Australian Sorghum Workshop, Too-woomba. 28 Feb.-1 Mar. 1989. Australian Institute of Agricultural Science, Brisbane.

Hammer, G.L. and Muchow, R.C. 1991. Quantifying climatic risk to sorghum in Australia's semiarid tropics and subtropics : Model development and simulation. p. 205-232. *In* R.C. Muchow and J.A. Bellamy (eds.) Climatic risk in crop production : models and management for the semiarid tropics and subtropics. C.A.B. International, Wallingford, UK.

Hammer, G.L., Sinclair, T.R., Boote, K.J., Wright, G.C., Meinke, H. and Bell, M.J. 1995. A peanut simulation model. 1. Model development and testing. Agron. J. 87: 1085-1093.

Hoogenboon, G. 2000. Contribution of agrometeorology to the simulation of crop production and its applications. Agril. and For. Meteorol. 103 : 137-157.

Hunt, L.A. 1993. Designing improved plant types: a breeders view point. p. 3-17. *In* F.W.T. Penning de Vries *et al.* (ed.) Systems approaches for sustainable agricultural development. Kluwer Academic Publishers, Dordrecht, The Netherlands.

ICAR 2000. Crop Statistics Reports. Indian Council of Agricultural Research, New Delhi, India.

Kiniry, J.R. and A.J. Bockholt 1998. Maize and sorghum simulation in diverse Texas environments. Agron. J. 90: 682-687.

Kiniry, J.R., W.D. Rosenthal, B.S. Jackson and G. Hoogenboom. 1991. Predicting leaf development of crop plants. p.29-42. *In* T. Hodges (ed.) Predicting Crop Phenology. CRC Press, Boca Raton, FL.

Kropff, M.J., A.J. Haverkort, P.K. Aggarwal and P.L. Kooman. 1995. Using systems approaches to design and evaluate ideotypes for specific environments. p. 417-435. *In* J. Bouma, A. Kuyvenhoven, B.A.M. Bouman, J.C. Luyten and H.G. Zandstra (eds.) Eco-regional approaches for sustainable land use and food production. Kluwer Academic Publishers, Dordrecht, The Netherlands.

Linneman, H., J. Dehoogh, M.A. Keyzer and H.D.J. van Heemst. 1979. Moira, model of international relations in agriculture. North Holland Publishing Company, Amsterdam.

Long, S.P., Baker, N.R. and Raines, C.A. 1993. Analysing responses of photosynthetic acclimation to long elevation of atmospheric CO_2 concentration. Vegetatio 104/104 : 33-45.

Mall, R.K. 1996. Some agrometeorological aspects of wheat crop and development of yield forecast models. Ph.D thesis (unpublished), Banaras Hindu University, Varanasi, India.

Meinke, H. and G.L. Hammer. 1997. Forecasting regional crop production using SOI phases : an example for the Australian peanut industry. Aust. J. Agric. Res. 48: 789-793.

Monteith, J.L. 2000. Agricultural meteorology: Evolution and application. Agri. For. Meteorol. 103(2000) 5-9.

Morrison, J.I.L. and Lawlor, D.W. 1999. Interactions between increasing CO_2 concentration and temperature on plant growth. Plant Cell and Environment 22 : 659-682.

Muchow, R.C., Sinclair, T.R. and Bennett, J.M., 1990. Temperature and solar radiation effects on potential maize yield across locations. Agron. J. 82 : 338-343.

Murthy, V.R.K. 1999. Studies on the influence of macro and micro meteorological factors on growth and yield of soybean. Unpublished Ph.D thesis submitted to ANGRAU, Hyderabad, India.

Murthy, V.R.K. 2002. Basic principles of Agricultural Meteorology. Book syndicate publishers, Koti, Hyderabad, India.

Ong, H.T. 1982. System approach to climatology of oil palm. 1. Identification of rainfall and dry spell aspects 2. Identification of temperature and sunshine. Oleagineux 37, 93,-443.

O'Toole, J.C. and C.O. Stockle. 1987. The role of conceptual and simulation modelling in plant breeding. Presented at the Int. Symp. on Improving Winter Cereals under Temperature and Soil Salinity Stresses, 26-29 October 1987, Cordoba, Spain.

Patel, H.R., Shekh, A.M., Bapuji Rao, B., Chaudhari, G.B. and Khushu, M.K. 1999. J. of Agromet. 1(2) : 149-154.

Penning de Vries, F.W.T. 1977. Evaluation of simulation models in agriculture and biology: conclusions of a workshop. Agricultural Systems 2: 99-105.

Penning de Vries, F.W.T., A.B. Brunsting and H.H.van Laar, 1974. Products, requirements and efficiency of biological synthesis, a quantitative approach. J. Theor. Biol. 45: 339-377.

Robertson, G.W. and Foong, S.F. 1977. Weather-based yield forecasts for oil palm fresh fruit bunches. International Development in Oil Palm, ISP, Kuala Lumpur.

Shorter, R., Lawn, R.J. and Hammer, G.L. 1991. Improving genotypic adaptation in crops – a role for breeders, physiologists and modelers. Exp. Agric. 27 : 155-175.

Sinclair, T.R. 1986. Water and nitrogen limitations in soybean grain production. I. Model development. Field Crops Res. 15 : 125-141.

Sivakumar, M.V.K. and Glinni, A.F. 2002. Applications of crop growth models in the semi-arid regions. pages 177-205. *In* Agricultural System Models in Field Research and Technology Transfer (Eds. L.R. Ahuja, L. Ma and T.A. Howell), Lewis Publishers, A CRC Press Company, Boca Raton, USA.

Sivakumar, M.V.K., Gommes, R. and Baier, W. 2000. Agrometeorology and sustainable agriculture. Agric. and For. Meteorol. 103: 11-26.

Thornton, P.K., W.T. Bowen, A.C. Ravelo, P.W. Wilkens, G. Farmer, J. Brock and J.E. Brink. 1997. Estimating millet production for famine early warning: an application of crop simulation modelling using satellite and ground-based data in Burkina Faso. Agricultural and Forest Meteorology 83: 95-112.

Unsworth, M.H. and Hogsett, W.E. 1996. Combined effects of changing CO_2, temperature, UV-B radiation on crop growth. pp. 171-197. *In* Global climate change and agricultural production; direct and indirect effects of changing hydrological, pedological and plant physiological processes (Eds. F. Bazzaz and W. Sombroek). Food and Agricultural Organization, Rome and John Wiley and Sons, West Sussex, England.

Van Keulen, H. and Wolf, J. (ed). 1986. Modelling of agricultural production: weather, soils and crops. Simulation Monographs. PUDOC, Wageningen, The Netherlands.

CROP GROWTH AND PRODUCTIVITY MONITORING AND SIMULATION USING REMOTE SENSING AND GIS

V.K. Dadhwal*
Crop Inventory and Modelling Division, ARG
Space Applications Centre (ISRO)
Ahmedabad

Abstract: Crop growth and productivity are determined by a large number of weather, soil and management variables, which vary significantly across space. Remote Sensing (RS) data, acquired repetitively over agricultural land help in identification and mapping of crops and also in assessing crop vigour. As RS data and techniques have improved, the initial efforts that directly related RS-derived vegetation indices (VI) to crop yield have been replaced by approaches that involve retrieved biophysical quantities from RS data. Thus, crop simulation models (CSM) that have been successful in field-scale applications are being adapted in a GIS framework to model and monitor crop growth with remote sensing inputs making assessments sensitive to seasonal weather factors, local variability and crop management signals. The RS data can provide information of crop environment, crop distribution, leaf area index (LAI), and crop phenology. This information is integrated in CSM, in a number of ways such as use as direct forcing variable, use for re-calibrating specific parameters, or use simulation-observation differences in a variable to correct yield prediction. A number of case studies that demonstrated such use of RS data and demonstrated applications of CSM-RS linkage are presented.

INTRODUCTION

Crop growth and yield are determined by a number of factors such as genetic potential of crop cultivar, soil, weather, cultivation practices (date of sowing, amount of irrigation and fertilizer) and biotic stresses. However, generally for a given area, year-to-year yield variability has been mostly modeled

(* *Present Address* : Indian Institute of Remote Sensing, Dehra Dun 248 001, India;
email: vkdadhwal@iirs.gov.in)

Satellite Remote Sensing and GIS Applications in Agricultural Meteorology
pp. 263-289

through weather as a predictor using either empirical or crop simulation approach. With the launch and continuous availability of multi-spectral (visible, near-infrared) sensors on polar orbiting earth observation satellites (Landsat, SPOT, IRS, etc) remote sensing (RS) data has become an important tool for yield modeling. RS data provide timely, accurate, synoptic and objective estimation of crop growing conditions or crop growth for developing yield models and issuing yield forecasts at a range of spatial scales. RS data have certain advantage over meteorological observations for yield modeling, such as dense observational coverage, direct viewing of the crop and ability to capture effect of non-meteorological factors. Recent developments in GIS technology allow capture, storage and retrieval and visualization and modeling of geographically linked data. An integration of the three technologies, viz., crop simulation models, RS data and GIS can provide an excellent solution to monitoring and modeling of crop at a range of spatial scales.

In this paper an attempt is made to introduce a basic framework and indicate through specific case studies, (a) how RS data are useful in estimating crop parameters like LAI, (b) introduce crop simulation models, (c) how GIS tools are used for crop monitoring with RS data and interfaced with models, and (d) how RS-derived parameters, crop simulation models and GIS are useful for crop productivity modeling. Details on some of the above topics can be obtained from recent reviews, such as Moulin *et al.* (1998), Dadhwal (1999), Hartkamp *et al.* (1999), Dadhwal and Ray (2000), Maracchi *et al.* (2000) and Dadhwal *et al.* (2003).

LAI estimation using RS-data

The leaf area index (LAI), defined, as the total one-sided leaf area per unit ground area, is one of the most important parameters characterizing a canopy. Because LAI most directly quantifies the plant canopy structure, it is highly related to a variety of canopy processes, such as evapotranspiration, light interception, photosynthesis, respiration and leaf litterfall. RS-based LAI estimation would greatly aid the application of LAI as input to models of photosynthesis, crop growth and yield simulation models, evapotranspiration, estimation of net primary productivity and vegetation/ biosphere functioning models for large areas. A number of techniques for space borne remote sensing data have been developed/tested, ranging from regression models to canopy reflectance model inversions with varying successes, which include (1) statistical models that relate LAI to band radiance (Badhwar *et al.*, 1986) or develop LAI-vegetation index relation (Chen and Cihlar, 1996 and Myneni *et al.*,

1997), (2) biophysical models like Price (1993), and (3) inversion of canopy reflectance using numerical model or LUT based model (Gao and Lesht, 1997, Qiu *et al.*, 1998, and Knyazighin *et al.*, 1998).

Myneni *et al.* (1997) developed a simple approach for estimating global LAI from atmospherically corrected NDVI using NOAA-AVHRR data. One- or three-dimensional radiative transfer models were used to derive land cover-specific NDVI-LAI relations of the form

$$LAI = a \times \exp(b \times NDVI + c)$$

where, coefficients a and c are determined by vegetation type and soil.

Chen *et al.* (2002) have described relations using NOAA-AVHRR simple NIR/Red ratio (SR). These equations are vegetation type dependent and are being used to generate Canada wide 1 km LAI maps every 10/11 day. The equations are summarized in Table-1 and require a background SR that is season dependent as an additional input. In case of another high repetivity coarse resolution sensor, VEGETATION onboard SPOT satellite, use of SWIR channel is made to compute a new vegetation index, namely Reduced Simple Ratio (RSR). RSR reduces between vegetation and understory/background effects, thus making possible use of simplified equations for retrieval of LAI (Table-1).

Table 1. Equations for obtaining regional LAI products from atmospherically corrected data from NOAA-AVHRR and SPOT-VEGETATION (Chen *et al.*, 2002)

Sensor	Vegetation Type	Model
NOAA-AVHRR	Coniferous forest	LAI = (SR – Bc)/ 1.153
	Deciduous forest	LAI = -4.1xln[(16-SR)/(16-Bd)]
	Mixed forest	LAI = -4.45 x ln[(14.5 – SR)/(14-Bm)]
	Other (crops, scrub etc.)	LAI = -1.6 x ln{14.5 – SR) / 13.5]
SPOT-VEGETATION		LAI = RSR/1.242
		LAI = -3.86 ln (1-RSR/9.5)
		LAI = -2.93 ln (1-RSR/9.3)
		LAI = RSR / 1.3

Bc, Bd, Bm are background NDVI for coniferous, deciduous and mixed forests, respectively.

Using MODIS data, onboard TERRA (launched in Dec. 1999), it is now possible to obtain operationally generated eight-day composite 'LAI product', at a spatial resolution of 1km, which incorporates model and look-up-table based LAI retrieval algorithms (Knyazighin *et al.*, 1999) as a part of MODLAND. However, there is a need to validate this product, before it can be utilized in operational applications. Pandya *et al.* (2003) describe results of a study to develop small area LAI maps using IRS-LISS-III data using field sampling and regression approach and using the generated maps to validate MODIS LAI product. The atmospheric measurements of aerosol optical thickness and water vapour content were performed concurrently with the LAI measurements at the time of satellite acquisition and were used to convert digital numbers into the ground reflectance. These images were geo-referenced and the fields within the region of interest, where LAI measurements carried out were identified on images. Using NDVI of these fields, empirical models based on site-specific NDVI-LAI relation were developed (Figure 1) and used to generate LAI maps for each acquisition and study site. The LAI images were aggregated to 1km spatial resolution and compared with MODIS LAI product and results indicated significant positive correlation between LAI derived from LISS-III data and MODIS data albeit with a positive bias, in the MODIS product (Figure 2).

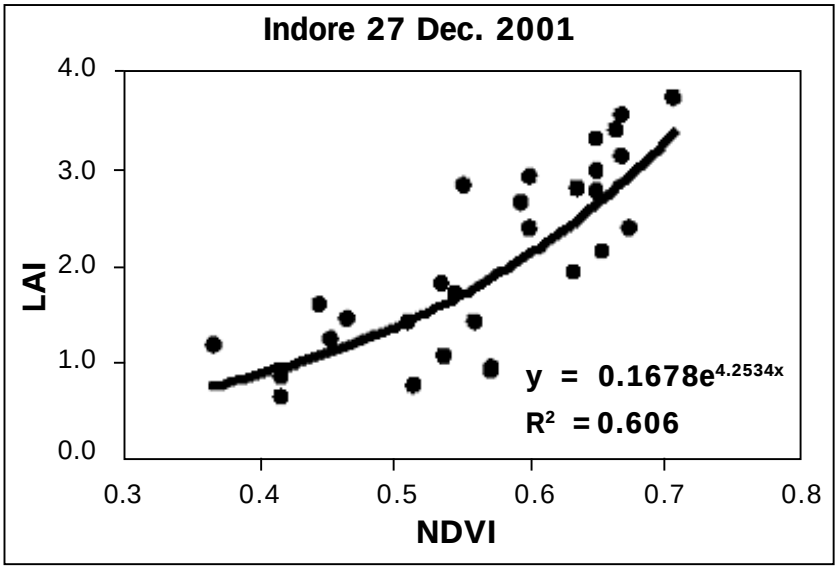

Figure 1: Relationship of ground measured LAI on wheat fields with IRS LISS-III derived NDVI at Indore (Madhya Pradesh, India) (Pandya *et al.*, 2003)

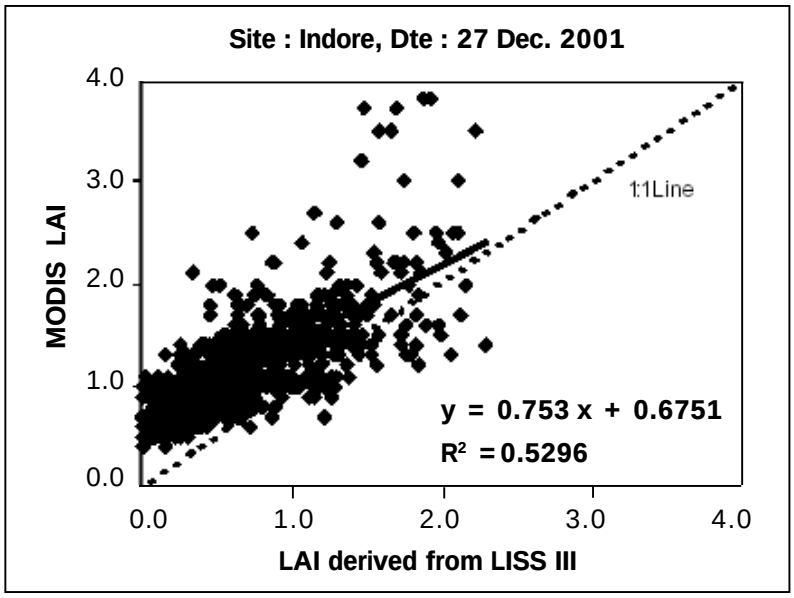

Figure 2: Comparison between LISS-III derived LAI and MODIS LAI at Indore (MP, India) (source: Pandya *et al.*, 2003)

Rastogi *et al.* (2000) tested Price model on farmers fields during 1996-97 season in Karnal (Haryana, India) and 1997-98 in Delhi using IRS LISS-III data and estimated wheat attenuation coefficients. The root mean square error (RMSE) between RS estimates and ground measured LAI ranged between 0.78-0.87 when LAI was in the range of 1-4, while for higher LAI range (4-6), the RMSE varied from 1.25 to 1.5 in two sites. Such errors can severely reduce utility of a model using field-level LAI as input.

Crop simulation models

Crop simulations models are based on physical plant processes and simulate the effects of change in growing environment on plant growth and development on a daily basis. A crop simulation model is a simple representation of a crop and is explanatory in nature. The processes essentially modeled are phenology, photosynthesis and dry matter production, dry matter partitioning, in simulation models aimed at potential production. Those aiming at crop-specific behaviour include modules for phyllochron, branching pattern and potential flowers/ grain filling sites. The response to water and nutrition limited environment is added by introducing models of soil water balance and uptake and transpiration by crop, and nitrogen transformations in soil, uptake and

remobilization within plant, respectively. Models of effects of weeds and pests are being developed and could be available in new generation of crop simulation models.

In dynamic crop simulation models, three categories of variables recognized are, state, rate and driving variables. The state variables are quantities like biomass, amount of nitrogen in soil, plant, soil water content, which can be measured at specific times. Driving variables, or forcing functions, characterize the effect of the environment on the system at its boundaries, and their values must be monitored continuously, e.g., meteorological variables. Each state variable is associated with rate variables that characterize their rate of change at a certain instant as a result of specific processes. These variables represent flow of material or biomass between state variables. Their value depends on the state and driving variables according to rules that are based on knowledge of the physical, chemical and biological processes that take place during crop growth.

Under the International Benchmark Sites Network for Agrotechnology Transfer (IBSNAT) project a computer software package called the Decision Support System for Agrotechnology Transfer (DSSAT) was developed which integrates 11 crop simulation models (CERES cereal, CROPGRO legume and other models) with a standardized input and output (Jones, 1993) and has been evaluated/ used in a number of countries. Use of CERES-Wheat included in DSSAT for regional wheat yield prediction has been demonstrated recently in India (Nain *et al.*, 2004).

GIS AND ITS USE FOR CROP MONITORING

Introduction to GIS

Burrough and McDonnell (1998) has defined GIS as a powerful set of tools for collecting, storing, retrieving at will, transforming and displaying spatial data from the real world for a particular set of purposes. The three major components of GIS are (i) computer hardware, (ii) computer software and (ii) digital geographic data. The information stored within a GIS is of two distinct categories. The spatially referenced information that can be represented by points, lines, and polygons, that are referenced to a geographic coordinate system and is usually stored in either raster (grid-cell) or vector (arc-node) digital format. The second category of information stored in a GIS is attribute data or information describing the characteristics of the spatial feature.

Using RS & GIS for crop monitoring

The use of GIS along with RS data for crop monitoring is an established approach in all phases of the activity, namely preparatory, analysis and output. In the preparatory phase GIS is used for (a) stratification/zonation using one or more input layers (climate, soil, physiolgraphy, crop dominance etc.), or (b) preparing input data (weather, soil and collateral data) which is available in different formats to a common format. In the analysis phase use of GIS is mainly through operations on raster layers of NDVI or computing VI profiles within specified administrative boundaries. The final output phase also involves GIS for aggregation and display of outputs for defined regions (e.g., administrative regions) and creating map output products with required data integration through overlays.

Wade *et al.* (1994) described efforts within National Agricultural Statistics Service (NASS) of U.S. Department of Agriculture (USDA) of using NOAA AVHRR NDVI for crop monitoring and assessment of damage due to flood and drought by providing analysts a set of map products. Combining satellite data in a GIS can enhance the AVHRR NDVI composite imagery by overlaying State and county boundaries. The use of raster-based (grid-cell) capabilities of ARC/INFO (GRID) for the generation of difference image helps compare a season with previous year or average of a number of years. Overlaying a crop mask helps in highlighting only effects on crops. Application of frost isolines is made to help analysts to locate average dates of the first frost for possible crop damage. Generation and overlay of contours of precipitation data generated using TIN function of ARC/INFO also is an aid to interpreting NDVI difference image.

Interfacing crop simulation models to GIS

Crop simulation models, when run with input data from a specific field/ site, produce a point output. The scope of applicability of these simulation models can be extended to a broader scale by providing spatially varying inputs (soil, weather, crop management) and policy combining their capabilities with a Geographic Information System (GIS). The main purpose of interfacing models and GIS is to carry out spatial and temporal analysis simultaneously as region-scale crop behaviour has a spatial dimension and simulation models produce a temporal output. The GIS can help in spatially visualizing the results as well as their interpretation by spatial analysis of model results.

While GIS and modeling tools have existed for so long, the integration, including the conceptual framework is being given attention only recently. Hartkamp *et al.* (1999) have reviewed GIS and agronomic modeling and suggested that 'interface' and 'interfacing' be used as umbrella words for simultaneously using GIS and modeling tools, and 'linking', 'combining' and 'integrating' as suitable terminology for degree of interfacing. These correspond to loose, tight and embedded coupling, respectively, as used by Burrough (1996) and Tim (1996). While there is a continuum between linking and combining, the terms are explained below:

(a) Linking: Simple linkage strategies use GIS for spatially displaying model outputs. A simple approach is interpolation of model outputs. An advanced strategy is to use GIS functions (interpolation, overlay, slope, etc.) to produce a database containing inputs of the model and model outputs are also exported to the same database. Communication between GIS and model is through identifiers of grid cells or polygons in input and output files, which are transferred in ascii or biary format between GIS and model (Figure 3a). Such an approach is not able to utilize full potential of the system and suffers from limitation due to (a) dependence on formats of GIS and model, (b) incompatibility of operating environments and (c) not fully utilizing the capabilities of GIS.

(b) Combining: Combining also involves processing data in a GIS and displaying model results, however, the model is configured with GIS and data are exchanged automatically. This is done with facilities in GIS package of macro language, interface programmes, libraries of user callable routines (Figure 3b). This requires more complex programming and data management than simple linking. Example of combining is AEGIS (Agricultural and Environmental GIS) with ArcView (Engel *et al.*, 1997).

(c) Integrating: Integration implies incorporating one system into the other. Either a model is embedded in GIS or a GIS system is included in a modeling system. This allows automatic use of relational database and statistical packages (Figure 3c). This requires considerable expertise, effort and understanding of the two tools.

Calixte *et al.* (1992) developed a regional agricultural decision support system, known as Agricultural and Environmental Geographic information System (AEGIS) that uses the DSSAT capabilities within ARC/INFO GIS for regional planning and productivity analysis. AEGIS allows the user to select

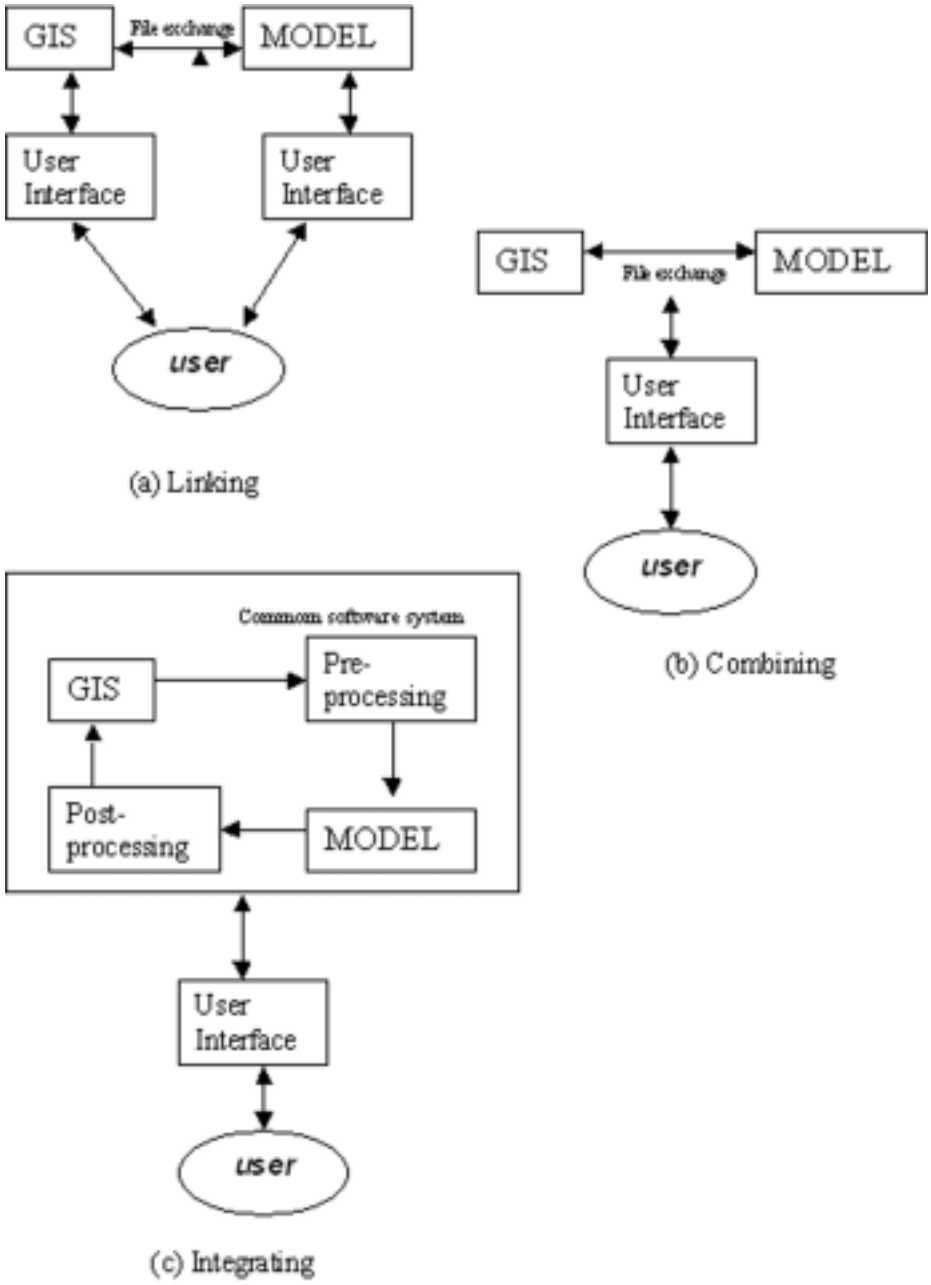

Figure 3: Organizational structure for (a) linking, (b) combining and (c) integrating GIS and crop models (Hartkamp *et al.*, 1999)

various combinations of crop management practices over space and evaluate potential crop production. Engel *et al.* (1997) modified the AEGIS into AEGIS/WIN (AEGIS for Windows) written in Avenue, an object-oriented macro scripting language, which links the DSSAT (Version 3) with the geographical mapping tool ArcView-2. Thornton *et al.* (1997a) developed spatial analysis software for the most recent release of the DSSAT, Version 3.1. This software standardized the links between crop models and GIS software and this allowed developers to make use of whatever GIS software is most suitable for a particular purpose, while ensuring that basic links to the DSSAT system and the crop models are the same. The spatial analysis software has two modules: (i) a geostatistical module to interpolate maps and produce probability surfaces from a network of data points, and (ii) a utility that calculates agronomic and economic output statistics from model simulations and maps the results as polygons. Another effort is development of a SPATIAL-EPIC linked to Arc/Info (Satya *et al.*, 1998).

Demonstrated applications of CSM interfaced with GIS

Current wide range of applications of interfacing of GIS and modelling are reviewed by Hartkamp *et al.* (1999) and covers spatial yield calculation (regional and global), precision farming, climate change studies, and agro-ecological zonation, etc.

CGMS (Crop Growth Monitoring System) of MARS (Monitoring Agriculture with Remote Sensing)

This project of European Union uses WOFOST model and Arc/Info for operational yield forecasting of important crops (Meyer-Roux and Vossen, 1994). The Crop Growth Monitoring System (CGMS) of the MARS integrates crop growth modelling (WOFOST), relational batabase ORACLE and GIS (ARC/INFO) with system analytical part for yield forecasting (Bouman *et al.*, 1997). There are databases on soil, weather, crop, and yield statistics that cover the whole of EU. The system-analytical part consists of three modules: agrometeorological module, a crop growth module and a statistical module. The meteorological module takes care of the processing of daily meteorological data that are received in real time to a regular grid of 50x50 km for use as input by crop growth model or for assessment of 'alarm' conditions. The crop growth module consists of the dynamic simulation model WOFOST in which crop growth is calculated and crop indicators are generated for two production levels: potential and water-limited. In CGMS, WOFOST is run on a daily bases for each so-called 'simulation unit', i.e. a unique combination of weather,

soil, and crop (mapping) units. In the statistical module, crop indicators (total above ground dry weight and dry weight storage organs) calculated with WOFOST are related to historical yield statistics through regression analysis in combination with a time-trend, for at least 15 years of simulated and historical data (Vossen, 1995). The resulting regression equations per crop per region are used to make actual yield forecast. CGMS generates on a 10 day and monthly basis three types of output on current cropping season: (i) Maps of accumulated daily weather variables on 50x50 km grid to detect any abnormalities, e.g. drought, frost, (ii) Maps of agricultural quality indicators based on comparison of simulated crop indicators with their long-term means, (iii) Maps and tables of yield forecasts.

Precision Farming

Han *et al.* (1995) developed an interface between PC ARC/INFO GIS and SIMPOTATO simulation model to study potato yield and N leaching distribution for site-specific crop management (precision farming) in a 50 ha field. The GIS input layers, corresponding to important distributed input parameters for the model, were irrigated water/N layer, soil texture layers and initial soil N layers. For each unique sub-area stored in the GIS database, the interface program extracts the attribute codes of that sub-area from the GIS database, converts the attribute codes to the input parameters of the SIMPOTATO and sends them to the model. After running the model, the interface program retrieves the output data (potato yield and N leaching), converts them to the attribute codes and stores the output data in the GIS database.

Agro-ecological Zonation

Aggarwal (1993) used WTGROWS to simulate potential and water-limited wheat yields for 219 weather locations spread all over the country. The district boundaries (as polygons) and model input parameters of soil, weather stations and agro-ecological regions were stored in ARC/INFO GIS. The model outputs of potential and rainfed productivity were stored in GIS as polygon attribute data. Based on potential and rainfed productivity, the districts were classified into 10 iso-yield zones and represented as map using GIS.

Evaluating Agricultural land use options

Aggarwal *et al.* (1998) studied the agricultural land use option for the state of Haryana using symphonic use of expert knowledge, simulation

modelling, GIS and optimization techniques. The study area was divided into agro-ecological land units by overlaying maps of soil, soil organic carbon and climatic normal rainfall in raster GIS IDRISI. The original soil mapping units based on 19 soil properties were reclassified based on soil texture, level and extent of salinity and sodicity, slope and ground water depth. The organic carbon and normal rainfall maps were generated by inverse square interpolation of observed data points followed by segmentation. The CSM for specific crops have been linked to GIS layers of administrative boundaries, physiographic features, climate, soil and agroclimatic zones and GCM outputs to study effect of future climatic changes on crop potential / productivity (Bacsi *et al.*, 1991; Carter and Saarikko, 1996).

LINKING CROP SIMULATION MODELS TO RS INPUTS & GIS

The use of remotely sensed information to improve crop model accuracy was proposed as early as two decades ago by Wiegand *et al.* (1979) and Richardson *et al.* (1982). They suggested using spectrally derived LAI either as direct input to physiological crop model or as an independent check to model calculation for its re-initialization. The main advantage of using remotely sensed information is that it provides a quantification of the actual state of crop for large area using less labour and material intensive methods than *in situ* sampling. While crop models provide a continuous estimate of growth over time, remote sensing provides a multispectral assessment of instantaneous crop condition with in a given area (Delecolle *et al.*, 1992).

The different ways to combine a crop model with remote sensing observations (radiometric or satellite data) were initially described by Maas (1988a) and this classification scheme was revised by Delecolle *et al.* (1992) and by Moulin *et al.* (1998). Five methods of remote sensing data integration into the models have been identified:

(a) the direct use of a driving variable estimated from RS data in the model;

(b) the updating of a state variable of the model (e.g., LAI) derived from RS ('forcing' strategy);

(c) the re-initialization of the model, i.e., the adjustment of an initial condition to obtain a simulation in agreement with the RS derived observations;

(d) the re-calibration of the model, i.e., the adjustment of model parameters to obtain a simulation in agreement with the remotely-sensed derived observations, also called 're-parameterization' strategy;

(e) the corrective method, i.e., a relationship is developed between error in some intermediate variable as estimated from remotely sensed measurement and error in final yield. This relationship may be applied to a case in which final yield is not known.

Direct use of driving variable

The driving variables of crop simulation models are weather inputs comprising daily observations of maximum and minimum temperature, solar radiation, relative humidity, and wind speed as a minimal subset. In a recent review on this subject, Moulin *et al.* (1998) cited inadequate availability of RS-derived parameters, due to cloud cover problem and intrinsic properties of sensors and platforms, as a major drawback, for adoption of this approach. However, this is a promising area, given the sparse distribution of weather observational network and recent progress in deriving some of these variables from sensors in space. Rainfall, solar radiation and intercepted/absorbed PAR have received maximum attention.

Maas (1988a) estimated the ratio of daily absorbed PAR (Q) to integrated daily PAR (R) from radiometric NDVI and generated daily values of Q/R by linear interpolation between NDVI measurements for use as driving variable in a simplified maize growth model. The model showed an overestimation of 6.2% in above ground biomass at anthesis. METEOSAT based decadal (10-day) rainfall using cold cloud duration has been used as input to CERES-Millet in Burkina Faso by Thornton *et al.* (1997b) to forecast provincial millet yields halfway through crop duration to within 15% of their final values.

Forcing strategy

The forcing strategy consists of updating at least one state variable in the model using remote sensing data. LAI has been the most commonly updated state variable. The concept of a simple crop simulation model and its modification for RS-derived LAI forcing is illustrated in Figure 4. Some examples of forcing spectrally derived LAI in crop simulation models are summarized in Table-2. The forcing could either be done only on day of RS observation (Maas, 1988a) or daily LAI profile is generated using some simple parametric model for use (Delecolle and Guerif, 1988).

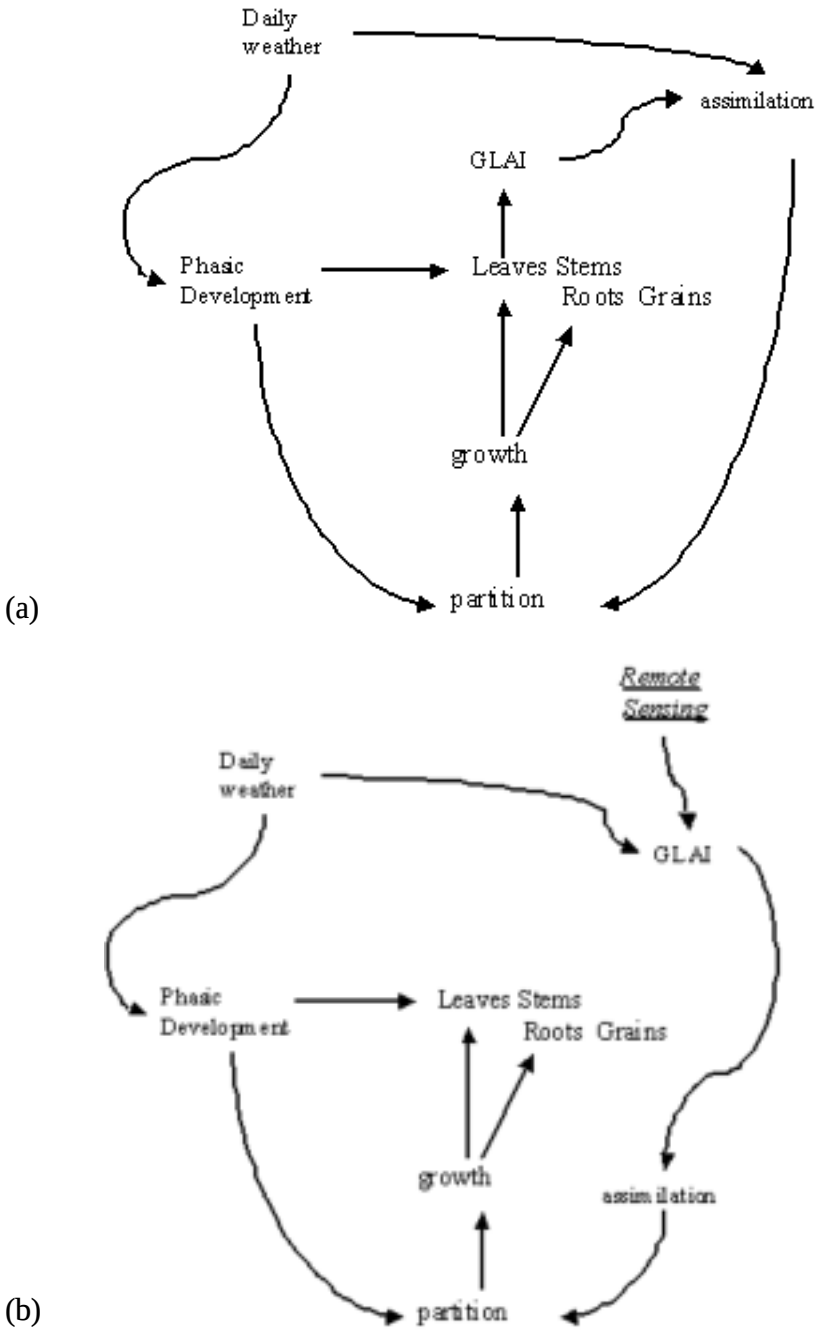

Figure 4: (a) Simple schematic of a crop simulation model. (b). Modified structure of crop simulation model with RS-based LAI forcing (Delecolle and Guerif, 1988)

Table 2. Selected case studies on use of RS-derived LAI for forcing crop simulation models

Crop	Model	LAI estimation & interfacing	Evaluation of performance	Reference
Maize	-	Ground NDVI-LAI on obs. Dates	AGDM estimation improved	[1]
Wheat	AFRCWHEAT	SPOT/HRV LAI-WDVI relation: Daily interpolated LAI	Yield RMSE decreased	[2]
Wheat	SUCROS	LAI-WDVI	Biomass at harvest	[3]

[1] Maas, 1988a; [2] Delecolle and Guerif, 1988; [3] Bouman, 1995

Re-initialization strategy

The re-initialization method takes advantage of the dependence of model performance on state variable initial condition. It involves adjustment of initial condition of state variable so as to minimize the difference between a derived state variable or the radiometric signal and its simulation. Maas (1988a) in his simplified maize model adjusted the initial value of LAI (L0) at emergence based on the minimization of an error function between remotely sensed LAI values and simulated LAI values during the course of simulation. Re-initialization using one observation produced results similar to updating (forcing). However, the stability of model estimates obtained through re-initialization increased as more observations were used. The observation at 51 days after emergence, which caused a 42% error using updating, resulted in less than a 3% error using re-initialization. Maas (1988b) demonstrated a similar study for sorghum using satellite observations. The simulation model was developed and verified using 10 fields in Central Texas in 1976 and the re-initialization approach was validated for the 37 fields in South Texas using Landsat MSS data and agronomic observations. Without using the initialization procedure, the average yield for the 37 fields was underestimated by 30%. Use of satellite derived green LAI data to initialize the same simulations resulted in a 2% overestimation of average yield.

Re-calibration/re-parameterization strategy

In this approach it is assumed that model is formally adequate but requires re-calibration. This is achieved by minimizing error between RS-derived state

variable and its simulation by the model. This makes such an approach sensitive to errors in deriving state variables from RS data. In this case also, the state variable matched is LAI. However, depending on the model structure, which parameter to tune and number of observations used in analysis is critical.

Maas (1988a) demonstrated the re-calibration for maize model with remotely sensed GLAI observations. A multi-dimensional error function minimization procedure was used which indicated more consistent estimates of LAI and biomass at anthesis as the number of parameters increased in multi-dimensional re-parameterization.

Delecolle *et al.* (1992) illustrated the use of re-calibration for rice crop using GRAMI model. Values of one to four parameters in the GRAMI model were re-calibrated to match the simulated LAI profile to observed LAI values. The results showed that improvement in simulated LAI profile by re-calibration depends largely on the number and timing of LAI observations. Clevers and Leeuwen (1996) used ground and airborne radiometric measurements over sugar beet fields to calibrate the SUCROS model. They derived LAI from measurements in optical and microwave wavebands. The adjusted parameters and initial conditions were sowing date, a growth rate, light use efficiency and maximum leaf area. The results showed that re-calibration with both optical and microwave observations estimated yield better than optical data alone. In the absence of optical remote sensing data, radar data yielded a significant improvement in yield estimation with the case of no remotely observed observations. Inoue *et al.* (1998) related paddy vegetation indices to the fraction of absorbed photosynthetically active radiation (fAPAR) as exponential equations with different parameters for the periods before and after heading. A real time recalibration module based on a simplex algorithm was developed and proved effective in linking remotely sensed fAPAR with a simple rice growth model.

Re-parameterization using Coupled Crop Simulation Models and Canopy-radiation Models

The re-initialization and re-parameterization of crop models can also make direct use of radiometric information instead of deriving canopy parameters from them (Moulin *et al.*, 1998). In this strategy, coupling a radiative transfer reflectance model to the crop production model reproduces the temporal behaviour of canopy surface reflectance, which can be compared with canopy reflectance observed from satellite. Adjusting initial conditions or model

parameters carries out the minimization of differences between the simulated and observed reflectance values.

Such an approach has been used by Clevers *et al.* (1994) and Guerif and Duke (1998) for sugarbeet. The LAI simulated by SUCROS on dates of spectral observations was passed on to PROSPECT-SAIL and SAIL model, respectively, and parameters of SUCROS model adjusted to minimize differences between observed WDVI and simulated WDVI. The re-parameterization of SUCROS reduced yield prediction errors. This approach was extended to microwave RS by Bouman *et al.* (1999) who simulated radar backscatter of agricultural crops (sugar beet, potato, winter wheat) by integrating LAI and leaf moisture from SUCROS with top soil moisture content by soil water balance model (SAHEL) and radar backscatter model (CLOUD).

Since canopy-radiation models such as SAIL have parameters in addition to LAI, their uncertainty could affect the results from this approach. Moulin and Guerif (1999) concluded that the error in canopy reflectance estimates as a result of omitting data on canopy leaf angle and soil reflectance, two parameters in SAIL model, is so large that direct use of simulated canopy reflectance in simulation models for yield prediction is severely affected. However, the use of vegetation indices drastically reduced the errors linked to crop structure (NDVI) and to soil reflectance (TSAVI).

Corrective approach

Sehgal *et al.* (2001b) used this strategy for generating the wheat yield maps for farmers' fields during rabi 1998-99 in Alipur block (Delhi). The RS inputs as estimated LAI were linked to wheat simulation model WTGROWS for yield mapping and results were validated with yield observations on farmers' fields. Biometric relation of grain yield and leaf area index (LAI) is derived from simulation model by running model for a combination of input resources, management practices and soil types occurring in the area. Then this biometric relationship is applied to all the crop fields of the study area for which the LAI is computed from remote sensing data. The WTGROWS simulated grain yield for the combination of inputs showed yields varying between 1.1 and 4.9 t ha^{-1}. The corresponding range of simulated LAI on 27 Jan 1999 was 0.6 to 4.2. The regression equation fitted between simulated LAI on 27th Julian day (i.e. 27-January-99) and simulated grain yield showed saturating logarithmic nature with a R^2 value of 0.81. The relationship is given below:

Yield (kg/ha) = 1571.2 * ln(LAI) + 2033.6 …[2]

This empirical biometric relation was applied to the LAI map of the wheat pixels and grain yield map for farmer's fields of Alipur block, Delhi, was generated. The predicted yields ranged from 2.1 to 4.8 tha^{-1}. The comparison of predicted grain yield and observed yield for the 22 farmers' fields showed high correlation coefficient of 0.8 and a root mean square error (RMSE) of 597 kg ha^{-1} which was 17 per cent of the observed mean yield (Figure 5).

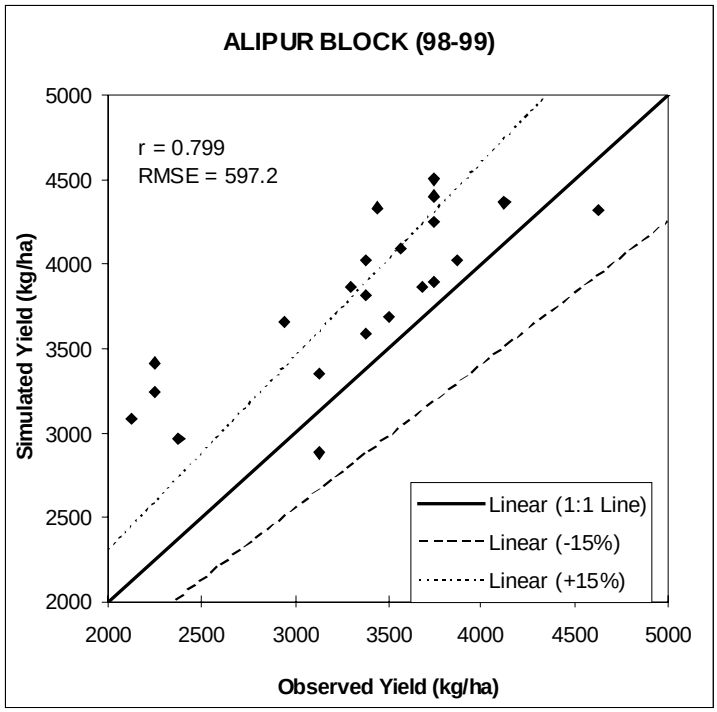

Figure 5: Comparison of predicted grain yield by modified corrective approach and observed values for 22 farmers' fields. The 1:1 line and its ±15 per cent band lines are also shown (Sehgal *et al.*, 2001b)

Development of a RS-based CGMS for wheat in India

Sehgal *et al.* (2001a) reported the development of a prototype Crop Growth Monitoring System (CGMS) for wheat using WTGROWS simulation model on a 5'x5' grid in GIS environment for generating daily crop growth maps and predicting district-wise grain yield. The inputs used were RS based wheat distribution map, daily weather surfaces, soil properties map and crop

management input databases in a GIS environment and analysis for wheat season of 1996-97 was carried out. The inputs, their processing in GIS and framework for CGMS are summarized in Figure 6. The grid-wise final simulated grain yields are shown in Figure 7. The figure clearly indicates spatial patterns in yield variability. The high grain yields in Kurukshetra and Karnal and low yields in Bhiwani, Rohtak, Yamunanagar and Ambala are brought out clearly. The comparison of simulated grain yields aggregated at district level and estimates by the State Department of Agriculture is shown in Figure 8. In general, the model simulated yields were higher than observed. This could be due to a number of yield reducing factors such as pest, weed, soil constraints, which operate in field but are not considered by the model. The model predicted yields were within ±10% of reported yields in 12 out 16 districts. The RMSE of 335.4 kg ha^{-1}, which is less than 10 per cent of the State mean yield, was obtained. Only in two districts, Mahendragarh and Bhiwani, the simulated district yields were lower than observed yields while for Kaithal, Karnal, Ambala and Yamunanagar, the simulated yields were higher than observed yields by more than 10 per cent.

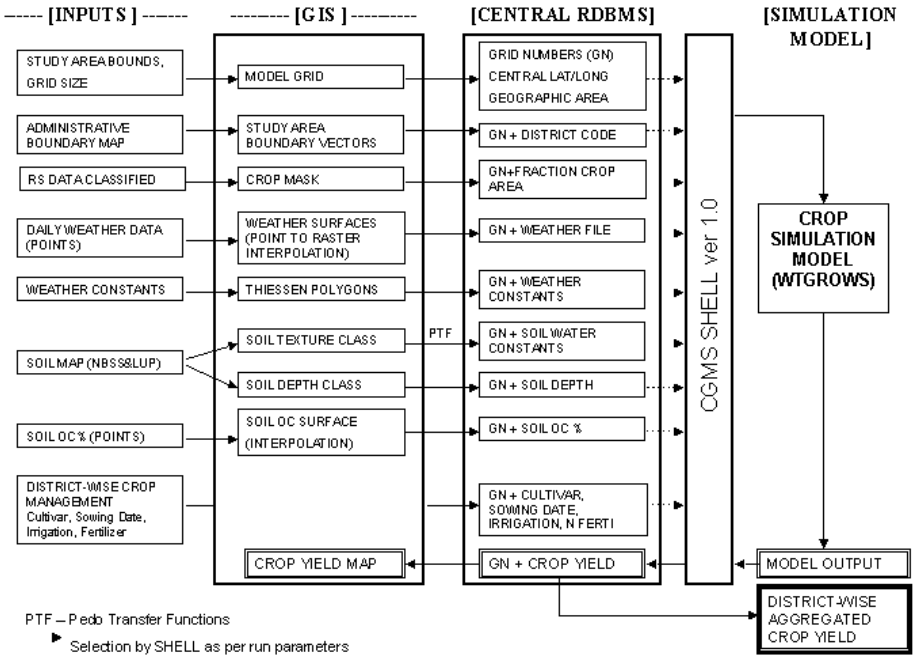

Figure 6. Schematic diagram of a crop growth monitoring system showing the linkages between inputs, spatial layers in GIS, and relational database to WTGROWS simulation model (Sehgal *et al.*, 2001a)

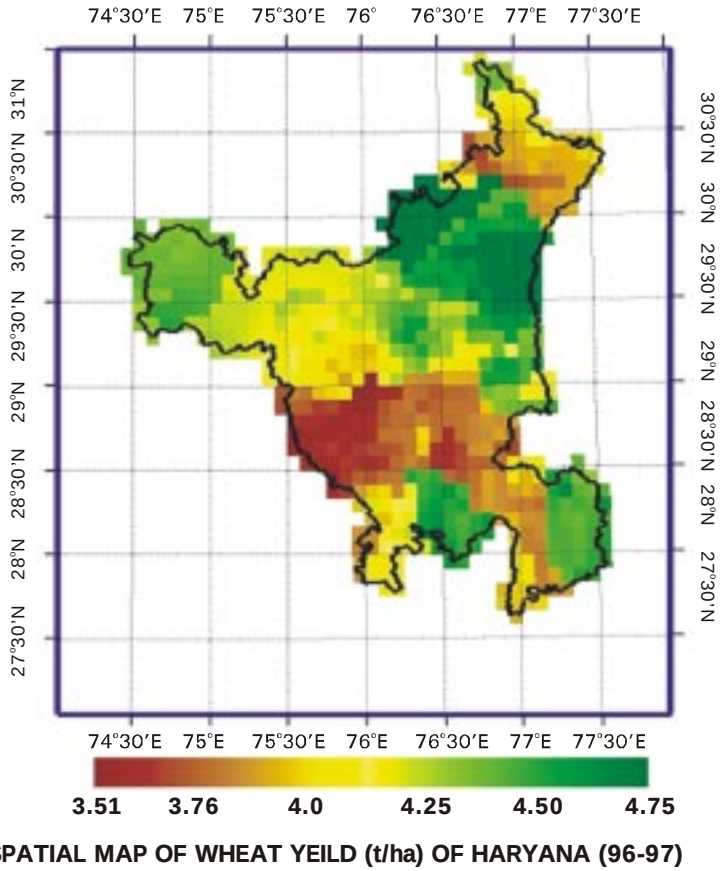

Figure 7: Grid-wise simulated wheat yields by WTGROWS simulation model for 1996-97 season in Haryana (Sehgal *et al.*, 2001a)

Sehgal *et al*. (2002) demonstrated a technique for estimating date of sowing (DOS) using RS-derived spectral-temporal crop growth profiles and CGMS simulation capability and evaluated the capability of CGMS for spatial yield mapping and district level yield prediction for Haryana State during 2000-01 crop season. The technique for estimating district-wise DOS matched the RS-derived date of peak NDVI (from multi-date WiFS sensor aboard IRS-1D satellite) to date of peak LAI simulated in CGMS for a range of plausible dates of sowing (Figure 9). The peak date of NDVI was computed by fitting Badhwar model to the multi-date NDVI values. The CGMS performance was evaluated by incorporating RS-derived date of sowing in predicting district level wheat yields with and without use of district-wise N fertilizer application

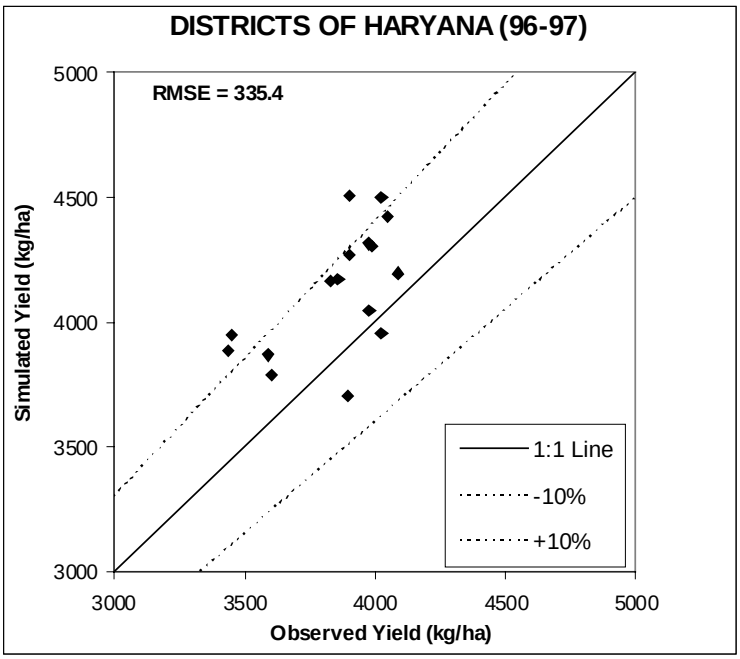

Figure 8: Comparison of simulated district wheat yields by CGMS with observed values reported by the State Department of Agriculture, Haryana , for 1996-97 season. The 1:1 line and its ±10 per cent band lines are also shown (Sehgal *et al.*, 2001a)

rate computed from district-wise fertilizer consumption statistics. The correlation between district yield simulated by CGMS and official State Department of Agriculture (SDA) estimates was only 0.163 when constant median/mean inputs of DOS, N fertilizer and irrigation application were specified for all the districts. The correlation increased to 0.52 when RS-CGMS-derived district-wise DOS was used as input and further increased to 0.74 when information from consumption statistics of N fertilizer use was additionally specified.

It is clear from the above studies that the potential of integrating crop simulation model, RS inputs and GIS has been well proven in a number of case studies. While techniques for geophysical and crop biophysical parameter retrieval are becoming available and producing products of required accuracy, the available crop simulation models need to be provided with GIS integration and iterative run options to benefit from this integration.

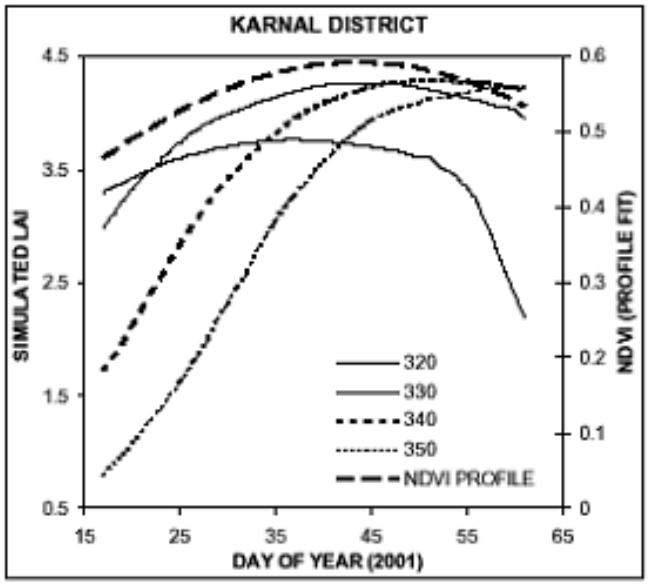

Figure 9: An illustration for obtaining date of sowing (DOS) for Karnal district by matching date of simulated LAI peak with date of fitted NDVI profile peak (Tmax). Different simulated LAI curves correspond to various dates of sowing (320 to 350) in year 2000 (Sehgal *et al.*, 2002)

CONCLUSIONS

Remote sensing data provide a complete and spatially dense observation of crop growth. This complements the information on daily weather parameters that influence crop growth. RS-crop simulation model linkage is a convenient vehicle to capture our understanding of crop management and weather with GIS providing a framework to process the diverse geographically linked data. Currently RS data can regularly provide information on regional crop distribution, crop phenology and leaf area index. This can be coupled to crop simulation models in a number of ways. These include, (a) direct use of RS inputs as forcing variable, (b) re-initializing or re-calibrating CSM so that its outputs of LAI match RS observations, and (c) using simulation model to estimate impact of variation in a state variable (e.g. LAI) and final yield and using CSM-RS differences to modeling yield predictions. These approaches have been demonstrated through case studies on wheat in India at different spatial scales (village, grid and district). CSM-RS linkage has a number of applications in regional crop forecasting, agro-ecological zonation, crop suitability and yield gap analysis and in precision agriculture.

In future the RS-CSM linkage will be broadened due to improvements in sensor capabilities (spatial resolution, hyper-spectral data) as well as retrieval of additional crop parameters like chlorophyll, leaf N and canopy water status. Thermal remote sensing can provide canopy temperatures and microwave data, the soil moisture. The improved characterization of crop and its growing environment would provide additional ways to modulate crop simulation towards capturing the spatial and temporal dimensions of crop growth variability.

REFERENCES

Aggarwal, P.K. 1993. Agro-ecological zoning using crop growth simulation models: characterization of wheat environments of India, pages 97-109. In: Systems Approaches for Agricultural Development, Vol. 2. (Penning de Vries, F.W.T., Teng, P. and Metselaar, K. eds.), Kluwer Academic Publishers, Dordrecht, The Netherlands.

Aggarwal, P.K., Kalra, N., Bandhyopadhyay, S.K., Pathak, H., Sehgal, V.K., Kaur, R., Rajput, T.B.S., Joshi, H.C., Choudhary, R. and Roetter, R. 1998. Exploring agricultural land use options for the State of Haryana: Biophysical modelling, pages 59-65. In: Exchange of methodologies in land use planning (Roetter, R., Hoanh, C.T., Luat, N.V., van lttersum, M.K. and van Laar, H.H. eds.), SysNet Research Paper Series No. 1, IRRI, Los Banos, Philippines.

Bacsi, Z., Thorton, P.K. and Dent, J.B. 1991. Impacts of future climate change on Hungarian crop production: An application of crop growth simulation models. Agric. Sys., 37: 435-450.

Badhwar, G. D., MacDonald, R.B., and Mehta, N.C. 1986. Satellite-derived LAI and vegetation maps as input to global cycle models-a hierarchical approach. Int. J. Remote Sensing, 7: 265-281.

Bouman, B.A.M. 1995. Crop modelling and remote sensing for yield prediction. Netherland J. Agric. Sci., 43: 143-161.

Bouman, B.A.M., van Dipen, C.A., Vossen, P. and van Der Wal, T. 1997. Simulation and systems analysis tools for crop yield forecasting, pages 325-340. In: Applications of Systems Approaches at the Farm and Regional Levels, Vol. 1. (Teng, P.S., Kropff, M.J., ten Berge, H.F.M., Dent, J.B., Lansigan, F.P. and van Laar, H.H. eds.), Kluwer Academic Publishers, Dordrecht, The Netherlands.

Bouman, B.A.M., van Kraalingen, D.W.G., Stol, W. and van Leeuwen, H.J.C. 1999. An ecological modeling approach to explain ERS SAR radar backscatter of agricultural crops. Remote Sens. Environ., 67: 137-146.

Burrough, P.A. and McDonnell, R.A. 1998. Principles of geographic information systems. Oxford University Press, Oxford, UK, pp. 10-16.

Burrough, P.A. 1996. Environmental modelling with geographical information system, pages 56-59. In: Models in Action, Quantitative Approaches in Systems Analysis (Stein, A., Penning de Vries, F.W.T. and Schotman, P.J. eds.), No 6, AB-DLO, Wageningen, The Netherlands.

Calixte, J.P., Beinroth, F.J., Jones, J.W. and Lai, H. 1992. Linking DSSAT to a geographic information system. Agrotechnology Transfer, 15: 1-7.

Carter, T.R. and Saariko, R.A. 1996. Estimating regional crop potential in Finland under a changing climate. Agric. For. Meteorol., 79: 301-313.

Chen, J.M. and Cihlar, J. 1996. Retrieving leaf area index of boreal conifer forests using Landsat TM images. Remote Sens.Environ., 55: 153-162.

Chen, J.M., Pavlic, G., Brown, L., Cihlar, J., Leblanc, S.G., White, H.P., Hall, R.J., Peddle, D.R., King, D.J., Trofymow, J.A., Swift, E., Van der Sanden, J., Pellikka, P.K.E. 2002. Derivation and validation of Canada-wide coarse-resolution leaf area index maps using high-resolution satellite imagery and ground measurements. Remote Sens. Environ., 80: 165-184.

Clevers, J.G.P.W., Buker, C., van Leeuwen, H.J.C. and Bouman, B.A.M. 1994. A framework for monitoring crop growth by combining directional and spectral remote sensing information. Remote Sens. Environ., 50: 161-170.

Clevers, J.G.P.W. and van Leeuwen, H.J.C. 1996. Combined use of optical and microwave remote sensing data for crop growth monitoring. Remote Sens. Environ., 56: 42 - 51.

Dadhwal, V.K. 1999. Remote Sensing and GIS for agricultural crop acreage and yield estimation. Internat. Arch. Photogramm. & Remote Sensing, XXXII, 7-W9, 58-67.

Dadhwal, V.K. and Ray, S.S. 2000. Crop Assessment using remote sensing – Part II: Crop condition and yield assessment. Indian J. Agric. Economics, 55 (2, Suppl.), 55-67.

Dadhwal, V.K., Sehgal, V.K., Singh, R.P. and Rajak, D.R. 2003. Wheat yield modeling using satellite remote sensing with weather data: Recent Indian experience. Mausum, 54(1): 253-262.

Delecolle, R. and Guerif, M. 1988. Introducing spectral data into a plant process model for improving its prediction ability. Proceedings of the 4th International Colloquium Signatures Spectrales d'Objects en Teledetection, 18-22 Jan, 1988, Aussois, France, pp. 125-127.

Delecolle, R., Maas, S.J., Guerif., M. and Baret, F. 1992. Remote sensing and crop production models: present trends. ISPRS J. Photogramm. Remote Sens., 47:145-161.

Engel, T., Hoogenboom, G., Jones, J.W. and Wilkens, P.W. 1997. AEGIS/WIN - a program for the application of crop simulation models across geographic areas. Agronomy J., 89: 919-928.

Gao, W. and Lesht, B.M. 1997. Model inversion of satellite measured reflectances to obtain surface biophysical and bi-directional reflectance characteristics of grassland. Remote Sens. Environ., 59: 461-471.

Guerif, M. and Duke, C. 1998. Calibration of SUCROS emergence and early growth module for sugar beet using optical remote sensing data assimilation. European J. Agronomy, 9: 127-136.

Han, S., Evans, R.G., Hodges, T. and Rawlins, S.L. 1995. Linking geographic information system with a potato simulation model for site-specific crop management. J. Environ. Qual., 24: 772-777.

Hartkamp, D.A., White, J.W. and Hoogenboom, G. 1999. Interfacing geographic information systems with agronomic modeling: A review. Agron. J., 91: 761-772.

Horie, T., Yajima, M. and Nakagawa, H. 1992. Yield forecasting. Agric. For. Meteorol., 40: 211-236.

Inoue, Y., Moran, M.S. and Horie, T. 1998. Analysis of spectral measurements in paddy field for predicting rice growth and yield based on a simple crop simulation model. Plant Production Sci., 1(4): 269-279.

Jones, J.W. 1993. Decision support systems for agricultural development, pages 459-471. In: *Systems Approaches for Agricultural Development*, Vol. 2. (Penning de Vries, F.W.T., Teng, P. and Metselaar, K. eds.), Kluwer Academic Publishers, Dordrecht, The Netherlands.

Knyazikhin, Y., Martonchik, J.V., Myneni, R.B., Diner, D.J. and Running, S.W. 1998. Synergistic algorithm for estimating vegetation canopy leaf area index and fraction of absorbed photosynthetically active radiation from MODIS and MISR data. J. Geophys. Res., 103: 32257-32275.

Maas, S.J. 1988a. Use of remotely sensed information in agricultural crop growth models. Ecol. Modelling, 41: 247-268.

Maas, S.J. 1988b. Using satellite data to improve model estimates of crop yield. Agron. J., 80: 655-662.

Maracchi, G., Perarnaud, V. and Kleschenko, A.D. 2000. Applications of geographical information systems and remote sensing in agrometeorology. *Agric. Forest Meteorol.*, 103: 119-136.

Meyer-Roux, J. and Vossen, P. 1994. The first phase of the MARS project, 1988-1993: overview, methods and results, pp. 33 – 85. In: Proceedings of the Conference on the MARS Project: Overview and Perspectives. Commission of the European Communities, Luxembourg.

Moulin, S. and Guerif, M. 1999. Impacts of model parameter uncertainties on crop reflectance estimates: a regional case study on wheat. Int. J. Remote Sens., 20(1): 213-218.

Moulin, S., Bondeau, A. and Delecolle, R. 1998. Combining agricultural crop models and satellite observations: from field to regional scales. Int. J. Remote Sens., 19(6): 1021-1036.

Myneni, R.B., Nemani, R.R. and Running, S.W. 1997. Estimation of global leaf area index and absorbed PAR using radiative transfer models. IEEE Trans. on Geosc. and Rem. Sensing, 35(6): 1380-1393.

Nain, A.S., Dadhwal, V.K. and Singh, T.P. 2004. Use of CERES-Wheat model for wheat yield forecast in central Indo-Gangetic plains of India. J. Agricultural Science (camb.), 142: 59-70.

Pandya, M.R., Chaudhari, K.N., Singh, R.P., Sehgal, V.K., Bairagi, G.D., Sharma, R. and Dadhwal, V.K. 2003. Leaf area index retrieval using IRS LISS-III sensor data and validation of MODIS LAI product over Madhya Pradesh. Current Science, 85(12): 1777-1782.

Price, J.C. 1993. Estimating leaf area index from satellite data. IEEE Trans. Geoscience Remote Sensing, 31: 727-734.

Qiu, J., Gao, W. and Lesht, B.M. 1998. Inverting optical reflectance to estimate surface properties of vegetation canopies. Int. J. Remote Sens., 19: 641-656.

Rastogi, A., Kalra, N., Agarwal, P.K., Sharma, S.K., Harit, R.C., Navalgund, R.R. and Dadhwal, V.K. 2000. Estimation of wheat leaf area index from satellite data using Price model. International J. Remote Sensing, 21(15): 2943- 2949.

Richardson, A.J., Wiegand, C.L., Arkin, G.F., Nixon, P.R. and Gerbermann, A.H. 1982. Remotely sensed spectral indicators of sorghum development and their use in growth modelling. Agric. Meteorol., 26: 11-23.

Satya, P., Shibasaki, R. and Ochi, S. 1998. Modelling Spatial Crop Production: A GIS approach. In: Proceedings of the 19th Asian Conference on Remote Sensing, 16-20 Nov., 1998, Manila, pp. A-9-1 – A-9-6.

Sehgal, V.K., Rajak, D.R. and Dadhwal, V.K. 2001a. Issues in linking remote sensing inputs in a crop growth monitoring system: results of a case study. In: Proc. of the ISRS National Symposium, Dec 11-13, 2001, Ahmedabad, India.

Sehgal, V.K., Sastri, C.V.S., Kalra, N. and Dadhwal, V.K. 2001b. Farm level yield mapping for precision crop management under Indian conditions using a simple approach of linking remote sensing information and crop simulation model. In: Proc. of the ISRS National Symposium, Dec 11-13, 2001, Ahmedabad, India.

Sehgal, V.K., Rajak, D.R., Chaudhary, K.N. and Dadhwal, V.K. 2002. Improved regional yield prediction by crop growth monitoring system using remote sensing derived crop phenology. Internat. Arch. Photogramm. Remote Sens. & Spatial Inf. Sci., 34 (7): 329-334.

Thornton, P.K., Bowen, W.T., Ravelo, A.C., Wilkens, P.W., Farmer, G., Brock, J. and Brink, J.E. 1997. Estimating millet production for famine early warning: an application of crop simulation modelling using satellite and ground-based data in Burkina Faso. Agric. For. Meteorol, 83: 95-112.

Tim, U.S. 1996. Coupling vadose zone models with GIS: Emerging trends and potential bottlenecks. J. Environ. Qual., 25: 535-544.

Vossen, P. 1995. Early assessment of national yields: the approach developed by the MARS-STAT project on behalf of European Commission, pages 327-347. In: Proceedings of the Seminar on Yield Forecasting, 24-27 Oct., 1995, Villerfranche-sur-Mer, France.

Wade, G., Mueller, R., Cook, P.W. and Doraiswamy, P.C. 1994. AVHRR Map products for Crop Condition Assessment: A Geographic Information Systems Approach. Photogrammetric Engineering & Remote Sensing, 60(9): 1145-1150.

Wiegand, C.L., Richardsons, A.J. and Kanemasu, E.T. 1979. Leaf area index estimates for wheat from LANDSAT and their implications for evapotranspiration and crop modeling. Agronomy J., 71: 336-342.

DROUGHTS & FLOODS ASSESSMENT AND MONITORING USING REMOTE SENSING AND GIS

A.T. Jeyaseelan

Crop Inventory and Drought Assessment Division
National Remote Sensing Agency
Department of Space, Govt. of India, Hyderabad

Abstract : Space technology has made substantial contribution in all the three phases such as preparedness, prevention and relief phases of drought and flood disaster management. The Earth Observation satellites which include both geostationary and polar orbiting satellites provide comprehensive, synoptic and multi temporal coverage of large areas in real time and at frequent intervals and 'thus' - have become valuable for continuous monitoring of atmospheric as well as surface parameters related to droughts and floods. Geo-stationary satellites provide continuous and synoptic observations over large areas on weather including cyclone monitoring. Polar orbiting satellites have the advantage of providing much higher resolution imageries, even though at low temporal frequency, which could be used for detailed monitoring, damage assessment and long-term relief management. Advancements in the remote sensing technology and the Geographic Information Systems help in real time monitoring, early warning and quick damage assessment of both drought and flood disasters. In this lecture the use of remote sensing and GIS and the global scenario for the drought and flood disaster management is discussed.

INTRODUCTION

Droughts and floods are water-related natural disasters which affect a wide range of environmental factors and activities related to agriculture, vegetation, human and wild life and local economies. Drought is the single most important weather-related natural disaster often aggravated by human action, since it affects very large areas for months and years and thus has a serious impact on regional food production, life expectancy for entire populations and economic performance of large regions or several countries. During 1967-1991, droughts

Satellite Remote Sensing and GIS Applications in Agricultural Meteorology
pp. 291-313

have affected 50 per cent of the 2.8 billion people who suffered from all natural disasters and killed 35 per cent of the 3.5 million people who lost their lives. In the recent years large-scale intensive droughts have been observed in all continents leading to huge economic losses, destruction of ecological resources, food shortages and starvation of millions people. Floods are among the most devastating natural hazards in the world, claiming more lives and causing more property damage than any other natural phenomena.

Several users such as top level policy makers at the national and international organisations, researchers, middle level policy makers at the state, province and local levels consultants, relief agencies and local producers including farmers, suppliers, traders and water managers are interested in reliable and accurate drought and flood information for effective management. The disaster management activities can be grouped into three major phases: The Preparedness phase where activities such as prediction and risk zone identification are taken up long before the event occurs; the Prevention phase where activities such as Early warning/Forecasting, monitoring and preparation of contingency plans are taken up just before or during the event; and the Response/Mitigation phase where activities are undertaken just after the event which include damage assessment and relief management.

Remote sensing techniques make it possible to obtain and distribute information rapidly over large areas by means of sensors operating in several spectral bands, mounted on aircraft or satellites. A satellite, which orbits the Earth, is able to explore the whole surface in a few days and repeat the survey of the same area at regular intervals, whilst an aircraft can give a more detailed analysis of a smaller area, if a specific need occurs. The spectral bands used by these sensors cover the whole range between visible and microwaves. Rapid developments in computer technology and the Geographical Information Systems (GIS) help to process Remote Sensing (RS) observations from satellites in a spatial format of maps - both individually and along with tabular data and "crunch" them together to provide a new perception - the spatial visualisation of information of natural resources. The integration of information derived from RS techniques with other datasets - both in spatial and non-spatial formats provides tremendous potential for identification, monitoring and assessment of droughts and floods.

REMOTE SENSING FOR DROUGHTS

Monitoring and assessment of drought through remote sensing and GIS depend on the factors that cause drought and the factors of drought impact.

Based on the causative factors, drought can be classified into Meteorological, Hydrological and Agricultural droughts. An extensive survey of the definition of droughts by WMO found that droughts are classified on the basis of: (i) rainfall, (ii) combinations of rainfall with temperature, humidity and or evaporation, (iii) soil moisture and crop parameter, (iv) climatic indices and estimates of evapotranspiration, and finally (v) the general definitions and statements.

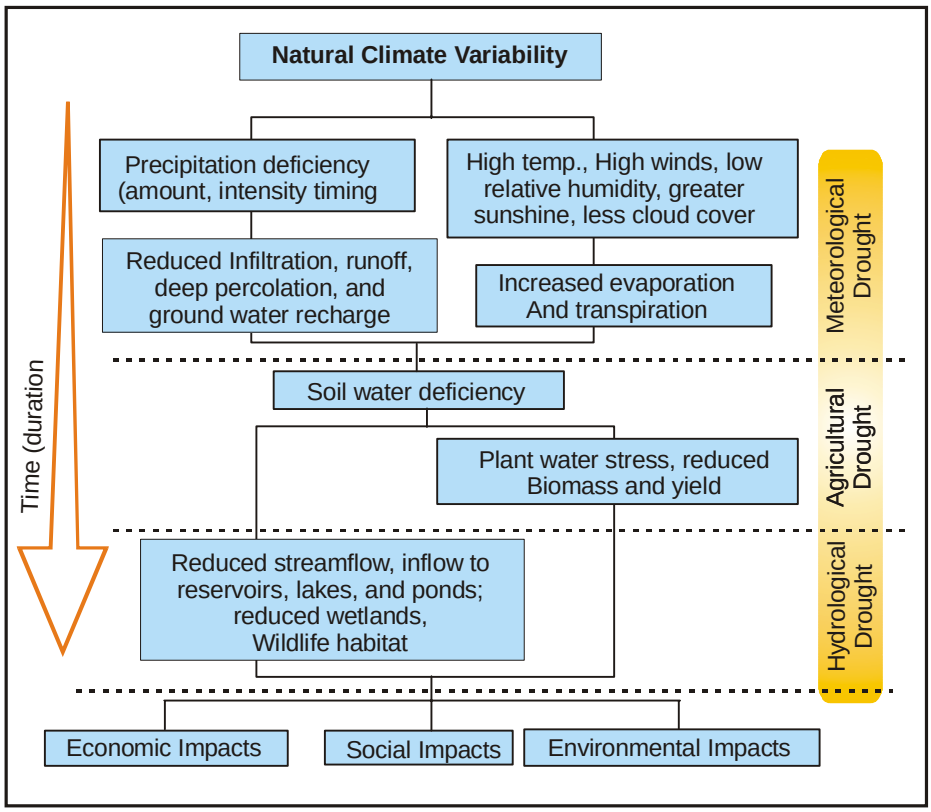

Figure 1: Sequence of Drought impacts

Drought is a normal, recurrent feature of climate and occurs in all climatic zones, although its characteristics vary significantly from one region to another. Drought produces a complex web of impacts that span many sectors of the economy and reach well beyond the area experiencing physical drought. Drought impacts are commonly referred to as direct or indirect. Reduced crop, rangeland, and forest productivity; increased fire hazard; reduced water levels; increased livestock and wildlife mortality rates; and damage to wildlife and fish

habitat are a few examples of direct impacts. The consequences of these impacts illustrate indirect impacts. The remote sensing and GIS technology significantly contributes to all the activities of drought management.

Drought Preparedness Phase

Long before the drought event occurs, the preparedness in terms of identifying the drought prone / risk zone area and the prediction of drought and its intensity is essential.

Drought Prone/Risk zone identification

The drought prone area or risk zone identification is usually carried out on the basis of historic data analysis of rainfall or rainfall and evaporation and the area of irrigation support. The conventional methods lack identification of spatial variation and do not cover man's influence such as land use changes like irrigated area developed and the area affected due to water logging and salinity. The remote-sensing based method for identification of drought prone areas (Jeyaseelan *et al.*, 2002) uses historical vegetation index data derived from NOAA satellite series and provides spatial information on drought prone area depending on the trend in vegetation development, frequency of low development and their standard deviations.

Drought prediction

The remote sensing use for drought prediction can benefit from climate variability predictions using coupled ocean/atmosphere models, survey of snow packs, persistent anomalous circulation patterns in the ocean and atmosphere, initial soil moisture, assimilation of remotely sensed data into numerical prediction models and amount of water available for irrigation. Nearly-global seasonal climate anomaly predictions are possible due to the successful combination of observational satellite networks for operational meteorological, oceanographic and hydrological observations. Improved coupled models and near-real time evaluation of *in situ* and remote sensing data - allows for the first time physically-based drought warnings several months in advance, to which a growing number of countries already relate their policies in agriculture, fisheries and distribution of goods.

The quality of seasonal predictions of temperature and precipitation anomalies by various centres such as the National Climate Research Centre

(NCRC) of United States, the European Centre for Medium Range Weather Forecasts (ECMWF), the India Meteorological Department (IMD), the National Centre for Medium Range Weather Forecast of India (NCMRWF) is a function of the quality and amount of satellite data assimilated into the starting fields (e.g., SST from AVHRR and profiles from TOVS on NOAA satellites, ERS-2 scatterometer winds, SSM/I on DMSP satellites and all geostationary weather satellites: Geostationary Operational Environmental Satellites (GOES), i.e. GOES-East, GOES-West of USA, METeorological SATellite (METEOSAT) of Europe, Geostationary Meteorological Satellites (GMS) of Japan, Indian National Satellites (INSAT) of India etc.). The new assimilation techniques have produced a stronger impact of space data on the quality of weather and seasonal climate predictions.

The potential contribution by existing satellites is by far not fully exploited, since neither the synergy gained by the combination of satellite sensors is used nor all the satellite data are distributed internationally. For example, better information flow is needed from satellite data producers to the intermediary services such as CLIPS (Climate Information and Prediction Services) project of World Meteorological Organisation (WMO), and prediction centres including the European Centre for Medium Range Weather Forecasts (ECMWF), National Centres for Environmental Predictions (NCEP), Japan Meteorological Agency (JMA), India Meteorological Department (IMD), National Centre for Medium Range Weather Forecast, India (NCMRWF) etc. to local services and ultimately to end users. Further the drought predictions need to be improved with El Niño predictions and should be brought down to larger scales.

Drought Prevention Phase

Drought Monitoring and Early Warning

Drought monitoring mechanism exists in most of the countries based on ground based information on drought related parameters such as rainfall, weather, crop condition and water availability, etc. Earth observations from satellite are highly complementary to those collected by *in-situ* systems. Satellites are often necessary for the provision of synoptic, wide-area coverage and frequent information required for spatial monitoring of drought conditions. The present state of remotely sensed data for drought monitoring and early warning is based on rainfall, surface wetness, temperature and vegetation monitoring.

Currently, multi channel and multi sensor data sources from geostationary platforms such as GOES, METEOSAT, INSAT and GMS and polar orbiting satellites such as National Oceanic Atmospheric and Administration (NOAA), EOS-Terra, Defense Meteorological Satellite Program (DMSP) and Indian Remote Sensing Satellites (IRS) have been used or planned to be used for meteorological parameter evaluation, interpretation, validation and integration. These data are used to estimate precipitation intensity, amount, and coverage, and to determine ground effects such as surface (soil) wetness.

Rainfall Monitoring

Rain is the major causative factor for drought. As the conventional method is based on the point information with limited network of observations, the remote sensing based method provides better spatial estimates. Though the satellite based rainfall estimation procedure is still experimental, the methods can be grouped into 3 types namely Visible and Infrared (VIS and IR) technique, passive microwave technique and active microwave technique.

VIS and IR technique: VIS and IR techniques were the first to be conceived and are rather simple to apply while at the same time they show a relatively low degree of accuracy. A complete overview of the early work and physical premises of VIS and thermal IR (10.5 – 12.5 μm) techniques is provided by Barrett and Martin (1981) and Kidder and Vonder Haar (1995). The Rainfall estimation methods can be divided into the following categories: cloud-indexing, bi-spectral, life history and cloud model. Each of the categories stresses a particular aspect of cloud physics properties using satellite imagery.

Cloud indexing techniques assign a rain rate level to each cloud type identified in the satellite imagery. The simplest and perhaps most widely used is the one developed by Arkin (1979). A family of cloud indexing algorithms was developed at the University of Bristol, originally for polar orbiting NOAA satellites and recently adapted to geostationary satellite imagery. “Rain Days” are identified from the occurrence of IR brightness temperatures (TB) below a threshold.

Bi-spectral methods are based on the very simple, although not always true, relationship between cold and bright clouds and high probability of precipitation, this is characteristic of Cumulonimbus. Lower probabilities are associated with cold but dull clouds (thin cirrus) or bright but warm (stratus) clouds. O’Sullivan *et al.* (1990) used brightness and textural characteristics

during daytime and IR temperature patterns to estimate rainfall over a 10 × 10 pixel array in three categories: no rain, light rain, and moderate/heavy rain. A family of techniques that specifically require geostationary satellite imagery are the life-history methods that rely upon a detailed analysis of the cloud's life cycle, which is particularly relevant for convective clouds. An example is the Griffith-Woodley technique (Griffith *et al.*, 1978). Cloud model techniques aim at introducing the cloud physics into the retrieval process for a quantitative improvement deriving from the overall better physical description of the rain formation processes. Gruber (1973) first introduced a cumulus convection parameterization to relate fractional cloud cover to rain rate. A one-dimensional cloud model relates cloud top temperature to rain rate and rain area in the Convective Stratiform Technique (CST) (Adler and Negri, 1988; Anagnostou *et al.*, 1999).

Passive microwave technique: Clouds are opaque in the VIS and IR spectral range and precipitation is inferred from cloud top structure. At passive MW frequencies, precipitation particles are the main source of attenuation of the upwelling radiation. MW techniques are thus physically more direct than those based on VIS/IR radiation. The emission of radiation from atmospheric particles results in an increase of the signal received by the satellite sensor while at the same time the scattering due to hydrometeors reduce the radiation stream. Type and size of the detected hydrometeors depends upon the frequency of the upwelling radiation. Above 60 GHz ice scattering dominates and the radiometers can only sense ice while rain is not detected. Below about 22 GHz absorption is the primary mechanism affecting the transfer of MW radiation and ice above the rain layer is virtually transparent. Between 19.3 and 85.5 GHz, frequency range radiation interacts with the main types of hydrometeors, water particles or droplets (liquid or frozen). Scattering and emission happen at the same time with radiation undergoing multiple transformations within the cloud column in the sensor's field of view (FOV). The biggest disadvantage is the poor spatial and temporal resolution, the first due to diffraction, which limits the ground resolution for a given satellite MW antenna, and the latter to the fact that MW sensors are consequently only mounted on polar orbiters. The matter is further complicated by the different radiative characteristics of sea and land surfaces underneath. The major instruments used for MW-based rainfall estimations are the SSM/I, a scanning-type instrument that measures MW radiation over a 1400-km wide swath at four separate frequencies, 19.35, 22.235, 37.0 and 85.5 GHz, the latter extending the spectral range of previous instruments into the strong scattering regime (as regards to precipitation-size particles).

Active microwave: The most important precipitation measuring instruments from space is the PR, precipitation radar operating at 13.8 GHz on board TRMM, the first of its kind to be flown on board a spacecraft. The instrument aims at providing the vertical distribution of rainfall for the investigation of its three-dimensional structure, obtaining quantitative measurements over land and oceans, and improving the overall retrieval accuracy by the combined use of the radar, and the TMI and VIRS instruments.

Surface Temperature Estimation

The estimation of water stress in crop/ vegetation or low rate of evapotranspiration from crop is another indicator of drought. As water stress increases the canopy resistance for vapor transport results in canopy temperature rise in order to dissipate the additional sensible heat. Sensible heat transport (ET) between the canopy (Ts) and the air (Ta) is proportional to the temperature difference (Ts-Ta). Therefore the satellite based surface temperature estimation is one of the indicators for drought monitoring since it is related to the energy balance between soil and plants on the one hand and atmosphere and energy balance on the other in which evapotranspiration plays an important role. Surface temperature could be quite complementary to vegetation indices derived from the combination of optical bands. Water-stress, for example, should be noticed first by an increase in the brightness surface temperature and, if it affects the plant canopy, there will be changes in the optical properties.

During the past decade, significant progress has been made in the estimation of land-surface emissivity and temperature from airborne TIR data. Kahle *et al.* (1980) developed a technique to estimate the surface temperature based on an assumed constant emissivity in one channel and previously determined atmospheric parameters. This temperature was then used to estimate the emissivity in other channels (Kahle, 1986). Other techniques such as thermal log residuals and alpha residuals have been developed to extract emissivity from multi-spectral thermal infrared data (Hook *et al.*, 1992). Based on these techniques and an empirical relationship between the minimum emissivity and the spectral contrast in band emissivities, a Temperature Emissivity Separation (TES) method has been recently developed for one of the ASTER (Advance Space borne Thermal Emission and Reflection Radiometer) products (ATBD-AST-03, 1996).

In addition, three types of methods have been developed to estimate LST from space: the single infrared channel method, the split window method which

is used in various multi-channel sea-surface temperature (SST) algorithms, and a new day/night MODIS LST method which is designed to take advantage of the unique capability of the MODIS instrument. The first method requires surface emissivity and an accurate radiative transfer model and atmospheric profiles which must be given by either satellite soundings or conventional radiosonde data. The second method makes corrections for the atmospheric and surface emissivity effects with surface emissivity as an input based on the differential absorption in a split window. The third method uses day/night pairs of TIR data in seven MODIS bands for simultaneously retrieving surface temperatures and band-averaged emissivities without knowing atmospheric temperature and water vapor profiles to high accuracy. This method improves upon the Li and Becker's method (1993), which estimates both land surface emissivity and LST by the use of pairs of day/night co-registered AVHRR images from the concept of the temperature independent spectral index (TISI) in thermal infrared bands and based on assumed knowledge of surface TIR BRDF (Bi-directional Reflectance Distribution Function) and atmospheric profiles.

Because of the difficulties in correcting both atmospheric effects and surface emissivity effects, the development of accurate LST algorithms is not easy. The accuracy of atmospheric corrections is limited by radiative transfer methods and uncertainties in atmospheric molecular (especially, water vapor) absorption coefficients and aerosol absorption/scattering coefficients and uncertainties in atmospheric profiles as inputs to radiative transfer models. Atmospheric transmittance/radiance codes LOWTRAN6 (Kneizys *et al.*, 1983), LOWTRAN7 (Kneizys *et al.*, 1988), MODTRAN (Berk *et al.*, 1989), and MOSART (Cornette *et al.*, 1994) have been widely used in development of SST and LST algorithms and the relation between NDVI and emissivities are used.

Soil Moisture Estimation

Soil moisture in the root zone is a key parameter for early warning of agricultural drought. The significance of soil moisture is its role in the partitioning of the energy at the ground surface into sensible and latent (evapotranspiration) heat exchange with the atmosphere, and the partitioning of precipitation into infiltration and runoff.

Soil moisture can be estimated from : (i) point measurements, (ii) soil moisture models and (iii) remote sensing. Traditional techniques for soil moisture estimation/ observation are based on point basis, which do not always represent

the spatial distribution. The alternative has been to estimate the spatial distribution of soil moisture using a distributed hydrologic model. However, these estimates are generally poor, due to the fact that soil moisture exhibits large spatial and temporal variation as a result of inhomogeneities in soil properties, vegetation and precipitation. Remote sensing can be used to collect spatial data over large areas on routine basis, providing a capability to make frequent and spatially comprehensive measurements of the near surface soil moisture. However, problems with these data include satellite repeat time and depth over which soil moisture estimates are valid, consisting of the top few centimetres at most. These upper few centimetres of the soil is the most exposed to the atmosphere, and their soil moisture varies rapidly in response to rainfall and evaporation. Thus to be useful for hydrologic, climatic and agricultural studies, such observations of surface soil moisture must be related to the complete soil moisture profile in the unsaturated zone. The problem of relating soil moisture content at the surface to that of the profile as a whole has been studied for the past two decades. The results of the study indicated following four approaches : (i) regression, (ii) knowledge based, (iii) inversion and (iv) combinations of remotely sensed data with soil water balance models.

Passive microwave sensing (radiometry) has shown the greatest potential among remote sensing methods for the soil moisture measurement. Measurements at 1 to 3 GHz are directly sensitive to changes in surface soil moisture, are little affected by clouds, and can penetrate moderate amounts of vegetation. They can also sense moisture in the surface layer to depths of 2 to 5 cm (depending on wavelength and soil wetness). With radiometry, the effect of soil moisture on the measured signal dominates over that of surface roughness (whereas the converse is true for radar). Higher frequency Earth-imaging microwave radiometers, including the Scanning Multichannel Microwave Radiometer (lowest frequency 6.6 GHz) launched on the Seasat (1978) and Nimbus-7 (1978-87) satellites, and the Special Sensor Microwave Imager (lowest frequency 19.35 GHz) launched on the DMSP satellite series have been utilized in soil moisture studies with some limited success. The capabilities of these higher frequency instruments are limited to soil moisture measurements over predominantly bare soil and in a very shallow surface layer (<5 cm). At its lowest frequency of 19.35 GHz the SSM/I is highly sensitive to even small amounts of vegetation, which obscures the underlying soil. Large variations in soil moisture (e.g., flood/no-flood) in sparsely vegetated regions and qualitative river flooding indices, are all that have been shown feasible using the SSM/I.

Vegetation Monitoring

The vegetation condition reflects the overall effect of rainfall, soil moisture, weather and agricultural practices and the satellite based monitoring of vegetation plays an important role in drought monitoring and early warning. Many studies have shown the relationships of red and near-infrared (NIR) reflected energy to the amount of vegetation present on the ground (Colwell, 1974). Reflected red energy decreases with plant development due to chlorophyll absorption in the photosynthetic leaves. Reflected NIR energy, on the other hand, will increase with plant development through scattering processes (reflection and transmission) in healthy, turgid leaves. Unfortunately, because the amount of red and NIR radiation reflected from a plant canopy and reaching a satellite sensor varies with solar irradiance, atmospheric conditions, canopy background, and canopy structure/ and composition, one cannot use a simple measure of reflected energy to quantify plant biophysical parameters nor monitor vegetation on a global, operational basis. This is made difficult due to the intricate radiant transfer processes at both the leaf level (cell constituents, leaf morphology) and canopy level (leaf elements, orientation, non-photosynthetic vegetation (NPV), and background). This problem has been circumvented somewhat by combining two or more bands into an equation or 'vegetation index' (VI). The simple ratio (SR) was the first index to be used (Jordan, 1969), formed by dividing the NIR response by the corresponding 'red' band output. For densely vegetated areas, the amount of red light reflected approaches very small values and this ratio, consequently, increases without bounds. Deering (1978) normalized this ratio from -1 to +1, with the normalized difference vegetation index (NDVI), by taking the ratio between the difference between the NIR and red bands and their sum. Global-based operational applications of the NDVI have utilized digital counts, at-sensor radiances, 'normalized' reflectances (top of the atmosphere), and more recently, partially atmospheric corrected (ozone absorption and molecular scattering) reflectances. Thus, the NDVI has evolved with improvements in measurement inputs. Currently, a partial atmospheric correction for Raleigh scattering and ozone absorption is used operationally for the generation of the Advanced Very High Resolution Radiometer. The NDVI is currently the only operational, global-based vegetation index utilized. This is in part, due to its 'ratioing' properties, which enable the NDVI to cancel out a large proportion of signal variations attributed to calibration, noise, and changing irradiance conditions that accompany changing sun angles, topography, clouds/shadow and atmospheric conditions. Many studies have shown the NDVI to be related to leaf area index (LAI), green biomass, percent green cover, and fraction of absorbed

photo synthetically active radiation (fAPAR). Relationships between fAPAR and NDVI have been shown to be near linear in contrast to the non-linearity experienced in LAI – NDVI relationships with saturation problems at LAI values over 2. Other studies have shown the NDVI to be related to carbon-fixation, canopy resistance, and potential evapotranspiration allowing its use as effective tool for drought monitoring.

Response/Mitigation phase

Assessment of Drought impact

Remote sensing use for drought impact assessment involves assessment of following themes such as land use, persistence of stressed conditions on an intra-season and inter-season time scale, demographics and infrastructure around the impacted area, intensity and extent, agricultural yield, impact associated with disease, pests, and potable water availability and quality etc. High resolution satellite sensors from LANDSAT, SPOT, IRS, etc. are being used.

Decision support for Relief Management

Remote sensing use for drought response study involves decision support for water management, crop management and for mitigation and alternative strategies. High resolution satellite sensors from LANDSAT, SPOT, IRS, etc. are being used. In India, for long term drought management, action plan maps are being generated at watershed level for implementation.

Global scenario on Remote Sensing use

The normalised difference vegetation index (NDVI) and temperature condition index (TCI) derived from the satellite data are accepted world-wide for regional monitoring.

The ongoing program on Africa Real-Time Environmental Monitoring using Imaging Satellites (ARTEMIS) is operational at FAO and uses METEOSAT rainfall estimates and AVHRR NDVI values for Africa.

The USDA/NOAA Joint Agricultural Weather Facility (JAWF) uses Global OLR anomaly maps, rainfall map, vegetation and temperature condition maps from GOES, METEOSAT, GMS and NOAA satellites.

Joint Research Centre (JRC) of European Commission (EC) issues periodical bulletin on agricultural conditions under MARS-STAT (Application of Remote sensing to Agricultural statistics) project which uses vegetation index, thermal based evapotranspiration and microwave based indicators. Agricultural Division of Statistics, Canada issues weekly crop condition reports based on NOAA AVHRR based NDVI along with agro meteorological statistics. National Remote Sensing Agency, Department of Space issues biweekly drought bulletin and monthly reports at smaller administrative units for India under National Agricultural Drought Assessment and Monitoring System (NADAMS) which uses NOAA AVHRR and IRS WiFS based NDVI with ground based weather reports. Similar programme is followed in many countries world-wide.

REMOTE SENSING FOR FLOODS

Floods are among the most devastating natural hazards in the world, claiming more lives and causing more property damage than any other natural phenomena. As a result, floods are one of the greatest challenges to weather prediction. A flood can be defined as any relatively high water flow that overtops the natural or artificial banks in any portion of a river or stream. When a bank is overtopped, the water spreads over the flood plain and generally becomes a hazard to society. When extreme meteorological events occur in areas characterized by a high degree of urbanization, the flooding can be extensive, resulting in a great amount of damage and loss of life. Heavy rain, snowmelt, or dam failures cause floods. The events deriving from slope dynamics (gravitational phenomena) and fluvial dynamics (floods) are commonly triggered by the same factor: heavy rainfall. Especially in mountainous areas, analyzing flood risk is often impossible without considering all of the other phenomena associated with slope dynamics (erosion, slides, sediment transport, etc.) whereas in plains damages are caused by flood phenomena mainly controlled by water flow.

Forms of Floods: River Floods form from winter and spring rains, coupled with snow melt, and torrential rains from decaying tropical storms and monsoons; Coastal Floods are generated by winds from intense off-shore storms and Tsunamis; Urban Floods, as urbanization increases runoff two to six times what would occur on natural terrain; Flash Floods can occur within minutes or hours of excessive rainfall or a dam or levee failure, or a sudden release of water.

Flood Preparedness Phase

Flood Prone/Risk zone identification

The flood information (data) and experience (intuition) developed during the earlier floods may help in future events. The primary method for enhancing our knowledge of a particular flood event is through flood disaster surveys, where results such as damage assessment, lessons learned and recommendations are documented in a report (see the Natural Disaster Survey Report on "The Great Flood of 1993," Scofield and Achutuni, 1994). Flood risk zone map is of two types: (1) A detailed mapping approach, that is required for the production of hazard assessment for updating (and sometimes creating) risk maps. The maps contribute to the hazard and vulnerability aspects of flooding. (2) A larger scale approach that explores the general flood situation within a river catchment or coastal belt, with the aim of identifying areas that have greatest risk. In this case, remote sensing may contribute to mapping of inundated areas, mainly at the regional level.

Flood Prevention Phase

Flood Monitoring

Though flood monitoring can be carried out through remote sensing from global scale to storm scale, it is mostly used in the storm scale using hydrodynamic models (Figure 2) by monitoring the intensity, movement, and propagation of the precipitation system to determine how much, when, and where the heavy precipitation is going to move during the next zero to three hours (called NOWCASTING). Meteorological satellites (both GOES and POES) detect various aspects of the hydrological cycle —precipitation (rate and accumulations), moisture transport, and surface/ soil wetness (Scofield and Achutuni, 1996). Satellite optical observations of floods have been hampered by the presence of clouds that resulted in the lack of near real-time data acquisitions. Synthetic Aperture Radar (SAR) can achieve regular observation of the earth's surface, even in the presence of thick cloud cover. NOAA AHVRR allows for a family of satellites upon which flood monitoring and mapping can almost always be done in near real time. High-resolution infrared (10.7 micron) and visible are the principal data sets used in this diagnosis. The wetness of the soil due to a heavy rainfall event or snowmelt is extremely useful information for flood (flash flood) guidance. SSM/I data from the DMSP are the data sets used in this analysis. IRS, SAR, SPOT, and to some extent high resolution

NOAA images can be used to determine flood extent and areal coverage. Various precipitable water (PW) products have been developed and are available operationally for assessing the state of the atmosphere with respect to the magnitude of the moisture and its transport. These products include satellite derived PW from GOES (Holt *et al.*, 1998) and SSM/I (Ferraro *et al.*, 1996), and a composite that includes a combination of GOES + SSM/I + model data (Scofield *et al.*, 1996, 1995).

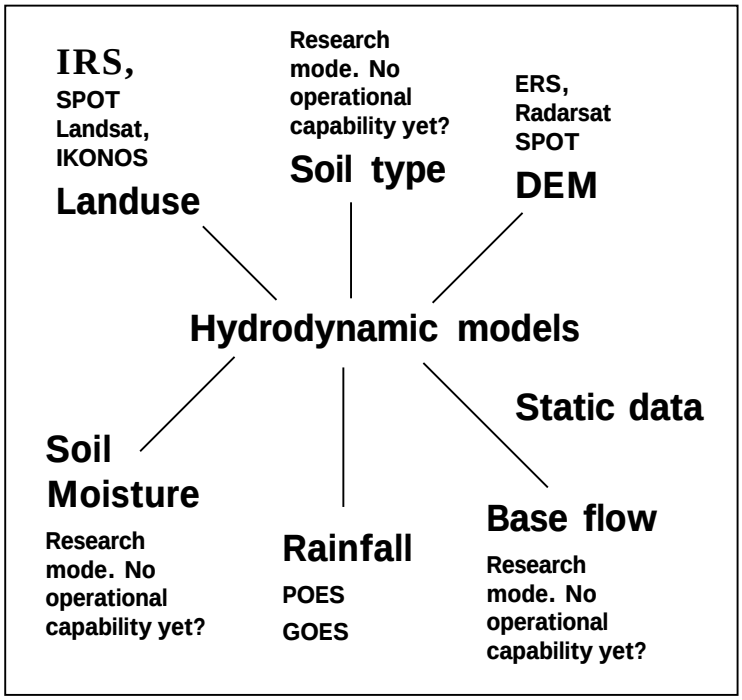

Figure 2: Remote sensing capabilities in Hydrodynamic models of flood

Flood Forecasting

Hydrologic models play a major role in assessing and forecasting flood risk. The hydrologic models require several types of data as input, such as land use, soil type, soil moisture, stream/river base flow, rainfall amount/intensity, snow pack characterization, digital elevation model (DEM) data, and static data (such as drainage basin size). Model predictions of potential flood extent can help emergency managers develop contingency plans well in advance of an actual event to help facilitate a more efficient and effective response. Flood forecast can be issued over the areas in which remote sensing is complementary to

direct precipitation and stream flow measurements, and those areas that are not instrumentally monitored (or the instruments are not working or are in error). In this second category, remote sensing provides an essential tool.

Quantitative Precipitation Estimates (QPE) and Forecasts (QPF) use satellite data as one source of information to facilitate flood forecasts. New algorithms are being developed that integrate GOES precipitation estimates, with the more physically based POES microwave estimates. An improvement in rainfall spatial distribution measurements is being achieved by integrating radar, rain gauges and remote sensing techniques to improve real time flood forecasting (Vicente and Scofield, 1998). For regional forecast, the essential input data are geomorphology, hydrological analysis, and historical investigation of past events and climatology. GOES and POES weather satellites can provide climatological information on precipitation especially for those areas not instrumentally monitored.

Forecast on the local scale requires topography, hydraulic data, riverbed roughness, sediment grain size, hydraulic calculations, land cover, and surface roughness. Remote sensing may contribute to mapping topography (generation of DEMs) and in defining surface roughness and land cover. In this case, remote sensing may contribute to updating cartography for land use and DEM. Complex terrain and land use in many areas result in a requirement for very high spatial resolution data over very large areas, which can only be practically obtained by remote sensing systems. There is also a need to develop and implement distributed hydrological models, in order to fully exploit remotely sensed data and forecast and simulate stream flow (Leconte and Pultz, 1990 and Jobin and Pultz, 1996). Data from satellites such as ERS, RADARSAT, SPOT and IRS can provide DEM data at resolutions of about 3 to 10 meters. Land use information can be determined through the use of AVHRR, Landsat, SPOT and IRS data. The rainfall component can be determined through the use of existing POES and GOES platforms. Although there are no operational data sources for estimating soil type, soil moisture, snow water equivalent and stream/river base flow, there has been considerable research on the extraction of these parameters from existing optical and microwave polar orbiting satellites.

Models can also assist in the mitigation of coastal flooding. Wave run-up simulations can help planners determine the degree of coastal inundation to be expected under different, user-specified storm conditions. These types of models require detailed near-shore bathymetry for accurate wave effect predictions. While airborne sensors provide the best resolution data at present, this data source can be potentially cost-prohibitive when trying to assess large areas of

coastline. In addition to DEM data, satellite based SAR can also be used to derive near-shore bathymetry for input into wave run-up models on a more cost-effective basis.

Response Phase

Assessment of Flood Damage (immediately during Flood)

The response category can also be called "relief," and refers to actions taken during and immediately following a disaster. During floods, timely and detailed situation reports are required by the authorities to locate and identify the affected areas and to implement corresponding damage mitigation. It is essential that information be accurate and timely, in order to address emergency situations (for example, dealing with diversion of flood water, evacuation, rescue, resettlement, water pollution, health hazards, and handling the interruption of utilities etc.). For remote sensing, this often takes the form of damage assessment. This is the most delicate management category since it involves rescue operations and the safety of people and property.

The following lists information used and analyzed in real time: flood extent mapping and real time monitoring (satellite, airborne, and direct survey), damage to buildings (remote sensing and direct inspections), damage to infrastructure (remote sensing and direct inspection), meteorological NOWCASTS (important real-time input from remote sensing data to show intensity/estimates, movement, and expected duration of rainfall for the next 0 - 3 hours), and evaluation of secondary disasters, such as waste pollution, to be detected and assessed during the crisis (remote sensing and others). In this category, communication is also important to speedy delivery.

Relief (after the Flood)

In this stage, re-building destroyed or damaged facilities and adjustments of the existing infrastructure will occur. At the same time, insurance companies require up-to-date information to settle claims. The time factor is not as critical as in the last stage. Nevertheless, both medium and high-resolution remote sensing images, together with an operational geographic information system, can help to plan many tasks. The medium resolution data can establish the extent of the flood damages and can be used to establish new flood boundaries. They can also locate landslides and pollution due to discharge and sediments. High-resolution data are suitable for pinpointing locations and the degree of damages. They can also be used as reference maps to rebuild bridges, washed-out roads, homes and facilities.

Global scenario on Remote Sensing use

There have been many demonstrations of the operational use of these satellites for detailed monitoring and mapping of floods and post-flood damage assessment. Remote Sensing information derived from different sensors and platforms (satellite, airplane, and ground etc.) are used for monitoring floods in China. A special geographical information system, flood analysis damage information system was developed for estimation of real time flood damages (Chen Xiuwan). Besides mapping the flood and damage assessment, high-resolution satellite data were operationally used for mapping post flood river configuration, flood control works, drainage-congested areas, bank erosion and developing flood hazard zone maps (Rao *et al.*, 1998). A variety of satellite images of the 1993 flooding in the St. Louis area were evaluated and combined into timely data sets. The resulting maps were valuable for a variety of users to quickly locate both natural and man-made features, accurately and quantitatively determine the extent of the flooding, characterize flood effects and flood dynamics. (Petrie *et al*., 1993). Satellite optical observations of floods have been hampered by the presence of clouds that resulted in the lack of near real-time data acquisitions. Synthetic Aperture Radar (SAR) can achieve regular observation of the earth's surface, even in the presence of thick cloud cover. Therefore, applications such as those in hydrology, which require a regularly acquired image for monitoring purposes, are able to meet their data requirements. SAR data are not restricted to flood mapping but can also be useful to the estimation of a number of hydrological parameters (Pultz *et al.*, 1996). SAR data were used for estimation of soil moisture, which was used as an input in the TR20 model for flood forecasting (Heike Bach, 2000). Floods in Northern Italy, Switzerland, France and England during October 2000 were studied using ERS-SAR data. Using information gathered by the European Space Agency's Earth Observation satellites, scientists are now able to study, map and predict the consequences of flooding with unprecedented accuracy. SAR images are also particularly good at identifying open water - which looks black in most images. When combined with optical and infra-red photography from other satellites, an extremely accurate and detailed digital map can be created. Quantitative Precipitation Estimates (QPE) and Forecasts (QPF) use satellite data as one source of information to facilitate flood and flash flood forecasts in order to provide early warnings of flood hazard to communities. New algorithms are being developed that integrate the less direct but higher resolution (space and time) images. An improvement in rainfall spatial distribution measurements is being achieved by integrating radar, rain gauges and remote sensing techniques to improve real time flood forecasting (Vicente and Scofield, 1998). Potential

gains from using weather radar in flood forecasting have been studied. (U.S. National Report to International Union of Geodesy and Geophysics 1991-1994). A distributed rainfall-runoff model was applied to a 785 km basin equipped with two rain gauges and covered by radar. Data recorded during a past storm provided inputs for computing three flood hydrographs from rainfall recorded by rain gauges, radar estimates of rainfall, and combined rain gauge measurements and radar estimates. The hydrograph computed from the combined input was the closest to the observed hydrograph. There has been considerable work devoted to developing the approach needed to integrate these remotely sensed estimates and in situ data into hydrological models for flood forecasting. A large-scale flood risk assessment model was developed for the River Thames for insurance industry. The model is based upon airborne Synthetic Aperture Radar data and was built using commonly used Geographic Information Systems and image processing tools. From the Ortho-rectified Images a land cover map was produced (Hélène M. Galy, 2000).

CONCLUSIONS

Droughts and Floods are among the most devastating natural hazards in the world, claiming more lives and causing extensive damage to agriculture, vegetation, human and wild life and local economies. The remote sensing and GIS technology significantly contributes in the activities of all the three major phases of drought and flood management namely, 1. Preparedness Phase where activities such as prediction and risk zone identification are taken up long before the event occurs. 2. Prevention Phase where activities such as Early warning/ Forecasting, monitoring and preparation of contingency plans are taken up just before or during the event and 3. Response/Mitigation Phase where activities just after the event includes damage assessment and relief management. In this lecture, brief review of remote sensing and GIS methods and its utilization for drought and flood management are discussed.

ACKNOWLEDGEMENTS

The author wishes to thank Dr. R.R. Navalgund, Director, Dr. A. Bhattacharya, Deputy Director (RS &GIS) and Dr. L. Venkataratnam, Group Director (A&SG) of NRSA for nominating the author to present the lecture in the WMO Sponsored Training/Workshop on Remote sensing data interpretation for Application in Agricultural Meteorology.

REFERENCES

Adler, R.F. and A.J. Negri, 1988. A satellite infrared technique to estimate tropical convective and stratiform rainfall. J. Appl. Meteorol., 27: 30-51.

Anagnostou, E.N., A.J. Negri and R.F. Adler, 1999. A satellite infrared technique for diurnal rainfall variability studies. J. Geophy. Res., 104: 31477-31488.

Arkin, P.A. 1979. The relationship between fractional coverage of high cloud and rainfall accumulations during GATE over the B-scale array. Mon. Wea. Rev., 106: 1153-1171.

ATBD-AST-03, 1996. Advance Space borne Thermal Emission and Reflection Radiometer (ASTER) products.

Barret, E.C. and D.W. Martin, 1981. The use of satellite data in rainfall monitoring. Academic Press, 340 pp.

Becker, F. 1987. The impact of spectral emissivity on the measurement of land surface temperature from a satellite. Int. J. Remote Sens. 11: 369-394.

Becker, F. and Z.L. Li 1990. Toward a local split window method over land surface. Int. J. Remote Sens. 11: 369-393.

Berk, A., L.S. Bemstein and D.C. Robertson, 1989. MODTRAN: A moderate resolution model for LOWTRAN 7. Rep. GLTR-89-0122, Burlington, MA: Spectral Sciences, Inc.

Chen Xiuwan. Flood Damage Real-Time Estimation-Model based on remote sensing and GIS. Institute of Remote Sensing and GIS, Peking University, Beijing, China. http://incede.iis.u-tokyo.ac.jp/reports/Report_11/Chen.pdf

Colwell, J.E. 1974. Vegetation canopy reflectance. Remote Sens. Environ., 3: 175-183.

Cornette, W.M., P.K. Acharya, D.C. Robertson and G.P. Anderson 1994. Moderate spectral atmospheric radiance and transmittance code (MOSART). Rep. R-057-94(11-30), La Jolla, CA: Photon Research Associates, Inc.

Ferraro, R.R., Weng, F., Grody, N.C. and Basist, A., 1996. An eight year (1987-94) climatology of rainfall, clouds, water vapor, snowcover, and sea-ice derived from SSM/I measurements. Bull. of Amer. Meteor. Soc., 77: 891-905.

Griffith, C.G., W.L. Woodley, P.G. Grube, D.W. Martin, J. Stout and D.N. Sikdar 1978. Rain estimation from geosynchronous satellite imagery- Visible and infrared studies. Mon.Wea. Rev., 106: 1153-1171.

Gruber, A. 1973. Estimating rainfall in regions of active convection. J. Appl. Meteorol., 12: 110-118.

Heike Bach. An Integrated Flood Forecast System Based on Remote Sensing Data, VISTA-Remote sensing applications in Geosciences.

Hélène M. Galy, Richard A. Sanders Willis, London, UK RGS-IBG Annual Conference, University of Sussex, January 4th – 7th 2000.

Holt, F.C., W.P. Menzel, D.G. Gray and T.J. Schmit 1998. Geostationary satellite soundings: new observations for forecasters. US Department of Commerce, NOAA, NESDIS, 30 pp.

Hook, S.J., A.R. Gabell, A.A. Green and P.S. Kealy 1992. A comparison of techniques for extracting emissivity information from thermal infrared data for geological studies. Remote Sens. Environ., 42: 123-135.

Jeyaseelan, A.T. and Chandrasekar, K. 2002. Satellite based identification for updation of Drought prone area in India. ISPRS-TC-VII, International Symposium on Resource and Environmental Monitoring, Hyderabad.

Jobin, D.I. and T.J. Pultz, 1996. Assessment of three distributed hydrological models for use with remotely sensed inputs. Third International Workshop on Applications of Remote Sensing in Hydrology, Greenbelt, MD, October 16-18, pp. 100-130.

Jordan, C.F. 1969. Derivation of leaf area index from quality of light on the forest floor. Ecology, 50: 663-666.

Kahle, A.B. 1986. Surface emittance, temperature and thermal inertia derived from Thermal infrared multispectral scanner (TIMS) data for Death Valley, California. Geophysics, 52 (7): 858-874.

Kahle, A.B., D.P. Madura and J.M. Soha, 1980. Middle infrared multispectral aircraft scanner data: analysis of geological applications. Appl. Optics, 19: 2279-2290.

Kerr, Y.H., J.P. Lagouarde and J. Imbernon, 1992. Accurate land surface temperature retrieval from AVHRR data with use of an improved split window algorithm. Remote Sens. Environ., 41(2-3): 197-209.

Kidder, S.Q. and T.H. Vonder Harr, 1995. Satellite Meteorology: An Introduction. Academic Press, 466 pp.

Kneizys, F.X., E.P. Shettle, L.W. Abreu, J.H. Chetwynd, G.P. Anderson, W.O. Gallery, J.E. A. Selby and S.A. Clough 1988. Users guide to LOWTRAN7. Rep. AFGL-TR-88-0177, Bedford, MA: Air Force Geophys. Lab.

Kneizys, F.X., E.P. Shettle, W.O. Gallery, J.H. Chetwynd, L.W. Abreu, J.E.A. Selby, S.A. Clough and R.W. Fenn, 1983. Atmospheric transmittance/Radiance: Computer code LOWTRAN 6. Rep. AFGL-TR-83-0187, Bedford, MA: Air Force Geophys. Lab.

Leconte, R. and T.J. Pultz, 1990. Utilization of SAR data in the monitoring of snowpack, wetlands, and river ice conditions. Workshop on Applications of Remote Sensing in Hydrology, Saskatoon, Saskatchewan, February 13-14, 1990, pp. 233-247.

Li, Z.L. and F. Becker, 1993. Feasibility of land surface temperature and emissivity determination from AVHRR data. Remote Sens. Environ, 43: 67-85.

O'Sullivan, F., C.H. Wash, M. Stewart and C.E. Motell, 1990. Rain estimation from infrared and visible GOES satellite data. J. Appl. Meteorol., 29: 209-223.

Ottle, C. and M. Stoll, 1993. Effect of atmospheric absorption and surface emissivity on the determination of land temperature from infrared satellite data. Int. J. Remote Sens., 14(10): 2025-2037.

Petrie, G.M., G.E. Wukelic, C.S. Kimball, K.L. Steinmaus and D.E. Evaluating 1993. Mississippi River Flood Developments Using ERS-1 SAR, Landsat, and Spot Digital Data. Beaver Pacific Northwest Laboratory, Richland, Washington http://www.odyssey.maine.edu/gisweb/spatdb/acsm/ac94108.html

Prata, A.J. 1994. Land surface temperatures derived from the advanced very high resolution radiometer and the along track scanning radiometer 2. Expeimental results and validation of AVHRR algorithm. J. Geophys. Res., 99(D6): 13025-13058.

Price, J.C. 1984. Land surface temperature measurements from the split window channels of the NOAA-7/AVHRR. J. Geophys. Res., 89: 7231-7237.

Pultz, T.J. and Yves Crevier, 1996. Early demonstration of RADARSAT for applications in hydrology. Third International Workshop on Applications of Remote Sensing in Hydrology, Greenbelt, MD, October 16-18, 1996, pp. 271-282.

Rao, D.P., V. Bhanumurthy and G.S. Rao, 1998. Remote Sensing and GIS in Flood Management in India. Memoir Geological Society of India, No. 41, 1998. pp. 195-218.

Scofield, R.A. and R. Achutuni, 1994. Use of satellite data during the great flood of 1993. Appendix C of the natural disaster survey report on The Great Flood of 1993, NOAA/NWS Report, U.S. Department of Commerce, Silver Spring, MD, C-1 — C-18.

Scofield, R.A. and R. Achutuni, 1996. The satellite forecasting funnel approach for predicting flash floods. Remote Sensing Reviews, 14: 251-282.

Scofield, R.A., D. Zaras, S. Kusselson and R. Rabin, 1996. A remote sensing precipitable water product for use in heavy precipitation forecasting. Proceedings of the 8th Conference on Satellite Meteorology and Oceanography, Atlanta, GA, 29 January - 2 February, 1996, AMS, Boston, MA, pp. 74- 78.

Scofield, R.A., S. Kusselson, D. Olander, and J. Robinson, 1995. Combining GOES, microwave, and raw insonde moisture data for improving heavy precipitation estimates and forecasts. Proceedings of the 14th Conference on Weather Analysis and Forecasting, Dallas, TX, 15 – 20 January, 1995, AMS, Boston, MA, (J4) 1 - (J4) 6.

Sobrino, J.A. and V. Caselles, 1991. A methodology for obtaining the crop temperature from NOAA-9 AVHRR data. Int. J. Remote Sens., 38: 19-34.

Vicente, G. and R.A. Scofield, 1998. The operational GOES infrared rainfall estimation technique. Bulletin of the American Meteorological Society, September 1998.

Vidal, A. 1991. Atmospheric and emissivity correction of land surface temperature measured from satellite using ground measurements or satellite data. Int. J. Remote Sens., 12(12): 2449-2460.

Wan, Z. and J. Dozier 1996. A generalized split-window algorithm for retrieving land-surface temperature from space. IEEE Trans. Geosci. Remote Sens., 34: 892-905.

Wan, Z. and Z.L. Li, 1997. A physics based algorithm for retrieving land-surface emissivity and temperature from EOS/MODIS data. IEEE Trans. Geosci. Remot. Sens., 27(3): 268-278.

WATER AND WIND INDUCED SOIL EROSION ASSESSMENT AND MONITORING USING REMOTE SENSING AND GIS

S.K. Saha
Agriculture and Soils Division
Indian Institute of Remote Sensing, Dehra Dun

Abstract : Water and wind induced soil erosion has adverse economic and environmental impacts. Large area in Asia-Pacific region is affected by soil erosion. This paper discusses various satellite remote sensing and GIS based modelling approaches for soil erosion hazard assessment such as empirical, semi-empirical and process based. Few case examples of soil erosion modelling by integrated use of remote sensing and GIS are included in this article.

INTRODUCTION

Soil degradation by accelerated water and wind-induced erosion is a serious problem and will remain so during the 21st century, especially in developing countries of tropics and subtropics. Erosion is a natural geomorphic process occurring continually over the earth's surface. However, the acceleration of this process through anthropogenic perturbations can have severe impacts on soil and environmental quality.

Accelerated soil erosion has adverse economic and environmental impacts (Lal, 1998). Economic effects are due to loss of farm income due to on-site and off-site reduction in income and other losses with adverse impact on crop/ animal production. The on-site and off-site effects of soil erosion on productivity are depicted in Figure 1 and Figure 2, respectively. Off-site economic impact of soil erosion is presented in Figure 3. Table 1 shows regional food production statistics for 1995 with and without soil erosion in the world. The data in Table 1 indicate total loss of food production at 31 M Mg for Africa, 190 M Mg for Asia and 18 M Mg for tropical America.

Satellite Remote Sensing and GIS Applications in Agricultural Meteorology
pp. 315-330

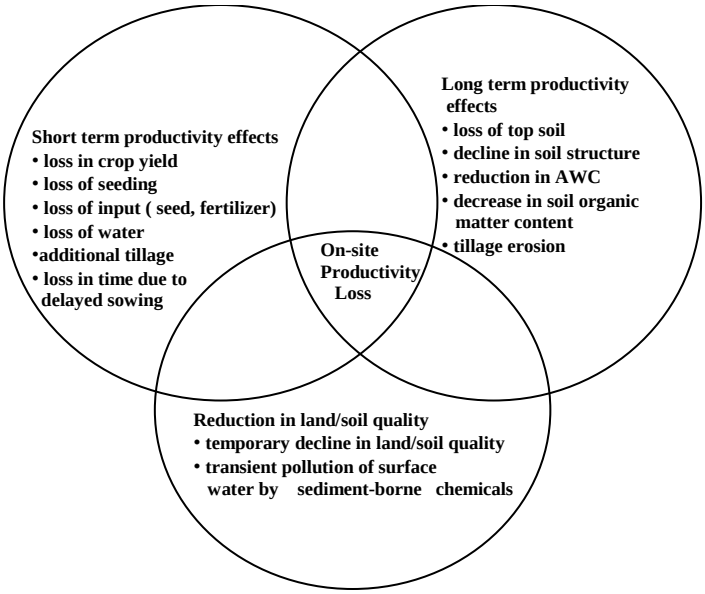

Figure 1: On-site effects of soil erosion on productivity are due to short-term and long-term effects, and on decline in soil quality (Lal, 2001)

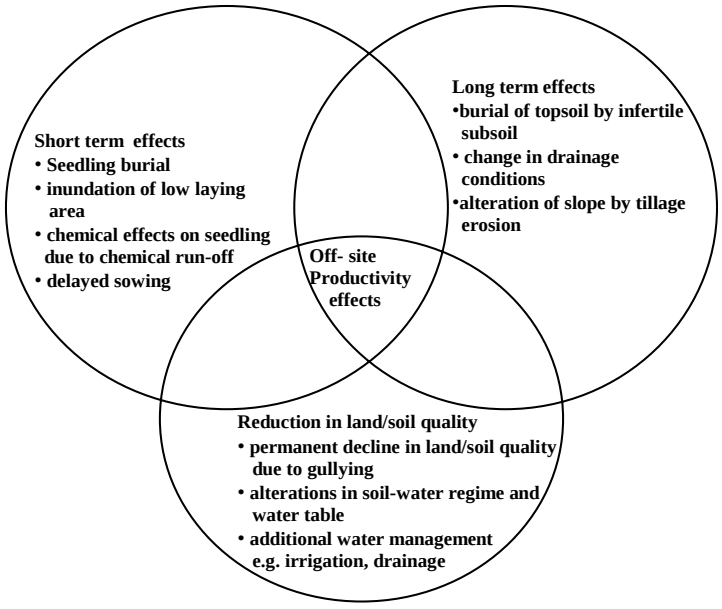

Figure 2: Off-site effects of soil erosion on productivity may be due to short-term or long-term and due to decline in land/soil quality (Lal, 2001)

Table 1. Regional food production statistics for 1995 with (a) and without (b) soil erosion (Lal, 2001)

Region	Cereals X 1000000		Soybeans X 1000000		Pulses X 1000000		Roots and tubers X 1000000	
	A	B	A	B	A	B	A	B
North Central America	358	376(5)	61	64(5)	6	65(b)	28	29(5)
Europe	268	281(5)	1	1(5)	6	6(5)	80	84(5)
Oceania	27	28(10)	-	-	2	2(15)	3	3(10)
Africa	100	110(10)	0.5	0.6(20)	7	8(20)	135	155(15)
Asia	929	1068(15)	21	23(10)	27	31(15)	248	293(18)
South America	90	99(10)	41	45(10)	4	4(10)	46	51(12)
Others	124	130(5)	3	3(5)	4	4(5)	69	72(5)
Total	1896	2092	126	136	50	61	609	687

GLOBAL EXTENT OF SOIL DEGRADATION BY EROSION

The total land area subjected to human-induced soil degradation is estimated at about 2 billion ha (Table 2; Lal, 2001). Of this, the land area affected by soil degradation due to erosion is estimated at 1100 Mha by water erosion and 550 Mha by wind erosion (Table 2). South Asia is one of the regions in the world where soil erosion by water and wind is a severe problem (Venkateswarulu, 1994 and Singh *et al.*, 1992) (Table 3).

Table 2. Global extent of human–induced soil degradation (Lal, 2001)

World Regions	Total Land Area (10 ha)	Human induced soil degradation (10 ha)	Soil erosion (10 ha)	
			Water	Wind
Africa	2966	494	227	186
Asia	4256	748	441	222
South America	1768	243	123	42
Central America	306	63	46	5
North America	1885	95	60	35
Europe	950	219	114	42
Oceania	882	103	83	16
World Total	13013	1965	1094	548

Table 3. Land area affected by soil erosion by water and wind in South Asia (Lal, 2001)

Country	Water erosion (Mha)	Wind erosion (Mha)	Total land area (Mha)
Afghanistan	11.2	2.1	65.3
Bangladesh	1.5	0	14.4
Bhutan	0.04	0	4.7
India	32.8	10.8	328.8
Iran	26.4	35.4	165.3
Nepal	1.6	0	14.7
Pakistan	7.2	10.7	79.6
Sri Lanka	1.0	0	6.6
Total	81.74	59.0	677.4

SOIL EROSION AND PROCESSES

Soil erosion is a three stage process : (1) detachment, (2) transport, and (3) deposition of soil. Different energy source agents determine different types of erosion. There are four principal sources of energy: physical, such as wind and water, gravity, chemical reactions and anthropogenic, such as tillage. Soil erosion begins with detachment, which is caused by break down of aggregates by raindrop impact, sheering or drag force of water and wind. Detached particles are transported by flowing water (over-land flow and inter-flow) and wind, and deposited when the velocity of water or wind decreases by the effect of slope or ground cover.

Three processes viz. dispersion, compaction and crusting, accelerate the natural rate of soil erosion. These processes decrease structural stability, reduce soil strength, exacerbate erodibility and accentuate susceptibility to transport by overland flow, interflow, wind or gravity. These processes are accentuated by soil disturbance (by tillage, vehicular traffic), lack of ground cover (bare fallow, residue removal or burning) and harsh climate (high rainfall intensity and wind velocity).

FACTORS OF SOIL EROSION

The soil erosion process is modified by biophysical environment comprising soil, climate, terrain and ground cover and interactions between them (Figure 4). Soil erodibility – susceptibility of soil to agent of erosion - is determined by inherent soil properties e.g., texture, structure, soil organic matter content, clay minerals, exchangeable cations and water retention and transmission properties. Climatic erosivity includes drop size distribution and intensity of rain, amount and frequency of rainfall, run-off amount and velocity, and wind velocity. Important terrain characteristics for studying soil erosion are slope gradient, length, aspect and shape. Ground cover exerts a strong moderating impact on dissipating the energy supplied by agents of soil erosion. The effect of biophysical processes governing soil erosion is influenced by economic, social and political causes (Figure 4).

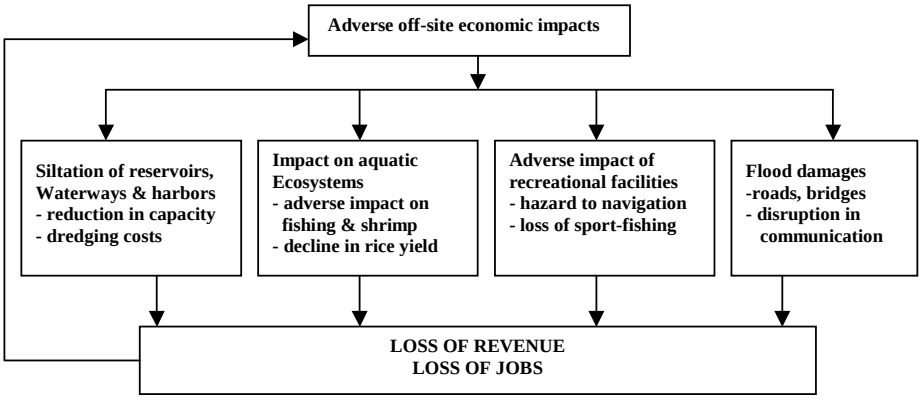

Figure 3: Off-site economic impact of soil erosion (Lal, 2001)

MODELLING SOIL EROSION

Field studies for prediction and assessment of soil erosion are expensive, time-consuming and need to be collected over many years. Though providing detailed understanding of the erosion processes, field studies have limitations because of complexity of interactions and the difficulty of generalizing from the results. Soil erosion models can simulate erosion processes in the watershed and may be able to take into account many of the complex interactions that affect rates of erosion.

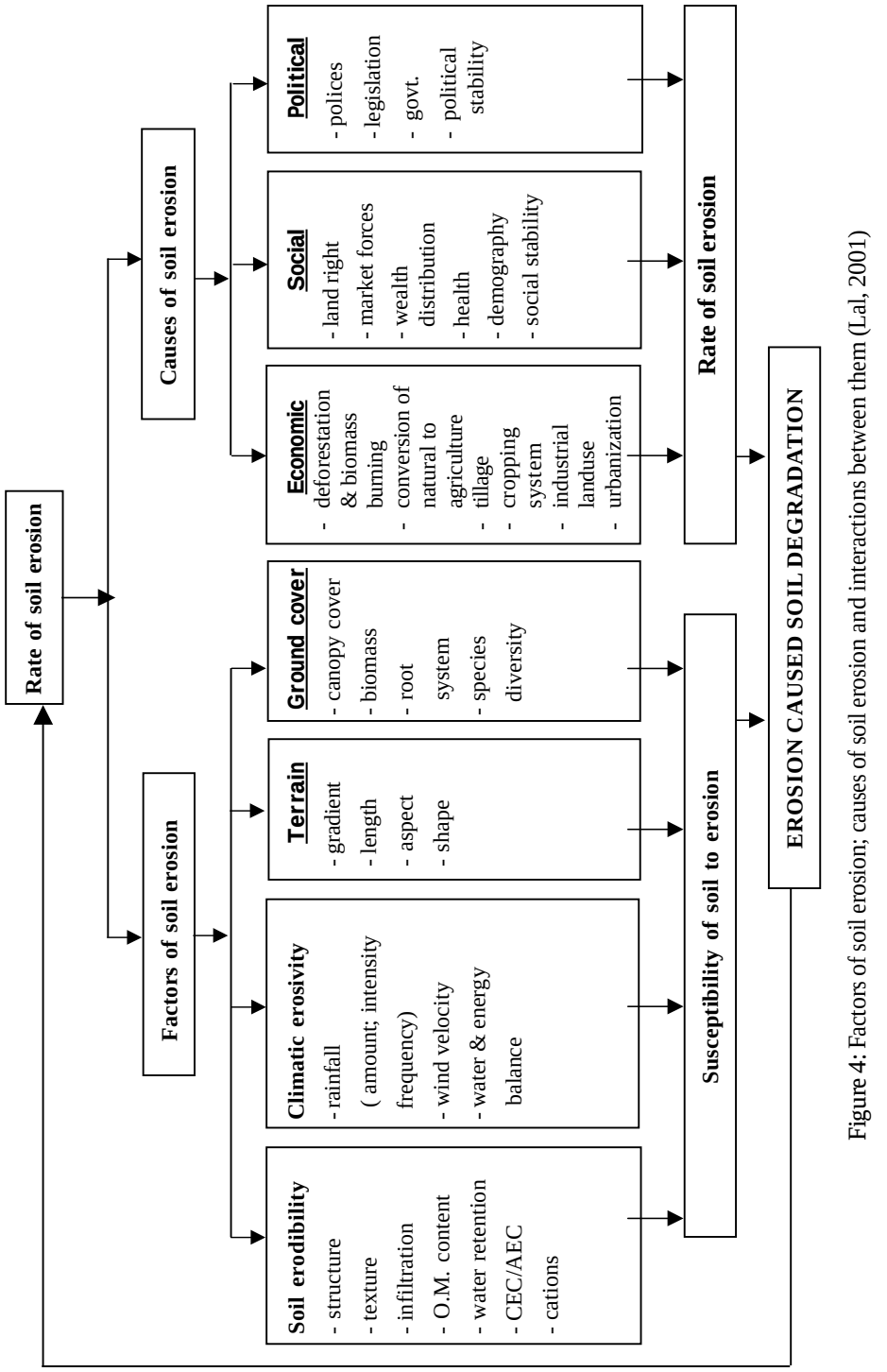

Figure 4: Factors of soil erosion; causes of soil erosion and interactions between them (Lal, 2001)

Soil erosion prediction and assessment has been a challenge to researchers since the 1930s' and several models have been developed (Lal, 2001). These models are categorized as empirical, semi-empirical and physical process-based models. Empirical models are primarily based on observation and are usually statistical in nature. Semi-empirical model lies somewhere between physically process-based models and empirical models and are based on spatially lumped forms of water and sediment continuity equations. Physical process-based models are intended to represent the essential mechanism controlling erosion. They represent the synthesis of the individual components which affect erosion, including the complex interactions between various factors and their spatial and temporal variabilities.

Some of the widely used erosion models are discussed below:

Empirical Models

Universal Soil Loss Equation (USLE)

USLE is the most widely used empirical overland flow or sheet-rill erosion equation. The equation was developed to predict soil erosion from cropland on a hillslope. The equation is given by –

$$A = R.K.L.S.C.P$$

Where, A is the average annual soil loss (mass/area/year); R is the rainfall erosivity index; K is the soil erodibility factor; L is the slope length factor; S is the slope gradient factor; C is the vegetation cover factor, and P is the conservation protection factor.

Revised Universal Soil Loss Equation (RUSLE)

The RUSLE updates the information on data required after the 1978 release, and incorporates several process-based erosion models (Renard *et al.*, 1997). RUSLE remains to be a regression equation –

$$A = R.K.L.S.C.P$$

A principal modification is in R factor which includes rainfall and run-off erosivity factor (run-off erosivity also includes snow melt where run-off is significant). There are also changes in C factor which is based on computation

of sub-factor called soil loss ratios (SLR). The SLR depends on sub-factors : prior landuse, canopy cover, surface cover, surface roughness and soil moisture (Renard *et al.,* 1997).

Semi-empirical Models

Modified Universal Soil Loss Equation (MUSLE)

Williams (1975) proposed a modified version of USLE that can be written as–

$$Sye = Xe.K.L.S.Ce.Pe$$

Where, Sye is the event sediment yield

$$Xe = \alpha. (Qe. qp) 0.56$$

Where, α is an empirical co-efficient; Qe is the run-off amount and qp is the peak run-off rate obtained during the erosion event and K.L.S.Ce & Pe are as defined for USLE.

Morgan, Morgan and Finney (MMF) Model

Morgan *et al.* (1984) developed a model to predict annual soil loss which endeavors to retain the simplicity of USLE and encompasses some of the recent advances in understanding of erosion process into a water phase and sediment phase. Sediment phase considers soil erosion to result from the detachment of soil particles by overland flow. Thus, the sediment phase comprises two predictive equations, one for rate of splash detachment and one for the transport capacity of overland flow. The model uses six operating equations for which 15 input parameters are required (Table 4). The model compares predictions of detachment by rain splash and the transport capacity of the run-off and assesses the lower of the two values as the annual rate of soil loss, thereby denoting whether detachment or transport is the limiting factor.

Physical Process-based Model

Empirical models have constraints of applicability limited to ecological conditions similar to those from which data were used in their development.

Further, USLE cannot deal with deposition; its applicability limits large areas and watersheds. Based on these considerations, several process-based models have been developed (e.g. WEPP, EUROSEM, LISEM (Lal, 2001)).

Table 4. Operative functions and input parameters of Morgan, Morgan & Finney Soil erosion model

Water phase:

$E = R * (11.9 + 8.7 * \text{Log } I)$ (1)

$Q = R * \exp(- R_C / R_0)$ (2)

Where,

$R_C = 1000 * MS * BD * RD * (E_t / E_0)^{0.5}$ (3)

$R_0 = R / R_n$ (4)

Sediment phase:

$F = K * (E * e^{-0.05 * A}) * 10^{-3}$ (5)

$G = C * Q^2 * \sin S * 10^{-3}$ (6)

- E - *kinetic energy of rainfall (J/m^2)*
- Q - *volume of overland flow (mm)*
- F - *rate of detachment by raindrop impact (kg/m^2)*
- G - *transport capacity of overland flow (kg/m^2)*
- R - *Annual rainfall (mm)*
- R_n - *Number of rainy days in the year*
- I - *Intensity of erosive rain (mm/h).*
- A - *Percentage of rainfall contributing to permanent interception and stream flow (%) .*
- E_t/E_0 - *Ratio of actual (E_t) to potential (E_0) evaporation.*
- MS - *Soil moisture content at field capacity or 1/3 bar tension (% w/w).*
- BD - *Bulk density of the top layer (Mg/m^3)*
- RD - *Top soil rooting depth (m) defined as the depth of soil from the surface to an impermeable or stony layer, to the base of A horizon; to the dominant root base.*
- K - *Soil detachability index (g/J) defined as the weight of soil detached from soil mass per unit of rainfall energy.*
- S - *Steepness of the ground slope expressed as slope angle.*
- C - *Crop cover management factor. Combines C and P factors of the USLE*

Water Erosion Prediction Project (WEPP) Model

WEPP is an example of widely used physically process-based erosion model (Renard *et al.*, 1996). It was developed as a system modeling approach for

predicting and estimating soil loss and selecting catchment management practices for soil conservation. Basic erosion and deposition equations in WEPP are based on the mass balance formulation that uses rill and inter-rill concept of soil erosion, which is a steady-state sediment continuity equation. The WEPP model computes erosion by rill and inter-rill processes. The sediment delivery to rill from inter-rill is computed by following equation –

$$Di = Ki. Ie^2. Ge. Ce. Sf$$

Where, Di is the delivery of sediment from inter-rill areas to rill ($kg/m^2/sec$); Ki is the inter-rill erodibility ($kg/m^4/sec$); Ie is the effective rainfall intensity (m/sec.); Ge is the ground cover adjustment factor and Sf is the slope adjustment factor calculated as per equation given below –

$$Sf = 1.05 – 0.85 \exp (-4 \text{ Sin } \alpha)$$

Where, α is the slope of the surface towards nearby rill. In comparison, rill erosion is the detachment and transport of soil particles by concentrated flowing water -

$$Dc = Kr. (T - Tc)$$

Where, Kr is the rill erodibility (sec/m); T is the hydraulic shear of flowing water (Pa) and Tc is the critical hydraulic shear that must be exceeded before rill detachment can occur (Pa).

Wind Erosion Model

Comparable to the USLE, a wind erosion model was proposed by Woodruff and Siddoway (1965) as shown in equation given below –

$$E = f (I, K, C, L, V)$$

Where, E is the mean annual wind erosion; I is the soil erodibility index; C is the climatic factor (Wind energy); L is the unsheltered median travel distance of wind across a field; V is the equivalent vegetative cover. This equation has been widely adopted and used for estimating erosion hazard in dry lands.

USE OF SATELLITE REMOTE SENSING AND GIS IN SOIL EROSION MODELING

The potential utility of remotely sensed data in the form of aerial photographs and satellite sensors data has been well recognized in mapping and assessing landscape attributes controlling soil erosion, such as physiography, soils, land use/land cover, relief, soil erosion pattern (e.g. Pande *et al.*, 1992). Remote Sensing can facilitate studying the factors enhancing the process, such as soil type, slope gradient, drainage, geology and land cover. Multi-temporal satellite images provide valuable information related to seasonal land use dynamics. Satellite data can be used for studying erosional features, such as gullies, rainfall interception by vegetation and vegetation cover factor. DEM (Digital Elevation Model) one of the vital inputs required for soil erosion modeling can be created by analysis of stereoscopic optical and microwave (SAR) remote sensing data.

Geographic Information System (GIS) has emerged as a powerful tool for handling spatial and non-spatial geo-referenced data for preparation and visualization of input and output, and for interaction with models. There is considerable potential for the use of GIS technology as an aid to the soil erosion inventory with reference to soil erosion modeling and erosion risk assessment.

Erosional soil loss is most frequently assessed by USLE. Spanner et al. (1982) first demonstrated the potential of GIS for erosional soil loss assessment using USLE. Several studies showed the potential utility of RS and GIS techniques for quantitatively assessing erosional soil loss (Saha *et al.*, 1991; Saha and Pande, 1993; Mongkosawat *et al.*, 1994). Satellite data analyzed soil and land cover maps and DEM derived and ancillary soil and agro-climatic rainfall data are the basic inputs used in USLE for computation of soil loss. Kudrat and Saha (1996) showed the feasibility of GIS to estimate actual and potential sediment yields following Sediment Yield Prediction Equation (SYPE) using RS derived soil and land use information, DEM derived slope and ancillary rainfall and temperature data. MMF model was used for quantification of soil loss by water erosion in Doon Valley, Dehra Dun, India, in GIS environment using various satellite remote sensing derived inputs (ASD, 2002).

The availability of GIS tools and more powerful computing facilities makes it possible to overcome difficulties and limitations and to develop distributed

continuous time models, based on available regional information. Recent development of deterministic models provides some spatially distributed tools, such as AGNPS (Young *et al.*, 1989); ANSWERS (Beasley *et al.*, 1980), and SWAT (Arnold *et al.*, 1993). The primary layers required for soil erosion modeling are terrain slope gradient and slope length which can be generated by GIS aided processing of DEM. Flanagan *et al.* (2000) generated the necessary topographic inputs for soil erosion and model simulations by linking WEPP model and GIS and utilizing DEM.

CASE EXAMPLES OF SOIL EROSION MODELING BY INTEGRATED USE OF REMOTE SENSING AND GIS

Soil Erosion Inventory in part of Bhogabati Watershed using RS & GIS following USLE

The study area is part of Bhogabati watershed which is located in Kolhapur district of Maharashtra, India. The area is characterized by warm, sub-humid tropical climate and the average annual rainfall is 1215 mm. The methodology adopted in this study for soil erosion modeling is depicted in Figure 5 (ASD, 2001). Soil and Land Use/Land Cover maps were prepared by analysis of IRS-1D : LISS III satellite data. Topographic factor (LS) was derived from DEM generated by GIS analysis. Various USLE factors and model derived erosional soil loss of the watershed are presented in Figure 6.

Regional Soil Erosion Inventory using RS & GIS following MMF model – a case study of Doon Valley

MMF modeling approach was tested for soil erosion inventory in Doon Valley, Dehra Dun district which is a part of northern India. The average annual rainfall ranges between 1600 to 2200 mm. The climate of the area is sub-tropical to temperate. The methodology adopted for this study for soil erosion modeling following MMF model is presented in Figure 7 (ASD, 2002). The various parameters of MMF model and model predicted erosional soil loss of the study area are presented in Figure 8.

CONCLUSIONS

Soil erosion involves complex, heterogeneous hydrological processes and models can only simulate these processes. USLE model is simple to use and conceptually easy to understand, but the greatest criticism of this model has

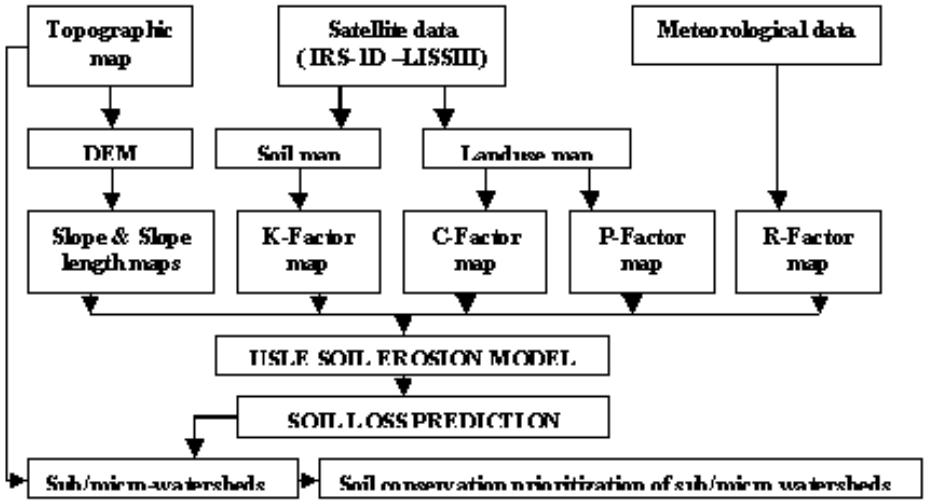

Figure 5: Flow diagram of methodology of soil erosion modeling using USLE

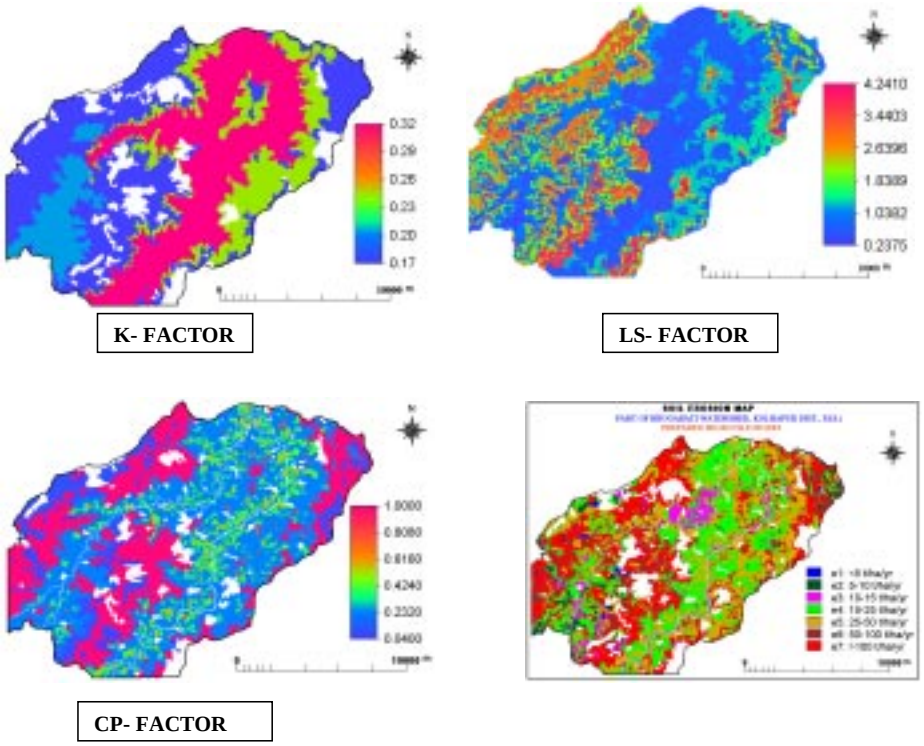

Figure 6: Factors of USLE and model predicted erosional soil loss (Bhogabati Watershed, Kolhapur District, Maharashtra, India)

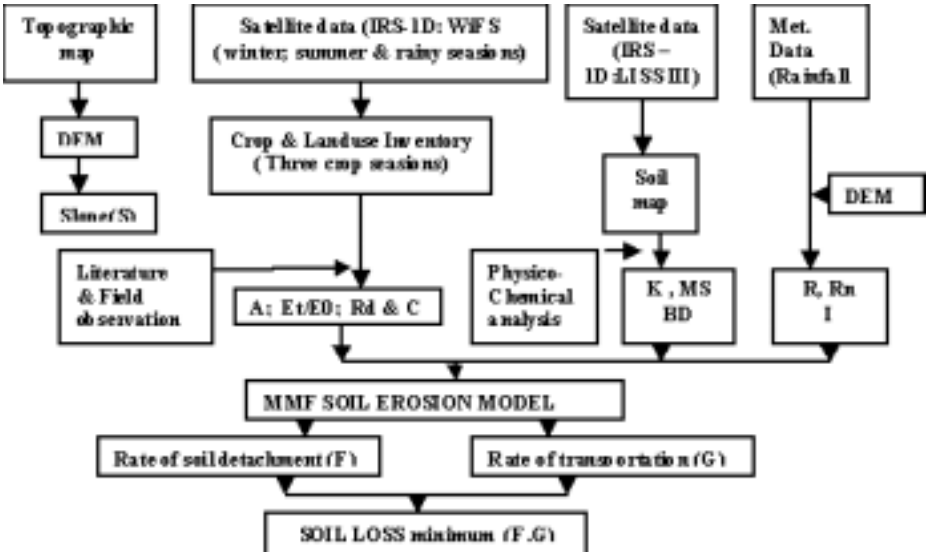

Figure 7: Flow diagram of methodology of soil erosion modeling using MMF model

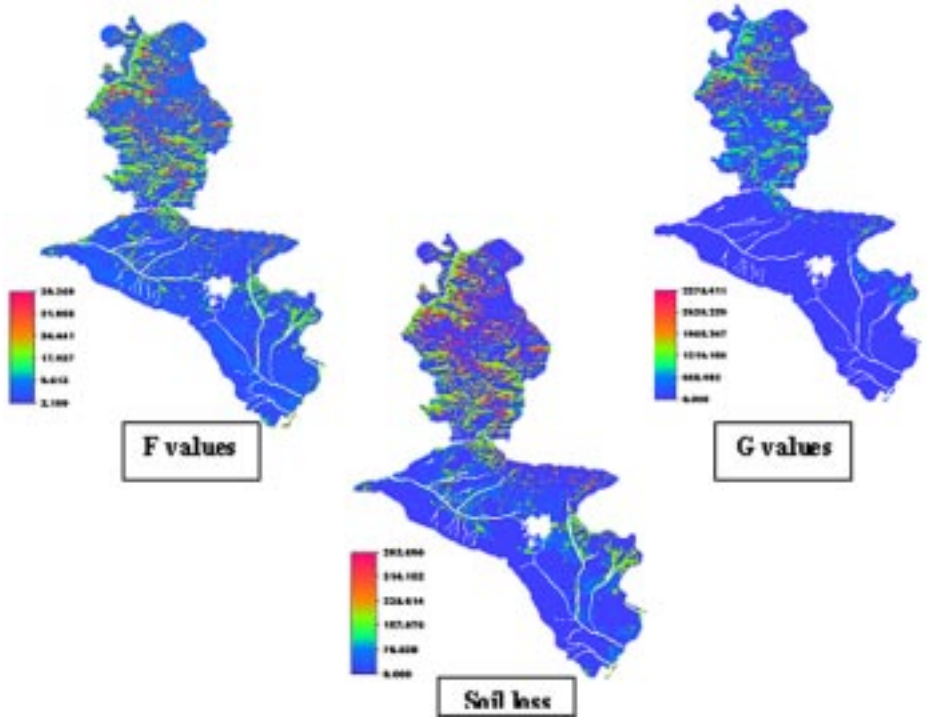

Figure 8: MMF model parameters F & G and model predicted erosional soil loss (Dehra Dun District, Uttaranchal, India)

been its ineffectiveness in applications outside the range of conditions for which it was developed. The process models and physically-based model have an advantage over simple statistical empirical models when individual processes and components that affect erosion are described simply and effectively. The disadvantages of these models are that the mathematical representation of a natural process can only be approximate and there are difficulties in the parameter prediction procedures. RS and GIS techniques are very effective tools for soil erosion modeling and erosion risk assessment.

REFERENCES

ASD 2001. Agriculture & Soils Division, IIRS P.G. Diploma Course pilot project report on Land Evaluation for Landuse Planning by integrated use of Remote Sensing and GIS – a case study of Bhogabati Watershed in Kolhapur district.

ASD 2002. Agriculture & Soils Division, IIRS P.G. Diploma Course pilot project report on Soil Erosion Inventory using IRS – WiFS data and GIS – a case study of Dehra Dun district (Uttaranchal).

Arnold, J.G., Engel, B.A. and Srinivasan, R. 1998. A continuous time grid cell watershed model. Proc. of application of Advanced Technology for management of Natural Resources.

Beasley, D.B.C., Huggins, L.F. and Monke, E.J. 1990. ANSWERS : a model for watershed planning. Transactions of ASAE. 23 : 938-944.

Flanagan, D.C., Renschler, C.S. and Cochrane, T.A. 2000. Application of the WEPP model with digital geographic information. 4th Int. Conf. on Integration of GIS and Environmental Modeling : Problems, Prospects and Research needs.

Lal, R. 1998. Soil erosion impact on agronomic productivity and environment quality: Critical Review. Plant Science, 17 : 319 – 464.

Lal, R. 2001. Soil degradation by erosion. Land Degradation & Development, 12 : 519 – 539.

Mongkolsawat, C., Thurangoon, P. and Sriwongsa 1994. Soil erosion mapping with USLE and GIS. Proc. Asian Conf. Rem. Sens., C-1-1 to C-1-6.

Morgan, R.P.C., Morgan, D.D.V. and Finney, H.J. 1984. A predictive model for the assessment of erosion risk. J. Agricultural Engineering Research 30: 245 – 253.

Pande, L.M., Prasad, J., Saha, S.K. and Subramanyam, C. 1992. Review of Remote Sensing applications to soils and agriculture. Proc. Silver Jubilee Seminar, IIRS, Dehra Dun.

Renard, K.G., Foster, G.R., Lane, I.J. and Laflen, J.M. 1996. Soil loss estimation. *In* Soil Erosion, Conservation and Rehabilitation; Agassi, M. (ed.). Marcel Dekkar, New York, 169-202.

Renard, K.G., Foster, G.R., Weesies, G.A., Mc Cool, D.K. and Yoder, D.C. 1997. Predicting soil erosion by water : A guide to conservation planning with the revised USLE. USDA Hand Book No. 703, USDA, Washington, D.C.

Saha, S.K. and Pande, L.M. 1993. Integrated approach towards soil erosion inventory for environmental conservation using satellite and agro-meteorological data. Asia-Pacific Rem. Sens. J., 5(2) : 21-28.

Saha, S.K., Kudrat, M. and Bhan, S.K. 1991. Erosional soil loss prediction using digital satellitee data and USLE, pages 369-372. *In* Applications of Remote Sensing in Asia and Oceania–environmental change monitoring (Shunji Murai ed.). Asian Association of Remote Sensing.

Spanner, M.A., Strahler, A.H. and Estes, J.E. 1982. Proc. Int. Symp. Rem. Sens. Environ., Michigan, USA.

Singh, G., Babu, R., Narain, P., Bhushan, L.S. and Abrol, I.P. 1992. Soil erosion rates in India. J. Soil Water Conservation, 47 : 93 – 95.

Venkateswarlu, J. 1994. Managing extreme stresses in arid zone of Western Rajasthan, India. *In* Stressed Ecosystem and Sustainable Agriculture. Virmani, S.M.; Katyal, J.C.; Eswaran, H. and Abrol, I.P. (eds.). Oxford & IBH Publishing, New Delhi, p. 161-171.

Williams, R. 1975. Sediment Yield Prediction with USLE using run-off energy factor. *In* Present and prospective technology for predicting sediment yields and sources. ARS-S-40, USDA, Washington D.C. : 244-252.

Woodruff, N.P. and Siddoway, F..H. 1965. A wind erosion equation. Soil Sci. Soc. Am. Proc., 29 : 602-608.

Young, R.A., Onstad, C.A., Bosch, D.D. and Anderson, W.P. 1989. AGNPS – Agriculture-Non-Point Source Pollution Model : A watershed analysis tool. Conservation Res. Report 35, USDA, ARS, Morris, MN, USA.

Zhang, L. 1994. A comparison of the efficiency of the three models to estimate water yield changes after forced catchment conversion. M.Sc. (Forest) Thesis, University of Melbourne, Australia.

SATELLITE BASED WEATHER FORECASTING

S.R. Kalsi
India Meteorological Department
Mausam Bhawan, Lodi Road, New Delhi

Abstract : Satellite data are increasingly being used in conjunction with conventional meteorological observations in the synoptic analysis and conventional weather forecast to extract information of relevance for agriculture in India. Synoptic applications of satellite imagery as in use at India Meteorological Department are highlighted in this report. Particular emphasis is laid on identification of large scale convective precipitation systems such as monsoon depressions and tropical cyclones. A brief review of national and international satellite systems of relevance to weather forecasts particularly for agriculture is provided. A summary of numerical products being derived from satellite data and their use in numerical models is also given. A brief on the New long range forecasting technique is included.

INTRODUCTION

Reliable weather prediction holds the key for socio economic development and is essential for food security of the human society. Since time immemorial, human race has been fascinated by the ever changing and highly dynamic atmosphere around him and has made concerted efforts to understand the controlling processes and achieve better capabilities of weather forecasting. The recent attempts for satellite based observations, made over the past two decades, have provided new insights in these processes. Synoptic coverage provided by satellites is ideally suited to study weather related atmospheric processes on different scales. The recent advances in satellite technology in terms of high resolution, multi-spectral bands covering visible, infrared and microwave regions have made space data an inevitable component in weather monitoring and dynamic modeling. The impact of satellite data is phenomenal in certain areas of meteorological applications such as short-range forecasts, Tropical Cyclone (TC) monitoring, aviation forecasts etc. With improving trend in accuracy of satellite retrievals, improvements could be carried out in models leading to improved forecasts, especially in the tropics.

Satellite Remote Sensing and GIS Applications in Agricultural Meteorology
pp. 331-346

CONTRIBUTIONS OF SPACE OBSERVATIONS

The launch of the first meteorological satellite TIROS-1 in April 1960 heralded the era of Space observations and gave the first glimpses of the dynamic cloud systems surrounding the Earth. Since then the technology has developed by leaps and bounds in observation capabilities in terms of spatial, spectral and temporal resolutions. A global system of Space observations with both geostationary and polar orbiting satellites has evolved.

The advantages of Space observations emanate from several factors such as:

- Synoptic view of large areas, bringing out the inter-relations of processes of different spatial scales.
- Frequent observations from geostationary satellites provide continuous monitoring while polar orbiting satellites give typical twice daily coverage; such data is relevant for study of weather system dynamics.
- The inherent spatial averaging is more representative than the point in-situ observations and readily usable for weather prediction models.
- High level of uniformity of space observations overcomes the problem of inter-calibration needed for ground based instruments.
- Filling of gaps in observations; Space data covers large oceanic areas and inaccessible and remote land areas, thus giving global coverage.
- New types of data and observations; parameters such as sea surface (skin) temperature, sea surface wind stress, sea level, cloud liquid water content, radiation balance, aerosol are some of the unique parameters provided only by satellites.
- Simultaneous observation of several dynamic parameters provided by different sensors in same platform facilitates study of inter-relationships and knowledge of processes (e.g. Sea Surface temperature and deep convection, cloud development and radiative forcing).

METEOROLOGICAL SATELLITES / PAYLOADS

Currently several operational meteorological satellites are providing global and regional observations. Six different types of satellite systems currently in

use are : 1) Visible/ Infrared/Water Vapour Imagers, 2) Infrared Sounders, 3) Microwave Imagers, 4) Microwave Sounders, 5) Scatterometers and 6) Radar Altimeters. Though the water vapour imaging capability is available only on the geostationary satellite, the visible and infrared imagers are available on geostationary as well as polar orbiting satellites. The last four are currently available only on polar orbiting systems. We first describe in detail below the INSAT system which is the primary satellite for weather surveillance in this part of the globe. It is a multipurpose geostationary satellite that caters to the requirements of Meteorology and Communication. It carries a met payload called Very High Resolution Radiometer (VHRR) that enables us to have visible, infrared and now even water vapour images. It is designed to provide the following services:

- Round the clock surveillance of weather systems including severe weather events around the Indian region.
- Operational parameters for weather forecasting – cloud cover, cloud top temperature, sea surface temperature, snow cover, cloud motion vector, outgoing long wave radiation etc.
- Collection and transmission of meteorological, hydrological and oceanographic data from remote/inaccessible areas through Data Collection Platforms.
- Timely dissemination of warning of impending disasters such as cyclones through Cyclone Warning Dissemination Systems.
- Dissemination of Meteorological information including processed images of weather systems through Meteorological Data dissemination system.

INSAT applications programme started with the launch of INSAT-1 series of satellites in early 1980s. INSAT-2 series that followed was designed based on user feedback. INSAT-2A and 2B launched in 1992 and 1993 carried VHRR payload with improved resolution of 2 km in visible and 8 km in thermal band. The imaging capability included three modes, viz. full frame, normal mode and sector mode of 5 minutes for rapid coverage of severe weather systems.

INSAT-2E launched in 1999 carried an advanced VHRR payload operating in three channels – visible (2 km), thermal and water vapour (8 km). The water vapour channel is capable of giving water vapour distribution and flow

patterns in the middle troposphere. Besides this, INSAT-2E also carried a CCD camera with 3 channels – visible, near infrared and short wave infrared with 1 km resolution to map the vegetation cover.

A geostationary meteorological satellite (METSAT) system devoted totally to meteorology was launched in 2002. It has been renamed as Kalpana-1 and is currently the operational satellite system being used by IMD.

INSAT-3A has been launched in April 2003 and carries identical payloads as in INSAT-2E. INSAT- 3D planned for future will also carry atmospheric sounder for temperature and water vapour profiles and split thermal channels for accurate sea surface temperature retrieval. Data from INSAT satellites are being used to retrieve a number of quantitative products. INSAT imagery is being used very exhaustively to provide support for synoptic analysis and weather forecasting. The quantitative products available from INSAT and its applications are described in subsequent sections.

Infrared Sounders

These systems are available on geostationary (GEOS N SERIES) and polar orbiting (NOAA 15-17/HIRS) Satellites. The primary application lies in direct assimilation of IR radiance in NWP models. IR sounders are going to have (2 orders of Magnitude) increase in the infrared channels. This will lead to large improvements in the vertical resolution of derived temperature and moisture profiles in clear areas and above cloud top level and improve the initial temperature and moisture fields.

Microwave Sounders

Similar to the microwave imager data, microwave sounder data from NOAA-15-17/AMSU instrument can provide valuable information below cloud top level. Tropospheric thermal measurements can be obtained in non-raining cloudy region. Microwave sounders data has proved to be very useful in determining upper tropospheric warm anomaly. This in turn is used in diagnosing intensity and intensity change of tropical cyclones (Brueske and Velden, 2000).

Microwave Imagers

VIS and IR provide proxy variables. Exact positioning of the eye is possible in VIS and IR imagery. Microwave (passive) sensors monitor radiation from

below the cirrus shield and provide information on atmospheric WV, cloud liquid water, precipitation, intensity and regions of convective activity. In June of 1987 the first satellite from the Defence Meteorological Satellite Programme (DMSP) carrying a microwave radiometer called Special Sensor Microwave/Image (SSM/I) was launched. It overlapped with the European Research Satellite (ERS-I) launched in July 1991 which carried a scatterometer. The swath width of the ERS-I scatterometer was only 500 km resulting, however, in the less than-complete coverage of the tropical regions each day.

The low horizontal resolution of some current radiometers may limit the usefulness of some parameters but the 15 km resolution of 85 GHz channel of SSM/I provides meso-scale information. This channel provides radar like imagery and is able to discern the circulation centres. Velden *et al.* (1989) describe the advantage of centre-fixing in TCs using 85 GHz imagery compared to conventional VIS and IR images where centres are covered in cirrus overcast. NASA launched a special satellite that aimed at making new measurements of meteorological quantities in the tropics. The Tropical Rainfall Measuring Mission (TRMM) has completed 3 years of successful data taking in 2000. With the change of its altitude from 350 km to 400 km, it will have enough fuel to provide continuous measurements upto 2005 (Velden and Hawkins, 2002). TRMM Microwave Imager (TMI) provides horizontal resolution of 5-7 km for 85 GHz channel which is 2-3 times better than the SSM/I, and the higher resolution TMI 37 GHz channel; can penetrate deeper into tropical cyclone to reveal additional details.

The Indian Remote Sensing Satellite (IRS-P4) launched in 1999 carried Multichannel Scanning Microwave Radiometer (MSMR). It is providing measurements at 6.6, 10, 18 and 21 GHz frequencies in both H&V polarizations. Attempts have been made to provide estimates of integrated water vapour, liquid water content, precipitation intensity, and SSTs over the global oceans (Gohil *et al.*, 2001).

Scatterometers

The primary application of the scatterometers is for Ocean Surface Wind Vectors. A scatterometer sends microwave pulses to the earth's surface and measures the backscattered power from the surface roughness elements. The back scatter power depends not only on the magnitude of the wind stress but also on the wind direction relative to the direction of the radar beam. The relation between backscatter signal and ocean surface winds is not well

established under the strong wind and rainy conditions of a cyclone because of lack of validation. After the failure of NASA's NSCAT system, there has been rapid deployment of a new system called Quikscat that provides a wide swath of 1800 km and unprecedented global ocean coverage. Wind fields from quikscat are available on near real-time to most TC forecast offices. The standard wind product has a 25 km spatial resolution. The data has provided the outer wind structure of tropical cyclones. It is also used to determine the radius of 35 knots (De Muth *et al.*, 2001), and for identifying closed circulations of developing systems and in providing lower limits for maximum sustained winds. Sarkar (2003) has reviewed techniques for surface wind measurements over global oceans from space platforms. The most successful wind sensor has been the microwave scatterometer.

Radar Altimeters

Many studies have shown that sub-surface thermal structure plays an important role in tropical cyclone intensification. The sub-surface structure can often be deduced from the satellite altimetry data. Research to better use these data in statistical forecast algorithms and the coupled ocean-atmosphere models has the potential to improve tropical cyclone intensity forecasts. The altimeter observations would be more useful with improved temporal and areal sampling. Multi-beam altimeters potentially can dramatically increase spatial sampling and fill the data voids.

SYNOPTIC APPLICATIONS IN IMD

The major application of satellite data has been the monitoring of Synoptic weather systems ranging from thunderstorms to cyclones and planetary scale phenomena such as monsoon. The dynamic nature of weather systems could be captured through the time series of satellite observations leading to better understanding of the process of genesis, growth and decay. This has led to satellite based technique (Dvorak technique) to assess the intensity of TC accurately and estimate the growth potential. The specific applications include identification of primary weather system such as low pressure, depression, troughs/ridges, jet streams regions of intensive convection, inter-tropical convergence zones etc. and onset and progress of monsoon system.

Following are the major applications of satellites images in operational weather forecasting:

i. Watch and monitor growth of weather phenomena like cumulonimbus cells, thunderstorm, fog etc. and their decay.

ii. Identify and locate primary synoptic systems like troughs/ridges, jet streams, regions of intense convection, inter tropical convergence zones etc.

iii. Monitor onset and progress of monsoon systems.

iv. Detect genesis and growth of TC and monitor their intensification and movement till landfall. This application is included in the next section.

Satellite imagery is being extensively used by synoptic network in conjunction with other available conventional meteorological data for analysis and weather forecasting. Zones of cloudiness are identified from the satellite imagery as regions of upward velocity and hence potential areas for occurrence of rainfall. Visible, infra red and water vapour images have distinctive uses and are complementary to each other.

We shall summarize below very briefly some of the very important applications in the operational synoptic analysis and weather forecasting.

Satellite imagery is very handy for remote and inaccessible areas such as Himalayas where heavy precipitation usually builds up. Though the characteristic cloud patterns of cold and warm fronts are not seen over India, the Western disturbances giving rise to heavy snow fall are well captured in the Satellite imagery (Kalsi and Mishra, 1983). The Cloud band ahead of well marked westerly trough is clearly seen in the Satellite imagery. The characteristic structure of snow is easily identified and its areal extent is monitored for estimating run-off and also for long range prediction of monsoon.

Deep penetrative CB clouds and thunderstorm complexes (Kalsi and Bhatia, 1992) are rather easy to be identified in visible and infrared imagery. Squall lines are clearly seen in the satellite loops. Satellite imagery provides powerful signals for forecasting severe weather (Purdom, 2003).

The rain bearing Southwest monsoon system advances northward usually as an intermittent band of cloudiness called inter-tropical convergence zone (ITCZ). It comprises of numerous rain showers and thunderstorms associated with the convergence in the shear zone. One of the earliest studies (Sikka &

Gadgil, 1980) showed the 30-40 day oscillatory nature of monsoon flow. The INSAT and NOAA sounding data have brought out the unique nature of monsoon onset with large scale changes in wind and moisture profiles in lower troposphere prior to monsoon onset. Using satellite data Joshi *et al.* (1990) have also noted a spectacular rise in the 300 mb temperature over the western central and eastern Tibetan Plateau and over the region of the heat low over Pakistan. They noted this rise commencing almost 2 weeks prior to the onset of monsoon rains over southwestern India. This appears to be an important parameter for monitoring the onset of monsoons and requires to be monitored in connection with forecast of the onset of monsoon operationally. Joseph *et al.* (2003) have identified conditions leading to onset of monsoon over Kerala using SST, OLR and winds obtained from satellite systems.

The monsoon depressions are the principal rain bearing systems of the southwest monsoon period over India. Substantial amounts of rainfall are generated by the westward passage of monsoon depressions forming in the bay. Monsoon depressions usually develop from innocuous looking cloud systems and from diffuse pressure fields over the head Bay of Bengal. Satellite imagery shows heavy overcast cloud mass in the southern sector with low level cumulus clouds determining the Low-Level Circulation Centre (LLCC) to the northeast. The LLCC is often free of deep convection. The widespread and heavy rainfall in the southwest sector is often accompanied with deep convection in that sector. Kalsi *et al.* (1996) have shown from satellite imagery that a few of these depressions acquire structure of marginal cyclones with almost vertical structure upto mid-tropospheric levels. Following Scoffield and Oliver (1977), Mishra *et al.* (1988) also used the enhanced infrared satellite imagery to compute satellite derived rainfall estimates which were found to be realistic. These signatures provide a lot of insight into physical and dynamical processes at work in the case of monsoon depressions and are extremely useful for short range forecasting.

The 16 parameter statistical model used by India Meteorological Department has several parameters that are provided by Satellite data such as the SST, Snow Cover, E1 Nino event etc. Several recent modeling studies show that a significant fraction of the inter-annual variability of monsoon is governed by internal chaotic dynamics (Goswami, 1998). The numerical weather prediction of monsoon received impetus from the satellite observations. The parameters of SST, cloud motion vector, OLR are found to have impact on model results.

RESEARCH AND APPLICATIONS IN THE FIELD OF TROPICAL CYCLONES

With its unmistakable spiral shape and central eye, the tropical cyclone is the most memorable feature on any satellite image. Indeed, if weather satellites detected nothing else besides these monster storms, they would be worth the money invested in them. A number of techniques have been developed to estimate the movement and intensity of tropical cyclones. One of the most widely accepted is the Dvorak (1984) technique which assigns an intensity based on the size and shape of the dense cloud mass adjacent to the centre of the circulation of the storm. TC intensity is estimated using VIS and IR imagery. Fixes are also made using scatterometer, TRMM, multispectral and special sensor microwave imager (SSM/I) data. IR imagery is the workhorse of the TC analysis because of its 24 hours availability. VIS imagery provides the highest resolution and is the best channel available for detection of surface features that may not be seen in the IR or WV imagery. Multispectral imagery which highlights features both at low and high levels is used to determine TC intensity and position. Satellite fixes of position are added to the fixes data base along with fixes from other sources. This is used to develop a Working Best Track and for input of TC bogus into numerical models. A lot of insight has been gained into physical and dynamical progress shaping development of TCs. Satellite imagery has also been very exhaustively used for the analysis of TCs developing in the north Indian Ocean (Kalsi 1999 & 2002). The satellite based observations have opened up new research areas for improved forecasting of intensity and track. Some of the emerging research areas are:

- The 'warm core approach' using MSU sounding data to analyse warm temperature anomalies in upper troposphere and correlate to central pressure fall and maximum winds (DeMuth *et al.*, 2001).
- The objective Dvorak technique (ODT) for intense cyclones (Velden *et al.*, 1998) and Advanced Objective Dvorak technique (AODT) for weak systems.
- Storm surge prediction using satellite derived radius of maximum winds, intensity, direction and speed of cyclones.
- Use of satellite data for synthetic vortex generation in numerical models.
- Assimilation of satellite data as mentioned under section 8 below.

Applications of Water Vapour channel data

Imaging in the water vapour channel greatly enhances insight into atmospheric circulation and humidity in the middle atmosphere. The physical basis of water vapour band is the strong absorption of emitted terrestial radiation by atmospheric water vapour. The water vapour channel peaks at 400 mb and the radiance is used for computation of mid-tropospheric moisture content (Velden *et al.*, 1997; Joshi *et al.*, 2001). Water vapour structure also correlates very well with atmospheric motion and thus can be used to delineate jet cores. Thick CB clouds with anvil appear prominently in both water vapour and thermal data. Water vapour appearing as plumes are indicators of heavy rainfall regions, leading to flash floods. IMD has also started using water vapour images. Some of the applications are:

- Water vapour plumes appearing as a tongue or stream of moisture indicating cyclonic circulation leading to heavy rainfall.
- Forecasting track of cyclones, such as recurvature indicated by the moisture envelop around the cyclone field (Bhatia *et al.*, 1999).
- Filling of gap in upper air observations (low density of radiosonde stations in tropics).

SATELLITE PRODUCTS GENERATED AT IMD

Kelkar (1995) has furnished an exhaustive review of quantitative products available from INSAT data. INSAT Meteorological Data Processing System (IMDPS) computes the following numerical products:

1. Cloud Motion Vectors (CMVs)
2. Quantitative Precipitation Estimates (QPEs)
3. Outgoing Long-wave Radiation (OLR)
4. Vertical Temperature Profiles (VTPRs)
5. Sea Surface Temperatures (SSTs)

CMVs, now also termed as atmospheric motions vectors (AMVs), computed from a triplet of satellite scans are disseminated operationally on Global Telecommunication System (GTS) for international consumption. Since the emphasis in the tropics is on the winds, the CMVs find relevance in the

analysis of wind field. They have significant impact on the accuracy of numerical models. Though no systematic validation studies of CMVs computed from INSAT data have been carried out, limited studies made by ECMWF in this regard indicate that the quality of this product has shown some improvement. The problems in the derivation of high quality CMVs in the region of active convective disturbances however, still continuing. There are no CMVs in the areas characterized by deep convection and height assignment is also leading to problems.

A large number of schemes have been developed over the years to infer the precipitation estimates from satellite pictures. Since in the tropics, there is preponderance of convective clouds, cloud history methods are of relevance for determination of QPEs. The arkin algorithm (Rao *et al.*, 1989) is being applied to derive operationally large-scale precipitation estimates on daily, weekly and monthly basis. Rainfall is used both as an input in the numerical model scheme for physical initialization and also for verifications of model predicted precipitation. The NWP schemes are unable to account adequately for the diabetic heating.

SSTs are derived from IR Channel (10.5-12.5μm) data from INSAT. A major anomaly in the accurate derivation of SST field is due to attenuation by the moisture in the overlying column, which is compounded by the fact that it is a single broad band channel data. Retrieval of SST during the monsoon season is badly affected due to heavy clouding. Though the seasonal gradients in the SST field are brought out, the accuracy is doubtful.

The Outgoing Longwave Radiation (OLR) is calculated using physical/ statistical algorithm on the IR window channel data received three hourly at IMDPS. Regular OLR derivation have been in progress since 1986. OLR has come out to be a proxy parameter for many of the research applications. OLR data derived from INSAT IR band is being operationally fed to NCMRWF, New Delhi where it is used in their schemes for physical initialization.

Khanna and Kelkar (1993) have described the system for derivation of temperature soundings of the atmosphere over the Indian region using satellite data. They employed physical retrieval method and generated regression estimates using SSU and MSU channels as initial guess. The high resolution sounding data from IMDPS is being assimilated in numerical models at IMD and NCMRWF.

IMPACT OF SATELLITE DATA ON NUMERICAL WEATHER PREDICTION MODELLING

A global spectral model (T-80/L/16) and a global data assimilation system based on short range forecast (six hours) of this model involving Spectral Statistical Interpolation (SSI) scheme of analysis has been operational at the NCMRWF since June 1994. The satellite data sets received on GTS along with many other data sets received directly from the satellite data sources are being routinely used on operational basis. Mitra *et al*. (2003) reported encouraging results made towards assimilation of different types of satellite data on the analysis and forecast system of NCMRWF. Inclusion of high density satellite winds improved the performance of the model in refining many of the flow features during the southwest monsoon season over India.

IMD is also running a limited area analysis and forecast system in which a variety of conventional as well as non-conventional data received on GTS system of WMO is being ingested. Prasad (1997) described the synthetic vortex generation scheme for numerical forecasting of TCs. The scheme basically generates radial distribution of surface pressure within the vortex from a empirical formula proposed by Holland (1980). Basic inputs for generating the surface pressure are the parameters like central pressure of the storm, its environmental pressure, radius of maximum wind, current position, movement and intensity of the storm, which are inferred from the satellite imagery. Surface winds are obtained from the gradient wind relationship. Upper winds are computed from surface winds by using composite vertical wind shear factors proposed by Anderson and Hollingsworth (1988). Recently a Quasi-Lagrangian Model (QLM) has also been installed. Inputs from the satellite data are quite important for initializing the vortex position.

Three areas wherein satellite data have significantly contributed to numerical weather prediction are: defining the initial conditions of the model, setting of the boundary conditions, and defining the forcing functions. The satellite derived parameters on SST, sea surface winds, temperature/humidity profiles etc. have been assimilated into the models and found to have significant impact on the forecast outputs. Boundary conditions play a crucial role in extended/seasonal/long-term predictions and several inputs such as SST-snow cover, vegetation cover, soil moisture, etc. are provided by satellite data. The impact studies carried out using the Extended Range Monsoon Prediction model (Pal *et al.*, 1999) using SST and soil moisture has given new insights into their crucial role. One of the important forcing functions namely radiation

budget operationally available from satellites is an important input to models. The most current research is focussing on assimilation of satellite inputs to models for improved performance.

FUTURE MISSIONS

Several satellite missions have been planned to support the operational data needs and ongoing research efforts. The future Metsat missions will carry improved VHRR and vertical sounders for temperature/humidity profiles. The Megha -Tropiques Mission scheduled for 2004 launch will be a joint project by ISRO and CNES, France with the objective of studying the water cycle and energy exchanges in the tropics. With an equatorial inclined orbit, the satellite will have high repetitively over tropical regions.

The future appears bright for our space-based observing system. Advanced, multispectral (visible, IR, and passive microwave) imagers, sounders (infrared and microwave) and scatterometers are planned for launch in the near future. Hyperspectral measurements from newly developed interferometers are expected to be flown experimentally by 2006. The information content will vastly exceed that of the current measuring devices. Instead of a few dozen viewing channels, these instruments will have more than a thousand channels over a wide spectral range. The satellite data downloads are expected to exceed several terabytes per day. Fortunately, communications and computing capacity are increasing at a rate that hopefully can accommodate this data explosion. Emerging new technologies (including the use of rapidly developing visualization tools) will be employed. It is important that the evolving space-based observational system keeps one step ahead of the demands being placed by the user community and advances in numerical weather prediction. While it will become an enormous task and challenge to assimilate this wealth of data into meaningful parameters, the outlook is bright for unlocking the still-unresolved mysteries towards improving our understanding and prediction of atmospheric circulation systems such as tropical cyclones.

CONCLUSIONS

Integrated use of satellite data and conventional meteorological observations is found to be very useful for synoptic analysis and conventional forecast to extract information relevant for agriculture in India. Synoptic applications of satellite images for operational weather-forecasting in India are discussed in this article. A summery of use of numerical products derived from meteorological satellite data in numerical climatic models is also presented.

ACKNOWLEDGEMENTS

The author is extremely grateful to Dr. R.R. Kelkar, Director General of Meteorology, India Meteorological Department, New Delhi to enable him to deliver lecture in the Training Workshop on Remote Sensing Data Interpretation for applications in Agricultural Meteorology Jointly organized by WMO, CSSTEAP, IIRS and IMD from July 7-11, 2003 at Dehradun. The author is also thankful to the organisers for inviting him to the workshop.

REFERENCES

Anderson, F. and Hollingsworth, A. 1988. Typhoon bogus observations in the ECMWF data assimilation systems.

Bhatia, R.C., Brij Bhushan and Rajeswara Rao, V. 1999. Application of water vapour imagery received from INSAT-2E. Current Science, 76: 1448-1450.

Brueske, K.F. and C.S. Velden, 2000. Tropical cyclone intensity estimation using the NOAA-KLM series AMSU : Preliminary results and future prospects. Preprints, 24th Conf. Hurr. Trop. Meteor., Fort Lauderdale, FL, Amer. Meteor. Soc., p. 258-259.

DeMuth, J.D., M. DeMaria, J. Knaff and T.H. VonderHaar, 2001. An objective method for estimating tropical cyclone intensity and structure from NOAA-15 AMSU data. Preprints 24th Conf. Hurr. Trop. Meteor., Fort Lauderdale FL, AMS, p. 484-485.

Dvorak, V.F. 1984. Tropical cyclone intensity analysis using satellite data. NOAA Tech. Rep. NESDIS. 11, 44 pp.

Goswami, B.N. 1998. International variations of Indian Summer Monsoon in a GCM : External conditions versus internal feedbacks. Jou. of Climate., 11: 501-502.

Gohil, B.S., Mathur, A.K. and Verma, A.K. 2001. Proceed. of Pacific Ocean Remote Sensing Conf., 2000, 5-8 December, 2000, NIO, Goa, India, 207-211.

Holland, G.J. 1980. An analytical model of the wind and pressure profiles in hurricanes. Mon. Wea. Rev., 108: 1212-1218.

Joseph, P.V., K.P. Sooraj and C.K. Rajan 2003. Conditions leading to Monsoon onset over Kerala and the associated Hadley cell. Mausam, 54(1): 155-164.

Joshi, P.C., Simon, B. and Desai, P.S. 1990. Atmospheric thermal changes over the Indian region prior to the onset as observed by satellite sounding data. Int. J. Clim., 10: 44-56.

Kalsi, S.R. and Mishra, D.K. 1983. On some meteorological aspects of snowfall over Himalayas and observed by satellite. Proc. of the First National Symp. on Seasonal Snow Cover, 28-30 April, 1983, New Delhi, p125-132.

Kalsi, S.R. and Bhatia, R.C., July-December 1992. Satellite observations of thunderstorm complexes in weakly forced environments. Vayu Mandal, 22: 65-76.

Kalsi, S.R., Rao, A.V.R.K., Misra, D.K., Jain R.K. and Rao, V.R. 1996. Structural variability of tropical disturbances in the Bay of Bengal. In Advances in Tropical Meteorology, Ed. by R.K. Datta. Concept Publishing Company, New Delhi. 449-458.

Kalsi, S.R. 1999. Multiple eyewall structure in an Arabian Sea Cyclone. Current Science 77 (8): 1175-1180.

Kalsi, S.R. 2002. Use of satellite imagery in tropical cyclone intensity analysis and forecasting. Meteorological Monograph, Cyclone Warning Division No. 1/2002, India Meteorological Department, New Delhi-110003, India.

Khanna, P.N. and Kelkar, R.R. 1993. Temperature sounding of the atmosphere over the Indian region using satellite data. Mausam, 42(2): 167-174.

Kelkar, R.R. 1995. Satellite products from IMD. WMO TMRP Series Rep. No. 52, 91-94.

Mishra, D.K., Kalsi, S.R. and Jain, R.K. 1988. The estimation of heavy rainfall using INSAT-1B. Mausam, 39(4): 19-40.

Mitra, A.K., Das Gupta, M., Prasad, V.S., Kar, S.C. and Rajan, D. 2003. Weather and Climate Modeling. New Age International Publishers, p. 23-36.

Pal, P.K., Prakash, W.J., Thapliyal, P.K. and Kishtwal, C.M. 1999. Technique of rainfall assimilation for dynamic extended range monsoon prediction. Meteo. Atmos. Phys. 71: 157-168.

Prasad, K. 1997. Prediction of tropical cyclones by numerical models-A review. Mausam, 48 (2): 225-238.

Purdom, J.F.W. 2003. Local severe storms monitoring and prediction using satellite systems. Mausam, 54(1): 141-154.

Rao, A.V.R.K., Kelkar, R.R. and Arkin, P.A. 1989. Estimation of precipitation and outgoing longwave radiation from INSAT-1B radiance data. Mausam, 40: 123-130.

Sarkar, A. 2003. Space based techniques for remote sensing of oceanic winds: A review. Mausam, 54(1):111-120.

Scoffield, R.A. and Oliver, V.J. 1977. A scheme for estimating convective rainfall from satellite imagery. NOAA Tech Memo NESS 86, Washington D.C., 47.

Sikka, D.R. and Gadgil, S. 1980. On the maximum cloud zone and the ITCZ over Indian longitudes during the southwest monsoon. Mon. Wea. Rev., 108: 1840-1853.

Velden, C.S., C.M. Hayden, S.J. Nieman, W.P. Manzel, S. Wanzong and S.J. Goerss, 1997. Upper tropospheric winds derived from geostationary satellite water vapour observations. Bulletin of Amer. Met.Soc., 78: 173-195.

Velden, C.S., T. Olander and R. Zehr, 1998. Evaluation of an objective scheme to estimate tropical cyclone intensity from digital geostationary satellite infrared imagery. Weather Forecasting, 13: 172-186.

Velden, C.S., Olson, W.S. and Roth, B.A. 1989. Tropical cyclone centre-fixing using SSM/1 data. Preprints of 4th conf. on Sat. Met. Ocean., AMS, Boston, MA 02108, J36-39.

Velden, C.S. and Hawkins, J.D. 2002. WMO TMRP Rep No. 67, Rapporteur Report on Topic 0.3.

SATELLITE-BASED AGRO-ADVISORY SERVICE

H. P. Das
Division of Agricultural Meteorology
Indian Meteorological Department, Pune

Abstract : Remote sensing techniques have been operationally used in many countries to provide basic information on crops, soils, water resources and the impact of drought and flood on agriculture. Procedures for pre-harvest acreage estimation of major crops such as wheat, rice and sorghum, using sampling and digital techniques based on remotely sensed data have improved greatly. Remote sensing can also provide data related to ocean and coastal zones like identifying potential area of fish concentration, environmental degradation that takes place in coastal zones due to over exploitation, etc. Other promising areas of applications include, disaster assessment, drought monitoring, environmental monitoring, forestry information, etc. all of which have advanced significantly.

The main users of crop maps and yield forecasts are governments and agribusiness who use them to assess demand, anticipate prices and plan the use of resources. Farmers do have a considerable interest, in knowing about problems in crops, and developments of the vegetation index concept could provide valuable information in stress management, for example in assessing irrigation demand, disease, pest and weed control, and crop nutrition. This information must be delivered or made accessible in sufficient time for the user to make professional sense and use these advisories appropriately in the management process.

INTRODUCTION

Ever since satellite remotely sensed data was available in digital format, the use of computers for analysis and interpretation of the data took roots. As the data actually depicted the state of the land as it existed at the time of observation, it was like bringing the ground to the office in the form of a picture to be studied by the various specialists. Data sets available from a variety of satellites have opened up tremendous possibilities of extracting a variety of information. In several cases of resources studies, the technique is operational, catering to several varied needs in the area of management of natural resources.

Satellite Remote Sensing and GIS Applications in Agricultural Meteorology
pp. 347-359

The major advantage in using satellite remotely sensed data is that it is the latest available at any given time.

Remote sensing techniques have been operationally used in many countries to provide basic information on crops, soils, water resources and the impact of drought and flood on agriculture. Integrated studies on soil and water conservation using remote sensing and GIS have been progressing with a view to raising agricultural production. In India procedures for pre-harvest acreage estimation of major crops such as wheat, rice and sorghum, using sampling and digital techniques based on remotely sensed data have improved greatly.

The question that arises is in what respect can remote sensing be used in agricultural information systems. In fact agricultural production encompasses myriad activities related to crops, soils, water resources, climate and local weather of the region. For some of the specific themes of these disciplines, remote sensing technology has been observed to be operational and in some others some more research may be needed to enable integration into the total agricultural information system.

Mainly, an agricultural resources inventory may need some knowledge of geology and geomorphology, forestry and vegetation, land use, and land degradation information, agricultural crops, water resources and agro-meteorology. The use of remote sensing data to obtain information and produce maps on a 1:50 000 scale is almost operational in all the aspects as mentioned above.

Agro-meteorological Information based on Remote Sensing data

Application potentials of remote sensing techniques on resources related to some important agrometeorological services are mentioned here :

- Agriculture (crops): One basic information that remote sensing can provide to agriculture is data related to crop identification and area measurement under different types of crops, or acreage estimation. This enables us to somewhat estimate the total production by understanding the yield per unit area. Such information has far-reaching consequences in providing adequate food security.

- Forestry and vegetation mapping: Remote sensing can aid in providing a) information about the extent of forest cover and give a general idea of the types of forest cover; b) forest canopy density condition ; c) detection of forest hazards like fire, disease and excessive felling.

- Water resources : Understanding water resources is important from agricultural point of view. Water supply to agriculturally related sectors depends upon the available resources, both in terms of quantity and quality. Remote sensing data is useful in assessing water resources, irrigated area studies and its monitoring and determining potential ground water zones.

Remote sensing can also provide data related to ocean and coastal zones like identifying potential area of fish concentration, environmental degradation that takes place in coastal zones due to over exploitation, etc. Other promising areas of applications include, disaster assessment, drought monitoring, environmental monitoring, etc. all of which have advanced significantly.

Assessment of Crop Condition and Estimation of Yields by Remote Sensing technique

The use of remote sensing data for estimating crop acreage estimation has reached a stage near operational level. Studies carried out for estimating acreage under different crops in many countries show a near 90 percent accuracy level. In many countries, production forecasting of certain crops, crop yield modeling and crop stress detection are done using remote sensing data. Yield is influenced by many factors, such as crop genotype, soil characteristics, cultural practices adopted, meteorological conditions and influences of diseases and pests. Many approaches have been followed to determine the integrated effects of various parameters that affect crop growth and crop yield. Several yield models have been developed in which data obtained from various types of satellites to cover some of the parameters have been used (Gupta, 1993; Doraiswamy *et al.*, 1996).

A major constraint however is a cloudy sky during the cropping season when normal optical remote sensing cannot give good data. However with the emergence of microwave remote sensed data, this can be overcome as such instruments can penetrate through clouds. To ensure complete success in predicting yields, some more research experiments may be needed to evolve a foolproof system.

Many countries have developed methods to assess crop growth and development from several sources of information such as, surveys of farm operators, crop condition reports from field surveys and local weather information. Remote sensing technology can provide supplemental spatial data

to provide timely information on crop condition and potential yields. The timely evaluation of potential yields is increasingly important because of the growing economic impact of agricultural production on world markets. The use of the NDVI parameter to estimate crop yields is a specific extension of the above general concept. The seasonal accumulated NDVI values correlate well with the reported crop yields in semi-arid regions (Groten, 1993).

Crop growth simulation models have been successfully used for predicting crop yields at the field level. However, numerous input requirements that are specific to the crop type, soil characteristics and management practices limit their applicability for regional studies. Integrating parameters derived from remotely sensed data with a growth model provides spatial integrity and near real time "calibration" of crop growth simulations. Remotely sensed data are incorporated in simulations of agricultural crop yields to calibrate or adjust model parameters during the simulation period to ensure agreement between the modeled and satellite observed parameters (Maulin *et al.*, 1995).

Real time Forestry Information from Satellite data

The use of satellite remote sensing data has been found to be a reliable and useful tool for gathering forest information. Gathering of real time forestry information enables us to compile gross forest vegetation resources data in a single format and monitor the changes in the areal coverage of the forest.

Since remote sensing satellites re-observe the same areas at periodic intervals, we have the added advantage of monitoring changes that occur in the area of coverage, to plan for remedial measures for any adverse happening, much sooner than what we were able to do in the past, when the facility of remote sensing from space altitudes was not available. It is in this context that we could view forest cover or vegetation cover of a large area, and the changes that occur to it, as the forest is a renewable natural resource which is very vital for human survival. The type of exercise also gives us the approximate rate at which the forest cover is changing and focusses attention on what should be done to ensure sustainability.

Identification of Fishing zone by Remote Sensing

Remote sensing methods have helped greatly in the optimisation of ocean resources. As 60 to 70 per cent of the world's population live within 20-30 km of the coastline, coastal zone management and optimisation of ocean

resources have grown in importance. With the advent of remote sensing methods using satellite and aerial survey, the data coverage and accessibility have increased. Several parameters relating to the oceans including fisheries can be studied using satellite and aircraft data.

While other ocean related applications have become possible on remotely sensed data from satellites, on a near real-time basis, here, it has been shown how a particular satellite and the sensor mounted on it have been used to obtain sea surface temperature and map it, on a regular basis, and pass it on to the fishermen who could concentrate on high potential areas and improve the catch.

The ocean colour as measured by the sensor is found to bear a direct relationship with the suspended material of the water, thermal characteristics and the location of greenish biological matter. One of the important parameters that can be measured with sufficient accuracy is the Sea Surface Temperature (SST), which has related to the concentration of fish population. This is an example of how a high technology has been applied at the grass-root level increasing the earning capacity by increased fish catches.

Fishing Zone Maps

SST derived from NOAA-AVHRR satellite serves as a very useful indicator of prevailing and changing environmental conditions and is one of the important parameters which decides suitable environmental conditions for fish aggregation. SST images obtained from satellite imagery over three or four days are composited and the minimum and maximum temperatures are noted down. These values are processed to obtain maximum contrast of the thermal information. This information is used to prepare relative thermal gradient images.

From these images, features such as thermal boundaries, relative temperature gradients to a level of 1 degree centigrade, level contour zones, eddies and upwelling zones are identified. These features are transferred using optical instruments to corresponding sectors of the coastal maps prepared with the help of Naval Hydrograph charts. Later, the location of the Potential Fishing Zone (PFZ) with reference to a particular fishing centre is drawn by identifying the nearest point of the thermal feature to that fishing centre. The information extracted consists of distance in kilometres, depth (for position fixing) in metres and bearing in degrees with reference to the North for a particular fishing centre.

Monitoring Natural Disasters by Remote Sensing

While aerial remotely sensed data were used for a long time, it is the satellite based remote sensing data which, because of its continuous availability and capacity to observe large areas, is considered a powerful medium to monitor the changes in the Earth's environment and take timely action. Remote sensing satellite information helps minimise damages e.g. the death of cattle, humans etc. and the damage of agricultural production in time of natural calamities by early warning system.

Floods occur mainly due to heavy rainfall in association with low pressure, depressions and cyclones. While floods and cyclones cannot be totally eliminated, careful monitoring and planning can certainly mitigate the destruction and help in evolving suitable rehabilitation measures based on remotely sensed data.

Attempts are being made to evolve a drought prediction system using remotely sensed data, but drought prediction is difficult, and a foolproof mechanism will probably take time. However, the severity of droughts can easily be assessed, thus providing information to the authorities for implementing relief measures.

Forest fires are considered a potential hazard with physical, biological, ecological and environmental consequences. Forest fires occur frequently in tropical countries particularly in the dry and hot seasons causing serious damage to the forest resources and agricultural production. Since the number of forest fires are increasing every year, continuous monitoring is of great importance, not only to understand present trends but also to devise a model to predict the possibility of fires in future. In a recent fire in the Rajiv Gandhi National Park situated in South Karnataka (India), remote sensing data was used for studying environmental aspects and the results were very encouraging.

Monitoring Pests and Disease from Satellite data

Various factors such as intensive cultivation, monocropping, changing weather conditions and indiscriminate use of pesticides have resulted in frequent outbreaks of crop pests and diseases causing huge crop losses. Minimising these losses is one way of enhancing grain production and remote sensing tool has been found very useful in monitoring large areas frequently. The Earth observing systems are useful in monitoring weather and ecological

conditions favourable for crop pests and diseases. Weather conditions such as temperature, humidity (moisture), sunshine hours (light) and wind play major influence on the densities of pest population and their natural enemies. Among the weather parameters that can be remotely sensed, type of cloud, extent of cloud cover, cold cloud duration (a surrogate for rainfall) are the most easily retrievable. Such information was used by phytopathologists to study rust diseases of wheat crop.

An aircraft fitted with a camera loaded with colour infrared films and flown over Kerala state (India), identified coconut areas severely affected by 'wilt' which could not be easily detected from the ground. This gave a clue to the area that could be viewed from satellite altitude.

Understanding the magnitude of crop losses is necessary to appreciate the importance of plant protection in crop production programmes. Losses can be due to biotic factors such as pests/diseases/weeds and abiotic factors such as drought, floods, cyclones and hailstorms. Damage caused by pests may be quantitative (overall reduction in yield), or qualitative such as change in colour and offensive odour. The regional disparities in crop condition assessment, the complex Centre-State relationships in handling relief measures and the introduction of crop insurance scheme, call for an unbiased, objective and timely information system to give early warning, to indicate the intensity of such hazards and to assess the loss.

FAO had organized an international training programme at National Remote Sensing Agency (NRSA) in India a decade ago, involving countries like India, Pakistan and Tanzania in the use of various remote sensing data to identify locust-breeding areas. The directorate of plant protection handles such issues. There is no proper information about the area affected by pests and diseases and other yield reducing factors on an all-India basis.

It is stated that the brown plant hopper (BPH) of rice is one of the dreaded insect pests in Asia. BPH is stated to be associated with synoptic weather conditions (depressions). Double cropping, extensive rice cultivation in the command area and indiscriminate use of fertilizers and pesticides aid the occurrence of BPH.

Desert Locust Forecasting

Desert locust plagues affect about 20 percent of the earth's surface spreading across Africa, the middle east and south-west Asia. They breed in areas that

have sufficient soil moisture and vegetation to support the early stages of this insect (viz. egg laying and hopper development). They migrate from west to east along with the passage of troughs moving in the westerlies and northward and southward along with the Inter-tropical Convergence Zone (ITCZ). The main weather systems bringing rainfall favourable for the development of desert locust are western disturbances, depressions over Arabian Sea and a few depressions developed over land.

Remotely sensed vegetation indices and rainfall estimates based on cold cloud duration and other cloud indexing techniques are the only cost-effective methods to survey the vast stretches of desert locust habitat.

A few studies have focussed on the collection of historical data on weather and habitat conditions with the dynamics of locust development stages, and synthesis of the data using Geographical Information System (GIS) and evolving decision support systems (Healey *et al.,* 1996). This system integrates remotely sensed landform soil texture, soil moisture and vegetation density with the daily weather data to forecast the suitable breeding sites and time of onset of locust upsurge in and around the study area.

Remote Sensing and Drought Monitoring

One of the natural calamities that affects us is lack of normal rainfall and consequent drought conditions which in turn affect agricultural productivity. Drought conditions can be monitored using data obtained from satellite. This system provides efficient and timely monitoring capability by integrating the timeliness and objectivity of space observations with details of ground perceptions.

During drought, physiognomic changes of vegetation may become apparent. Satellite sensors are capable of discerning many such changes through spectral radiance measures and manipulation of such measures into vegetation indices, which are sensitive to the rate of plant growth as well as to the amount of growth. Such indices are also sensitive to the changes in vegetation affected by moisture stress. The visible and near infrared bands on the satellite multi-spectral sensors allow monitoring of the greenness of vegetation. This property is used in the case of monitoring drought, as the stressed vegetation and other bare ground, water, etc. reflect differently. Besides, moisture stress in vegetation, resulting from prolonged rainfall deficiency, is reflected by lowering of vegetation index values. Such decrease could also be caused by other stresses

such as pest/disease attack, nutrient deficiency or soil geo-chemical effects. But this does not show up well in coarse resolution data which covers very large areas at a time.

Reliable drought interpretation requires a Geographical Information System (GIS) based approach, since the topography, soil type, spatial rainfall variability, crop type and variety, irrigation support and management practices are all relevant parameters.

In recent years, many investigations have demonstrated the capability of satellite-borne sensors to provide information on various drought indicators, which helps to monitor drought more effectively. The following paragraphs discuss remote sensing of rainfall, soil moisture, and vegetation/crop conditions, which are helpful in delineating agricultural drought.

Rainfall Estimation by Remote Sensing

Satellite estimation of rainfall is not likely to be better than rainfall measured through conventional rain gauges, but nevertheless is useful to fill in spatial and temporal gaps in ground reports. Nageswara Rao and Rao (1984) demonstrated an approach for preparing an indicative drought map based on NOAA AVHRR derived rainfall estimation at the seedling stage of crop growth. For drought monitoring, quantitative point-specific rainfall estimates on the daily basis all over the country may not be required. What is needed, however, is a capability to spatially distribute the point rainfall observations over the areal unit in a qualitative manner.

Remote Sensing of Soil Moisture

Microwave sensors are probably the best soil moisture sensors, considering the strong physical relationship between the microwave response and soil moisture and the capability of microwaves to penetrate clouds, precipitation, and herbaceous vegetation. The principle advantage of active microwave sensors is that high spatial resolution can be obtained even at satellite altitudes.

Microwave sensors can provide estimates of soil moisture only in surface layers up to 10 cm thick. This depth is too shallow, compared to the 1-2 m root zone of many field crops in the tropics. Using the water content in the top 10 cm of the surface layer, the moisture content can be calculated within acceptable limits and with minimum error when the surface soil moisture estimation is made just before dawn.

Some investigations are under way at the National Remote Sensing Agency, Space Application Centre, and elsewhere to evaluate ERS- ISAR data for soil moisture estimates in the surface layers.

Remote Sensing of Vegetation status

During periods of drought conditions, physiological changes within vegetation may become apparent. Satellite sensors are capable of discerning many such changes through spectral radiance measurements and manipulation of this information into vegetation indices, which are sensitive to the rate of plant growth as well as to the amount of growth. Such indices are also sensitive to the changes in vegetation affected by moisture stress (Das, 2000).

The visible and near infrared (IR) bands on the satellite multispectral sensors allow monitoring of the greenness of vegetation. Stressed vegetation is less reflective in the near IR channel than nonstressed vegetation and also absorbs less energy in the visible band. Thus the discrimination between moisture stressed and normal crops in these wavelengths is more suitable for monitoring the impact of drought on vegetation.

The NDVI varies with the magnitude of green foliage (green leaf area index, green biomass, or percentage green foliage ground cover) brought about phenological changes or environmental stresses. The temporal pattern of NDVI is useful in diagnosing vegetation conditions

Moisture stress in vegetation, resulting from prolonged rainfall deficiency is reflected by lower NDVI values. Such a decrease could also be caused by other stresses, such as pest/disease infestation, nutrient deficiency, or soil geochemical effects. Discrimination of moisture stress from other effects does not present a problem in coarse resolution data over large areal units, as neither pest/disease attack nor nutrient stress is selected in terms of area or crop type.

National Agricultural Drought Assessment and Monitoring System (NADAMS)

Since 1989, National Agricultural Drought Assessment and Monitoring System (NADAMS) in India has been providing biweekly drought bulletins through the kharif season (June to December) for 246 districts in most of the peninsular and northern India. The bulletins, which describe prevalence, relative severity level, and persistence of drought through the season at the

district level, are being sent to the concerned state and central administrators as well as to district-level officers. The drought assessment is based on a comparative evaluation of satellite observed green vegetation cover (both area and greenness) of a district in any specific time period to cover in similar periods in the previous year. The trend of seasonal vegetation development until the reporting period is also compared with trends of previous years. The drought interpretation takes into account rainfall and aridity anomaly trends. This nationwide early warning services has been found to be useful for providing early assessment of drought conditions.

Dissemination of the Information through Agro-met Advisory service

Agrometeorological information is rarely provided as a finished product to the clients. Often it is used to complement the purely meteorological products, or delivered in combination with other remotely sensed products, such as information in soil wetness, land or vegetation cover (NDVI), likely presence of pests and/or diseases, estimates of the areal coverage of irrigated or flood-retreat crops, incidence of bush fires, etc. By the nature of their capacity to indicate the probable areal extent of a condition, and of the still very rapid evolution of the parameters that can be measured or derived, remotely-sensed data and their derived products will be a growing resource for the supply of agrometeorological products to clients.

How information is delivered to the users of the product is, finally, of extreme importance. There are a number of issues that fall into information delivery. These include clearly defined users, user-friendly information, cooperation and coordination between producers and users of the product, proper training, and timeliness of information delivery. Hard copy publication sent via mail allows detailed text and graphics, but its effectiveness may be hampered by the timeliness of receipt. Delivery by radio allows rapid dissemination but limits the amount of information that may be provided. Internet technology combines the strengths of detailed information and rapid delivery but is definitely constrained by lack of Internet access in many developing countries.

The product must be delivered or made accessible in sufficient time for the user to make professional sense from the information and use it appropriately in the management process. Formal lines of communication can be developed through user surveys and open forums. Information mechanisms, such as telephone, facsimile, or email exchange should also be encouraged.

Once established, such mechanisms for communication should become a routine occurrence to accommodate changing user needs, new technological innovations, and more efficient distribution procedures. Constructive feedback mechanisms promote an active dialogue to encourage improvements that not only technically enhance the bulletin but also increase its usefulness. Information delivery by Internet communication offers great opportunity to move quality products to the decision-maker rapidly. The computer age technology also allows efficient feedback mechanisms, which in turn may increase the demand for additional information (Motha, 2001).

CONCLUSIONS

The use of satellite based remote sensing has proved itself as a strong and unbiased information system at regular intervals of time. While agricultural scientists have shown some interest in developing its usage, there is still a long way to go, as it is only the agricultural scientists who can clearly define what information is actually needed. Besides, they should integrate the remotely sensed information system with their agricultural information system to derive optimum usage, timely recovery of degraded land and refrain from unsustainable activities by use of other advanced technologies to their benefit and to enable increasing productivity through alternate farming system.

ACKNOWLEDGEMENT

The author is grateful to Dr. R. R. Kelkar, Director General of Meteorology, Indian Meteorological Department, New Delhi for permission to present this paper in the workshop.

REFERENCES

Das, H.P. 2000. Monitoring the incidence of large scale droughts in India. pages 181-195. *In* Drought A Global Assessment(Donald A. Wilhite (Ed.)), Vol. 1, Routeldge London and New York.

Doraiswamy, P. C., Zara, P. and Stem, A. 1996. Satellite remotely sensed data application in estimating crop condition and yields, pages 220 -240. Remote Sensing Applications. Narosa Publishing House.

Groten, S.M.E. 1993. NDVI-Crop monitoring and early yield assessment of Burkina Faso. International Journal of Remote Sensing, 14(8): 1495-1515.

Gupta, R.K. 1993. Comparative study of AVHRR ratio vegetation index and normalized difference vegetation index in district level agricultural monitoring. International Journal of Remote Sensing : 14(1): 55-73.

Healey, R.G., Robertson, S.G., Magor, J.I., Pender, J. and Gressman, K. 1996. A GIS for Desert Locust Forecasting and Monitoring, International Journal of Remote Sensing: 10(1): 117-136.

Motha, R.P. 2001. Agrometeorological Bulletins. How can we improve them. Proceedings of the Inter-Regional Workshop, Barbados.

Moulin, S., Fisher, A., Dedieu, G. and Delcolle, R. 1995. Temporal variation in satellite reflectances at field and regional scales compared with values simulated by linking crop growth and SAIL models. Remote Sensing of Environment, 54: 261-272.

Nageswara Rao, P.P. and Rao, V.R. 1984. An approach for agricultural drought monitoring using NOAA/AVHRR and Landsat imagery. pages 225 –229. *In* Remote Sensing-From Research towards Operational Use (T.D. Guyenne and J.J. Hunt (eds)), (International Geoscience and Remote Sensing Symposium, Strasbourg, France, 27-30 August), Noordwijk, Netherlands : ESA Scientific and Technical Pulications Branch.

FOREST FIRE AND DEGRADATION ASSESSMENT USING SATELLITE REMOTE SENSING AND GEOGRAPHIC INFORMATION SYSTEM

P.S. Roy*
Indian Institute of Remote Sensing (NRSA)
Dehra Dun

Abstract : India, with a forest cover of 20.55% of geographical area, contains a variety of climate zones, from the tropical south, north-western hot deserts to Himalayan cold deserts. Enriched with ample diversity of forests bloomed with a rich array of floral and faunal life forms. With increasing population pressure, the forest cover of the country is deteriorating at an alarming rate. Along with various factors, forest fires are a major cause of degradation of Indian forests. According to a Forest Survey of India report, about 50 per cent of forest areas in the country are prone to fire. It is estimated that the proportion of forest areas prone to forest fires annually ranges from 33% in some states to over 90% in others. While statistical data and geospatial information on forest fire are very weak or even not available. About 90% of the forest fires in India are started by humans. The degree of forest fire risk analysis and frequency of fire incidents are very important factors for taking preventive measures and post fire degradation assessment. Geospatial techniques are proving to be powerful tools to assess the forest fire risk and degradation assessment. The present paper describes the present state of forests, methodology, models and case studies of forest fire risk and degradation assessment in context to Indian forests.

INTRODUCTION

Fire has been a source of disturbance for thousand of years. Forest and wild land fires have been taking place historically, shaping landscape structure, pattern and ultimately the species composition of ecosystems. The ecological role of fire is to influence several factors such as plant community development, soil nutrient availability and biological diversity. Forest and wild land fire are considered vital natural processes initiating natural exercises of vegetation

* *Present address* : National Remote Sensing Agency, Hyderabad, 500037, India

Satellite Remote Sensing and GIS Applications in Agricultural Meteorology
pp. 361-400

succession. However uncontrolled and misuse of fire can cause tremendous adverse impacts on the environment and the human society.

Forest fire is a major cause of degradation of India's forests. While statistical data on fire loss are weak, it is estimated that the proportion of forest areas prone to forest fires annually ranges from 33% in some states to over 90% in others. About 90% of the forest fires in India are started by humans. Forest fires cause wide ranging adverse ecological, economic and social impacts. In a nutshell, fires cause: indirect effect on agricultural production; and loss of livelihood for the tribals as approximately 65 million people are classified as tribals who directly depend upon collection of non-timber forest products from the forest areas for their livelihood.

A combination of edaphic, climatic and human activities account for the majority of wild land fires. High terrain steepness along with high summer temperature supplemented with high wind velocity and the availability of high flammable material in the forest floor accounts for the major damage and wide wild spread of the forest fire. Figure-1 shows triangle of forest fire. The contribution of natural fires is insignificant in comparison to number of fires started by humans. The vast majority of wild fires are intentional for timber harvesting, land conversion, slash – and- burn agriculture, and socio-economic conflicts over question of property and landuse rights. In recent years extended droughts (prolonged dry weather), together with rapidly expanding exploitation

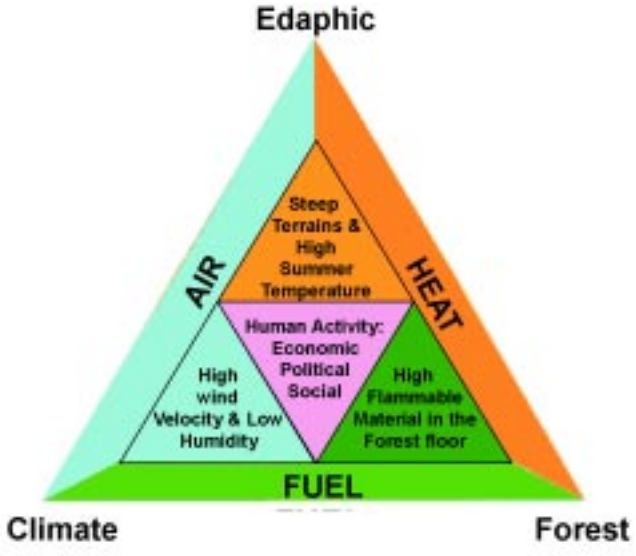

Figure 1: Triangle of forest fire

of tropical forest and the demand for conversion of forest to other land uses, have resulted in significant increase in wild fire size, frequency and related environmental impacts.

Recent wild fires have an immense impact in Indonesia, Brazil, Mexico, Canada, USA, France, Turkey, Greece, India and Italy. Large-scale fires and fire hazards were also reported in eastern parts of the Russian Federation and in China northeastern Mongolia autonomous region. There has been a continuous increase of application of fire in landuse system in forest of South East Asian region. This has resulted in severe environmental problems and impacts on society. Wild fires often escape from landuse fire and take unprecedented shape causing problems of transboundary pollution. The paper analyzes the forest and wild land fires issues with particular reference to South East Asia and emphasizes on development of national and regional fire management plans considering the complexity and diversity of fire. The paper also attempts to assess the current status of application of satellite remote sensing for fire detection, monitoring and assessment. According to a classification of forest fires by type and causes, three types of forest fires are prevalent;

a) Ground fires: Ground fires occur in the humus and peaty layers beneath the litter of un-decomposed portion of forest floor with intense heat but practically no flame. Such fires are relatively rare and have been recorded occasionally at high altitudes in Himalayan fir and spruce forests (Fig. 2).

Figure 2: Ground fire

b) Surface fires: Surface fires occurring on or near the ground in the litter, ground cover, scrub and regeneration, are the most common type in all fire-prone forests of the country (Fig. 3).

c) Crown fires: Crown fires, occurring in the crowns of trees, consuming foliage and usually killing the trees, are met most frequently in low level coniferous forests in the Siwaliks and Himalayas (NCA Report, 1976) (Fig. 4).

Figure 3: Surface fire

Figure 4: Crown fire

Impact of the Forest Fire on the Global Environment

Forest fires controlled or uncontrolled have profound impacts on the physical environment including: landcover, landuse, biodiversity, climate change and forest ecosystem. They also have enormous implication on human health and on the socio-economic system of affected countries. Economic cost is hard to quantify but an estimate by the economy and environment can be provided. The fire incidence problem for South East Asia put the cost of damages stemming from the Southeast Asian fires (all causes) at more than $4 billion. Health impacts are often serious. As per one estimate 20 million people are in danger of respiratory problems from fire in Southeast Asia.

Most pronounced consequence of forest fires causes their potential effects on climate change. Only in the past decade researchers have realized the important contribution of biomass burning to the global budgets of many radiatively and chemically active gases such as carbon dioxide, carbon monoxide, methane, nitric oxide, tropospheric ozone, methyl chloride and elemental carbon particulate. Biomass burning is recognized as a significant global source of emission contributing as much as 40% of gross Carbon dioxide and 30% of tropospheric ozone (Andreae, 1991).

Most of the world burnt biomass matter is from savannas, and because 2/3rd of the earth savannas are in Africa, that continent is now recognized as

"burnt center" of the planet. Biomasss burning is generally believed to be a uniquely tropical phenomenon because most of the information we have on its geographical and temporal distribution is based on the observation of the tropics. Because of poor satellite coverage, among other things, little information is available on biomass burning in boreal forests, which represent about 29% of the world's forests.

Table 1. Global estimates of annual amounts of biomass burning and resulting release of carbon into the atmosphere

Source of burning (Tg dry matter/year)	Biomass burned	Carbon released (TgC/year)
Savannas	3690	1660
Agricultural waste	2020	910
Tropical forests	1260	570
Fuel wood	1430	640
Temperate and boreal forests	280	130
Charcoal	20	30
World total	8700	3940

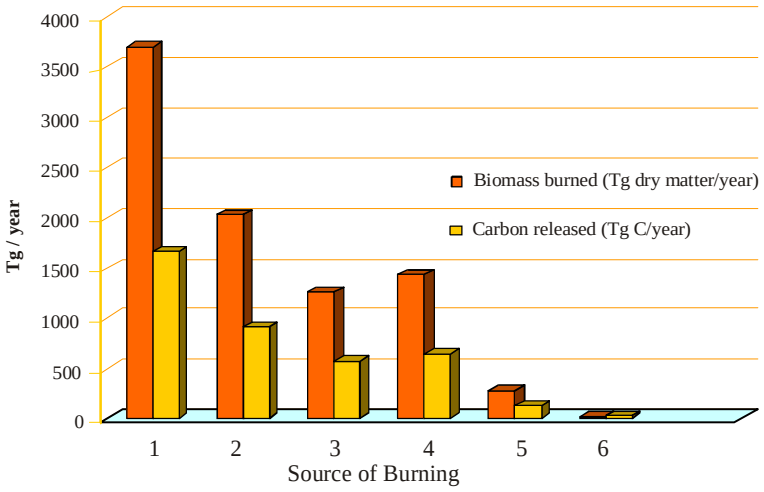

Figure 5: Global estimates of annual amounts of biomass burning and of the resulting release of carbon into the atmosphere (Andreae *et al.*, 1991). Where, 1. Savannas; 2 Agricultural waste; 3. Tropical Forests; 4. Fuel Wood; 5. Temperate & Boreal Forest and 6. Charcoal.

Knowledge of the geographical and temporal distribution of burning is critical for assessing the emissions of gases and particulates to the atmosphere. One of the important discoveries in biomass burning research over the past years, based on a series of field experiments, is that fires in diverse ecosystems differ widely in the production of gaseous and particulate emissions. Emissions depend on the type of ecosystem; the moisture content of the vegetation; and the nature, behavior and characteristics of the fire.

Fire regimes in tropical forests and derived vegetation are characterized and distinguished by return intervals of fire (fire frequency), fire intensity (e.g. surface fires vs. stand replacement fires) and impact on soil. Basic tropical and subtropical fire regimes are determined by ecological and anthropogenic (socio-cultural) gradients.

Lightning is an important source of natural fires which have influenced savanna-type vegetation in pre-settlement periods. The role of natural fires in the "lightning-fire bioclimatic regions" of Africa was recognized early (e.g. Phillips 1965; Komarek 1968). Lightning fires have been observed and reported in the deciduous and semi-deciduous forest biomes as well as occasionally in the rain forest. Today the contribution of natural forest to the overall tropical wildland fire scene is becoming negligible. Most tropical fires are set intentionally by humans (Bartlett 1955, 1957, 1961) and are related to several main causative agents (Goldammer 1988) :

- deforestation activities (conversion of forest to other land uses, e.g. agricultural lands, pastures, exploitation of other natural resources);
- traditional, but expanding slash-and-burn agriculture;
- grazing land management (fires set by graziers, mainly in savannas and open forests with distinct grass strata [silvopastoral systems]);
- use of non-wood forest products (use of fire to facilitate harvest or improve yield of plants, fruits, and other forest products, predominantly in deciduous and semi-deciduous forests);
- wildland/residential interface fires (fires from settlements, e.g. from cooking, torches, camp fires etc.);
- other traditional fire uses (in the wake of religious, ethnic and folk traditions; tribal warfare) and
- socio-economic and political conflicts over questions of land property and land use rights.

Comparatively little is known empirically about the vegetation fire regime of Southeast Asia when viewed at larger scales. This is despite the importance of fire as an agent of regional land cover change and in modifying atmospheric chemistry. Fire is widely used in rice cultivation in Asia where 94 % of the world's crop is grown (Nguyen et al., 1994). It also has a high incidence within forests in tropical Asia (Hao and Liu, 1994) where it is mainly associated with shifting cultivation (McNeely *et al.*, 1991). As with the tropics and the African tropics, Southeast Asian tropical forests are of considerable ecological and economic importance and make up about 20% of the world's tropical forest resource (after FAO, 1993). Information on biomass burning within the Indo-Malayan region is needed to assist in the modelling of large-scale atmospheric pollution and climate change phenomena and for regional use by landuse managers, habitat conservationists, and national and regional policy makers. Mainland Southeast Asia is the focus of the Southeast Asian fire, since it is more strongly seasonal and less humid than many parts of insular South-east Asia (Nix, 1983) and thus both favour the use of fire as a land management tool and support more fire-prone ecosystems (54% of forest formations are tropical seasonal forest compared to 4% within insular regions, FAO, 1993). The mainland Southeast Asian product offers an analysis of the spatial and temporal distribution of vegetation fire in mainland Southeast Asia using AVHRR 1 km resolution data for the period of single dry season (that chosen is from November 1992 to April 1993).

The Socio-Economic and Cultural Background of Forest Fires

While many of the publications cited above contain information on fire causes, there are only few in-depth studies available on the socio-economic and cultural aspects of managing the fire problem. The forest fire management system in Thailand has its strong base on a fire prevention approach which is being realized by a close cooperation with the local population (cf. Contribution by S. Akaakara, this volume). The same refers to the IFFM approach in Indonesia (cf. Contribution by H. Abberger, this volume; see also the work of Otsuka [1991] on forest management and farmers in East Kalimantan). A basic study on the socio-economic and cultural background of forest fires in the pine forests of the Philippines was conducted in the late 1980s and reveals the usefulness of such surveys for further management planning (Noble, 1990).

Despite the initial efforts it must be stated that there is a tremendous gap of expertise and available methodologies of socio-economic and cultural approaches in integrating people into operational fire management systems.

According to the IFFN (2002) the ecological and socio-economic consequences of wild land fires in India include -

- Loss of timber, loss of bio-diversity, loss of wildlife habitat, global warming, soil erosion, loss of fuelwood and fodder, damage to water and other natural resources, loss of natural regeneration. Estimated average tangible annual loss due to forest fires in country is Rs.440 crore (US$ 100 millions approximately).
- The vulnerability of the Indian forests to fire varies from place to place depending upon the type of vegetation and the climate. The coniferous forest in the Himalayan region comprising of fir (*Abies* spp.), spruce (*Picea smithiana*), *Cedrus deodara, Pinus roxburghii* and *Pinus wallichiana* etc. is very prone to fire. Every year there are one or two major incidences of forest fire in this region. The other parts of the country dominated by deciduous forests are also damaged by fire (see Table 1).

Various regions of the country have different normal and peak fire seasons, which normally vary from January to June. In the plains of northern and central India, most of the forest fires occur between February and June. In the hills of northern India fire season starts later and most of the fires are reported between April and June. In the southern part of the country, fire season extends from January to May. In the Himalayan region, fires are common in May and June.

Table 2. Susceptibility and vulnerability of Indian forests to wildfire (IFFN, 2002)

Type of Forests	Fire Frequent (%)	Fire Occasional (%)
Coniferous	8	40
Moist Deciduous	15	60
Dry Deciduous	5	35
Wet/Semi-Evergreen	9	40
North-Eastern Region	50	45

Fire Policy and Legal Aspects

The issue of a fire policy and relevant legislation and regulations are the most important prerequisites for any fire management activities. A fire policy,

which would be a basic commitment to the fire problem and the definition of a national concept of policies to encounter fire-related problems, needs to embrace the following basic considerations (if not at national level, a policy may also be formulated at the regional or district level):

a. A general statement on the role and impacts of fire in the most important forests and other vegetation of the country (or management unit).

b. A general statement regarding how to counter the negative impacts of fire.

c. Definition of an overall fire management strategy. Definition of fire management policy in the various geographic regions in accordance with vegetation type, demographics and land uses.

d. Definition of the role of the population in participating in fire management activities, especially in fire prevention.

A variety of legal aspects needs to be considered for the implementation of a fire policy and for coherent fire management planning, in general e.g. :

a. Clear definition of landownership and availability of a landownership register.

b. Development of a landscape plan in which clear definitions are given of the land uses permitted or practiced on a defined area of land.

c. Regulations concerning construction in forests and wildlands, especially on burned areas.

d. Clear definition of fire management responsibilities as related to the various types of land ownerships and different tasks in fire management, e.g. fire prevention, fire detection, and fire suppression (including coordination and cooperation).

e. Rehabilitation of burned lands.

f. Law enforcement.

Regional Co-operation in Forest Fire Management

Beginning in 1992, as a consequence of the regional smog problems caused by land-use fires, member states of the Association of South East Asian Nations (ASEAN) created joint activities to encounter problems arising from

transboundary haze pollution. ASEAN workshops held in Balikpapan (1992) and Kuala Lumpur (1995) summarized the problems and urged appropriate initiatives. The ASEAN Conference on "Transboundary Pollution and the Sustainability of Tropical Forests" is one of the first important steps to materialize the conceptual framework proposed during the past years.

Most important in future regional ASEAN-wide cooperation in fire management will be the sharing of resources. The foci will be :

- predicting fire hazard and fire effects on ecosystems and atmosphere;
- detection, monitoring and evaluating fires; and
- sharing fire suppression technologies.

The ASEAN Fire Forum during this meeting will provide important recommendations on joint future actions. The ASEAN region will potentially serve as a pilot region in which resource sharing will be based on the fact that two distinct fire problem seasons exist within the region. While within Indonesia the fire season is mainly during the months of September to November (southern hemisphere dry season), the fire season in monsoon-influenced SE Asia is between January and May. Sharing resources means that hard and software technologies and required personnel can concentrate on the hemispheric fire problems, and even costly fire suppression equipment, e.g. airplanes, can be used more economically throughout the whole year.

Forest Degradation & Fire Disasters in India during the Past Few Years

The normal fire season in India is from the month of February to mid June. India witnessed the most severe forest fires in the recent time during the summer of 1995 in the hills of Uttar Pradesh and Himachal Pradesh in the Himalayas in northern part of India. The fires were very severe and attracted the attention of whole nation. An area of 677, 700 ha was affected by fires. The quantifiable timber loss was around US$ 45 million. The loss to timber increment, loss of soil fertility, soil erosion, loss of employment, drying up of water sources and loss to biodiversity were not calculated by the Committee appointed by the Government to enquire into the causes of fires, as these losses are immeasurable but very significant from the point of view of both economy as well as ecology. The fires in the hills resulted in smoke in the area for quite a few days. The smoke haze, however, vanished after the onset of rains. These fires caused changes in the micro-climate of the area in the form of soil moisture balance and increased

evaporation. Lack of adequate manpower, communication and, water availability in the hills helped this fire spread rapidly reaching the crown level. The thick smoke spread over the sky affecting visibility up to 14,000 feet.

Assessment of Forest Degradation

The statistics on forest fire damage are very poor in the country. In the absence of proper data, it is difficult to arrive at the accurate losses from the forest fires. Moreover, the losses from fires in respect of changes in biodiversity, carbon sequestration capability, soil moisture and nutrient losses etc are very significant from the point of view of ecological stability and environmental conservation. To a certain extent, the loss due to forest fires can be estimated based on the inventories made by the Forest Survey of India (FSI) as reported in the state of forest report 1995 and subsequent field observations conducted by them. The statistics of losses from forest fires from the various states of the union is still very sketchy and fragmented. Much of the data available does not reflect the ground situation and is grossly under reported. The total reported loss from the states of the union is around US$ 7.5 million annually.

The Forest Survey of India data indicate 50% of the forest areas as fire prone. This does not mean that country's 50% area is affected by fires annually. Very heavy, heavy and frequent forest fire damage are noticed only over 0.8%, 0.14% and 5.16% of the forest areas respectively. Thus, only 6.17% of the forests are prone to severe fire damage. In absolute terms, out of the 63 million ha of forests an area of around 3.73 million ha can be presumed to be affected by fires annually. At this level the annual losses from forest fires in India for the entire country can be moderately estimated at US$ 107 million. This estimate does not include the loss suffered in the form of loss of biodiversity, nutrient and soil moisture and other intangible benefits. Based on the UNDP project evaluation report of 1987, if 40 million ha of forests are saved annually from forest fires due to implementation of modern forest fire control methods, the net amount saved at todays' prices would come to be US$ 6.8 million.

Remote Sensing & Geographic Information System

Satellite observations providing a global survey of the composition of biomass burning plumes and their dispersal in the global atmosphere will become available by the middle to late 1990s and will be an important contribution to this task. Global mapping of CO and O_3 columns can be achieved by the Global Ozone Monitoring Experiment (GOME) and Scanning Imaging

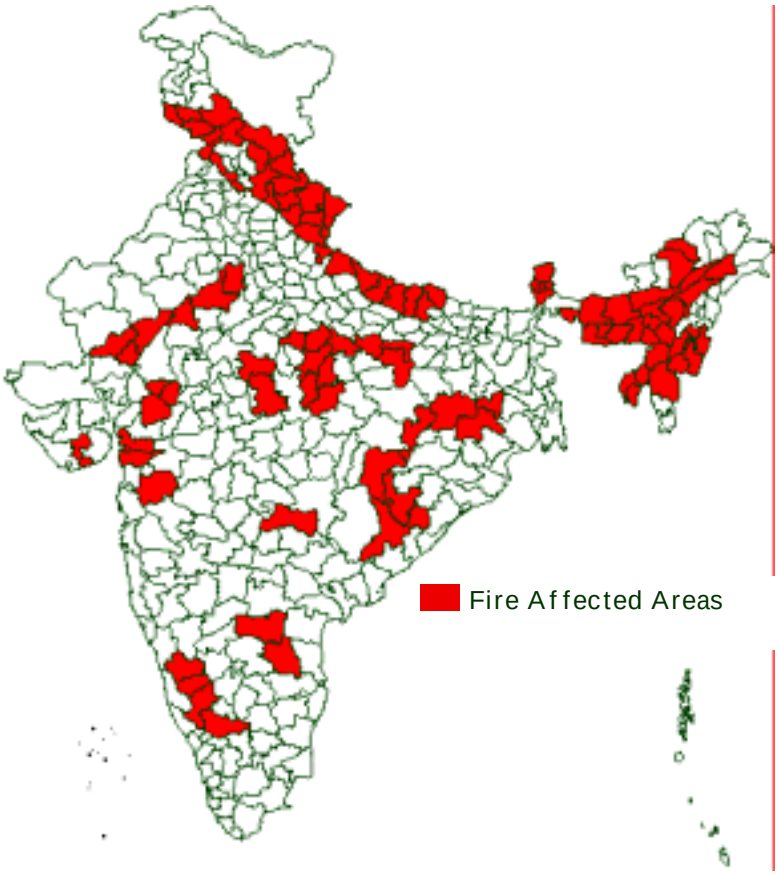

Figure 6: Map f India showing the districts with regular interval of forest fire (Source: Forest Survey of India, Dehra Dun)

Absorption Spectrometer for Atmospheric Chartography/Chemistry (SCIAMACHY) sensor, scheduled for inclusion on the ESA ERS-2 (European Space Agency Remote Sensing Satellite) in 1993-94 and/or later launches. Global mapping CO is available on the EOS-A platform in the late 1990s, using the MOPPITT (Measurement of Pollution in The Troposphere) or TRACER sensors. The sensor TES, planned for launching on the EOS-B platform, will provide horizontal and vertical mapping of a number of trace species including CO, O_3, NO_X and HNO_3.

Potentials of Satellite Remote Sensing

The inability to detect wild land fires during initial stages and take rapid aggressive action on new fires is perhaps the most limiting factor in controlling

such wild land fires. This is especially true for fires in areas with limited access. Providing an effective response to wildland fires requires four stages of analysis and assessment:

- Determining fire potential risk
- Detecting fire starts
- Monitoring active fires
- Conducting post-fire degradation assessment

The technological advancement in space remote sensing has been widely experimented in last three decades to obtain the desired information.

Fire Potential

Fire potential depends on the amount of dead and live vegetation and moisture contents in each. The amount of dead and live vegetation is estimated from a high quality landcover map derived from (ideally) a high resolution sensor, such as the IRS, Landsat TM or SPOT multispectral scanner or from lower resolution sensor such as NOAA-AVHRR or NASA Moderate Resolution Imaging Spectrometer (MODIS). These satellites can be used to monitor changes in the vegetation vigor, which is correlated with the moisture of the live vegetation. The moisture in the dead vegetation is estimated from knowledge of local weather conditions. Thus, a baseline land cover map and immediate estimate of vegetation condition are needed.

The research project FIRE in global Resource and Environmental monitoring (FIRE) was initiated in 1994 by the Monitoring of Tropical Vegetation unit (MTV) of the Commission of the European Union Joint Research Centre in order to address such issues. A key objective of this initiative was the documentation of vegetation fire patterns for the entire globe and the analyses of such patterns in relation to land use/land cover dynamics in tropical and inter-tropical regions. Obviously, such vegetation fires represent only part of the overall biomass burning activity, which also includes the burning of domestic fuels, occurring at the surface of the Earth. Due to both the characteristics of the phenomenon and to the multiscale objective, the fire monitoring system under development in the MTV Unit relies on remote sensing techniques as the main source of information. This is the case since earth observation from space provides systematic and consistent measurements of a series of parameters

related to fire and fire impacts, and, consequently, is an ideal medium for the study of vegetation fire. The AVHRR on the NOAA satellites is the main source of data for the studies done by the FIRE project. For the 5 km GAC (Global Area Coverage) data, historical archives exist that extend back to 1981 and consist of daily images covering the entire globe. More limited data sets, from the same AVHRR sensor but at 1 km resolution also exist at global, continental and regional level. A mobile AVHRR data receiving station is also used by the FIRE project.

Fire Detection

Satellite-borne sensors can detect fires in the visible, thermal and mid-infrared bands. Active fires can be detected by their thermal or mid-infrared signature during the day or by the light from the fires at night. For their detection the sensors must also provide frequent overflights, and the data from the overflights must be available fast. Satellite systems that have been evaluated for fire detection include AVHRR, which has a thermal sensor and makes daily overflights, the Defense Meteorological Satellite Program (DMSP) Optical Linescan System (OLS) sensor, which makes daily overflights and routinely collects visible images during its nighttime pass, and the NOAA Geostationary Operational Environmental Satellite (GOES) sensor, which provides visible and thermal images every 15 minutes over the United States and every 30 minutes elsewhere. Therefore AVHRR has been used most extensively for detecting and monitoring wildfires.

Fire Monitoring

Fire monitoring differs from fire detection in timing and emphasis rather than in the methods used to process the satellite image information. Satellite sensors typically provide coarse resolution fire maps which show the general location and extent of wildland fires. Detailed fire suppression mapping requires the use of higher resolution airborne thermal infrared sensors to accurately map small fire hot-spots and active fire perimeters. Higher-resolution fire maps are needed to deploy fire suppression crews and aerial water or retardant drops.

Fire Assessment

Once fires are extinguished, a combination of low resolution images (AVHRR) and higher-resolution images (SPOT, Landsat and Radar) can be used to assess the extent and impact of the fire. Radar has proved effective in

monitoring and assessing the extent and severity of fire scars in the boreal forests (Kasischke *et al.*, 1994), for quantifying biomass regeneration in tropical forests (Luckman *et al.*, 1997) and for modeling ecosystem recovery in Mediterranean climates (Vietma *et al.*, 1997). Low resolution visible and infrared sensors such as AVHRR have proved useful for automated fire mapping (Fernandes *et al.*, 1997) and for evaluating the impact of fire on long-term land cover change (Ehrlich *et al.*, 1997). Multi-resolution studies incorporating both AVHRR and Landsat images reveal the scale-related influences of analyzing post-fire vegetation regeneration (Steyaert *et al.*, 1997).

Information related to new fire scars and vegetation succession within the scars can be used to update the baseline vegetation map used for fire prediction. Continued monitoring of the fire scars provides extensive information on land cover transitions involving changes in productivity and biodiversity, which in turn influence fire potential. Knowledge of the extent and intensity of fire scars provides important information for the rehabilitation of the burn areas.

Globally no reliable statistics about the exact location and annual areas burnt by forest fire are available. The information required and what can be achieved using Remote Sensing data are presented as Table 3.

Table 3. Forest Fire Assessment

Class of Information	Type of Information
a) *alpha type*	Fire : start and end dates, location, size and cause
b) *beta type*	Fuels biome classification and fuel loading forest inventory (number), age class, size class
c) *gamma type*	Fire characterisation (crown, surface etc.), fuel consumption and structural involvement (wildland urban interface)
d) *delta type*	Number of fires, areas burnt (by forest type), cause of fires (number)
e) *epsilon type*	Gas and aerosol emission data
f) *eta type*	Total expenditure of fire programme, total fire suppression costs and total direct losses of merchantable timber, structure losses

Detection and Monitoring of Fire

Space borne remote sensing technologies have improved the capability to identify fire activities at local, regional and global scales by using visible and infrared sensors on existing platforms for detecting temperature anomalies, active fires, and smoke plumes. Geosynchronous satellites such as GOES and polar orbiting sensors such as the NOAA AVHRR have been used successfully to establish calendars of vegetation state (fire hazard) and fire activities. Other satellites with longer temporal sampling intervals, but with higher resolution, such as Landsat and SPOT, and space borne radar sensors, deliver accurate maps of active fires, vegetation state and areas affected by fire. Fire scar (burned area) inventories for emission estimates are difficult to conduct, especially in the region of the Maritime Continent in which cloud cover inhibits ground visibility of many sensors. Radar sensors such as SAR offer good potential application in fire scar characterisation. ASEAN scientists (candidate institutions: ASEAN Specialized Meteorological Centre (ASMC) and the Indonesian National Institute of Aeronautics and Space (LAPAN) should consider appropriate research.

Table 4. Different sensors and possible potential applications to study forest fires

Sensors	:	Potential Applications
Video Images	:	Fire characterisation, burnt area estimation, fire propagation, estimate of fire density and burnt scars
IRS PAN	:	Exact location of forest fires, extent of fires and types of land cover of fires, impact of human activities on incidence of forest fire
IRS LISS III Landsat TM	:	Land cover characterisation and forest non forest mapping
IRS WiFS AVHRR-HRPT	:	Fire characterisation, land cover characterisation and monitoring
AVHRR-GAC	:	Characterisation, land cover characterisation, seasonal variations in land cover, inter annual variation in land cover, land cover change and burnt area estimation
ERS-ATSR	:	Burnt area estimation

The fire episode of 1997 in Indonesia has clearly demonstrated that the "hot spot" information generated by the NOAA AVHRR is of limited value. New sensors are currently developed which are specifically aimed to satisfy the demands of the fire science and management community, e.g., the BIRD satellite project of the Deutsche Forschungsanstaltfur Luft- und Raumfahrt (DLR) (with a two-channel infrared sensor system in combination with a wide-angle optoelectronic stereo scanner) and the envisaged fire sensor component FOCIS on the International Space Station (Briess *et al.*, 1997; DLR 1997). Indonesia's Ministry for Research and Technology (BPPT) is interested to collaborate with the DLR in testing and validating the BIRD satellite.

Fire Weather and Fire Danger Forecasts

Weather forecasts at short to extended time ranges and global to regional space scales can be utilized for wildland fire management, e.g. the recent proposal by the US National Centre for Environmental Prediction (NCEP). The Normalized Difference Vegetation Index (NDVI) has been successfully used for estimating fire danger. A recent (not yet published, 1997) report of the IDNDR (IDNDR 1997) gives an overview on a series of candidate systems for early warning of fire precursors which should investigated by Indonesian scientists.

The proposed Canadian project "Fire Danger Rating System for Indonesia : An Adaptation of the Canadian Fire Behavior Prediction System" will be an important contribution towards improving the basic knowledge on the weather-fuel-fire/fire behaviour relationships.

The fire danger rating systems which are already in use in some parts of Indonesia (IFFM-GTZ), however, may be more readily available to produce a regional early warning system within a relatively short time period of a few months. The ministry of Environment of Singapore has indicated interest to test the system at ASEAN level.

The ASEAN Fire Weather Information System (ASFWIS) is a co-operation between ASEAN and the Canadian Forest Service. It provides maps describing the current fire weather situation in South East Asia. This system is based upon the Canadian Forest Fire Danger Rating System (CFFDRS) (for further information to the CFFDRS refers to ASFWIS). Studies have shown that the CFFDRS is applicable outside of Canada. Currently it is also used in a modified form in New Zealand. In New Zealand the Fire Weather Indices Fine Fuel

Moisture Code (FFMC) and the Initial Spread Index (ISI) represent the fire danger in the scrublands. The Duff Moisture Code (DMC) is also applicable in South East Asia, because it potentially describes the moisture state of the upper peat layers in peat and peat swamp forests. All three parameters may serve as a suitable indicator of forest fire danger in South East Asia.

CASE STUDIES

Forest Fire Assessment

Forest Fire Prone Area Mapping – A Case Study in GIR-Protected Area

The following study had been carried out in GIR forest which is located in the Saurashtra Peninsula of Gujarat. It is the largest biologically intact contours tract of forest and the only abide of the Asiatic Lion in the world. The main objective of the study is to design, develop and demonstrate RS/GIS based approach in order to prepare region/type level fire danger rating system taking into consideration risk, hazard, meteorological parameters and human interventions and also to prepare forest fire risk area/disaster map for GIR forest Gujarat. Two types of data are used in the study i.e. spatial and non spatial. Spatial data mainly includes Remote Sensing data, forest block, compartment boundaries, road/railway network and the most important existing water bodies in that area where the non-spatial data pertains to meteorological data on temperature, relative boundary, rainfall, wind, socio-economic data.

The methodology adopted was visual, digital and hybrid method for Remote Sensing data analysis. IRS 1C/1D LISS III FCC's were used for visual interpretation for classification of vegetation in the entire GIR-PA region. To identify fire scars digital data of IRS 1C/1D WiFS had been used. WiFS data had also been used to delineate water bodies and fire scars. The parameters used for modelling the fire risk zone were –

- Fire occurrence maps for three or more seasons
- Classified vegetation map (two seasons)
- Road network (Proximity analysis)
- Maximum temperature
- Relative humidity

- Rainfall data
- Forest block compartments
- Rivers, streams and water bodies
- Settlements location map (Proximity analysis)

All these parameters have direct/indirect influence on the occurrence of fire and were integrated using GIS and a multi parametric weighted index model has been adopted to derive the 'fire-risk' zone map. It is classified into 6 risk zones. It was observed that very high and high zones are mostly at the fringe of the protected area or within 100 m of the roads passing through the region with temperature above 40^{o}C and humidity less than 35%. Apart from human interference the analysis has shown that vegetation type and meteorological parameters have vital importance for hazard zonation.

Spatial Modelling Techniques for Forest Fire Risk Assessments

The study attempted to give insight in the use of RS and GIS for fire management. Spatial modelling and analysis have been done in GIS environment for identification of areas prone to fire risk and subsequently response routes were suggested for extinguishing forest fires (Jain *et al.*, 1996 and Porwal *et al.*, 1997). Some of the necessary components contributing to the fire behaviour viz., fuel (vegetation types), topography (slope and aspect etc.) and the causes of fire (i.e., roads and settlements) have been given due weightages.

The study has been done in part of Rajaji National Parks covering an area of approximately 115 km^{2}. The topography is variable within the altitude ranging between 300-700 m above msl. The climate is subtropical type with the temperature varying from 13.1^{o}C in January to 38.9^{o}C in May & June. The area is dominated by moist Siwalik sal forest, moist mixed deciduous forest, dry mixed deciduous forest, chirpine and shrubs.

Landsat TM false colour composite (FCC) and SPOT images on 1:50,000 scale have been visually interpreted to obtain primary map layers viz. Forest cover type map, density map etc. The contour map, road network settlement etc. have been obtained from Survey of India toposheets. This spatial data in the form of map was digitized and transformed in machine-readable form for integration of thematic information. However, before their integration (Fig. 7) these were converted into index map viz., fuel type index maps from forest

cover type map, aspect and slope index map from the slope and aspect map and distance index from the road map.

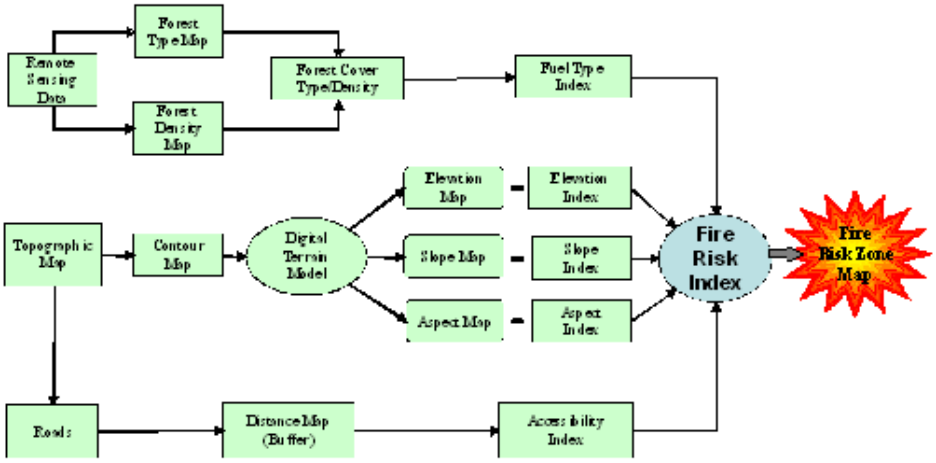

Figure 7: Fire risk zonation model

Spatial modelling has been done to obtain the combined effect of fuel type index, elevation index, slope index, aspect index and the distance/accessibility index. Weightages have been assigned as per the importance of particular variable contributing in fire environment. In this case the highest weightage has been given to fuel type index because fuel contributes to the maximum extent because of inflammability factor. The second highest weightage has been given to aspect because sun facing aspects receives direct sun rays and makes the fuel warmer and dry. The model output i.e., cummulative fire risk index (CFRISK) value map was obtained by integrating in ILWIS.

$$CFRISK = FUI * 4 + ASI * 3 + SLI * 2 + ACI + ELI1$$

Where FUI, ASI, SLI, ACI and ELI are the fuel type index, aspect index, slope index, accessibility index and elevation index. The fire risk index values in this map were ranging from 12-66. Based on statistics this map was reclassified and final fire risk zone map was obtained.

In another study in Dholkhand range integration of various influencing factors has been done by following a hierarchical system on the basis of experience and the opinion of experts in the field and weightages were assigned to different variables on a 1-10 scale.

$$FR = [10Vi = 1\text{-}10\ (5H_{j} = 1\text{-}4 + 5R_{k\ =\ 1\text{-}5} + 3\ S_{l\ =\ 1\text{-}4})$$

Where FR is the numerical index of fire risk, V*i* the vegetation variable (with 1-10 classes), H_j indicates the proximity to human habitation (with 1-4 classes), S_l indicates slope factor (with 1-4 classes) and R_k is road/fire line factor (with 1-5 classes). The subscripts i, *j, k, l* indicate sub-classes based on importance determining the fire risk.

After obtaining the fire risk map (Fig. 8) in Motichur range (part of Rajaji National Park) attempt was made to suggest response routes for extinguishing forest fires. The forest type maps obtained by using Remote Sensing data have been used to assign non-directional costs under different vegetation category and digital elevation model was used for giving directional costs using GDIRGRAD programme compatible to be used in ILWIS. Finally the GROUTES programme was used to trace final response route plan from the source i.e., forest range head quarter to high fire risk areas (Porwal, 1998). A final map showing response routes planned and dropped out fire risk map obtained in the beginning was developed.

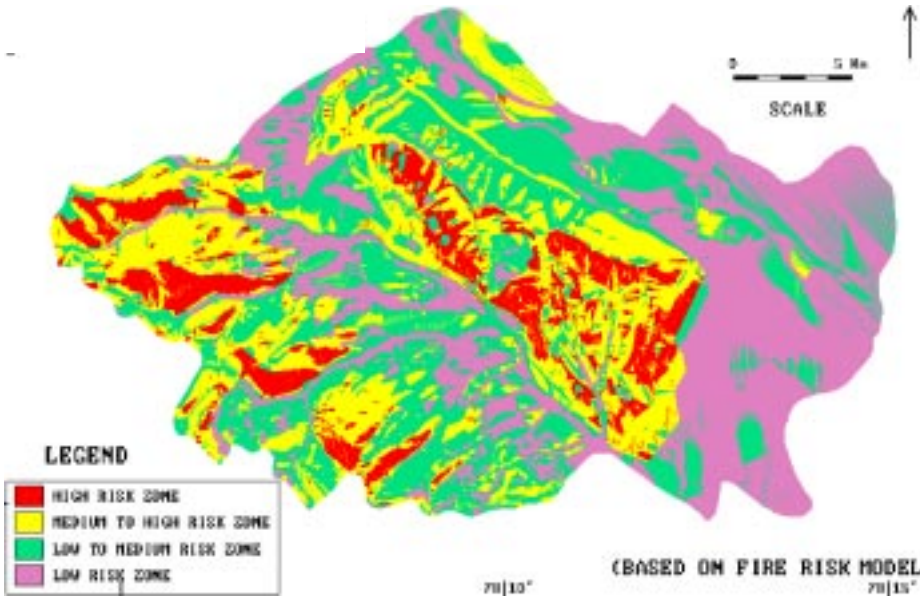

Figure 8: Fire Risk Map (part of Rajaji National Park)

Forest fires cause significant damage to the forest ecosystem. In Central Himalayan region forest fires occur between April to June annually when the weather is hot and dry. Usually the south facing slopes are prone to fire due to direct sun insulation and inflammable litters of pine and dry deciduous trees at the forest floor. The presence of habitation, roads, footpaths etc., and their distance from such sites indicate an additional yardstick for the occurrence of forest fires. Extensive forest area during summer of 1995 in the Western and Central Himalaya drew wide attention of the forest managers and environmentalists. This study attempts to provide estimates about forest fire damaged areas using digital satellite remote sensing data in the Tehri district of Garhwal Himalaya (Pant *et al.*, 1996).

The study area is characterized by hilly and mountainous terrain supporting varied forest types and composition controlled by altitude, variety of land use/ land cover types along with perpetual snow cover on the mountain peaks. Pine is the dominant forest type and is most susceptible to fire almost every year particularly near habitation.

The Indian Remote Sensing Satellite-1B, LISS-II (IRS-B, LISS-II) data of pre-fire and post fire period (1993-95) were studied and analysed digitally in the IBM RS/6000, EASI/PACE computer system. The supervised per pixel classification and digital enhancement approaches have been used to identify the forest fire affected areas along with other cover types. Prior to this digital geometric correction of satellite images have been done using 1:250,000 scale Survey of India topographical sheets and both the images were masked with respect to district boundary. Digital enhancement techniques facilitated to choose correct training sets for supervised classification technique using maximum likelihood classifier. The training sets were assigned based on the ground truth information collected from fire burnt areas and surrounding cover types. Out of the various enhancement techniques the best result has been obtained by making the colour composite image of IR, NDVI and intensity under equal stretching.

The total area affected under forest fire has been estimated as 910.01 km^2 or 20.58% of total geographical area of 4421.26 km^2. This includes forest burnt area as 168.88 km^2 or 3.38% of total geographical area, partially burnt forest area (area under active fire) as 473.69 km^2 or 10.71% of total geographical area and the partially burnt fallow land/grassland/scrub land as 267.44 km^2 or 6.05%. The forested area identified under smoke plumes has been estimated

as 130.96 km^2 or 2.96% of total forests area. The overall accuracy of classification has been assessed as 88%.

FOREST DEGRADATION ASSESSMENT

Deforestation Monitoring

The pressure on forests is greatest in the developing countries. The primary causes of deforestation are encroachment of forest area for agricultural production and exploitation of forest cover for meeting housing and industrial needs. Deforestation leads to an increase in the loading of CO_2 in the atmosphere. Increased albedo and change in aerodynamic roughness over deforested areas alter the energy balance bearing implications on atmospheric circulation patterns and rainfall statistics. Deforestation leads to soil erosion and gradual loss of biodiversity.

The amount of vegetation loss/deforestation due to encroachment can be estimated by the use of remote sensing technique. The impact of slash and burn during and after the 'jhumming' (slash and burn agriculture) operations is clearly visible from remote sensing imageries. The representative relationship between the population density and the percent of forest cover provides information about the rate of deforestation and thereby helps in formulating the mitigation plan. Utilization of remote sensing tool for stock mapping and growing stock estimation for forest management improves reliability. Assam is well known for its large forest tracts. The recorded forest area in Assam is 39.15% of the geographical area. These forests are repositories of a rich biological diversity. At the same point there is tremendous pressure on these forest lands. There has been an overall decrease of 1,031 sq. km of dense forest from 1997 to 1999 in Assam. This decrease is more pronounced in the Brahmaputra valley in the areas like Sonitpur and others. This study was undertaken after large-scale deforestation was observed in above district by IIRS team of scientists working in Arunachal Pradesh. The objective was to assess the large-scale deforestation and loss in biodiversity.

This study covers the entire Sonitpur district (5,103 km^2) located in upper Assam valley. Land use within the area is divided primarily among tropical semi-evergreen forest, moist deciduous forest, riverain forest, pasture land, agriculture and tea gardens. Good quality Landsat-TM and IRS-1C LISS-III false colour composites of dry season pertaining to 1994, 1999 and 2001 periods were used to monitor the loss of biodiversity. All scenes were radiometrically

and geometrically corrected and on-screen visually interpreted into forest and non-forest cover classes. The total number of plant species, species diversity, economically important and endemic species in similar forests in Assam were worked out in field to understand the type of loss incurred due to large scale deforestation.

The forest cover type of 1994, 1999 and 2001 are shown in Fig. 9. All three types of forests viz., semi-evergreen, moist deciduous, and riverain could be mapped from three data sets of different time periods. Results indicate that moist deciduous forests occupy the maximum area followed by tropical semi-evergreen and riverain. A loss of 86.73 km^2 (1.68%) was observed between 1994-99 and 145.44 km^2 between 1999-2001. An increase of 5.0 km^2 area was observed in moist deciduous forest. The loss in semi-evergreen forests was found to be 0.52 km^2 (0.01%) from 1994 to 1999 while between 1999-2000/2001 it was 2.04 km^2 (0.04%). There was no loss in case of riverain forests. Table 5 gives the area under different forest types during different periods.

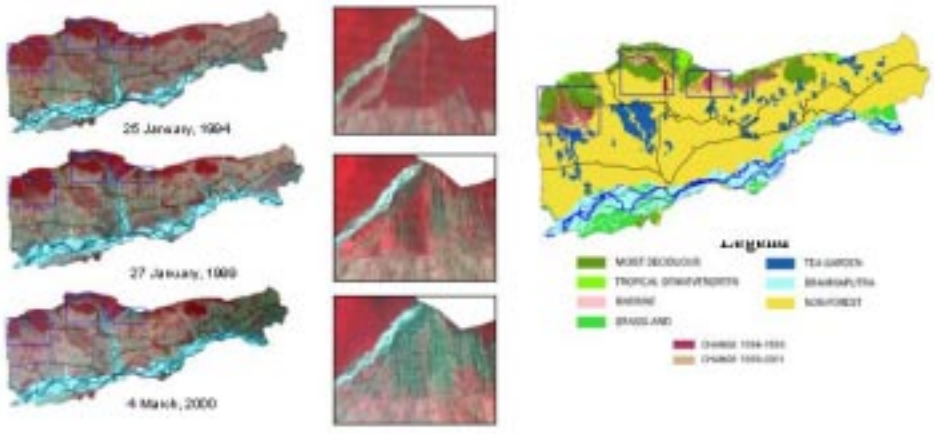

Figure 9: Deforestation monitoring in Sonitpur District of Assam

The results of field survey show that moist deciduous forests possess highest biodiversity (Shannon and Wiener Index -6.49) followed by evergreen (5.60) and semi-evergreen (5.45) forests.

Table 5. Area (km^2) under different forest and non-forest categories in Sonitpur

Land cover	1994	1999	2001	Net change
Moist deciduous	743.00	656.76	513.36	(-)229.64
Semi-evergreen	59.71	59.19	57.15	(-)2.56
Riverain	7.65	7.65	7.65	No change
Grassland	249.03	251.07	250.56	(+)1.53
Tea garden	383.24	385.28	384.77	(+)1.53
River	658.80	658.80	658.80	No change
Non-forest	3001.58	3084.25	3230.71	(+)229.13
Total	5103.00	5103.00	5103.00	No change

The spatial distribution of different forest types from 1994 to 2001 shows that forest cover in the Sonitpur district undergoing massive reduction with time. The rate of deforestation in the district worked out to be 10.7% from 1994 to 1999 and 20% from 1999 to 2001. The overall rate of forest degradation was estimated to be 28.65% between 1994 and 2001, which may be the highest rate of deforestation anywhere in the country. The findings of the field survey suggest that we have lost very invaluable moist deciduous and semi-evergreen forests in the ongoing deforestation in Sonitpur district. Ironically, these forests happen to be the climax vegetation in the region, known for their immense ecological and economic value.

Forest Canopy Density Assessment

Forest cover is of great interest to a variety of scientific and land management applications, many of which require not only information on forest categories, but also tree canopy density. Forest maps are a basic information source for habitat modelling, prediction and mapping of forest insect infestations, and plant and animal biodiversity assessment. Foresters and forest managers especially require information for gap filling activities to restore forest wealth. Forest managers require accurate maps of forest type, structure, and seral state for fire (Roy, *et al*., 1997) and insect damage assessment and prediction (Chandrasehkhar *et al.*, 2003), wildlife habitat mapping, and regional-scale ecosystem assessment (Blodgett *et al.*, 2000). Few attempts have been reported to stratify the forest density using satellite remote sensing digital data (Roy *et al*. 1990). Previous efforts to estimate tree canopy density as a continuous

variable have utilized linear spectral mixture analysis or linear regression techniques (Iverson *et al*., 1989; Zhu and Evans, 1994; DeFries *et al*., 2000). Other techniques such as physically based models and fuzzy logic have also been explored but are probably premature for use over large areas (Baret *et al*., 1995; Maselli *et al.,* 1995). International Tropical Timber Organisation (ITTO) and Japan Overseas Forestry Consultants Association (JOFCA) while working on project entitled "Utilization of Remote Sensing" developed methodology wherein biophysical spectral indices were developed to stratify forest density (Anon., 1993 and Rikimaru, 1996). In this study the methodology has been validated on an Indian test site.

Study Area

The study site is selected keeping in view the area covering different forest types, structure and undergrowth conditions. Southern part of the Doon valley of the Dehra Dun district of Uttaranchal state (lat. 30° 00' to 30° 16' N; long. 78° 00' to 78° 18' E) was selected for the study. The terrain of the area is irregular and undulating. The summer temperature varies from 38.5°C to 16.7°C and in winters it ranges from 23.6°C to 5.4°C. Precipitation varies from 175 cm to 228.6 cm per annum. The slope ranges from moderate to little bit steep towards the stream lines. The climate is relatively moist tropical. The forest types are mainly North Indian tropical moist Sal forest, North Indian tropical dry deciduous forest, khair and sissoo dominated riverine forest, scrub and degraded forests.

Materials and Methods

The Landsat Thematic Mapper (Landsat-TM) data was taken as an input for the FCD (Forest Canopy Density) model. The FCD model comprises bio-physical phenomenon modeling and analysis utilizing data derived from four indices: Advanced Vegetation Index (AVI), Bare Soil Index (BI), Shadow Index or Scaled Shadow Index (SI, SSI) and Thermal Index (TI). It determines FCD by modeling operation and obtaining from these indices. Landsat-TM (Path-Row 146-039) of 14-09-1996 and Enhanced Thematic Mapper (ETM+) data (Path-Row 146-039) of 14-10-2002 has been used for the digital analysis of forest canopy density. Phenology of the vegetation is one of the important factors to be considered for effective stratification of the forest density. Optimum season for the assessment of forest canopy density in the present study is August – November months of the year. Pre-processing is done in Erdas Imagine to enhance spectral signature of digital data and then enhanced image is imported into BIL format to make it compatible with FCD mapper.

The Forest Canopy Density (FCD) model combines data from the four indices (VI, BI, SI and TI) (Fig. 10). The canopy density is calculated in percentage for each pixel. Vegetation index response to all of vegetation cover such as the forest, scrub land and the grass land was computed. Advanced vegetation index (AVI) reacts sensitively the vegetation quantity. Shadow index increases as the forest density increases. Thermal index increases as the vegetation quantity increases. Black colored soil area shows a high temperature. Bare soil index increases as the bare soil exposure degree of ground increase. These index values are calculated for every pixel.

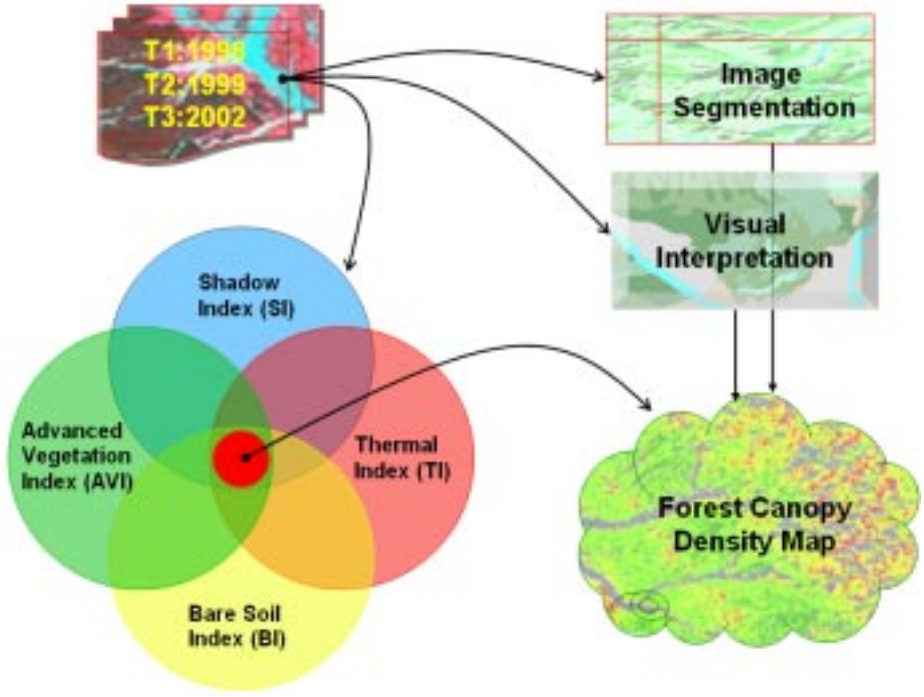

Figure 10: Approach used in the forest canopy density stratification

Note that as the FCD value increases there is a corresponding increase in the SI value. In other words where there is more tree vegetation there is more shadow. Concurrently, if there is less bare soil (i.e. a lower BI value) there will be a corresponding decrease in the TI value. It should be noted that the VI is "saturated" earlier than SI. This simply means that the maximum VI values that can be regardless of the density of the trees or forest. On the other hand, the SI values are primarily dependent on the amount of tall vegetation such as tree which casts a significant shadow.

Vegetation Density is calculated using vegetation index and bare soil index as a prime inputs. It is a pre-processing method which uses principal component analysis. Because essentially, VI and BI have high negative correlation. After that, set the scaling of zero percent point and a hundred percent point. The shadow index (SI) is a relative value. Its normalized value can be utilized for calculation with other parameters.

The SSI was developed in order to integrate VI values and SI values. In areas where the SSI value is zero, this corresponds with forests that have the lowest shadow value (i.e. 0%). Areas where the SSI value is 100, correspond with forests that have the highest possible shadow value (i.e.100%). SSI is obtained by linear transformation of SI. With development of SSI one can now clearly differentiate between vegetation in the canopy and vegetation on the ground. This constitutes one of the major advantages of the new methods. It significantly improves the capability to provide more accurate results from data analysis than was possible in the past. Integration of VD and SSI means transformation for forest canopy density value. Both parameters have dimension and percentage scale unit of density. It is possible to synthesize both these indices safely by means of corresponding scales and units of each

$$FCD = (VD+SSI+1)^{½-1}$$

Forest canopy stratification is carried out using object oriented image analysis. In this approach, the tone and texture are considered for the base level segmentation. Segmented objects are again put into hierarchical stratification by selecting the test and training area based on the ground truth. Finally, forest densities have been stratified using standard nearest neighbour classification scheme. Semi-conventional onscreen visual interpretation of digital data is carried out to map the forest canopy density. Details about the methodology and techniques used for visual interpretation are discussed else where (Roy *et al*., 1989).

Results and Discussion

The output FCD map generated from the semi-expert system (Fig. 11) is sliced in to five density classes and same density stratification is also followed in object oriented image analysis (image segmentation) (Fig. 12) and visual image interpretation of digital data. Details of each density class are shown in the Table 6. Overall analysis of forest canopy density in all the cases indicates that majority of the forests in the study area have canopy closure of 40% to

80%. However, some deviation has been observed between these techniques, class I (> 80 %) shows very high per cent difference, it is also observed that the deviation is reduced with decrease in the canopy density (Table 6 and Fig. 13).

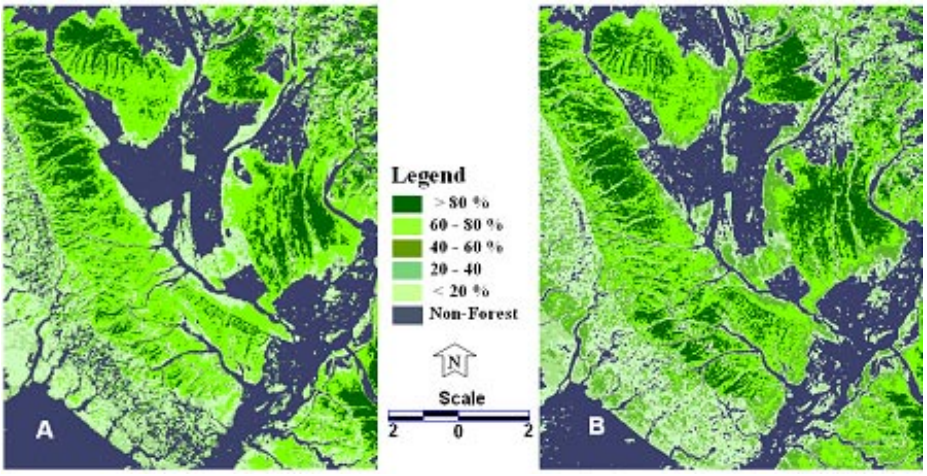

Figure 11: FCD map derived from Landsat TM and ETM+ (A: 14 Sep. 1996 and B: 16 Oct. 2002)

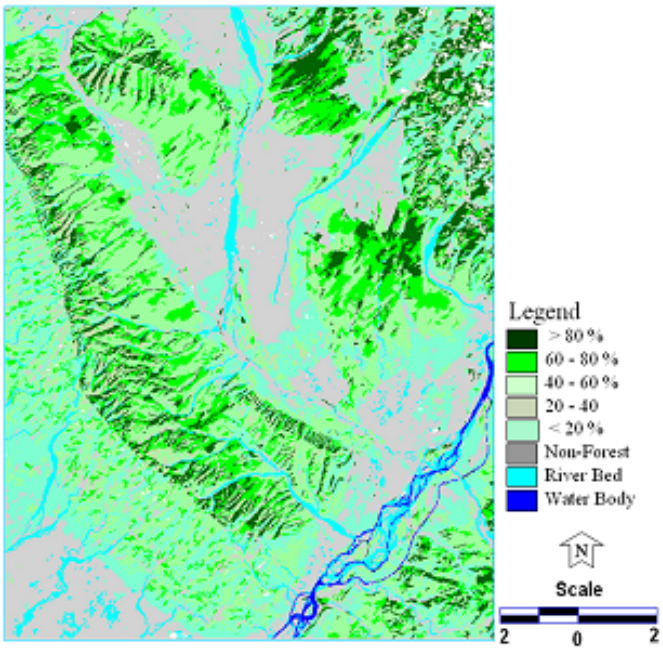

Figure 12: Forest canopy density map derived from object oriented image segmentation

Table 6. Forest canopy density classes and area comparison between different techniques

Density strata	Visual Interpretation (ha)	FCD Mapper Semi-expert (ha)	Object oriented Image Analysis (ha)
> 80%	8493.21	2917.73	3435.30
60 to 80%	11411.82	12803.76	10421.25
40 to 60%	15002.10	10808.26	6284.70
20 to 40%	8506.53	10832.58	12718.16
< 20%	7715.52	4966.11	7012.98
Non-forest	13701.40	26103.78	3088.08
Riverbed	3599.64	—	25472.70
Total	68430.22	68432.22	68433.17

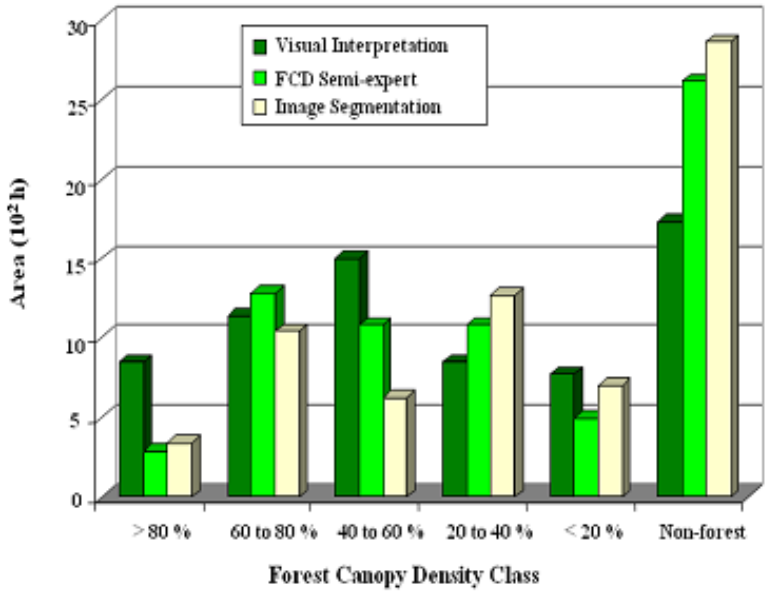

Figure 13: Variation in forest canopy density classes extracted from different techniques

The accuracies of density maps generated from all the methodologies have been assessed to validate the technique. Comparison of the density stratification accuracies have been carried out with reference to ground control points and

different techniques. Accuracy is estimated from the confusion matrix over the training class, in terms of percentage of number of correctly classified category against the total number of classes, viz., class 1 (> 80 %), class 2 (60 – 80 %), class 3 (40 – 60 %), class 4 (20 – 40 %) and class 5 (< 20 %).

It has been observed that overall classification accuracy giving satisfactory results, FCD mapper semi-expert system shows 80.21% accuracy followed by object oriented image analysis of 87.50% and 71.88% respectively. The correlation coefficient value of FCD model with visual interpretation and image segmentation are found to be 0.95 and 0.84 respectively.

Delineation of forest vegetation from the other objects is considered to be very important factor for precise analysis of forest change detection and landuse processes. FCD model shows acceptable degree of delineation of forest vegetation from the other non-forest classes. However, same inputs used for analysis in image segmentation of *eCongnition v2.1* and unsupervised cluster analysis of *Erdas Imagine v8.5* shows boarden inter mixing of forest vegetation with other classes (Fig. 14).

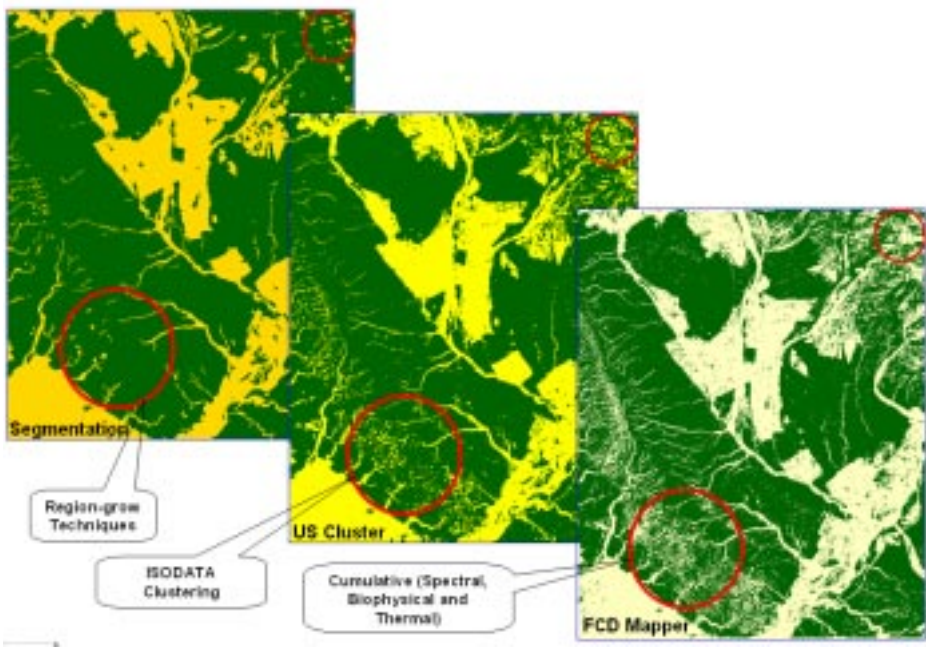

Figure 14: Comparison of various methods used for forest and non-forest separation. Red circles indicates fraction of the delineation of forest from non-forest

The time factor is also considered in the analysis of the models, there is a big difference in the time taken for forest canopy density mapping in the techniques adapted. Visual interpretation took 4 days where as FCD mapper semi expert system took only half a day to complete the job. However, about half of the times of visual interpretation have been spent on object oriented image analysis. Overall analysis and assessment of the techniques used in the present study indicate that FCD semi-expert shows satisfactory results. It requires less manpower and limited ground checks. Therefore FCD model would be a very useful tool especially for foresters for better monitoring and management of forests for the future. Detailed and accurate maps of forest condition and structure are a necessity for rigorous ecosystem management. Forest cover type map along with density maps are the fundamental source of information for fire behaviour modeling, animal habitat management, prediction and mapping of forest insect infestations, and plant and animal biodiversity assessment.

Application of Forest Canopy Density Map derived from FCD Model

Forest canopy density maps derived from FCD Mapper semi-expert system can be used for various purposes. Practical applications of FCD map have been demonstrated by taking two important forestry applications in the present study. In the first case, FCD maps derived from two data sets with an interval of 6 years i.e., 1996 and 2002 have been used for the detection of change in Sal (*Shorea robusta*) forest canopy density. Change detection assessment of this time interval shows that there is reduction in forest canopy in some isolated locations as shown in Fig. 15 indicated by red circle. The canopy density of > 80% reduced to 60 - 80% categories. This is a result of infestation Sal heart wood borer around the period 1998 to 2000. Most of the affected trees are removed from the stand and some trees lost canopy and became moribund which has crated openings in the Sal forest stand. However, some area shows development and expansion of the tree crown over 6 years as indicated with yellow circles in the same figure. These areas are unaffected by the insect infestation.

Some of the important forestry operations where forest canopy density map could be useful are listed below.

FCD model can used for following important forestry operations viz.,

- To plan afforestation and reforestation activities

- Identification of forest canopy gaps for enrichment planting
- Rehabilitation of encroached and logged over areas
- Planning of operational silvicultural systems
- Preparation of Working Plans (Maps at beet / coupe level)
- Regeneration or Gap filling
- Wildlife habitat management
- Planned timber extraction
- Can be used as a base line data for scientific work
- Detection of disease affected areas
- Change detection in forest and non-forest
- Predictive analysis of change in forest canopy density

In the second case, three data sets (1996, 1999 and 2002) are used to derive forest canopy map of the same study area. Change detection of 1996 to 1999, 1999 to 2002 and 1996 to 2002 have been carried out to assess the

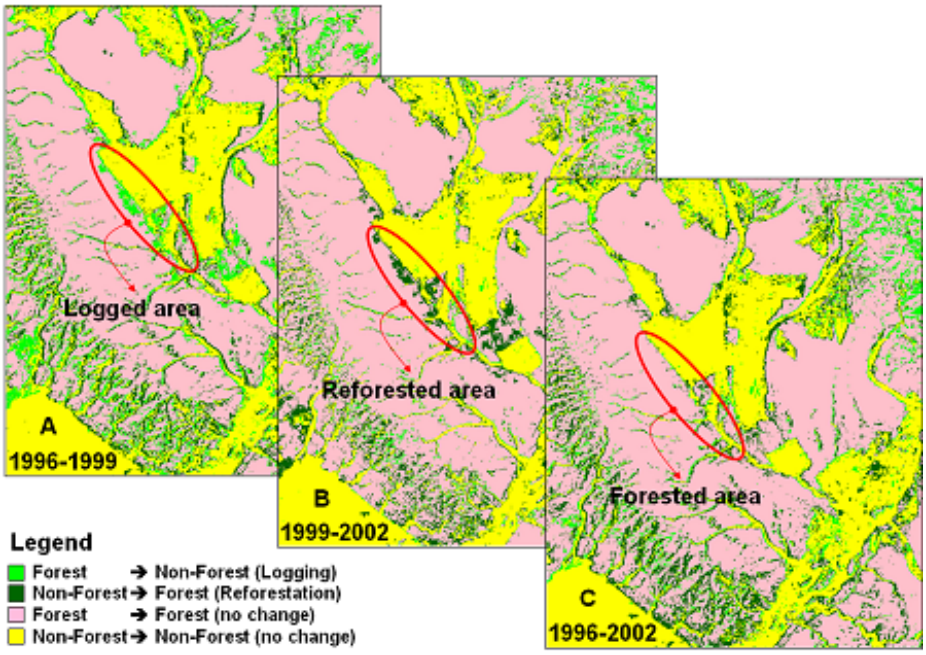

Figure 15: Change in forest canopy density. Red ellipse on green area indicates reduction of forest density due to infestation of Sal heartwood borer

logged over area and reforested area. There was a forest as indicated by red ellipse in the Figure 16 which was removed around end of the year 1996. Change detection between the period 1996 to 1999 shows logged over area (Fig. 15). Same logged area was again replanted with high density *Eucalyptus* plantation in the end of the year 1999. Change map of the area between the periods 1999 to 2002 shows reforested area as indicated by red ellipse (Fig. 16). This kind of results help in management of forest cover in the local level.

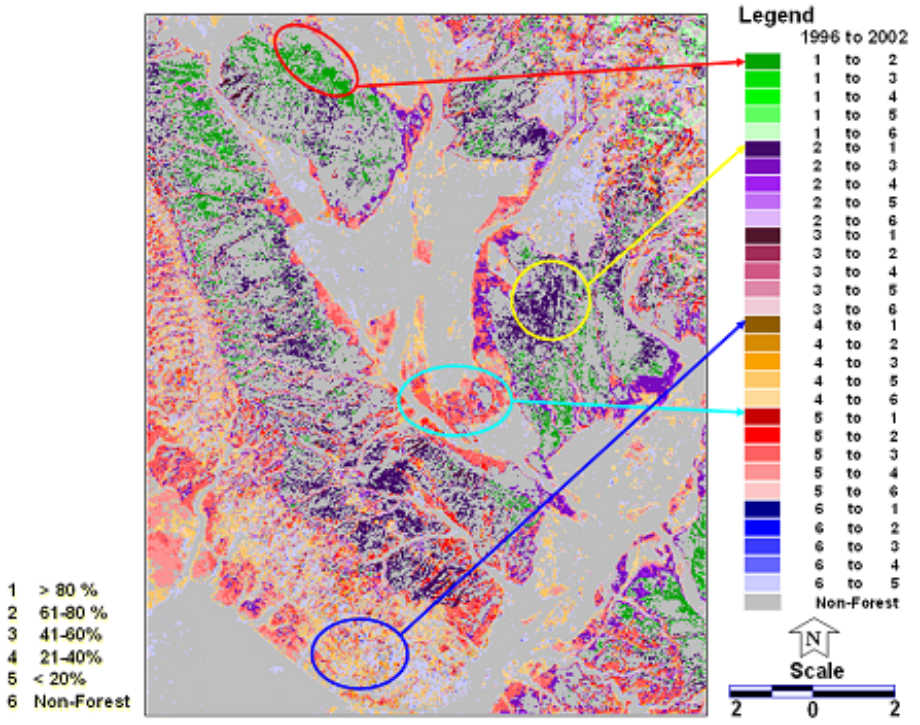

Figure 16: Change detection of logged over area and reforested area from 1996 to 2002

Forest Canopy density is one of the most useful parameters considered in the planning and implementation of rehabilitation. Conventional remote sensing methodology is based on qualitative analysis of information derived from study area i.e. ground truthing. This has certain disadvantages in terms of time and cost required for training area establishment and also requires expertise. The JOFCA-ITTO semi expert system is useful tool for better management of forests. The model has been validated for its high accuracy. Compared to other methods, FCD Mapper has shown good results with respect to class interval, time taken for analysis and mapping accuracy. Cluster analysis of forest canopy density

map derived from FCD Mapper and Conventional methods have showed similar trends with respect to percent area of forest and non-forest. Gregarious occurrence of bushy vegetation like Lantana poses problem in delineation of forest canopy density as their reflectance is similar to that of the forest. Further improvement can done to incorporate geographic coordinate system, map composition and one click data import facility so that user can get the full-fledged utility of the semi expert system.

CONCLUSIONS

Increasing population pressure with multiplied demand for the domestic needs have carved out separate fracture in the biosphere by modifying the forest ecosystems. In the process we have been loosing green cover at faster rate than expected. Sustainable management of forest resources has become key agenda of the century. The assessment of the forest fire and degradation is one of the important factors to be considered for better management of the forest resources. However, the lack of reparative analysis with synoptic coverage has been one of the limitations in the conventional assessment techniques which can be potentially over come by using geospatial approach. Hence, satellite remote sensing has provided holistic view to the planet Earth. The satellite remote sensing has enabled to map and monitor vegetation resources in varying scale and time. The geographic information system enables to organize the data sets for analysis and decision making process. India has made significant efforts to build state of art satellite systems and develop applications to manage the natural resources. Forest cover mapping using space technology is already an operational tool. Under a national scientific initiative India has developed comprehensive data base on vegetation types, disturbance regimes, fragmentation and biological richness at landscape level in the important eco-regions. Satellite images have a considerable value for mapping forest fire and degradation assessment. It helps in decision making processes for the proper establishment of the green cover over the affected areas.

Extensive areas are burnt and deforested every year, leading to widespread environmental and economic damage. The impact of this damage involves not only the amount of timber burnt but also environmental damage to forested landscapes leading, in some cases, to land and forest degradation and the prevention of vegetation recovery. However, further more improvement required to enhance the process of better assessment, monitoring and management of the forest resources of the planet earth.

REFERENCES

Anonymous 1993. Rehabilitation of logged over Forests in Asia/Pacific region. Final Report of Sub Project II International Tropical Timber Organization- Japan Overseas Forestry Consultants Association, 1-78.

Abhineet Jainl, Shirish A. Ravan, R.K. Singh, K.K. Das and P.S. Roy, 1996. Forest fire risk modelling using Remote Sensing and Geographic Information System . Current Science, 70(10): 928-933.

Baret, F. J., G. P. W. Clevers, and M. D. Steven, 1995. The robustness of canopy gap fraction estimates from red and near-infrared reflectances: a comparison of approaches. Remote Sensing of Environment, 54(2): 141-151.

Bapedal. 1996. National Coordination Team on Land and Forest Fire Management. Int. Forest Fire News, No. 14, 27-28.

BAPPENAS. 1992. International Workshop on Long-Term Integrated Forest Fire Management in Indonesia, Bandung, 17-18 June 1992. BAPPENAS/GTZ, Jakarta, Indonesia. 34 p. (mimeo).

Bartlett, H.H. 1955, 1957, 1961. Fire in relation to primitive agriculture and grazing in the tropics : annotated bibliography, Vol. 1-3. Mimeo. Publ. Univ. Michigan Bot. Gardens, Ann Arbor, USA.

Blodgett, C., Jakubauskas, M., Price, K., and Martinko, E. 2000. Remote Sensing-based Geostatistical Modeling of Forest Canopy Structure. ASPRS 2000 Annual Conference, Washington, D.C., May 22-26.

Chandrashekhar, M.B., Sarnam Singh, N.K. Das and P.S. Roy. 2002. Wildlife-Human conflict analysis in Kalatop Khajjiar Wildlife Sanctuary, Himachal Pradesh: Geospatial approach. National Seminar on Relevance of Biosphere reserve, National parks and Wildlife sanctuaries (Protected Habitats) in present context. May 25-26, 2002, held at Gurukula Kangri University, Hardwar (U.A.).

Cole, M.M. 1986. The savannas. Biogeography and Botany. Academic Press, London, UK.

DeFries, R. S., M. C. Hansen, and J. R. G. Townshend, 2000. Global continuous fields of vegetation characteristics: a linear mixture model applied to multi-year 8km AVHRR data. International Journal of Remote Sensing, 21(6/7): 1389-1414.

De Ronde, C., J.G. Goldammer, D.D. Wade, and R.V. Soares 1990. Prescribed fire in industrial pine plantations. In: J.G. Doldammer (editor), Fire in the tropical biota. Ecosystem processes and global challenges. Ecological Studies 84. Springer-Verlag, Berlin-Heidelberg. pp. 216-272.

Ehrlich D., E.F. Lambin and J. Malingreau 1997. Biomass Burning and Broad-scale Land Cover Changes in Western Africa. Remote Sensing of the Environment, 61: 201-209.

Fernandez A., P. Illera and J.L. Casanova 1997. Automatic Mapping of Surfaces Affected by Forest Fires in Spain Using AVHRR NDVI Composite Image Data. Remote Sensing of the Environment, 60: 153-162.

Flasse S.P. and Ceccato P.S. 1996. A contextual algorithm for AVHRR fire detection, *International Journal of Remote Sensing,* 17(2): 419-424.

Goldammer, J.G. 1988. Rural land use and fires in the tropics. Agroforestry Systems, 6 : 235-253.

Goldammer, J.G. (ed.) 1990. Fire in the tropical biota. Ecosystem processes and global challenges. Ecological Studies 84, Berlin-Heidelberg : Springer-Verlag.

Goldammer, J.G., and S.R. Penafiel 1990. Fire in the pine-grassland biomes of tropical and subtropical Asia. *In :* J.G. Goldammer (editor) Fire in the tropical biota. Ecosystem processes and global challenges. Ecological Studies 84. Srpinger-Verlag, Berlin-Heidelberg, Germany. pp. 44-62.

Goldammer, J.G. 1991. Tropical wildland fires and global changes : Prehistoric evidence, present fire regimes, and future trends. *In :* J.S. Levine (editor), Global biomass burning. The MIT Press, Cambridge, Massachussetts, USA. pp. 83-91.

Goldammer, J.G. 1993. Feuer in Waldokosystemen der Tropen and Subtropen. Birkhauser-Verlag, Basel-Boston, Schweiz. 251 p.

Goldammer, J.G. 1994. Interdisciplinary research projects for developing a global fire science. A paper presented at the 12th Confer. Forest Meteorology, October 26-28, 1993, Jekyll Island, Georgia. Society of American Foresters Publ. 94-02 : 6-22.

Goldammer, J.G., B. Seibert, and W. Schindele. 1996. Fire in dipterocarp forests. *In :* A. Scheulte and D. Schone (editors), Dipterocarp forest ecosystems : Towards sustainable management. World Scientific Publ., Singapore-New Jersey-London-Hongkong. pp. 155-185.

Iverson, L. R., E. A. Cook, and R. L. Graham, 1989. A technique for extrapolating and validating forest cover across large regions: calibrating AVHRR data with TM data. International Journal of Remote Sensing 10(11): 1805-1812.

Justice C.O., and Dowty P. 1993. IGBP-DIS Satellite fire detection alogrithm workshop technical report. IGBP-DIS Working Paper No. 9, 88pp., Feb. 1993, NASA/GSFC, Greenbelt, Maryland, USA.

IFFM (Integrated Forest Fire Management Project). 1996. Integrated Forest Fire Management Project in East Kalimantan. Int. Forest Fire News, 14 : 29-30.

IFFN (International Forest Fire News), 2002. Fire Situation In India. Int. Forest Fire News, 26: 23-27.

IGAC (International Global Atmospheric Chemistry Project). 1992. Biomass Burning Experiment : Impact on the Atmosphere and Biosphere. An Activity of the International Global Atmospheric Chemistry (IGAC) Project, IGAC Core Project Office. The MIT Press, Cambridge, Massachussetts, USA. 19 pp. + App.

Kasischke, E.S., L. L. Bourgeau-Chavez and N.H.F. French 1994. Observations of Variations in ERS-1 SAR Image Intensity Associated with Forest Fires in Alaska. IEEE Transactions on Geoscience and Remote Sensing, 32(1): 206-210.

Komarek, E.V. 1968. Lightning and lightning fires as ecological forces. *In :* Proc. Ann. Tall Timbers Fire Ecol. Conf. 8. Tall Timbers Research Station. Tallahassee, Florida, USA. pp. 169-197.

Kowal, N.E. 1966. Shifting cultivation, fire and pine forest in the Cordillera Central, Luzon, Philippines. Ecol. Monogr., 36 : 389-419.

Luckman, A., J. Baker, T. M. Kuplich, C. C. Yanasse and A.C. Frery 1997. A Study of the relationship between Radar Backscatter and Regenerating Tropical Forest Biomass for Spaceborne SAR Instruments. Remote Sensing of the Environment, 60: 1-13.

Maselli, F. C., Conese, T. D. Filippis, and S. Norcini, 1995. Estimation of forest parameters through fuzzy classification of TM data. IEEE Transactions on Geoscience and Remote Sensing, 33 (1): 77-84.

Noble, B. 1990. Socio-economic and cultural background of forest fires in the Benguet pine forests. FAO TCP Assistance in Forest Fire Management, the Philippines Working Paper No. 2. FAO Rome, TCP/PHI/8955, 50 p. (mimeo).

Nye, P. H., and D.J. Greenland. 1960. The soil under shifting cultivation. Tech. Comm. 51, Commonwelath Bureau of Soils. Harpenden, UK.

Otsuka, M. 1991. Forest management and farmers. Towards the sustainable land use – A case study from East Kalimantan, Indonesia. Master Program of Environmental Sciences. The University of Tsukuba, Japan (unpubl.).

Pancel, L., and C. Wiebecke 1981. "Controlled Burning" in subtropischen Kiefernwaldern und seine Auswirkungen auf Erosion and Artenminderung im Staate Uttar Pradesh. Forstarchiv, 52 : 61-63.

Phillips, J. 1965. Fire as master and servant : its influence in the bioclimatic regions of Trans-Saharat Africa. *In :* Proc. Tall Timbers Fire Ecol. Conf. 4. Tall Timbers Research Station. Tallahassee, Florida, USA. pp. 7-109.

Porwal, M.C., M.J.C. Meir, Y.A. Hussin and P.S. Roy : 1997 : Spatial Modelling for fire risk zonation using Remote Sensing and GIS. Paper presented in ISPRS Commission VII Working Group II Workshop on Application of Remote Sensing and GIS for Sustainable Development, Hyderabad, 1997.

Prins, E.M., and Menzel, W.P. 1992. Geostationary satellite detection of biomass burning in South America. International Journal of Remote Sensing, 13(15): 2783-3462.

Rikimaru, A. 1996. LANDSAT TM Data Processing Guide for forest Canopy Density Mapping and Monitoring Model. ITTO workshop on utilization of remote sensing in site assessment and planning for rehabilitation of logged-over forest. Bangkok, Thailand, July 30- August 1,1996.1-8.

Roy, P.S., R.N. Kaul, M.R. Sharma Roy and S.G. Garbyal, 1985. Forest type stratification and delineation of shifting cultivation areas in eastern part of Arunachal Pradesh using Landsat MSS data. International Journal of Remote Sensing, 6(3): 411-418.

Roy, P.S., Diwakar, P.G., Vohra, T.P.S. and Bhan, S.K.1990. Forest Resource Management using Indian Remote Sensing Satellite data. Asian -Pacific Remote Sensing J. 3 (1): 11-22.

Roy, P.S., S. Miyatake and A. Rikimaru, 1997. Biophysical Spectral Response Modeling Approach for Forest Density Stratification. Proc.The 18th Asian Conference on Remote Sensing, October 20-24, 1997, Malaysia.

Steyaert, L.T., F.G. Hall and T.R. Loveland 1997. Land Cover Mapping, Fire Regeneration, and Scaling Studies in the Canadian Boreal Forest with 1-km AVHRR and Landsat TM data. Journal of Geophysical Research, 102(d24): 29581-29598.

Stott, P., J.G. Goldammer, and W.L. Werner. 1990. The role of fire in the tropical lowland deciduous forests of Asia. *In :* J.G. Goldammer (editor), Fire in the tropical biota. Ecosystem processes and global challenges. Ecological Studies 84. Springer-Verlag. Berlin-Heidelberg, Germany, pp. 21-44.

Stuttard, M., S. Boardman, P. Ceccato, I. Downey, S. Flasse, M. Gooding and K. Muirhead, 1995. Global Vegetation Fire Product. Final Report to the JRC. Contract 100444-94-09-FIEP ISP GB. Earth Observation Sciences Ltd.

Viedma, O., J. Meli, D. Segarra and J. Garc'a-Haro 1997. Modeling Rates of Ecosystem Recovery after Fires by Using Landsat TM data. Remote Sensing of Environment, 61: 383-398.

Watters, R.F. 1971. Shifting cultivation in Latin America. FAO for Dev. Pap. 17. Food and Agricultural Organisation of the United Nations, Rome, Italy.

Zhu, Z. and D. L. Evans, 1994. US forest types and predicted percent forest cover from AVHRR data. Photogrammetric Engineering & Remote Sensing, 60(5): 525-531.

DESERT LOCUST MONITORING SYSTEM – REMOTE SENSING AND GIS BASED APPROACH

D. Dutta, S. Bhatawdekar, B. Chandrasekharan, J.R. Sharma,
S. Adiga*, Duncan Wood** and Adrian McCardle**
Regional Remote Sensing Service Centre, CAZRI Campus, Jodhpur, Rajasthan
** NNRMS/RRSSC, ISRO Headquarters, Bangalore*
*** RADARSAT International, Richmond BC, Vancouver, Canada*

Abstract : Desert locusts (DL) are a serious problem during April to August in the deserts and semi-deserts of Republic of Kazakhstan and causing extensive crop damage. There is no institutional and functional mechanism to forecast the habitat of locusts and most of the area remains unnoticed after laying eggs. The key to improve DL forecasting and control depends on the collection and generation of historical database on locust, weather and habitat from affected region. Looking at the problem a Decision Support System (DSS) has been developed on ARC/INFO GIS with ergonomic user interface for ingestion and subsequent analysis of locust related information vis-à-vis bio-physical and climatic data acquired from various satellite sensors and hydromet weather server respectively to identify high frequency breeding areas well before the physiological development is completed. Weather based analytical models for physiological development of DL has been dovetailed with the DSS for facilitating historic and present data analysis in relation to locust activity. This will enhance the surveying capability and better forecasting.

INTRODUCTION

Desert locusts (*Schistocerca gregaria*, Forskl) are known to be one of the dreaded insects since time immemorial for agricultural production. More than 60 countries are affected at varying degrees during plague development caused by several consecutive generation of successful breeding triggered by a favourable sequence of heavy and widespread rainfall. Normally in solitary phase density remains low and poses no economic threat but under favourable bio-climatic condition population increases very fast over space and time and forms gregarious swarms which can devastate agricultural lands. It is during this period that locusts can cause enormous damage to standing crops even

Satellite Remote Sensing and GIS Applications in Agricultural Meteorology
pp. 401-423

several hundred kilometers away from their origin. However, early detection of locust growth and breeding sites are two key issues for efficient surveillance and control of desert locusts (DL). Locating high frequency breeding areas over temporal and spatial scale warrants analysis of large number of biophysical and bio-climatic variables in relation to locust physiology. Nevertheless the most difficult part of forecasting is migration of adult winged locusts, which is influenced by large number of weather parameters at synoptic scale.

To manage the locust devastation and its timely warning there is a need for structured geospatial database in GIS environment and interfacing with other analytical and modeling tools to form sophisticated spatial Decision Support System (Healy *et al.*, 1996). This paper describes one such system and the approach to meet forecasting need using ARC/INFO GIS and a host of digital data especially from optical and microwave satellites sensors. GIS and Remote Sensing technology dramatically improves the ability of forecasting through effective manipulation of large volume and variety of spatially referenced and descriptive data. The logical aspects of database design employs integration of all application requirements in a database structure that supports the view and processing needs of these applications. The physical aspects refers to evalusation of alternative implementations and choosing storage structure, query mechanism and access methods (Navathe and Schkolnik, 1978).

The major plague of 1985-89 prompted the world acridologists to improve the forecasting tools and methodologies in order to maximize the effectiveness of pesticides and reduce the toxicity in aquatic environment. The highest priority was assigned to modeling and validating the spread of infestations over space and time in relation to concurrent changes in weather and vegetation (FAO, 1989).

In the present study effort has been made to provide interface to handle population dynamics, physiological development, habitat suitability as well as climate suitability for breeding and migration. The locusts biology in relation to weather and other environmental factors have been used in forecasting process. The DSS essentially adheres with norms of database design standard, customization, validation, integration before actual query mechanism and performing modeling operations.

Locusts in Kazakhstan

Locusts are a recurring problem in Kazakhstan but the problem has been intensified since 1996 mostly due to collapse of uncompetitive farming and

unusually warm weather in recent past. In 2000, 27% of total food grain production i.e. 5 million ton was destroyed and more than 8.8 million ha land was affected. The perennial dynamics of locust population has strong relationship with transformation of landuse fabric in the republic from 1954 to 1992 onwards. The landuse distribution of Kazakhstan is dominated by semi desert and deserts (77.2%), and grassland and forests of 9.4%. The grasslands used to serve as ecological niche for the desert locusts confined to smaller pockets from which they used to migrate in adjoining fringe of agricultural lands. But the land development history of Kazakhstan has adversely affected the natural habitats of locusts while passing through 4 different phases since 1954.

i. Active development of virgin and fallow lands (1954-1964).

ii. Use of soil protection system in agriculture (1965-1974).

iii. Intensive use of agrotechnology (1976-1992) and indiscriminate use of pesticides which has caused locust insurgence.

iv. Continuous shrinking of agricultural lands due to economic constraints, giving rise to multistage fallow (1992 onwards).

As a result of this multi-phasic land transformation large portion of arable lands have been infested with wild grasses and bushes. The extent of such lands has largely expanded and redistributed in the contact zones between cultivated and uncultivated lands in the territory forming excellent habitat for DL scattered over large areas especially in the west, south-east and south. Out of 35 species of DL found in Kazakhstan mostly 3 types are dominating namely Asian, Italian and Moroccan. In the east Italian locusts (*Calliptamus italicus*) dominate, whereas in south-east Asian locusts (*Locusta migratoria*) and in south Moroccan locusts (*Dociostaurus maroccanus*) are prevalent. The situation is getting worse not only in Kazakhstan but also in adjoining countries viz. Russia, Uzbekistan and Kyrgystan. The locusts are also spreading from their traditional breeding grounds to further west. Many new areas have been reported first time since 80 years.

Key issues in DL control

The major issues related to DL control can be summarized as follows.

- Acquisition of bio-physical information from vast inaccessible and hostile terrain (locust habitats) using satellite remote sensing technology with better temporal sampling capability.
- Parameterization and accurate translation of remote sensing information in relation to ground segment for model input.
- Use of spatial variables for process modeling and subsequent field validation.
- Bio-climatic modeling for locust physiology and migration based upon historical locust events and ground intelligence.
- Operationalization for forecasting of high frequency breeding areas and flight behavior.

Satellite remote sensing helps to examine relationships between distributions of insect pests, rainfall and green vegetation in the seasonally dry tropics. For migration and dispersal modeling there is a need for studying historical records for plague development and forecasting. Current weather data could help to examine downwind airborne dispersal of insect pests over a range of temporal and spatial scales. Based upon the survey of ecological conditions in potential breeding and outbreak areas, aerial and ground survey is organized that become potentially suitable after rainfall incidence. Following the survey operation strategies are chalked out to control DL populations when exceeds above a specific threshold limit, mainly in known outbreak areas.

Requirement for a GIS to support Forecasting

DSS facilitates incorporation and integration of a variety of information, relevant for modeling of locust population on spatial and temporal context on a common platform. It maximizes the opportunities for early intervention and management of locust swarms. Characteristically it is ergonomic with user interface to facilitate both data capture and analysis through a series of menus for accessing separate information management tools with data display on spatial context. It is desirable to bring together all the information sources used by forecasting and field staff to aid in decision making process. The characteristic features of the DSS are expected to be as follows (Healey *et al.*, 1996).

i. Access to historical records of locust sightings and associated environmental conditions, with ability to cross-reference related events.

ii. Structured access to reference material for new and existing locust case studies the later being derived from sources such as the published Desert Locust Forecasting Manual (Pedgley, 1981).

iii. Rapid input and storage of accurately located sightings.

iv. Facilities to display and analyze locust events in the context of both current and antecedent environment conditions, both meteorological and vegetation-related.

v. Ability to compare the present spatio-temporal configuration of locust events, together with prior dynamics, to past analogue spatio-temporal sequences from previous plagues and recession periods.

vi. Interfacing between GIS and other analytical tools for modeling of locust development and migration.

vii. Capacity of handling historical locust data for analysis of past locust events and analogue development from previous upsurge based on similarity / matching index.

viii. Capability of handling raster, vector and descriptive data as well as comparison of multiple raster and vector maps for analysis of the relationships between locust events and bio-climate.

ix. Analysis of daily weather data for bio-climatic modeling for breeding, upsurge and duration of life stage.

x. Organisational requirements to meet in-house procurement standards for hardware and software.

What is Geo-LIMIS

Geo-LIMIS (Geographically Encoded Locust Impact Minimization Information System) is a Decision Support System (DSS) developed on ARC/ INFO 8.0 NT platform using ARC macro language, ODE tools and Visual Basic. The aim is to provide operational decision support for locust habitat suitability, surveillance, prioritization of critical areas and weather conditions on spatial context to enable timely control measures at the field level over the target areas. There is an unique amalgamation of data from various sources such as remote sensing data from optical and microwave satellites along with daily meteorological data downloaded from internet and ground based information on locust generated by the line departments. The thematic maps

used in habitat suitability mapping include landuse/landcover, vegetation density, landform, soil texture and soil moisture supplemented with a large number of reference maps viz. road, rail, stream, administrative units, settlement location, meteorological stations etc. The conceptual diagram of working of Geo-LIMIS is given in Figure 1 and the main menu in Figure 2.

Functionally Geo-LIMIS comprises of six modules viz. i) Spatial database dictionary, ii) database validation as per the database standard formulated for the project, iii) database integration with the query shell using validated database, iv) Inputting locust information from field observation to create spatial database along with the descriptive data i.e. the swarm type, species, density of egg/ hopper/adult as per field survey and other ancillary information on ground condition, v) Geo-LIMIS query shell – It is the main habitat suitability analysis module. Query shell provides facilities for display of single or multiple themes, locust ground observations, theme overlay, generation of integrated layer for habitat suitability, *in situ* report generation from locust sighting regarding the prevailing ground condition during locust observation which finally is used as knowledge based input for generating habitat suitability map for the entire area from known sample area known as cohort distribution, vi) Life cycle builder – It necessarily uses daily weather data and analyzes the locust breeding suitability under prevailing weather condition, egg and hopper development and flight suitability.

Figure 2: Geo-LIMIS main menu

Spatial Database Dictionary

The package has devised suitable database structure for spatial and non-spatial database elements. Database elements, required to be integrated, with the package must adhere to these standards. To explore and analyze these database elements efficiently and provide ease to the users in executing various tasks of the package, all the database elements and components should be known to the shell. For this purpose, Geo-LIMIS maintains a spatial database dictionary, named as LWTHEME.LWS (INFO table), to store details of various database elements. This dictionary can be updated and extended by the user through a user friendly GUI (Figure 3). User can browse through the spatial dictionary, update or extend it.

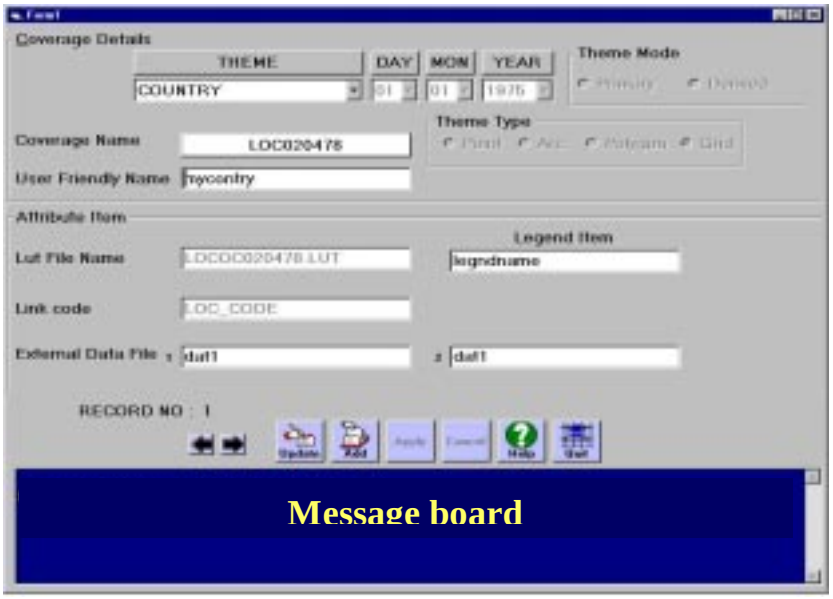

Figure 3: Spatial database dictionary interface

This module (Figure 4) performs the validation of each database element (spatial layers) and also checks the integrity of the database and validates each database element whether it adheres to Geo-LIMIS database design and standards or not. It generates a validation report after critically examining the data. The spatial database elements, which have an entry in the spatial database dictionary will only be considered for validation. During database validation the package performs following validation checks vis-à-vis Geo-LIMIS database design and standards.

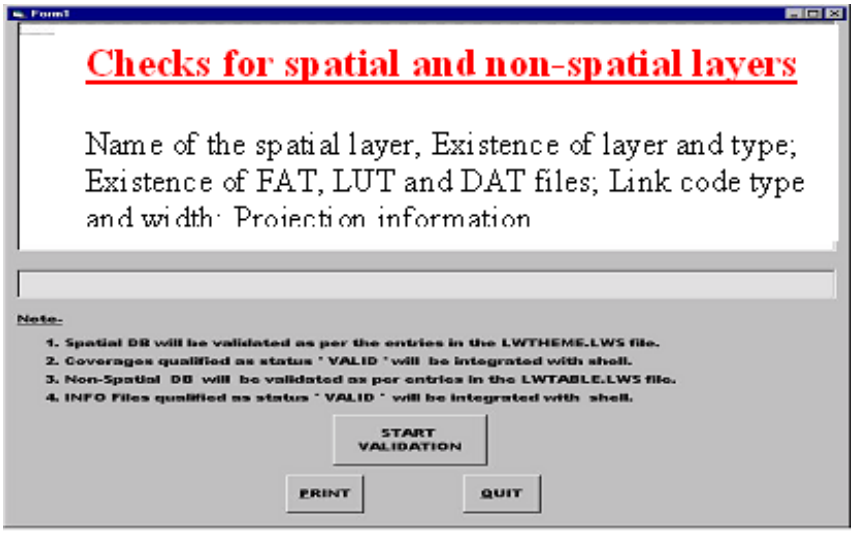

Figure 4: Database validation module

i. Name of the spatial layers.

ii. Existence of layers and type of layers, feature attribute table (FAT), look up table files. (.LUT) and files containing data for non-spatial themes (.DAT).

iii. Existence of link-code in feature attribute table (FAT), .LUT and .DAT files.

iv. Definition of link-code i.e. width and each entry of link-code.

v. Projection information.

5.3 Database Integration Module

This module performs the pre-processing and integration of each validated database element (spatial layers) and prepares them for further analysis. Database integration can be performed either for all the themes or for selected themes (Figure 5a and 5b). The spatial database elements, which have an entry in the spatial dictionary and have been validated successfully, will only be considered for database integration. Integration is performed in either of the following cases.

Figure 5a: Database integration

Figure 5b: Database integration

i. Whenever the database is being integrated for the first time.

ii. After updating any spatial layer, either spatial features or its feature attribute table or associated .LUT files.

iii. Whenever a new layer is added to the database.

Major tasks performed during database integration include –

i. Generation of intermediate GRID's for using by the Geo-LIMIS query shell for virtual masking.

ii. Creation of projection files (.PRJ) required for projection transformation from one system to another.

iii. Generation of Theissen polygon layer from point meteorological station data. As a result the entire area is spatially divided into number of polygons each represented by a meteorological station.

Input Locust Information Module

This module (Figure 6a) is provided to convert non-spatial locust information into spatial data. It is important to understand the soil-vegetation and climatic information in the locust sight points. The knowledge gained in terms of ground condition during locust reporting helps to build the complex query for habitat suitability analysis. This module generates date wise spatial file dovetailed with field attribute information. Each point entry is automatically projected into desired system and records the data against the

point entered. Efforts are ongoing to directly input GPS measurements from field. Besides entry of field points graphically/key board, the module also supports entry of point layers generated outside in ARC/INFO or Arcview environment. User can browse through all the points of sighting and visualize the detailed locust information, edit or update (Figure 6b). For enhancing the referencing capability, layers such as roads, rail, settlement and administrative boundaries can be set in the back environment to precisely ingesting the locust sight point.

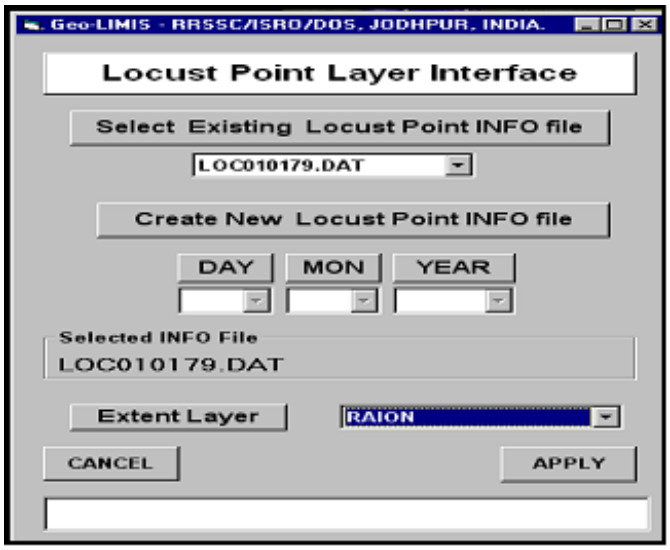

Figure 6a: Locust input interface

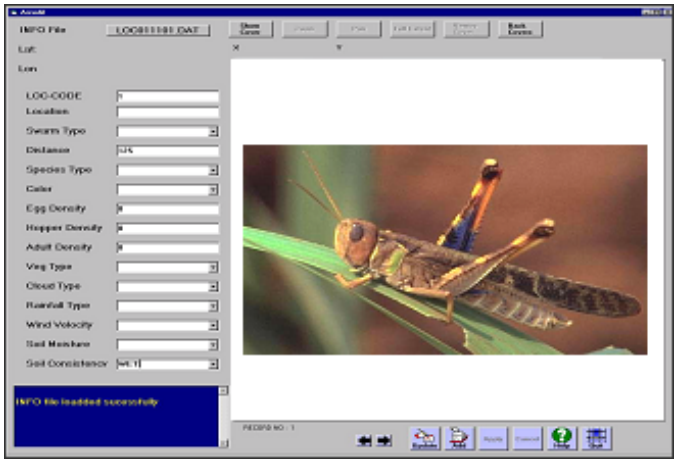

Figure 6b: Spatial database generation with attributes

From locust sighting files those observations would be sorted where the density of locust are above a certain threshold to be critical. The points, thus identified, are used for generation of buffer of specified width (as per the ground spread). The objective of doing so is to identify the biophysical condition underneath buffer, which is supposed to be critical in terms of locust. The information extracted from the buffer area, is used by the Geo-LIMIS query shell, for habitat suitability analysis.

QUERY SHELL MODULE

Geo-LIMIS Query Shell

It is the main display analysis and query shell module (Figure 7) which facilitates display of spatial and non-spatial data, identification of theme attributes, overlay of themes, visual query of single of multiple themes, generation of integrated layers, building queries for suitable locust sites and habitat suitability map in desired scale as well as statistics generation. Besides query shell hosts a number of other functionalities viz. symbol updating, choice of text font and color, zooming/panning, saving of map output in various formats etc.

Figure 7: Query shell main menu

SELECT_AOD (Selection of area of display): This is the first option which facilitates user to select desired area of display (Figure 8). Selection could be made for one or more polygons, by defining as irregular area or by specifying the geographic coordinates. The area could be selected by clicking on the graphics or by name through a pull down menu. The selected area of display (AOD) will be used for all display purpose. Area outside the AOD will be virtually masked.

SPATIAL_DISPLAY (Spatial display of themes, Primary or Derived): The option is used for display of selected theme (primary or derived) pertaining to the AOD (Figure 9a, b, c, d). Along with map the legend, display scale, north arrow and index map is also displayed.

NON_SPATIAL _DISPLAY (For displaying of locust and meteorological data): This facility provides display of locust related information viz. density

of egg/hopper/adult etc in the form of spot/ratio (Figure 10a, b) as well as meteorological data of selected variable on monthly basis in graphical form. The size of the spot varies proportionately with the value of density. The detailed information of any locust sight could be visualized as a text file using sight-info button. The some of the climate data that could be plotted include temperature, humidity, wind velocity, cloudiness and rainfall in the form of bar or line diagram. For climate data display the EXCEL file must be available in the user's workspace. The package automatically coverts .xls files for corresponding meteorological station into INFO file. In the EXCEL to INFO conversion interface, the user can specify the name of the station along with the year of interest.

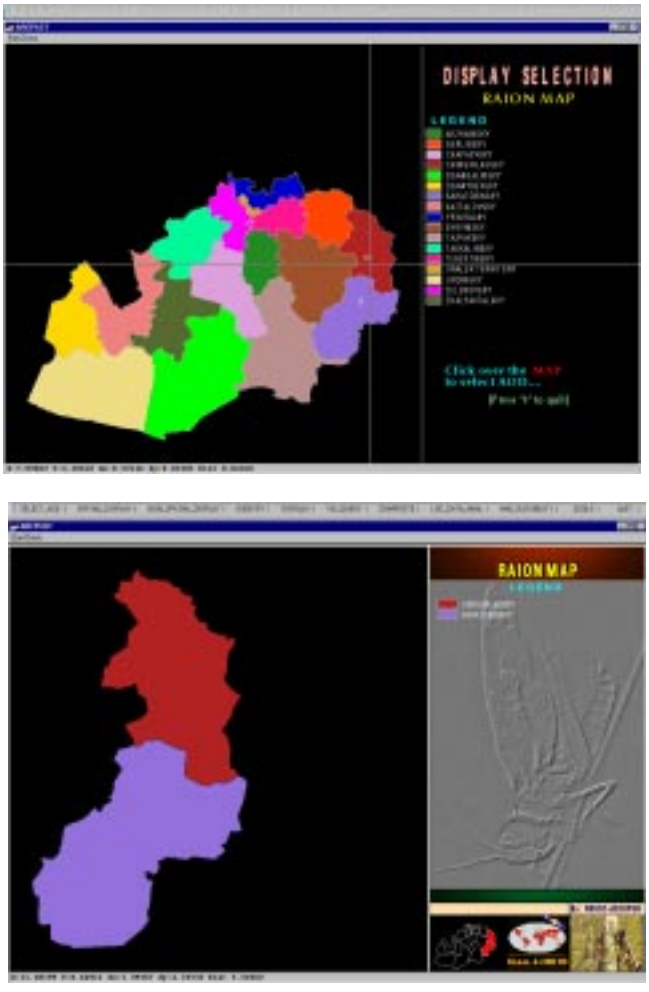

Figure 8: Selection of area of display

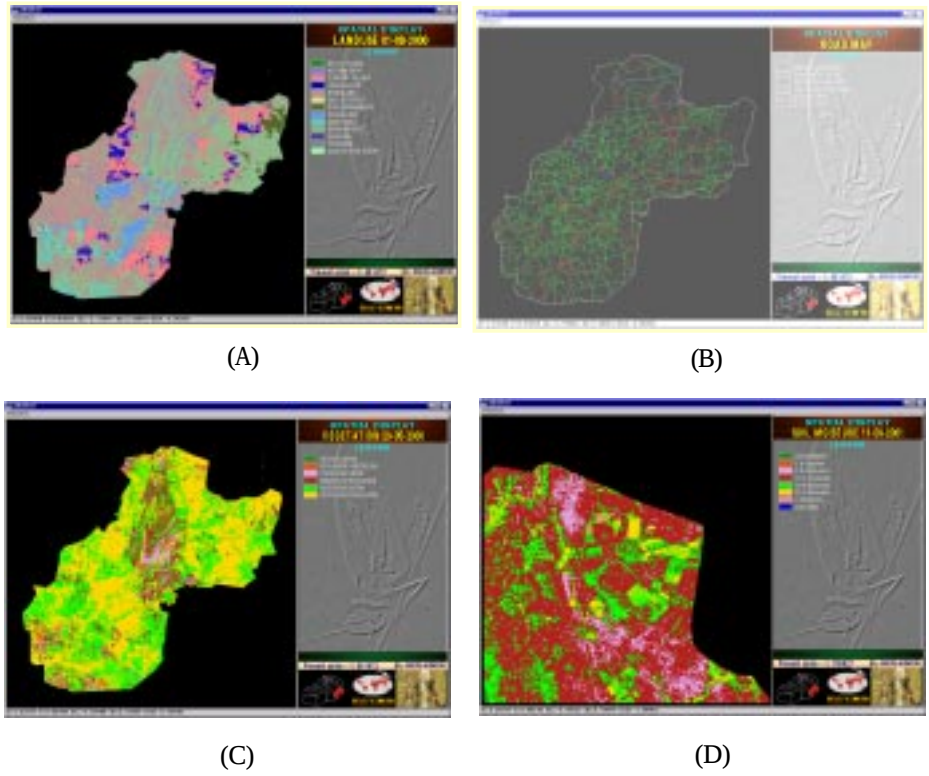

(A) (B)

(C) (D)

Figure 9: Spatial display of themes

IDENTIFY (To identify attribute of the themes at user specified location): It helps the user to identify attributes at user specified location (Figure 11). Identification could be for currently displayed theme, selected themes or multi-themes.

OVERLAY (For overlaying selected features of a theme on the displayed theme): It facilitates the user to overlay selected features of a theme on the displayed theme. Overlaid theme is displayed in the form of polygon, lines, points or hatched polygons (for themes of GRID type) with selected color/ pattern (Figure 12).

VIS_QUERY (For visual query of single or multiple themes): The purpose of this option is to perform visual query of single theme or across multiple themes i.e. to display selected subset of features (attributes) using query builder. The area satisfying the user defined query is only displayed (Figure 13). In the query builder menu the name of the selected theme appears along with

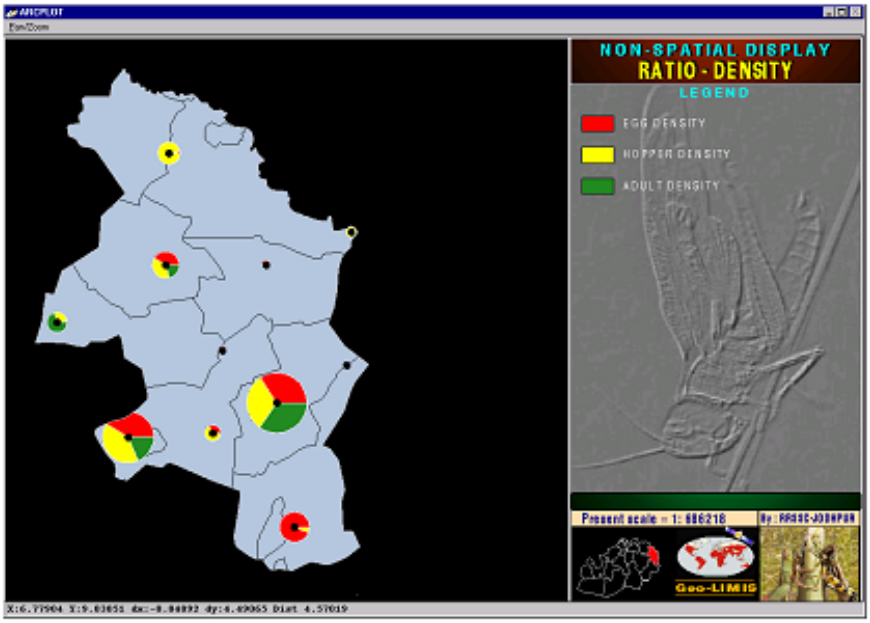

(A)

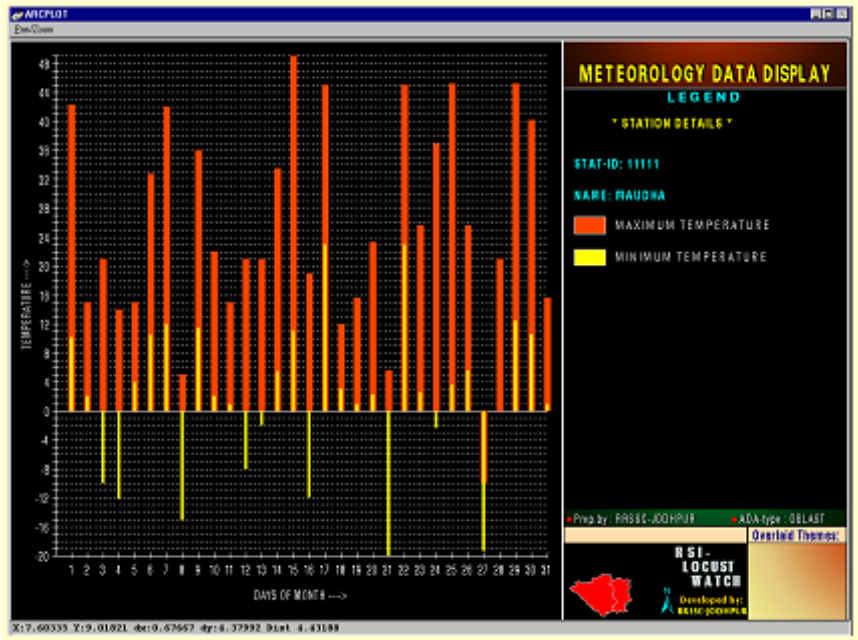

(B)

Figure 10: Non-spatial data display

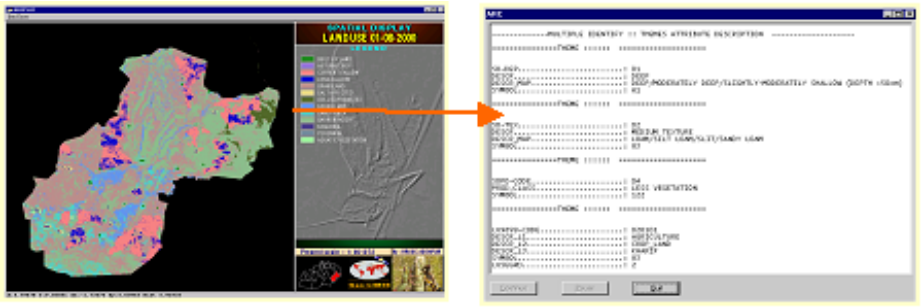

Figure 11: Attribute identification specific location

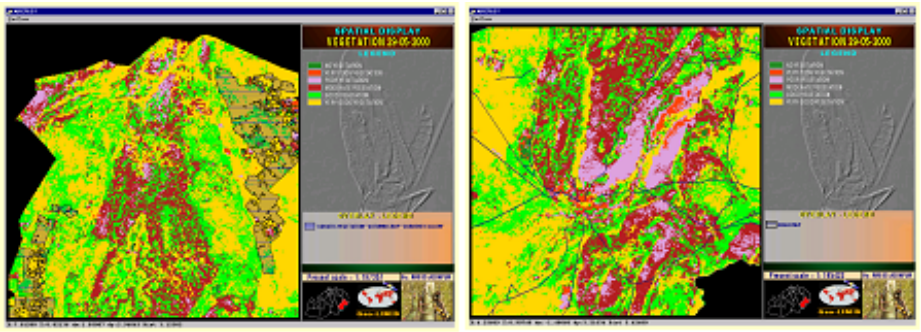

(a) (b)

Figure 12: Overlay of themes (a) polygon-polygon (b) polygon-line

relational operators – AND, OR along with choice for the attribute. Once the attribute of a theme is selected it can be added to the query set. The existing query can however, be added or edited. Once all the theme specific queries are put together in the query set the 'DRAW' button executes plotting of areas satisfying the criteria defined in the query set.

COMPOSITE (To generate integrated layers viz. SOLSCAPE and SOMVI and the final composite layer): The layers to be used for the generation of habitat suitability can be grouped into tow broad derived layers based on temporal sampling requirements for analysis. It is presumed that landform and soil texture are relative static geophysical properties in temporal scale and could be generated afresh once in 7-10 years time frame. Similarly is the case of broad landuse, which remained almost unchanged over the years in Kazakhstan except the current fallows are becoming permanent. Only the biomass cover changes drastically with summer and spring. Hence it was felt logical to integrate these three layers to generate SOLSCAPE layer, which could be used as it is for 2 or more consecutive seasons.

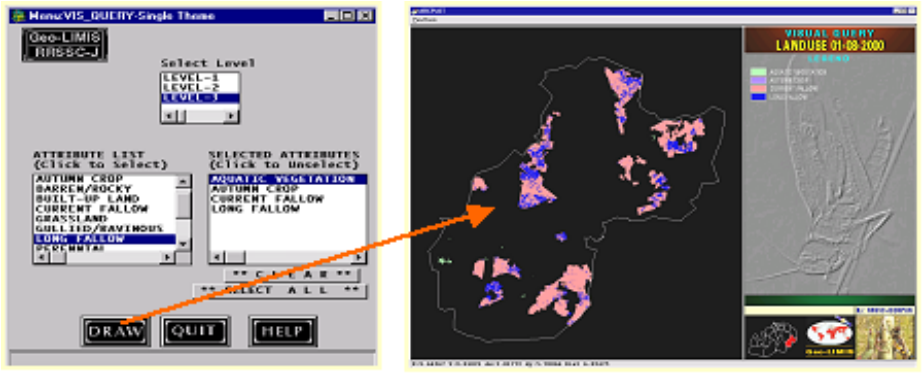

Figure 13: Visual query for single and multiple themes

On the other hand vegetation density and soil moisture are highly dynamic in temporal and spatial scale. Hence there is a need to map both of these parameters in every 7-10 days interval. Coarse resolution satellite data thought to be adequate for such dynamic features as the locust activity is a regional phenomena and not does not affect by local changes. These two parameters were combined together to generate an integrated layer called SOMVI. Integration of both SOLSCAPE and SOMVI generate final COMPOSITE layer which is the precursor for habitat suitability analysis.

LOC_DATA_ANAL (Analysis of locust data for input to query builder): Locust information in conjunction with ground and meteorological data is a prerequisite for developing expert system through the process of "knowledge gain". Historic locust data such as swarm type, species type, egg/hopper/adult density, area infested vis-à-vis concurrent weather during infestation will help the modeler to predict optimal range and combination of weather parameters in relation to locust response (Figure 14).

Besides climatic suitability locust data is also utilized to analyze in reference to in situ condition in the ground segment. The land condition underneath buffer area gives valuable input about locust preference for soil moisture, texture, vegetation etc and cohort distribution based on known sampling area. The buffer area generates report across multiple themes and displays as per cent distribution of various classes of each theme.

HABITAT_SUITABILITY (To generate habitat suitability layer): Based on locust data analysis the query set is generated and each set is given a class name such as most favourable, favourable, medium favourable and not

favourable (Figure 15). This file is saved as .qry file for eventual use in habitat suitability map generation.

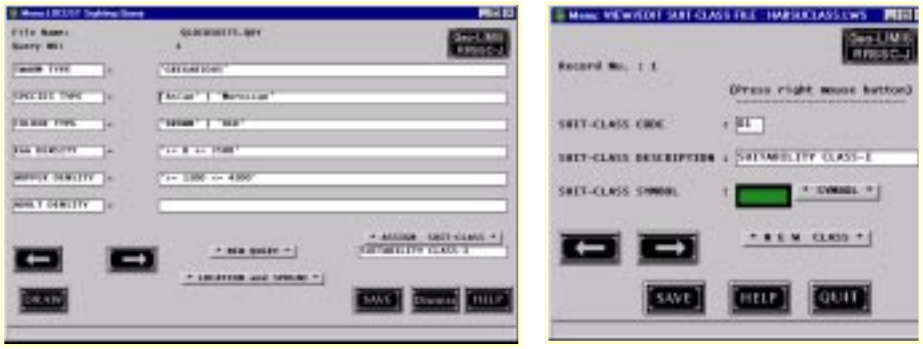

Figure 14: Locust data analysis interface

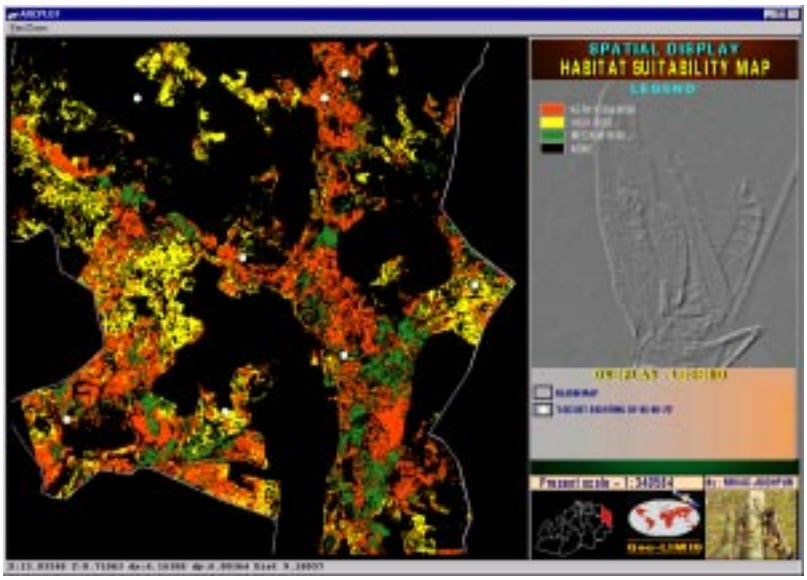

Figure 15: Habitat suitability map

TOOLS (Miscellaneous functions): The other functions include zooming and panning, saving of image in desired format, statistics generation, setting of text font and color, viewing of symbolset, updating of symbols and execution of ARCPLOT commands externally.

Life Cycle Builder

This module (Figure 16) works independently to query shell and analyses daily weather data downloaded from internet for forecasting of i) climate suitability for breeding of locusts and ii) suitability for flight. Besides thermal growth curve for egg incubation and hopper development specific to desert locust have been used to model the growth and development of locusts, which is an important indicator for locust control at temporal scale. Detailed physiology and locust life cycle have been studied to jot down environmental growth parameters in conjunction to ground intelligence for programming logic.

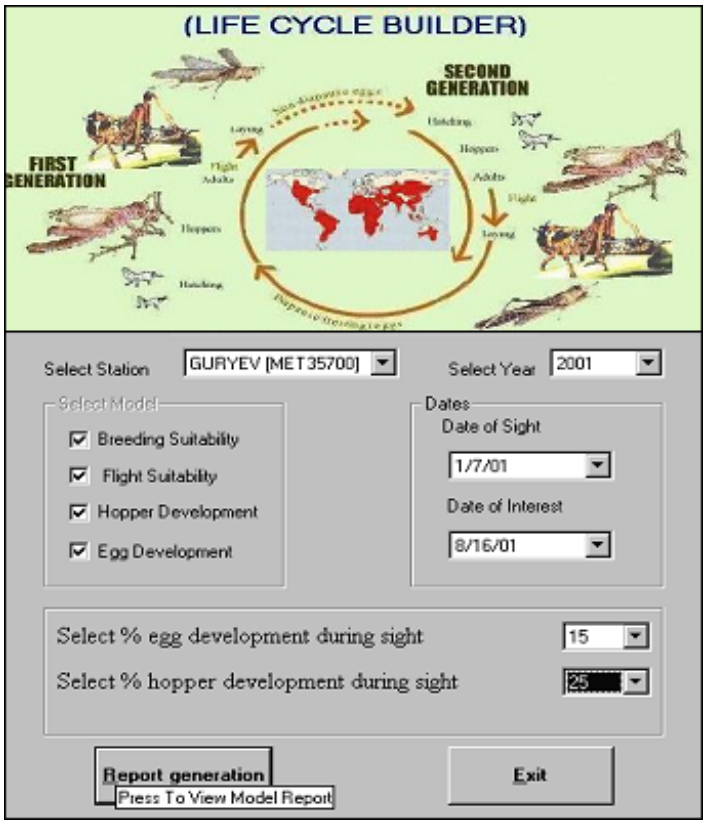

Figure 16: Life cycle builder interface

The database for climate was generated by downloading daily weather data from (http://meteo.infospace.ru.wond.html.index.ssi) Russian Hydromet Server. Year and location wise weather file is generated.

Climate suitability for Locust Breeding

For breeding of desert locusts, consecutive rain is required over 3 to 4 weeks to keep surface soil moist. If the surface soil remain moist for 10-15 days the adult locusts start oviposition. Besides soil moisture, soil temperature is also important to avoid desiccation of the egg pods. Hence to model breeding suitability past 3 weeks data pertaining to rainfall type, number of occurrence, maximum difference between two consecutive rain is analysed (indicates the duration of soil wetness). After analysis the model returns the output as a text file indicating whether the prevailing weather over past 3 weeks was suitable or not.

Climate suitability for Locust Migration/Flight

Migration and long march of adult locusts is a function of temperature, saturation deficit, wind velocity and direction, cloudiness and the upper atmospheric condition i.e. vertical distribution of atmospheric water vapour and mixing zones of upper atmosphere especially in the convergence zones. There is a minimum threshold temperature for flight muscle activation (greater than 17^{o}C), on the other hand above 42 ^{o}C thermal inactivation of muscle take place and flight is rare. Most optimum temperature is nearer to 35 ^{o}C. Similar to air temperature, humidity also play role in maintaining water balance during flight. Threshold wind velocity required for flight of DL is 13 m/s as the swarms prefer to move passively downwind with +/-10 degree deviation along its direction. Below the threshold wing movement is limited to hopping and saltation. In a cloudy day however, locusts do not fly. All the above constraints were used in programming logic to evaluate the chances of flight.

Per cent Egg Incubation undergone

This module essentially employs the temperature-growth model (Figure 17) of desert locust based on experiment carried out by Symmons et al., 1973. The percent incubation per day is calculated against daily ambient temperature from the model and integrated over the period of interest. If the percent development value exceeds 100 it prompts that incubation is complete. Besides it also compares with thermal degree days required for DL to complete its incubation. This gives idea about the degree of development undergone till date since it's reporting in the field. Here the inputs required are date of sighting of egg pods in the field along with approximate development till that

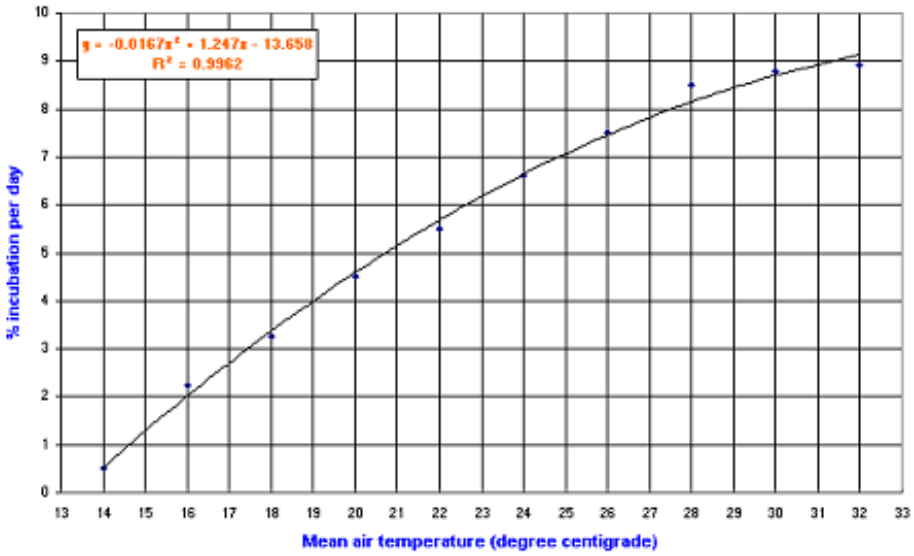

Figure 17: Air temperature vs per cent egg incubation of desert locust

time and the date on which percent incubation is sought. For generalization the model uses the growth curve of DL but with availability of species specific growth curve choices could be given to the users for selection of model.

Per cent Hopper Development undergone

Similar to egg incubation this model (Figure 18) calculates per cent development of hopper through various instars using daily air temperature. Like egg incubation per cent development undergone per day is integrated over the requested period and the value is returned. Here the inputs required are date of sighting of hoppers in the field along with approximate development till that time and the date on which percent development is sought. For generalization the model uses the growth curve of DL but with availability of species specific growth curve choices could be given to the users for selection of model.

The output menu of the Life Cycle Builder is given in Figure 19.

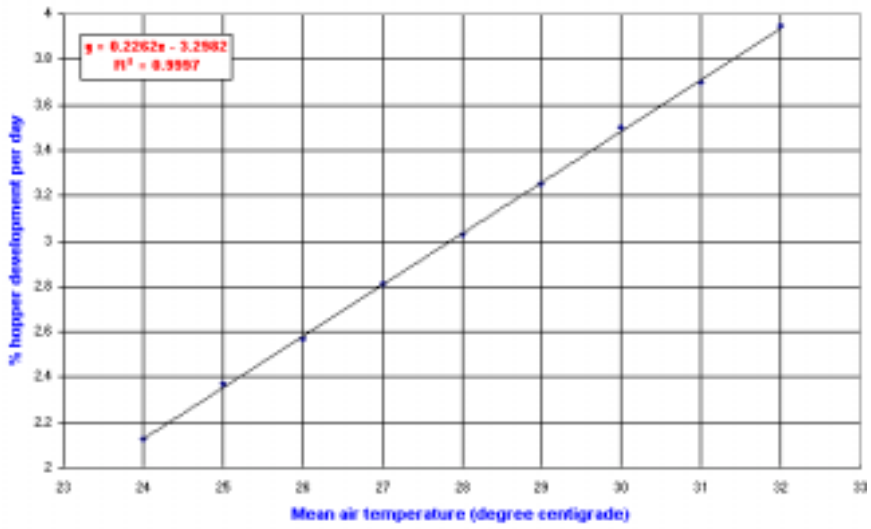

Figure 18: Air temperature vs per cent hopper development of desert locust

Figure 19: The Life Cycle Builder output

CONCLUSIONS

A Decision Support System on ARC/INFO GIS was developed to meet the need of locust forecasting requirements and operational use in the republic of Kazakhstan in the locust season. Various needs for the user has been taken into account by introducing ergonomics in the user interface design as well as coupling of analytical tools for efficient and meaningful outputs generation. The DSS developed can handle complex spatio-temporal configuration of locust events, generation of locust sighting as spatial database, cohort distribution based upon known sampling areas and utilization of internet downloaded daily weather data for locust life stage development. As the DSS uses wide variety of cartographic and remotely sensed sources, provision is kept for handling of raster, vector and descriptive data as well as comparison of multiple raster and vector maps for analysis of the relationships between locust events and bio-climate. Introduction of the mobile GIS and Global Positional System in surveying techniques will improve the accuracy and timely availability of data as model input to forecast in near real time.

One of the important aspects of locust data analysis for near real time forecasting depends upon the dissemination of field information to the center where data analysis is performed. Data on distribution, density and life stages of locust as well as habitat condition could be collected using GPS and palmtop computer and sent to GIS based DSS located at the headquarter where further analysis is performed through high frequency radio modems. The survey data could be converted to GIS format point features for visualization and used as input to run spatially explicit development models for predicting critical events at various life stages. The next important aspect is to combine operationally the outputs of various environmental models in relation to locust biology and critical events of life cycle like DYMEX professional model of Australia. A climate matching function can be used in the absence of any knowledge of the distribution of a species. This option can help the user to directly compare the temperature, rainfall and relative humidity of a given location with any number of other locations. It will provide a method of identifying sites with similar climates for assessing risk zones. Species-specific models could be developed after availability of detailed ground based information for event modeling. In the Life Cycle Builder module of Geo-LIMIS could be enhanced for calculating the values of its output variables at each time step. The sub-modules could be connected to an appropriate output variable of another or the same module by linking each of their input variables. During simulation, the value of that output variable can be used as

the input value. Scope is there that model designer can configure most modules to adapt them for required task. Geo-LIMIS with little change in the input layers and habit suitability criteria interfaced with life stage builder specific to the species concerned could be used for modeling other exotic insect pests and near real time forecasting for ground surveillance and control strategy.

ACKNOWLEDGEMENTS

The authors express their deep sense of gratitude to Dr K. Kasturirangan, Chairman, ISRO and Secretary, DOS, for his constant encouragement and guidance during this study. We are grateful to Shri V. Sundaramaiya, Scientific Secretary, ISRO for his guidance and support to bring out this manuscript. The authors are also thankful to the Director, Space Research Institute, Kazakhstan for extending support and valuable information for successful completion of the project.

REFERENCES

Deveson, E.D. and Hunter, D.M. 2001. Decision Support for Australian Locust Management using Wireless Transfer of Field Survey Data and Automatic Internet Weather Data Collection (Unpublished).

FAO, 1989. Desert Locust Research Priorities. Report of the FAO Research Advisory Panel, 2-5 May, 1989, Rome (FAO).

FAO, 1994. The Desert Locust Guidelines 1. Biology and Behavior, Rome.

Healey, R.G., Robertson, S.G., Magor, J.I., Pender, J. and Cressman, K. 1996. A GIS for Desert Locust Forecasting and Monitoring. Int. J. Geographical Information System, 10 (1): 117-136.

http://pest.cpitt.uq.edu.au/forecast/intro.html.

http://www.environment.gov.au/land/monitoring/green.html.

Navathe, S. and Schkolnick, M. 1978. View Representation in logical database design. In Proceedings of ACK-SIGMOD International Conference on Management of Data. Austin, TX. (ACM Press), pp. 144-156.

Pedgley, D.E. (editor) 1981. Desert Locust Forecasting Manual. Volume 1. (London: HMSO).

WORKSHOP EVALUATION

M.V.K. Sivakumar
World Meteorological Organization
7bis Avenue de la Paix, 1211 Geneva 2, Switzerland

INTRODUCTION

The Training Workshop (RA II) on Satellite Remote Sensing & GIS Applications in Agricultural Meteorology, was co-sponsored by the World Meteorological Organization (WMO), the India Meteorological Department (IMD), the Centre for Space Science and Technology Education in Asia and the Pacific (CSSTEAP), the Indian Institute of Remote Sensing (IIRS), the National Remote Sensing Agency (NRSA) and the Space Applications Centre (SAC).

The Commission for Agricultural Meteorology (CAgM) of WMO recognizes that training of technical personnel to acquire, process and interpret the satellite imagery is a major task. This training workshop was organized in response to the recommendations of the CAgM session in Ljubljana, Slovenia in 2002 with the objective of helping the participants from the Asian countries in learning new skills and updating their current skills in satellite remote sensing and GIS applications in agricultural meteorology.

Sixteen participants from thirteen Asian countries, including Bangladesh, China, India, Kazakhstan, Lao PDR, Maldives, Mongolia, Nepal, Saudi Arabia, Sri Lanka, Tajikistan, Thailand and the United Arab Emirates participated in this training workshop.

FORMAT FOR THE TRAINING WORKSHOP

The training workshop was designed for agrometeorologists from Asia with little or no background in satellite remote sensing and GIS applications in agricultural meteorology.

The workshop started with a thorough introduction to various aspects of satellite and remote sensing along with practical exercises on the digital analysis of satellite data. This was followed by lectures on digital image processing,

Satellite Remote Sensing and GIS Applications in Agricultural Meteorology
pp. 425-427

fundamentals of GIS and Geopositioning Systems (GPS) and spatial data analysis and practical demonstration of GIS software.

The participants were then introduced to both theoretical and practical aspects of retrieval of agrometeorological parameters using satellite remote sensing data. This was followed by a lecture on remote sensing and GIS application in agro-ecological zoning.

Remote sensing and GIS are very useful tools in crop growth and productivity monitoring and simulation as well as assessment and monitoring of droughts, floods, water and wind induced soil erosion. Lectures were given on all these aspects followed by practical demonstrations.

Participants were then introduced to satellite applications in weather forecasting, agro-advisory services, desert locust monitoring, forest fire and degradation assessment.

WORKSHOP EVALUATION

In order to facilitate the evaluation of the Seminar and help obtain feedback from the participants, an evaluation form was circulated on the final day. A summary of participant evaluation of the Seminar is shown in Table 1. About 94% of the participants felt that the programme met the expressed objectives of the workshop. The quality of the workshop programme was rated by 100% of the participants as being very good to good. Sixty two percent of the participants rated the workshop as excellent while 19% rated it as very successful.